

---

**ASPECTS OF QUANTUM  
CORRELATIONS IN INFORMATION  
PROCESSING**

---

*Thesis submitted for the degree of*  
**DOCTOR OF PHILOSOPHY (SCIENCE)**

*in*  
**PHYSICS (THEORETICAL)**

*by*  
**SHOUNAK DATTA**

**DEPARTMENT OF PHYSICS  
UNIVERSITY OF CALCUTTA**

2022

*To*  
*Late Sankar Chandra Dutta*  
*and*  
*Late Renu Dutta*

# Abstract

Since the famous Einstein-Podolsky-Rosen paradox, quantum theory surpasses the classical understanding of the world by featuring quantum entanglement among two or more microscopic particles. Quantum correlations arising from the entangled states play vital roles in shaping quantum information theory. This thesis investigates different forms of spatial quantum correlations present, largely in bipartite qubit systems and their information theoretic applications.

At first, we show the correspondence between an asymmetric quantum correlation, *viz.* quantum steering and the secret key rate in one-sided device-independent quantum cryptographic scenarios. Then we propose a technique of weak measurement and its reversal to preserve a lower bound of the secret key rate linked with quantum steering under the environmental interaction designed via amplitude damping decoherence. It is even possible to improve the aforementioned bound of the secret key rate to some extent when the technique is averaged over the success and failure of the post-selection method. Next, we quantify bipartite quantum steering through the decomposition of a correlation in terms of the extremal non-signalling correlations in the context of steering. We show that the quantifier, named steering cost, is a bonafide measure of quantum steering under the resource theoretic framework and is useful to detect steering for two well-known families of correlations.

We subsequently probe the framework of sharing quantum correlations in the presence of multiple observers for one of the strongest classes of steerable correlations, namely the nonlocal advantage of quantum coherence(NAQC). We show that all the forms of NAQC correlations between two qubits can be shared by at most one observer per side. Finally, we study the sharing of an information-theoretic task, *viz.* the remote preparation of a qubit at the lab of a single receiver, performed by a sequence of independent senders. By considering various bipartite pure and mixed initial states, we show that at most six sequential senders can achieve the quantum mechanical advantage with the receiver in the given framework when every sender prepares a remote state from the equatorial great circle of the Bloch sphere and a single copy of a maximally entangled pure state is shared initially.

# Acknowledgements

It is my privilege to pay extreme regards to my supervisor, Prof. Archan S. Majumdar for his continuous support and encouragement throughout my research career. He unfolded a vibrant atmosphere from where I, as a beginner, learned a lot about the global academic functioning of the researchers in our field. I have not only been enriched through the uncountable number of discussions on several topics of quantum theory with him but also experienced support in non-academic matters in many ways. It is a great pleasure for me to recollect the lessons that I gained from Prof. Guruprasad Kar, Prof. Dipankar Home, Prof. Debasis Sarkar, Prof. Sibasish Ghosh and Prof. Arun K. Pati.

The support from my friends, colleagues, office staffs and faculty members of S. N. Bose National Centre for Basic Sciences(SNBNCBS), Kolkata will remain memorable for me. Specially I want to mention Dr. Tanumoy Pramanik, Dr. Shiladitya Mal, Dr. C. Jebarathinam, Dr. Nirman Ganguly, Dr. Samyadeb Bhattacharya, Dr. Manik Banik, Dr. Arup Roy, Dr. Debarshi Das and Sourav Karar during my tenure in the centre.

I want to acknowledge financial support from the Department of Science and Technology, Govt. of India through project, INSPIRE fellowship program and SNBNCBS as well.

The contribution of my grandparents in my life and their demise in the midst of my research career left the deepest impression on me. And of course, the sacrifice and affection of my parents always inspire me in the journey of my life.

# List of Publications

## Publications forming part of the thesis:

1. **S. Datta**, S. Goswami, T. Pramanik, and A. S. Majumdar, '*Preservation of a lower bound of quantum secret key rate in the presence of decoherence*', *Phys. Lett. A*, **381**, 897 (2017).
2. D. Das, **S. Datta**, C. Jebaratnam, and A. S. Majumdar, '*Cost of Einstein-Podolsky-Rosen steering in the context of extremal boxes*', *Phys. Rev. A*, **97**, 022110 (2018).
3. **S. Datta** and A. S. Majumdar, '*Sharing of nonlocal advantage of quantum coherence by sequential observers*', *Phys. Rev. A*, **98**, 042311 (2018); *Phys. Rev. A* **99**, 019902(E) (2019).
4. **S. Datta**, S. Mal, A. K. Pati, and A. S. Majumdar, '*Remote qubit state preparation by multiple observers using a single copy of a two-qubit entangled state*', [arXiv:2109.03682 \[quant-ph\]](https://arxiv.org/abs/2109.03682) (2021).

## Additional publications not forming part of the thesis:

1. D. Das, **S. Datta**, S. Goswami, A. S. Majumdar, and D. Home, '*Bipartite qutrit local realist inequalities and the robustness of their quantum mechanical violation*', *Phys. Lett. A*, **381**, 3396 (2017).
2. A. G. Maity, **S. Datta**, and A. S. Majumdar, '*Tighter Einstein-Podolsky-Rosen steering inequality based on the sum-uncertainty relation*', *Phys. Rev. A*, **96**, 052326 (2017).
3. S. Gupta, **S. Datta**, and A. S. Majumdar, '*Preservation of quantum nonbilocal correlations in noisy entanglement-swapping experiments using weak measurements*', *Phys. Rev. A*, **98**, 042322 (2018).
4. **S. Datta**, S. Mal, and A. S. Majumdar, '*Protecting temporal correlations of two-qubit states using quantum channels with memory*', [arXiv:1808.10345 \[quant-ph\]](https://arxiv.org/abs/1808.10345) (2018).
5. S. Karar, **S. Datta**, S. Ghosh, and A. S. Majumdar, '*Anharmonicity can enhance the performance of quantum refrigerators*', [arXiv:1902.10616 \[quant-ph\]](https://arxiv.org/abs/1902.10616) (2019).
6. S. Gupta, D. Das, C. Jebarathinam, A. Roy, **S. Datta**, and A. S. Majumdar, '*"All-versus-nothing" proof of genuine tripartite steering and entanglement certification in the two-sided device-independent scenario*', *Quantum Stud.: Math. Found.* **9**, 175 (2022).
7. D. Tiwari, **S. Datta**, S. Bhattacharya, S. Banerjee, '*Dynamics of two qubit central spin under fermionic environment*', [arXiv:2205.04135 \[quant-ph\]](https://arxiv.org/abs/2205.04135) (2022).

# Contents

<b>Abstract</b>	<b>iii</b>
<b>Acknowledgements</b>	<b>iv</b>
<b>List of Publications</b>	<b>v</b>
<b>List of Figures</b>	<b>x</b>
<b>List of Tables</b>	<b>xii</b>
<b>1 Introduction</b>	<b>1</b>
1.1 Axioms of Quantum Mechanics	2
1.1.1 Features of a qubit	4
1.1.1.1 Mixedness	4
1.1.1.2 Coherence	5
1.1.1.3 Imaginarity	6
1.1.2 Schmidt decomposition	7
1.2 Entanglement	8
1.2.1 Bipartite entanglement measures	9
1.2.1.1 Distance based measure	10
1.2.1.2 Entropy of entanglement	10
1.2.1.3 Entanglement of formation	11
1.2.1.4 Concurrence	11
1.2.1.5 Negativity	11
1.2.2 Applications of entanglement	12
1.2.2.1 Quantum teleportation	13
1.2.2.2 Quantum dense coding	15
1.2.2.3 Quantum cryptography	16
1.3 Bell nonlocality	18
1.3.1 EPR theorem	18
1.3.2 Bell's theorem	19
1.3.3 Bell nonlocality measure	22
1.3.3.1 Nonlocal cost	22
1.3.4 Applications of Bell nonlocality	24
1.4 Quantum steering	24
1.4.1 Steering inequalities	26

1.4.1.1	Utility of uncertainty relations . . . . .	26
1.4.1.2	Analogous CHSH inequality . . . . .	30
1.4.1.3	Criterion of $n$ -measurement settings per side . . . . .	32
1.4.2	Quantum steering measures . . . . .	33
1.4.2.1	Steering weight . . . . .	34
1.4.2.2	Robustness of steering . . . . .	34
1.4.3	Applications of quantum steering . . . . .	34
1.5	Nonlocal advantage of quantum coherence . . . . .	35
1.5.1	Coherence complementarity relations . . . . .	35
1.5.2	Coherence steering inequalities . . . . .	36
1.5.3	Applications of NAQC . . . . .	37
1.6	Quantum discord . . . . .	37
1.6.1	Geometric measure . . . . .	38
1.6.2	Applications of discord . . . . .	38
1.6.2.1	Remote state preparation . . . . .	38
1.7	Hierarchy of quantum correlations . . . . .	40
1.8	Generalized measurements . . . . .	41
1.9	Quantum channels . . . . .	46
1.10	Plan of the thesis . . . . .	48
<b>2</b>	<b>Preservation of a quantum correlation</b>	<b>51</b>
2.1	Technique of weak measurement plus ADC . . . . .	52
2.2	1s-DIQKD associated with steering . . . . .	54
2.3	Quantum secret key rate under ADC . . . . .	57
2.3.1	Case-I: Single interaction . . . . .	58
2.3.2	Case II: Double interaction . . . . .	59
2.4	Improvement of quantum secret key rate . . . . .	61
2.4.1	Case-I: Single interaction . . . . .	62
2.4.2	Case-II: Double interaction . . . . .	64
2.5	Summary and Outlook . . . . .	67
<b>3</b>	<b>Cost of a quantum correlation</b>	<b>70</b>
3.1	Extremal non-signalling boxes . . . . .	71
3.2	Steering scenario in the context of extremal boxes . . . . .	73
3.3	Quantifying EPR steering . . . . .	75
3.3.1	Definition . . . . .	75
3.3.2	Consistency with the resource theory of steering . . . . .	75
3.3.2.1	Faithfulness . . . . .	77
3.3.2.2	Monotonicity . . . . .	77
3.3.2.3	Convexity . . . . .	81
3.4	Illustrations . . . . .	84
3.4.1	White-noise BB84 family . . . . .	85
3.4.2	Colored-noise BB84 family . . . . .	90
3.5	Steering cost versus steering weight . . . . .	94
3.5.1	Illustrations . . . . .	95
3.5.1.1	Example 1. . . . .	96
3.5.1.2	Example 2. . . . .	97
3.6	Summary and Outlook . . . . .	97

<b>4</b>	<b>Sharing of a quantum correlation</b>	<b>99</b>
4.1	NAQC under unsharp measurement formalism . . . . .	101
4.2	Sharing of $l_1$ -norm of NAQC . . . . .	105
4.2.1	Alice <sup>1</sup> in the given scenario . . . . .	105
4.2.2	Alice <sup>2</sup> in the given scenario . . . . .	106
4.3	Sharing of relative entropy of NAQC . . . . .	108
4.3.1	Alice <sup>1</sup> in the given scenario . . . . .	108
4.3.2	Alice <sup>2</sup> in the given scenario . . . . .	109
4.4	Sharing of skew-information of NAQC . . . . .	110
4.4.1	Alice <sup>1</sup> in the given scenario . . . . .	110
4.4.2	Alice <sup>2</sup> in the given scenario . . . . .	111
4.5	Summary and Outlook . . . . .	112
<b>5</b>	<b>Sharing of an information processing task</b>	<b>114</b>
5.1	Recapitulation of RSP . . . . .	117
5.2	Optimal classical strategy . . . . .	119
5.2.1	Case I . . . . .	120
5.2.2	Case II . . . . .	121
5.3	RSP under unsharp measurement formalism . . . . .	122
5.4	Sequential RSP with maximally entangled pure state . . . . .	126
5.4.1	RSP from equatorial great circle . . . . .	128
5.4.1.1	Geometric discord vs concurrence . . . . .	130
5.4.2	RSP from non-equatorial circles . . . . .	137
5.4.2.1	Illustration: RSP with $\theta = \frac{\pi}{2} \pm (\frac{\pi}{2} - \tan^{-1} \sqrt{2})$ . . . . .	143
5.5	Sequential RSP with non-maximally entangled pure state . . . . .	144
5.6	Sequential RSP with mixed entangled state . . . . .	148
5.7	Summary and Outlook . . . . .	151
<b>6</b>	<b>Concluding remarks</b>	<b>154</b>
	<b>References</b>	<b>160</b>

# List of Figures

1.1	Hierarchy of quantum correlations, named after NAQC for Nonlocal Advantage of Quantum Coherence, BNL for Bell nonlocality, quantum steering and ENT for entanglement, are sketched. Additionally, the set of entangled states is comprised within the space of discordant states. . . . .	40
2.1	Lower bound of the quantum secret key rate for the initial Bell state $ \Psi^\pm\rangle$ given by Eq.(2.10) is plotted versus the decoherence parameter $D$ . The upper (blue) curve corresponds to Case-I ( <i>i.e.</i> single interaction) while the lower (green) curve corresponds to Case-II ( <i>i.e.</i> double interaction). . . . .	60
2.2	Lower bound of quantum secret key rate for the initial Bell state $ \Phi^\pm\rangle$ given by Eq.(2.10) is plotted versus the decoherence parameter $D$ . The upper (blue) curve corresponds to Case-I ( <i>i.e.</i> single interaction) while the lower (green) curve corresponds to Case-II ( <i>i.e.</i> double interaction). . . . .	61
2.3	Lower bound of quantum secret key rate is plotted against the strength of decoherence $D_B = D$ ( $x$ -axis) and the strength of weak measurement $p_B$ ( $y$ -axis). The upper (green) surface is for the secret key rate given by Eq.(2.26) using the technique of weak measurement while the lower (blue) one is for the secret key rate given by Eq.(2.14) <i>i.e.</i> without using such technique. . . . .	64
2.4	Lower bound of quantum secret key rate is plotted against the strength of decoherence $D_A = D_B = D$ ( $x$ -axis) and the strength of weak measurement $p_A = p_B = p$ ( $y$ -axis). The upper (blue) surface corresponds to the secret key rate associated with $\rho'_R$ obtained successively from the initial state given by Eq.(2.10) where the technique of weak measurement is utilized and the lower (green) surface corresponds to the secret key rate associated with the state $\rho''_{AB}$ given by Eq.(2.15) where the technique of weak measurement is not utilized. . . . .	66
2.5	The average of quantum secret key rate, $r_{Av}$ is plotted (blue surface) against the strength of decoherence $D_A = D_B = D$ ( $x$ -axis) and the strength of weak measurement $p_A = p_B = p$ ( $y$ -axis). The green surface corresponding to the case without weak measurement is the same as in Fig.2.4. It can be seen from the blue surface that, the improvement of the average secret key rate is possible for a certain range of values of the strength of decoherence and weak measurement. . . . .	67
2.6	The improvement factor $r_I$ (yellow surface) is plotted against the decoherence strength, $D(= D_A = D_B)$ ( $x$ -axis) and the weak measurement strength, $p(= p_A = p_B)$ ( $y$ -axis). By utilizing the weak measurement technique, the improvement of the given lower bound of the average secret key rate can be seen well above the green plane representing $r_I = 1$ for a certain region in $\{D, p\}$ space. . . . .	67

4.1	Schematic diagram of sharing the task of NAQC by sequential Alices in order to steer the local quantum coherence of Bob's subsystem. . . . .	104
5.1	The optimum classical bound on the RSP-fidelity, <i>i.e.</i> $f_{cl}^{\max}$ is plotted against the polar angle $\theta$ of a fixed circle on the Bloch sphere from where Bob chooses a state to prepare at Alice's side remotely. . . . .	122
5.2	Schematic diagram of remote state preparation at Alice's lab by multiple Bobs. The local unitary operations, $\{\mathbb{1}_2, \sigma_z\}$ and their reverse are applicable for remote states chosen from the equatorial circle of the Bloch sphere. . . . .	125
5.3	The optimally available geometric discord and concurrence for different number of Bobs is presented whenever the implementation of RSP is achievable upto its previous Bobs with non-classical advantage at Alice's side. . . . .	132
5.4	Schematic diagram of a Bloch sphere. $\{ 0\rangle,  1\rangle\}$ forms the computational basis, whereas $\{ 0_{x(y)}\rangle,  1_{x(y)}\rangle\}$ are the basis corresponding to $x(y)$ direction. $\{ \psi^i\rangle,  \psi_{\perp}^i\rangle\}$ are two mutually orthogonal states with a polar angle $\theta$ . Traversing over all azimuthal angles $\phi_i \in [0, 2\pi]$ implies, in effect, the precession over the curved surface of the double cone. . . . .	138
5.5	The minimum sharpness of measurements <i>i.e.</i> $\{(\lambda_i)_{\min}\}_1^6$ specified by the respective Bobs are plotted against different polar angles of the remote state ( $\theta$ ) such that, the average RSP-fidelities can attain the non-classical values for $(\lambda_i)_{\min} < \lambda_i \leq 1 \forall i$ , while the singlet state is shared initially and the sharpness of measurements, manifested by the previous Bobs (up to $\text{Bob}^{i-1}$ ), are maintained with the corresponding non-classical region of average RSP-fidelities. . . . .	140
5.6	The data points corresponding to the minimum sharpness of measurements, <i>i.e.</i> $(\lambda_i)_{\min}(\theta)$ to attain the non-classical advantage of the average RSP-fidelities are plotted w.r.t. the number of Bobs ( $i \leq n$ ) while sharing the singlet state initially and the remote states are prepared every time from a non-equatorial circle (with a fixed polar angle, $\theta$ ) of the Bloch sphere such that, corresponding to $\text{Bob}^{n+1}$ in the given scenario $(\lambda_{n+1})_{\min} > 1$ . Purple, green, blue, brown data points represent $\theta = \frac{\pi}{2}, \frac{3\pi}{8}, \frac{\pi}{4}$ and $\frac{\pi}{8}$ respectively. The total number of data points for a given $\theta$ is indicated by $n$ . . . . .	142
5.7	The minimum sharpness of measurements, <i>i.e.</i> $\{(\lambda_i)_{\min}\}_1^6$ to achieve the quantum mechanical advantage of average RSP-fidelities are plotted against the state parameter $\xi$ of the initially shared non-maximally entangled pure state where the remote states from the equatorial great circle ( $\theta = \frac{\pi}{2}$ ) of the Bloch sphere are chosen to be prepared by each Bob up to $\text{Bob}^i$ . . . . .	146
5.8	The data points corresponding to the minimum sharpness of measurements, <i>i.e.</i> $(\lambda_i)_{\min}(\xi)$ to achieve the quantum advantage of the RSP-protocol are plotted w.r.t. the number of Bobs ( $i \leq n$ ) such that, for $\text{Bob}^{n+1}$ in the given scenario $(\lambda_{n+1})_{\min} > 1$ while a non-maximally entangled pure state with parameter $\xi$ is shared initially and a remote state from the equatorial great circle of the Bloch sphere is prepared every time. Hence by fixing $\theta = \frac{\pi}{2}$ , purple, green, blue and brown colored data points correspond to the initial states with $\xi = \frac{\pi}{4}, \frac{\pi}{6}, \frac{\pi}{8}$ and $\frac{\pi}{10}$ respectively. The total number of data points for a given $\xi$ implies the optimal bound on the number of Bobs ( $n$ ). . . . .	147
5.9	The minimum sharpness of measurements, <i>i.e.</i> $\{(\lambda_i)_{\min}\}_1^6$ are plotted against the Werner state parameter $c$ of the initial state where the remote states are picked from the equatorial great circle ( $\theta = \frac{\pi}{2}$ ) of the Bloch sphere in order to obtain the non-classical value of the average RSP-fidelity corresponding to $\text{Bob}^i$ . . . . .	149

# List of Tables

5.1	The leftover amount of geometric discord and concurrence, that can be maximally utilized by different numbers of Bobs in the given scenario where each Bob prepares remote state from the equatorial great circle of the Bloch sphere by making use of the singlet state as the initial quantum resource. . . . .	131
5.2	The domain of sharpness of measurements for which 6 subsequent Bobs can altogether attain the average fidelity $> \frac{3}{4}$ for preparing remote qubits from the equatorial plane of the Bloch sphere when a single copy of the initially shared state is one among the maximally entangled pure states. . . . .	136
5.3	At most $n$ -number of Bobs can sequentially prepare the remote states having a fixed polar angle $\theta$ on the surface of the Bloch sphere such that every Bob attains the average RSP-fidelity greater than $f_{cl}^{\max}$ by utilizing the singlet state initially. . . . .	141
5.4	The range of sharpness parameters $\lambda_i \in ((\lambda_i)_{\min}, 1]$ for which 3 Bobs can independently prepare the remote states with polar angle $\theta = \frac{\pi}{2} \pm (\frac{\pi}{2} - \tan^{-1} \sqrt{2})$ at Alice's side with average fidelity $f_{av}^{AB^i} > 0.803$ by using the singlet state initially. . . . .	143
5.5	At most $n$ -number of Bobs can sequentially prepare the remote states from the equatorial circle ( $\theta = \frac{\pi}{2}$ ) of the Bloch sphere such that, every Bob up to Bob $^n$ attains the average RSP-fidelity $> \frac{3}{4}$ whenever a single copy of the non-maximally entangled pure state is shared initially. . . . .	146
5.6	At most $n$ -number of Bobs can sequentially prepare the remote states from equatorial circle ( $\theta = \frac{\pi}{2}$ ) of the Bloch sphere such that every Bob up to Bob $^n$ are capable of doing RSP with average RSP-fidelity $> \frac{3}{4}$ by sharing Werner state initially. . . . .	150

## Introduction

Since the beginning of the 20th century, the classical idea of physics faced several challenges when it was found to be incompetent to explain several experimental observations on the microscopic particles. From the spectral analysis of black body radiation, the well-known Rayleigh-Jeans law failed to provide the correct energy spectrum at the ultraviolet region of wavelength, which is called as *ultraviolet catastrophe*. The phenomenon of interference from the double-slit experiment is another salient signature of such incompetence. There are several other instances, which clearly indicate the genesis of a new physics, called as Quantum Mechanics(QM). Subsequently, the mathematical framework, with the help of functional analysis, has been formulated to describe QM. In 1935, Einstein, Podolsky and Rosen described QM as incomplete [EPR35] by introducing an entangled state, which is famously called as *EPR paradox*. Whereas several counter-intuitive phenomena in the presence of entanglement, having their advantages in computational and information-theoretic aspects, established QM as an experimentally accurate theory, where the standard classical predictions are utterly impossible. The modern outlook of quantum information theory is developed through the persistent effort of the physicists, computer scientists and mathematicians. In this thesis, we investigate some features of quantum mechanical correlations present in a joint state of two spatially separated microscopic particles with their useful applications.

## 1.1 Axioms of Quantum Mechanics

The fundamental postulates of QM are given below:

**A1.** A physical system, completely characterized by a state, is associated with a Hilbert space  $\mathcal{H}$ .

The dimension of  $\mathcal{H}$  depends upon the degrees of freedom for that physical system. For example, a harmonic oscillator requires infinite dimensional Hilbert space. A qubit is the smallest quantum system with a Hilbert space of dimension 2. A spin- $\frac{1}{2}$  particle or a photon having two states of polarization is representative of a two-level system.  $\mathcal{H}$  is a complete inner product space where the vectors, denoted by  $|\psi\rangle$  satisfy positivity ( $\langle\psi|\psi\rangle > 0$ ), linearity ( $\langle\vartheta|(a_1|\psi_1\rangle + a_2|\psi_2\rangle) = a_1\langle\vartheta|\psi_1\rangle + a_2\langle\vartheta|\psi_2\rangle$ ) and skew symmetry ( $\langle\vartheta|\psi\rangle^* = \langle\psi|\vartheta\rangle$ ). A ray in QM is a vector, equivalent under multiplication with a complex number and is normalized ( $\langle\psi|\psi\rangle = 1$ ). In general, a state is represented by a positive trace class operator, such as a qubit state in 2-dim complex Hilbert space  $\mathbb{C}^2$  is represented by

$$\rho = \frac{1}{2}(\mathbb{1}_2 + \vec{n} \cdot \vec{\sigma}) \quad (1.1)$$

where  $\mathbb{1}_2$  is a  $2 \times 2$  identity matrix,  $\vec{n} = (n_x, n_y, n_z)$  is the directional vector and  $\vec{\sigma} = (\sigma_x, \sigma_y, \sigma_z)$  is a set of Pauli matrices along x-, y-, z-directions respectively. Here  $\sigma_x = \begin{pmatrix} 0 & 1 \\ 1 & 0 \end{pmatrix}$ ,  $\sigma_y = \begin{pmatrix} 0 & -i \\ i & 0 \end{pmatrix}$  and  $\sigma_z = \begin{pmatrix} 1 & 0 \\ 0 & -1 \end{pmatrix}$  respectively ( $i = \sqrt{-1}$ ).  $\rho$  satisfies  $\text{Tr}(\rho) = 1$  and is called as density matrix.

**A2.** Observables or measurable properties of a physical system are associated with self-adjoint operators on the Hilbert space  $\mathcal{H}$ .

The condition for a self-adjoint operator in QM or self-adjoint matrix say,  $\mathcal{A}$  is that,  $\mathcal{A} = \mathcal{A}^\dagger$ .  $\mathcal{A}$  always yields real eigenvalues say,  $\{a_i\}$  and the corresponding eigenvectors are  $\{|\psi_i\rangle\}$ . Then one can write  $\mathcal{A} = \sum_i a_i |\psi_i\rangle\langle\psi_i|$  on  $\mathcal{H}$ .

**A3.** Measurement of an observable results in one of its eigenvalues and the probability

of getting the outcome is generated by Born's rule.

Suppose, a measurement of  $\mathcal{A}$  is performed on a system prepared in a state  $\rho$ . Then according to the Born's rule, the probability of getting outcome  $a_i$  is given by  $p_i = \text{Tr}[\rho |\psi_i\rangle\langle\psi_i|]$ . The expectation or average value of  $\mathcal{A}$  in the state  $\rho$  is  $\text{Tr}[\rho\mathcal{A}]$ . The operator  $|\psi_i\rangle\langle\psi_i| \forall i$  is called a projector and the measurement is called a projective measurement.

If we consider, in general that, a measurement operator  $\mathfrak{M}_i$  is acting upon the state  $\rho$ , then the probability of getting  $i$ -th outcome becomes  $\text{Tr}[\mathfrak{M}_i\rho\mathfrak{M}_i^\dagger]$  or  $\text{Tr}[\mathfrak{M}_i^\dagger\mathfrak{M}_i\rho]$ . The set of positive elements  $\{\mathfrak{M}_i^\dagger\mathfrak{M}_i\}_i$  satisfy completeness relation and constitute a Positive Operator Valued Measure (POVM). It can be reduced to a projective measurement if the projectors are its elements. The post-measurement state corresponding to different outcomes can be obtained through the following transformation,

$$\rho \rightarrow \frac{\mathfrak{M}_i\rho\mathfrak{M}_i^\dagger}{\text{Tr}[\mathfrak{M}_i\rho\mathfrak{M}_i^\dagger]} \quad \forall i \quad (1.2)$$

**A4.** The evolution of a closed system in QM is governed by a unitary operator which depends on the Hamiltonian acting upon the system.

Suppose that, a physical system is described by  $\rho(t_1)$  at time  $t_1$  and by  $\rho(t_2)$  at a later instant  $t_2$ . Then for a unitary operator  $U(t_1, t_2)$  the following transformation exists

$$\rho(t_1) \rightarrow \rho(t_2) = U(t_1, t_2)\rho(t_1)U(t_1, t_2)^\dagger \quad (1.3)$$

where,  $U(t_1, t_2) = \exp[-\frac{iH(t_2-t_1)}{\hbar}]$  and  $H$  is the Hamiltonian acting on the system.

**A5.** If a system labeled by  $A$  is associated with the Hilbert space  $\mathcal{H}_A$  and the system labeled by  $B$  is associated with the Hilbert space  $\mathcal{H}_B$ , then the composite system between  $A$  and  $B$  is associated with the tensor product Hilbert space  $\mathcal{H}_A \otimes \mathcal{H}_B$ .

### 1.1.1 Features of a qubit

The simplest density matrix to represent the state of a physical system is a qubit. Several aspects of a qubit are discussed below.

#### 1.1.1.1 Mixedness

Usually, Von-Neumann entropy [Neu55] is used to measure the mixedness of a qubit state  $\rho$ , which is given as

$$\begin{aligned} S(\rho) &= -\text{Tr}(\rho \log_2 \rho) \\ &= -\sum_l \omega_l \log_2 \omega_l \end{aligned} \quad (1.4)$$

where  $\{\omega_l\}$  are the set of eigenvalues of  $\rho$ . This is to quantify quantum states emitted from a source in terms of bits. If  $S(\rho)$  is approximated up to first order of  $\rho$  given by Eq.(1.1), then it is called as linear entropy with the form  $\sim 1 - \text{Tr}(\rho^2) \sim \frac{1-|\vec{n}|^2}{2}$  where  $|\vec{n}| = \sqrt{n_x^2 + n_y^2 + n_z^2}$ . Hence the linear entropy is invariant under the basis representation of density matrix and numerically less demanding than the Von-Neumann entropy. The measure of linear entropy was originally introduced in [PWK04].

A qubit  $\rho$  is pure if  $|\vec{n}| = 1$  or  $\rho^2 = \rho$  and is mixed if  $|\vec{n}| < 1$  or  $\rho^2 < \rho$ . The linear entropy is zero for a pure qubit and maximum of  $\frac{1}{2}$  for  $\frac{\mathbb{1}_2}{2}$ . The representation of a pure qubit  $\rho$  in terms of spherical polar co-ordinates is given by  $\vec{n} = (\sin \theta \cos \phi, \sin \theta \sin \phi, \cos \theta)$  and it lies on the curved surface of the Bloch sphere. The corresponding vector form of a pure state is  $|\psi\rangle = \cos(\frac{\theta}{2})|0\rangle + \exp(i\phi) \sin(\frac{\theta}{2})|1\rangle$  ( $0 \leq \theta \leq \pi$ ,  $0 \leq \phi \leq 2\pi$ ) where the z-basis states  $\{|0\rangle, |1\rangle\}$  are comparable with the computational bits with a possibility of superposition between them. Whereas the mixed states correspond to the points lying inside the surface of the Bloch sphere. Quantum information is about knowing the information hidden in a quantum state through operations like measurements. The least informative quantum state is a maximally mixed qubit state *i.e.*  $\frac{\mathbb{1}_2}{2}$  where all outcomes are equally probable.

### 1.1.1.2 Coherence

The notion of coherence depends upon the quantum mechanical description of a physical system *i.e.* the off-diagonal elements of a density matrix. Now coherence of a density matrix implies the superposition of orthogonal pure states in a fixed basis. Suppose that, a pure state  $|\psi\rangle$  can be written as,  $|\psi\rangle = \sum_i c_i |\psi_i\rangle$  in terms of basis states  $\{|\psi_i\rangle\}_i$  where  $c_i \neq 0 \exists i$ . This suggests that the density matrix  $\rho = |\psi\rangle\langle\psi|$  has coherence for that basis. If the density matrix is represented in another basis, then quantum coherence for that basis will differ. We know that a pure state in a particular basis can not be expressed in terms of other pure states in that basis. Hence from  $|0_x\rangle = \frac{1}{\sqrt{2}}(|0_z\rangle + |1_z\rangle)$  where  $|0_x\rangle, |0_z\rangle$  and  $|1_z\rangle$  denote up-spin along x-direction, up and down spin along z-direction respectively, we can say that,  $|0_x\rangle$  has no coherence in x-basis whereas has optimum coherence in z-basis. Now there are three quantifiers according to the resource theoretic formulation of quantum coherence given by Baumgratz *et al* [SAP17, BCP14a].

1.  **$l_1$ -norm:** It is given by [BCP14a]

$$C^1(\rho) = \sum_{\substack{i,j \\ i \neq j}} |\rho_{ij}| \quad (1.5)$$

where  $\rho_{ij}$  is the element corresponding to i-th row and j-th column of the density matrix  $\rho$ . Using Eq.(1.1), we have  $C_i^1(\rho) = \sqrt{|\vec{n}|^2 - n_i^2} \quad \forall i \in \{x, y, z\}$  in the basis i.

2. **Relative entropy:** It is given by [BCP14a]

$$C^E(\rho) = S(\rho_D) - S(\rho) \quad (1.6)$$

where  $S(\rho)$  is Von-Neumann entropy of state  $\rho$  and  $\rho_D$  is the diagonal matrix formed by the diagonal elements of  $\rho$  in a fixed basis. Using Eq.(1.1), we have for i-th basis  $C_i^E(\rho) = H(\frac{1+n_i}{2}) - H(\frac{1+|\vec{n}|}{2}) \quad \forall i \in \{x, y, z\}$  where  $H(\alpha) = -\alpha \log_2(\alpha) - (1 - \alpha) \log_2(1 - \alpha)$ .

3. **Skew information:** In  $\sigma_i$  basis, it has the form [Gir14],

$$C^S(\rho) = -\frac{1}{2} \text{Tr}[[\sqrt{\rho}, \sigma_i]^2] = \text{Tr}[\rho \cdot \sigma_i \cdot \sigma_i - \sqrt{\rho} \cdot \sigma_i \cdot \sqrt{\rho} \cdot \sigma_i] \quad (1.7)$$

where  $[x, y] = xy - yx$  is the commutator between two matrices  $x$  and  $y$ . However, the observable quantity of  $C^S(\rho)$  is a certain lower bound *i.e.*  $-\frac{1}{4} \text{Tr}[[\sqrt{\rho}, \sigma_i]^2]$ . By making use of Eq.(1.1) in the basis  $i$ , we obtain  $C_i^S(\rho) = \frac{1}{|\vec{n}|^2} (|\vec{n}|^2 - n_i^2) (1 - \sqrt{1 - |\vec{n}|^2})$   $\forall i \in \{x, y, z\}$ .

In general, the quantifiers satisfy the following trade-off for a qubit  $\rho$ ,

$$C_i^{L1}(\rho) \geq C_i^E(\rho) \geq C_i^S(\rho) \quad \forall i \in \{x, y, z\}$$

### 1.1.1.3 Imaginarity

Complex numbers play a significant role in the formulation of quantum mechanics. The presence of complex numbers in the elements of density matrix can be seen from Eq.(1.1). For example, the up or down eigenstate of  $\sigma_y$  can be written in terms of the eigenstates of  $\sigma_z$  as,  $|0_y\rangle = \frac{1}{\sqrt{2}}(|0_z\rangle + i|1_z\rangle)$  or  $|1_y\rangle = \frac{1}{\sqrt{2}}(|0_z\rangle - i|1_z\rangle)$  ( $i = \sqrt{-1}$ ). It implies that the eigenstates of  $\sigma_y$  have maximum imaginarity in  $\sigma_z$  eigenbasis, whereas it has no imaginarity in  $\sigma_y$  eigenbasis as no pure state can be expressed by other pure states in the same basis. Hence imaginarity is another basis-dependent property of a qubit. According to the resource theoretic formulation of quantum imaginarity proposed by Wu *et al* [WKR<sup>+</sup>21a, WKR<sup>+</sup>21b], there are two non-equivalent quantifiers of imaginarity.

1. **Geometric imaginarity:** For pure states  $|\psi\rangle$ , it is given by

$$\mathcal{I}_g(|\psi\rangle) = \frac{1 - |\langle \psi^* | \psi \rangle|}{2} \quad (1.8)$$

where  $|\psi^*\rangle$  is the complex conjugate of  $|\psi\rangle$ . Whereas for mixed states having the

form,  $\rho = \sum_j p_j |\psi_j\rangle\langle\psi_j|$ , it is given by

$$\mathcal{I}_g(\rho) = \min \sum_j p_j \mathcal{I}_g(|\psi_j\rangle) \quad (1.9)$$

considering all pure state decompositions of  $\rho$ .

**2. Robustness of imaginarity:** In general, for a qubit  $\rho$ , it is given by,

$$\mathcal{I}_R(\rho) = \frac{1}{2} \|\rho - \rho^T\|_1 \quad (1.10)$$

where,  $\rho^T$  is the transpose of  $\rho$  and the trace norm of matrix  $V$  is given by  $\|V\|_1 = \text{Tr}[\sqrt{V^\dagger V}]$ . For a pure qubit  $\rho = |\psi\rangle\langle\psi|$ , we have  $\mathcal{I}_R(\rho) = \sqrt{1 - |\langle\psi^*|\psi\rangle|^2}$ . With respect to the three mutually orthogonal basis in 2-dim, the robustness of imaginarity for the qubit state given by Eq.(1.1) are as follows,  $\mathcal{I}_R^x(\rho) = \mathcal{I}_R^z(\rho) = n_y, \mathcal{I}_R^y(\rho) = n_x$ .

## 1.1.2 Schmidt decomposition

A pure state of a composite system in Hilbert space  $\mathcal{H}_A \otimes \mathcal{H}_B$  can be expressed as,

$$|\psi\rangle_{AB} = \sum_{n=1}^d \sqrt{\mu_n} |\alpha_n\rangle \otimes |\beta_n\rangle, \quad (1.11)$$

where the subsystems  $A$  and  $B$  have orthonormal basis  $\{|\alpha_n\rangle\}$  and  $\{|\beta_n\rangle\}$  in their respective state subspaces and  $d \leq \min\{d_A, d_B\}$ .  $d_A$  and  $d_B$  are the dimension of  $\mathcal{H}_A$  and  $\mathcal{H}_B$  respectively. The simplest joint state of a composite system is a state of two-qubit system belonging to  $\mathbb{C}^2 \otimes \mathbb{C}^2$ .

## General two-qubit representation

The generalized form of a bipartite qubit system can be represented as [Fan83]

$$\rho_{AB} = \frac{1}{4} [\mathbb{1}_2 \otimes \mathbb{1}_2 + \vec{m} \cdot \vec{\sigma} \otimes \mathbb{1}_2 + \mathbb{1}_2 \otimes \vec{n} \cdot \vec{\sigma} + \sum_{i,j=1}^3 t_{ij} (\sigma_i \otimes \sigma_j)] \quad (1.12)$$

where,  $\mathbb{1}_2$  is  $2 \times 2$  identity matrix,  $\vec{\sigma} = (\sigma_1, \sigma_2, \sigma_3) = (\sigma_x, \sigma_y, \sigma_z)$  is Pauli spin vector, the real 3-vectors corresponding to first and second subsystems *i.e.*  $\vec{m} \in \mathbb{R}^3$  and  $\vec{n} \in \mathbb{R}^3$  satisfy  $|\vec{m}| \leq 1$  and  $|\vec{n}| \leq 1$  respectively. The real elements  $t_{ij} = \text{Tr}[\rho_{AB}(\sigma_i \otimes \sigma_j)]$  form a  $3 \times 3$  correlation matrix  $T := \{t_{ij}\}_{i,j}$ . The subsystems of  $\rho_{AB} \in \mathbb{C}^2 \otimes \mathbb{C}^2$  can be obtained by an operator map called partial trace *i.e.*  $\mathfrak{T}(\mathcal{H}_A \otimes \mathcal{H}_B) \mapsto \{\mathfrak{T}(\mathcal{H}_A), \mathfrak{T}(\mathcal{H}_B)\}$  where  $\mathfrak{T}$  is a branch space of trace-class operators on the Hilbert space. Partial trace with respect to second and first subsystem give the density operators of first and second subsystems respectively as given by,  $\rho_A = \text{Tr}_B[\rho_{AB}]$  and  $\rho_B = \text{Tr}_A[\rho_{AB}]$ .

There may be many different quantum correlations present in composite systems with the simplest version of interpretation in  $\mathbb{C}^2 \otimes \mathbb{C}^2$ . The most important of these correlations is quantum entanglement.

## 1.2 Entanglement

A composite system described by a joint state may not always be written as the product of individual subsystems. These states are known as entangled states. In reality, an individual subsystem is expected to remain in a particular state which can be known through a measurement. But Einstein, Podolsky and Rosen in a seminal paper in 1935 [EPR35] showed that, though a system can not simultaneously remain in an eigenstate of two incompatible observables predicted by QM, still measurements reveal the occurrence of it with certainty for an individual subsystem after measuring the other subsystem. It is a paradox that, if entanglement exists, then the description of QM is not complete and there must be an underlying theory that gives correct experimental predictions. Even Schrödinger [Sch35] agreed with Einstein's criticism of entanglement as *spooky action at a distance*.

The joint state of a composite system  $\rho_{AB}$  is called entangled if it can not have the following decomposition w.r.t. individual subsystems,

$$\rho_{AB} = \sum_{\lambda} p(\lambda) \rho_A^{\lambda} \otimes \rho_B^{\lambda} \quad (1.13)$$

where,  $\sum_{\lambda} p(\lambda) = 1$ .  $\rho_A^{\lambda}$  and  $\rho_B^{\lambda}$  correspond to subsystems  $A$  and  $B$  respectively.

Entanglement is solely the property of a state. However, it can be revealed through local measurements on both sides. Suppose that, an observable  $\mathcal{A}$  is measured on the subsystem labeled by  $A$  and it results an outcome  $a$ . Similarly, the measurement of an observable  $\mathcal{B}$  on the subsystem labeled by  $B$  yields an outcome  $b$ . Then the non-existence of the following joint probability distribution implies that the state is entangled.

$$p(a, b | \mathcal{A}_x, \mathcal{B}_y) = \sum_{\lambda} p(\lambda) p_Q(a | \mathcal{A}_x, \rho_A^\lambda) p_Q(b | \mathcal{B}_y, \rho_B^\lambda) \quad (1.14)$$

The subscript  $Q$  stands for 'Quantum' as the description of both the subsystems are considered to be quantum. Hence the probabilities for each subsystem from Born's rule can be obtained as,  $p_Q(a | \mathcal{A}_x, \rho_A^\lambda) = \text{Tr}[\Pi_{\mathcal{A}_x}^a \rho_A^\lambda]$  and  $p_Q(b | \mathcal{B}_y, \rho_B^\lambda) = \text{Tr}[\Pi_{\mathcal{B}_y}^b \rho_B^\lambda]$ , where  $\{\Pi_{\mathcal{A}_x}^a, \Pi_{\mathcal{B}_y}^b\}$  are the corresponding projectors for subsystems  $A$  and  $B$  respectively. A state which is not entangled is called as a separable state.

### 1.2.1 Bipartite entanglement measures

A resource is a property of a composite system that enables one to perform certain tasks which can not be done without it. Quantum entanglement [HHHH09] is a resource for tasks like teleportation [BBC<sup>+</sup>93], super dense coding [BW92] etc. The resource present in a shared state can be quantified either in terms of the degree of success for such a task or in terms of the cost of preparing maximum resource out of it. A resource theory essentially depends on the description of free states and free operations. Free states are the states which do not have the resource and free operations are the operations by which the generation of resource is not possible from free states. The set of all separable states form the free states in the resource theory of entanglement while the set of Local Operation and Classical Communication (LOCC) [CLM<sup>+</sup>14] in both ways between the two subsystems are the set of free operations in this case. LOCC can be recognized as a Completely Positive Trace Preserving (CPTP) map to transform the density matrices in the space of linear trace class operators. The definition of the CPTP map is discussed later.

Suppose for a joint state  $\rho_{AB}$ ,  $\mathcal{E}(\rho_{AB})$  is a good entanglement measure according to the

resource theory [BDSW96, VPRK97], then it satisfies the following properties:

- **Faithfulness.** If and only if  $\rho_{AB}$  is a separable state, then  $\mathcal{E}(\rho_{AB}) = 0$ .
- **Monotonicity.** Suppose that,  $\Xi(\rho_{AB})$  implies an operation of LOCC on the state  $\rho_{AB}$ , then entanglement is non-increasing under LOCC, *i.e.*  $\mathcal{E}(\Xi(\rho_{AB})) \leq \mathcal{E}(\rho_{AB})$ .
- **Convexity.** For a given decomposition of  $\rho_{AB} = \sum_i \mathcal{P}_i \rho_{AB}^i$ , entanglement is not increasing *i.e.*  $\mathcal{E}(\rho_{AB}) \leq \sum_i \mathcal{P}_i \mathcal{E}(\rho_{AB}^i)$ .

Most of the bipartite entanglement monotones are convex, *e.g.* entanglement of formation, negativity etc. Some important quantifiers of bipartite entanglement are given below.

### 1.2.1.1 Distance based measure

It is calculated by minimizing the distance of an entangled state from the set of separable states, *i.e.*

$$\mathcal{E}_D(\rho_{AB}) = \inf_{\sigma_{AB} \in \text{SEP}} \mathcal{D}(\rho_{AB}, \sigma_{AB}) \quad (1.15)$$

Trace norm or relative entropy may be considered as the distance metric. Relative entropy of entanglement shows merits in quantum computation and in information-theoretic arguments [Ved02] and can be expressed as,

$$\mathcal{E}_{RE}(\rho_{AB}) = \inf_{\sigma_{AB} \in \text{SEP}} \text{Tr} \rho_{AB} (\log_2 \rho_{AB} - \log_2 \sigma_{AB}) \quad (1.16)$$

### 1.2.1.2 Entropy of entanglement

It is a measure for only pure entangled states [BDSW96]. If  $\rho_A$  and  $\rho_B$  are the reduced density matrices for subsystems  $A$  and  $B$  respectively coming from  $|\psi\rangle_{AB}$  as,  $\rho_{A(B)} = \text{Tr}_{A(B)}(|\psi\rangle_{AB}\langle\psi|)$ , then entropy of entanglement can be expressed as,

$$\mathcal{E}_E(|\psi\rangle_{AB}) = S(\rho_A) = S(\rho_B) \quad (1.17)$$

where,  $S(\rho_{A(B)})$  is Von Neumann entropy for subsystem  $A(B)$ .

### 1.2.1.3 Entanglement of formation

Suppose a mixed entangled state  $\rho_{AB}$  can be formed as  $\rho_{AB} = \sum_i p_i |\psi^i\rangle_{AB} \langle \psi^i|$  from all possible pure state ensembles  $\{p_i, |\psi^i\rangle_{AB}\}$ . Then the least amount of entanglement that can be prepared from the given ensembles is called as the entanglement of formation [BDSW96].

$$\mathcal{E}_F(\rho_{AB}) = \min_{\text{decompositions}} \sum_i p_i \mathcal{E}_E(|\psi^i\rangle_{AB}) \quad (1.18)$$

In fact, the entanglement of formation in asymptomatic limit merges with another measure, named as entanglement cost under the method of regularization [HHT01].

### 1.2.1.4 Concurrence

Wootters constructed a matrix  $\mathcal{C}(\rho_{AB}) = \sqrt{\sqrt{\rho_{AB}} (\sigma_y \otimes \sigma_y) \rho_{AB}^* (\sigma_y \otimes \sigma_y) \sqrt{\rho_{AB}}}$ , which is called as concurrence matrix [HW97, Woo98] where  $\rho_{AB}^*$  is the complex conjugate of  $\rho_{AB}$ . If its eigenvalues  $\{\Upsilon_i\}_{i=1}^4$  are arranged in decreasing order, then the measure of concurrence can be defined as given below,

$$\mathcal{E}_C(\rho_{AB}) = \max\{0, \Upsilon_1 - \Upsilon_2 - \Upsilon_3 - \Upsilon_4\} \quad (1.19)$$

Entanglement of formation and concurrence are directly related as,

$$\mathcal{E}_F(\rho_{AB}) = H\left(\frac{1 + \sqrt{1 - \mathcal{E}_C^2(\rho_{AB})}}{2}\right) \quad (1.20)$$

where,  $H(\alpha) = -\alpha \log_2(\alpha) - (1 - \alpha) \log_2(1 - \alpha)$ .

### 1.2.1.5 Negativity

The measure of negativity for  $\rho_{AB}$  is given by,

$$\mathcal{E}_N(\rho_{AB}) = \frac{\|\rho_{AB}^{T_B}\|_1 - 1}{2} \quad (1.21)$$

where, the trace norm of a matrix  $M$  is  $\|M\|_1 = \text{Tr}[\sqrt{M^\dagger M}]$  and  $\rho_{AB}^{T_B}$  is the partial transposition of the density matrix  $\rho_{AB}$  w.r.t. subsystem  $B$ . The definition of negativity does not change if the partial transposition w.r.t. subsystem  $A$  is considered. Now the effect of partial transposition of a matrix  $X$  is denoted by the displacement of the matrix elements in the following way,  $\{X_{ij,kl}\}^{T_B} = \{X_{il,kj}\} \forall i, j, k, l$ . Let us consider that,  $\rho_{AB}^{T_B}$  has at least one negative eigenvalue  $e$ , then  $\mathcal{E}_N(\rho_{AB}) = |e|$ . Otherwise  $\mathcal{E}_N(\rho_{AB}) = 0$ . This comes from the PPT (Positive Partial Transpose) criterion or Peres-Horodecki criterion of separability [Per96, HHH96], which is a necessary condition of any bipartite state, in general. But it is both the necessary and sufficient condition of separability for only the qubit-qubit and qubit-qutrit systems. According to this criterion, the partial transposition of a bipartite separable state necessarily has all positive eigenvalues, or it is a PPT state. Whereas an entangled state is a NPT (Negative Partial Transpose) state iff it comes from  $2 \otimes 2$  or  $2 \otimes 3$  dimensional Hilbert space. A PPT state may be entangled in higher dimensional Hilbert space which is called as bound entangled state. We restrict our analysis in the domain of  $2 \otimes 2$  dim Hilbert space in this thesis.

There are other quantifiers, *e.g.* distillable entanglement [BDSW96], robustness of entanglement [VT99] etc. The measures are not practically useful tools for the detection of entanglement.

## 1.2.2 Applications of entanglement

Entanglement between quantum systems acts as a resource for multiple information-theoretic tasks which are otherwise impossible with classical systems. Using entanglement, one can teleport an unknown qubit to remote places [BBC<sup>+</sup>93], send 2-cbit (classical bit) information by super dense coding [BW92], generate secret key protected from eavesdropping [BB84, Eke91] etc. Other applications of entanglement include the distinguishability of states via LOCC [TDL01, GKR<sup>+</sup>01], the conversion of information into thermodynamic work [OHHH02] etc. Cryptographic advantages can also be seen in multipartite entanglement scenario [HBcvB99, idZZHW98].

### 1.2.2.1 Quantum teleportation

Quantum teleportation is a task of sending an unknown qubit instantly at a remote location by using entanglement. Let us consider that, Alice is the sender and Bob is the receiver and the qubit is unknown to both of them. The task of teleportation [BBC<sup>+</sup>93] is different from the cloning of an unknown qubit as prohibited by quantum theory [Die82, WZ82] because during teleportation the information about the unknown qubit is completely destroyed at the sender's end when it is prepared at the receiver's end. Suppose that, an unknown pure qubit  $|p\rangle_{A'} = a|0\rangle_{A'} + b|1\rangle_{A'}$  has to be teleported from Alice to Bob using the entanglement between them. The entangled state shared between Alice and Bob is given by,  $|\Phi^+\rangle_{AB} = \frac{1}{\sqrt{2}}(|00\rangle_{AB} + |11\rangle_{AB})$ . Then the three-particle state between Alice and Bob has the following form:

$$\begin{aligned}
|\Psi\rangle_{A'AB} &= |p\rangle_{A'} \otimes |\Phi^+\rangle_{AB} \\
&= \frac{1}{2} [ |\Phi^+\rangle_{AA'} \otimes (a|0\rangle_B + b|1\rangle_B) + |\Phi^-\rangle_{AA'} \otimes (a|0\rangle_B - b|1\rangle_B) \\
&\quad + |\Psi^+\rangle_{AA'} \otimes (a|1\rangle_B + b|0\rangle_B) + |\Psi^-\rangle_{AA'} \otimes (a|1\rangle_B - b|0\rangle_B) ] \\
&= \frac{1}{2} [ |\Phi^+\rangle_{AA'} \otimes |p\rangle_B + |\Phi^-\rangle_{AA'} \otimes (\sigma_z |p\rangle_B) \\
&\quad + |\Psi^+\rangle_{AA'} \otimes (\sigma_x |p\rangle_B) + |\Psi^-\rangle_{AA'} \otimes (\sigma_y |p\rangle_B) ] \tag{1.22}
\end{aligned}$$

where the four Bell states or the maximally entangled pure bipartite qubit states are given by,  $|\Phi^\pm\rangle_{AA'} = \frac{1}{\sqrt{2}}(|00\rangle \pm |11\rangle)$  and  $|\Psi^\pm\rangle_{AA'} = \frac{1}{\sqrt{2}}(|01\rangle \pm |10\rangle)$ . If Alice measures her particles in the Bell basis  $\{|\Phi^\pm\rangle, |\Psi^\pm\rangle\}$ , then the four outcomes can be encoded in 2-cbits (*i.e.*  $\{00, 01, 10, 11\}$  respectively) which Alice can send to Bob through some classical channel. Then Bob applies local unitary transformations *i.e.*  $\{\mathbb{1}_2, \sigma_z, \sigma_x, \sigma_y\}$  respectively depending on the measurement outcomes shared by Alice. In this way, Bob can obtain the unknown qubit  $|p\rangle_B$  in his side without the physical transfer of the particle. The protocol of quantum teleportation involves 2-cbit of classical information, 1-ebit (entangled bit) of quantum information, which is impossible classically. After the protocol, the entanglement between Alice and Bob breaks down completely. Many real experiments are performed to verify quantum teleportation in distant locations [BBDM<sup>+</sup>98, MHS<sup>+</sup>12].

Let us suppose that, Alice wants to prepare an unknown pure qubit state  $|\psi^d\rangle = \cos(\frac{\theta^d}{2})|0\rangle + e^{i\phi^d} \sin(\frac{\theta^d}{2})|1\rangle$  in Bob's lab without transferring the particle physically. It is the most general representation of a pure qubit from the surface of the Bloch sphere in Hilbert space  $\mathbb{C}^2$ . Here Alice is not allowed to exploit any quantum resource that can be initially shared between Alice and Bob. Alice is only allowed to make use of the classical channel by which he can send 1 cbit of information to Bob and Bob is free to prepare a qubit upto local operations. If the prepared state in Bob's lab is  $\rho^p$ , then the closeness of the desired state and the prepared state is  $\langle\psi^d|\rho^p|\psi^d\rangle$ , which is  $|\langle\psi^d|\psi^p\rangle|^2$  for pure state  $\rho^p = |\psi^p\rangle\langle\psi^p|$ . The classical fidelity can be calculated by averaging the closeness over infinitely many runs where in each run Alice is given different  $|\psi^d\rangle$ . If the classical communication (CC) is not allowed from Alice to Bob, then Bob has to randomly guess the desired state which will either match or does not match with the desired state. Hence the fidelity becomes  $\frac{1}{2}$  which is the lower bound of classical fidelity in any circumstances. If CC is allowed from Alice to Bob, then Alice measures a dichotomic observable  $\vec{n}_A \cdot \vec{\sigma}$  where  $\vec{n}_A = (\sin \theta_A \cos \phi_A, \sin \theta_A \sin \phi_A, \cos \theta_A)$  with  $0 \leq \theta_A \leq \pi, 0 \leq \phi_A \leq 2\pi$  and sends the outcome (either up or down) to Bob by a classical channel. The probability of getting up(down) outcome is given by  $\langle\psi^d|\frac{\mathbb{1}_2 \pm \vec{n}_A \cdot \vec{\sigma}}{2}|\psi^d\rangle = \text{Tr}[(\frac{\mathbb{1}_2 \pm \vec{n}_A \cdot \vec{\sigma}}{2}) \cdot |\psi^d\rangle\langle\psi^d|]$ . Now Bob can prepare either  $|\psi_1^p\rangle$  or  $|\psi_2^p\rangle$  depending upon the outcomes either up or down.

Now according to Massar-Popescu model [MP95, BG13], the input states  $|\psi^d\rangle$  can be chosen uniformly from the surface of the Bloch sphere ( $0 \leq \theta^d \leq \pi, 0 \leq \phi^d \leq 2\pi$ ) which is consistent with the standard scheme of teleportation. Let us suppose that,  $|\psi_i^p\rangle = \cos(\frac{\theta_i^p}{2})|0\rangle + e^{i\phi_i^p} \sin(\frac{\theta_i^p}{2})|1\rangle$  ( $0 \leq \theta_i^p \leq \pi, 0 \leq \phi_i^p \leq 2\pi$ )  $\forall i \in \{1, 2\}$ . Now by taking average over all input states  $|\psi^d\rangle$  from the surface of the Bloch sphere, the fidelity expression for a

classical strategy becomes

$$\begin{aligned}
f_{cl} &= \frac{1}{4\pi} \int_0^{2\pi} \int_0^\pi \left( \langle \psi^d | \frac{\mathbb{1}_2 + \vec{n}_A \cdot \vec{\sigma}}{2} | \psi^d \rangle \langle \psi^d | \psi_1^p \rangle \langle \psi_1^p | \psi^d \rangle \right. \\
&\quad \left. + \langle \psi^d | \frac{\mathbb{1}_2 - \vec{n}_A \cdot \vec{\sigma}}{2} | \psi^d \rangle \langle \psi^d | \psi_2^p \rangle \langle \psi_2^p | \psi^d \rangle \right) \sin \theta^d d\theta^d d\phi^d \\
&= \frac{1}{2} + \frac{1}{12} [\cos \theta_A \cos \theta_1^p - \cos \theta_A \cos \theta_2^p \\
&\quad + \cos(\phi_A - \phi_1^p) \sin \theta_A \sin \theta_1^p - \cos(\phi_A - \phi_2^p) \sin \theta_A \sin \theta_2^p] \\
&\leq \frac{2}{3}
\end{aligned} \tag{1.23}$$

The classical fidelity is optimized with respect to the measurement direction chosen by Alice and the parameters of the states prepared by Bob. The equality holds for  $\theta_A = 0, \theta_1^p = 0, \theta_2^p = \pi$ , *i.e.* when Alice measures  $\sigma_z$  and Bob prepares either  $|0\rangle$  or  $|1\rangle$  (*i.e.* one of the eigenstates of  $\sigma_z$ ) accordingly. Hence without using a quantum resource between the sender and the receiver, the fidelity of preparing an unknown state, by choosing uniformly from the surface of the Bloch sphere, can attain the optimal value of  $\frac{2}{3}$  classically. But when the sender and the receiver share an entangled state between them, then the fidelity of preparing an unknown state under the standard protocol of quantum teleportation, can achieve the value greater than  $\frac{2}{3}$  and may reach up to a faithful limit of 1.

### 1.2.2.2 Quantum dense coding

According to the Holevo bound [Hol73], a qubit can utmost carry 1-cbit of information. It means that 2 messages can be sent by using a qubit. However, if entanglement is shared apriori between the sender, Alice and the receiver, Bob, then by sending just a qubit, Alice can convey 4 messages to Bob. So the theme of dense coding by virtue of entanglement is that 2-cbits of information can be carried by sending a qubit [BW92].

Let us consider that, Alice and Bob share a Bell state  $|\Phi^+\rangle_{AB}$  where the qubit A is possessed by Alice and the qubit B is possessed by Bob. Now Alice wants to send one of the four messages to Bob. For this, Alice applies one of the four unitary operations  $\{\mathbb{1}_2, \sigma_z, \sigma_x, -i\sigma_y\}$  ( $i = \sqrt{-1}$ ) on her qubit and sends her qubit to Bob. As Bell states are invariant under local unitary transformations, *i.e.*  $(\mathbb{1}_2 \otimes \mathbb{1}_2)|\Phi^+\rangle_{AB} = |\Phi^+\rangle_{AB}$ ,

$(\sigma_z \otimes \mathbb{1}_2)|\Phi^+\rangle_{AB} = |\Phi^-\rangle_{AB}$ ,  $(\sigma_x \otimes \mathbb{1}_2)|\Phi^+\rangle_{AB} = |\Psi^+\rangle_{AB}$  and  $(-i\sigma_y \otimes \mathbb{1}_2)|\Phi^+\rangle_{AB} = |\Psi^-\rangle_{AB}$  respectively where,  $\{\sigma_x, \sigma_y, \sigma_z\}$  are Pauli spinors along  $x$ -,  $y$ -,  $z$ - directions respectively, hence Bob possesses one of the four orthogonal Bell states which are distinguishable by Bell basis measurements at Bob's side. Thus by sending 1 qubit, Alice sends 2-cbit of information to Bob. Here entanglement apriori acts as a memory of the information which was not considered by Holevo. Experiments are also performed to verify quantum dense coding by using polarized photons [MWKZ96], nuclear magnetic resonance(NMR) [FZF<sup>+</sup>00] etc.

### 1.2.2.3 Quantum cryptography

To send a secret message from Alice to Bob, Alice has to encrypt the message with the help of a key which is known by Bob beforehand. After getting the encrypted message, Bob can decrypt the original message with the help of that key. Either Alice and Bob privately meet to settle the key or they have to generate the key by sending a particle from Alice to Bob and by making a conversation through some public channel. There may be a possibility of eavesdropping if the key is not fully secure. The state of the particle can be easily determined by an eavesdropper as allowed by classical physics without disturbing it anyway. However, it is not qualified by quantum theory where a measurement disturbs the state of a quantum system by collapsing it to one of its eigenstates. The secure quantum key generation protocol was first proposed by Bennett and Brassard in 1984 which is famously known as BB84 protocol [BB84].

Suppose that, Alice sends particles to Bob which are the in eigenstates of spin observables  $\sigma_z$  or  $\sigma_x$  in 2-dim. After receiving each particle, Bob measures its spin either in  $z$ - or in  $x$ - direction. Bob publicly announces the choice of the basis of his measurement to Alice while keeping secret the outcomes. Alice compares the prepared basis of the states of the particles and the basis of measurement by Bob. When the two bases do not match, they discard it. Otherwise they obtain a string of matched basis for which they assign bit values as follows:  $\{|0_z\rangle, |0_x\rangle\} \mapsto 0$  and  $\{|1_z\rangle, |1_x\rangle\} \mapsto 1$  where ( $|0_z\rangle$  or  $|0\rangle$ ) and ( $|1_z\rangle$  or  $|1\rangle$ ) form the basis of  $\sigma_z$  (also called as computational basis) and  $|0_x\rangle$  and  $|1_x\rangle$  form the basis of  $\sigma_x$ .

In this way, the raw key can be generated. The concept of the above BB84 correlation can thus be represented by the joint probability distribution of having outcomes  $a$  and  $b$  from the measurements  $\mathcal{A}$  and  $\mathcal{B}$  done on the joint state of particles possessed by Alice and Bob respectively and it is given by  $p(a = b | \mathcal{A}, \mathcal{B}) = 1$  for  $\mathcal{A} = \mathcal{B}$  and  $p(a = b | \mathcal{A}, \mathcal{B}) = \frac{1}{2}$  for  $\mathcal{A} \neq \mathcal{B}$ . If an eavesdropper intervenes in the process by measuring the particles sent by Alice before reaching to Bob, then the state of the particles may not be the same after the intervention. When Bob obtains and measures the particle, it may not result into the same particle which Alice prepared and sent though the choice of basis remains the same for both. Therefore the error can be detected when Bob compares his measurement outcomes with Alice through some public channel. When the rate of error is high, then Alice and Bob agree to postpone the protocol. Thereby the secrecy of the protocol is assured. However, if the states of the particles are non-orthogonal, then the eavesdropper can not gain any information without disturbing the systems.

Apart from sending a particle physically, Alice and Bob can generate a secret key based on the entanglement shared between them initially. This was first proposed by Ekert in 1991 [Eke91]. The copies of the singlet state shared between Alice and Bob can be represented as,

$$|\Psi^-\rangle_{AB} = \frac{1}{\sqrt{2}}(|0_z 1_z\rangle - |1_z 0_z\rangle) = \frac{1}{\sqrt{2}}(|0_x 1_x\rangle - |1_x 0_x\rangle) \quad (1.24)$$

which can be simplified from Eq.(1.12) with  $|\vec{m}| = |\vec{n}| = \{t_{ij} | i \neq j\} = 0$  and  $\{t_{ii}\} = -1$ . Now Alice and Bob measure their particles randomly in the eigenbasis of  $\sigma_z$  or  $\sigma_x$ . Then they share their chosen basis publicly and discard the cases where their chosen basis are not the same. As the outcomes of Alice and Bob are anti-correlated according to Eq.(1.24), hence they assign the bit values of their respective outcomes as  $\{|0_z\rangle, |0_x\rangle\} \mapsto 0$  and  $\{|1_z\rangle, |1_x\rangle\} \mapsto 1$  for Alice and  $\{|1_z\rangle, |1_x\rangle\} \mapsto 0$  and  $\{|0_z\rangle, |0_x\rangle\} \mapsto 0$  for Bob. Under the attack of an eavesdropper, the entanglement between Alice and Bob breaks down and the anti-correlation statistics can never be reproduced by a pure product state. Hence when Alice and Bob compare some of their measurement outcomes publicly, they will come to know the presence of an eavesdropper. If the eavesdropper tries to gain information without disturbing the entangled state, then the state of the eavesdropper will remain com-

pletely uncorrelated due to the monogamy of entanglement [CKW00]. As Alice and Bob share the maximally entangled state, so that a third party can in no way be correlated with any of them. If Alice and Bob have entanglement but not the maximally entangled state, then the third party's interference can be caught from the Bell inequality violation [Bel64] provided the measurement outcomes of Alice and Bob are shared publicly. Therefore, an eavesdropper can not be able to gain information from the entanglement-based protocol.

## 1.3 Bell nonlocality

Einstein, Podolsky and Rosen (EPR) in 1935 [EPR35] questioned the completeness of quantum theory through the contradiction of quantum theory with locality and physical reality. Surprisingly the operationally viable measurement statistics on the entangled particles is not compatible with the assumption of local realism. This was proved by J. Bell in 1964 [Bel64] by the construction of a local realist model. This gives birth to a quantum mechanical correlation called Bell nonlocality [BCP<sup>+</sup>14b].

### 1.3.1 EPR theorem

Einstein, Podolsky and Rosen pointed out the incompatibility of quantum mechanics with the two assumptions of classical world-view [EPR35], which are provided below.

- **Locality.** The elements of reality revealed by the measurement on one system can not be affected by the choice of measurement on another system separated at a distance.
- **Reality.** If the value of a physical quantity can be predicted with certainty without disturbing the system, then there exists a physical reality for that physical quantity.

A theory is not complete without all the elements of physical reality in that theory.

The claim of EPR comes from the rotational invariance of the singlet state given by Eq.(1.24), where Bob's subsystem collapses to one of the eigenstates of either  $\sigma_z$  or  $\sigma_x$  spin observable if Alice chooses to measure either  $\sigma_z$  or  $\sigma_x$  on her subsystem kept at a distance from the Bob's subsystem. As Alice can not influence the physical reality of

Bob's subsystem, hence without measuring or disturbing Bob's subsystem anyway, the physical reality assigned to Bob's subsystem after Alice's measurement correspond to the spin along z-direction as well as the spin along x-direction. However, a system can not simultaneously remain in the eigenbasis of  $\sigma_z$  and  $\sigma_x$ . Through this contradiction, EPR claimed that, there is no element of physical reality in the theory of quantum mechanics. Therefore quantum theory is incomplete and there is a space left for the construction of an operationally sound underlying theory which also encompasses all the elements of physical reality.

### 1.3.2 Bell's theorem

J. Bell in 1964 introduced an operational level inequality by incorporating the assumptions of locality and reality [Bel64] which shows by its violation the strength of quantum correlation than that predicted by classical mechanics. Let us suppose that, Alice and Bob interact with each other or an external source prepares their joint state  $\mathcal{P}$  before they are separated spatially. Alice and Bob then measure the observables  $\mathcal{A}_x$  ( $x \in \{0, 1\}$ ) and  $\mathcal{B}_y$  ( $y \in \{0, 1\}$ ) on their subsystems to obtain the outcomes  $a$  ( $a \in \{-1, +1\}$ ) and  $b$  ( $b \in \{-1, +1\}$ ) respectively. This yields the expectation value  $\langle \mathcal{A}_x \mathcal{B}_y \rangle = \sum_{a,b=-1}^{+1} ab p(a,b|\mathcal{A}_x \mathcal{B}_y, \mathcal{P})$ , where  $p(a,b|\mathcal{A}_x \mathcal{B}_y, \mathcal{P})$  or simply  $p(a,b|\mathcal{A}_x, \mathcal{B}_y)$  is the joint probability of having outcomes  $a$  and  $b$  after measuring  $\mathcal{A}_x$  and  $\mathcal{B}_y$   $\forall a,b,x,y$  at Alice's and Bob's side respectively. If quantum theory is not complete and by imposing an ontic or underlying hidden variable  $\lambda$ , which satisfy the assumptions of local realism at the ontic level, may present a complete theory with the following reproducibility condition by averaging over the entire ontic space(OS) of variables.  $\lambda$  is often called as the value of shared randomness.

$$p(a,b|\mathcal{A}_x \mathcal{B}_y) = \sum_{\lambda \in OS} p(\lambda) p(a,b|\mathcal{A}_x, \mathcal{B}_y, \lambda) \quad (1.25)$$

where  $\sum_{\lambda \in OS} p(\lambda) = 1$ .

An ontological theory is

1. local iff  $p(a|\mathcal{A}_x, \mathcal{B}_y, \lambda) = p(a|\mathcal{A}_x, \lambda) \forall a,x,y$  and  $p(b|\mathcal{A}_x, \mathcal{B}_y, \lambda) = p(b|\mathcal{B}_y, \lambda) \forall b,x,y$ ,

2. deterministic iff  $p(a, b | \mathcal{A}_x, \mathcal{B}_y, \lambda) \in \{0, 1\}$  which implies  $p(a | \mathcal{A}_x, \mathcal{B}_y, b, \lambda) = p(a | \mathcal{A}_x, \mathcal{B}_y, \lambda)$   
and  $p(b | \mathcal{A}_x, \mathcal{B}_y, a, \lambda) = p(b | \mathcal{A}_x, \mathcal{B}_y, \lambda)$

Combining local determinism, the following factorizability condition follows,

$$p(a, b | \mathcal{A}_x, \mathcal{B}_y, \lambda) = p(a | \mathcal{A}_x, \lambda) p(b | \mathcal{B}_y, \lambda) \quad (1.26)$$

and hence from Eq.(1.25) we get

$$p(a, b | \mathcal{A}_x, \mathcal{B}_y) = \sum_{\lambda \in OS} p(\lambda) p(a | \mathcal{A}_x, \lambda) p(b | \mathcal{B}_y, \lambda) \quad (1.27)$$

Another assumption that is hidden in Eq.(1.25) is the assumption of *free will* or *measurement independence*, i.e.  $p(\lambda | \mathcal{A}_x, \mathcal{B}_y) = p(\lambda)$  which implies the independence of Alice and Bob to choose the measurements freely. Eq.(1.27) represents the Local Hidden Variable (LHV) model for a local-deterministic theory.

Now using Eq.(1.27), the expectation value of the joint measurement done on the preparation state  $\mathcal{P}$  becomes

$$\begin{aligned} \langle \mathcal{A}_x \mathcal{B}_y \rangle &= \sum_{\lambda} p(\lambda) \left( \sum_a a p(a | \mathcal{A}_x, \lambda) \right) \left( \sum_b b p(b | \mathcal{B}_y, \lambda) \right) \\ &= \sum_{\lambda} p(\lambda) \langle \mathcal{A}_x \rangle_{\lambda} \langle \mathcal{B}_y \rangle_{\lambda} \end{aligned} \quad (1.28)$$

where  $\langle \mathcal{A}_x \rangle_{\lambda} \in \{-1, +1\} \forall x$  and  $\langle \mathcal{B}_y \rangle_{\lambda} \in \{-1, +1\} \forall y$ .

Using Eq.(1.28) for different measurement correlations involving  $x, y \in \{0, 1\}$ , one can construct that,

$$\begin{aligned} B_{CHSH} &= |\langle \mathcal{A}_0 \mathcal{B}_0 \rangle + \langle \mathcal{A}_0 \mathcal{B}_1 \rangle + \langle \mathcal{A}_1 \mathcal{B}_0 \rangle - \langle \mathcal{A}_1 \mathcal{B}_1 \rangle| \\ &= \sum_{\lambda} p(\lambda) |\langle \mathcal{A}_0 \rangle_{\lambda} \langle \mathcal{B}_0 \rangle_{\lambda} + \langle \mathcal{A}_0 \rangle_{\lambda} \langle \mathcal{B}_1 \rangle_{\lambda} + \langle \mathcal{A}_1 \rangle_{\lambda} \langle \mathcal{B}_0 \rangle_{\lambda} - \langle \mathcal{A}_1 \rangle_{\lambda} \langle \mathcal{B}_1 \rangle_{\lambda}| \\ &\leq \sum_{\lambda} p(\lambda) (|\langle \mathcal{B}_0 \rangle_{\lambda} + \langle \mathcal{B}_1 \rangle_{\lambda}| + |\langle \mathcal{B}_0 \rangle_{\lambda} - \langle \mathcal{B}_1 \rangle_{\lambda}|) \\ &\leq 2 \sum_{\lambda} p(\lambda) = 2 \end{aligned} \quad (1.29)$$

where the first inequality in the right hand side of Eq.(1.29) comes from  $\langle \mathcal{A}_0 \rangle_\lambda, \langle \mathcal{A}_1 \rangle_\lambda \in \{-1, +1\}$  and the second inequality in the right hand side of Eq.(1.29) comes from  $\langle \mathcal{B}_0 \rangle_\lambda, \langle \mathcal{B}_1 \rangle_\lambda \in \{-1, +1\}$ . The inequality  $B_{CHSH} \leq 2$  is known as Bell's inequality or Bell-CHSH (Clauser, Horne, Shimony, Holt) inequality [Bel64, CHSH69] which is the necessary and sufficient condition for testing local realism in bipartite qubit states involving two dichotomic measurements per side (2-2-2 scenario). As in quantum theory, the entangled states violate this inequality, hence classical assumptions turn out to be incompatible with the observations of quantum mechanics. Bell's inequality for a generalised bipartite qubit state *i.e.* given by Eq.(1.12) can be reduced to a state based criterion derived by Horodecki *et al* [HHH95] which is given by  $\max B_{CHSH}(\rho_{AB}) = 2(\mu + \mu') \leq 2$  where,  $\mu$  and  $\mu'$  are the two largest eigenvalues of the matrix  $TT^t$ . Here  $T$  denotes the correlation matrix corresponding to Eq.(1.12) and  $T^t$  is the transpose of  $T$  and the maximization of the left hand side of Bell's inequality is taken over all possible measurement settings for both sides. Considering the maximally entangled singlet state given by Eq.(1.24) and the observables on both sides as  $\mathcal{A}_0 = \frac{\sigma_z + \sigma_x}{\sqrt{2}}, \mathcal{A}_1 = \frac{\sigma_z - \sigma_x}{\sqrt{2}}, \mathcal{B}_0 = \sigma_z, \mathcal{B}_1 = \sigma_x$ , we obtain

$$B_{CHSH}(|\Psi^-\rangle_{AB}) = 2\sqrt{2} > 2 \quad (1.30)$$

by using the condition  ${}_{AB}\langle \Psi^- | \vec{p}_x \cdot \vec{\sigma} \otimes \vec{q}_y \cdot \vec{\sigma} | \Psi^- \rangle_{AB} = -\vec{p}_x \cdot \vec{q}_y = -\cos \theta_{p_x, q_y}$  for the observables  $\mathcal{A}_x = \vec{p}_x \cdot \vec{\sigma}$  ( $x \in \{0, 1\}$ ) and  $\mathcal{B}_y = \vec{q}_y \cdot \vec{\sigma}$  ( $y \in \{0, 1\}$ ). Here the angle  $\theta_{p_x, q_y}$  denotes the angle between the directions  $p_x$  and  $q_y$  on the Bloch sphere. Though the algebraic maximum of Bell's inequality is 4, the maximum violation of it, that is allowed by quantum mechanics, is  $2\sqrt{2}$  as shown by Cirel'son [Cir80]. It is achieved by one of the maximally entangled bipartite pure qubit states including the singlet state, which are commonly known as *Bell states*. It is to note that, a correlation between two particles must satisfy non-signalling condition to make quantum mechanics consistent with the special theory of relativity. The non-signalling correlations satisfy  $\sum_b p(a, b | \mathcal{A}_x, \mathcal{B}_y) = \sum_b p(a, b | \mathcal{A}_x, \mathcal{B}_{y'}) = p(a | \mathcal{A}_x) \forall a, x, y, y'$  and  $\sum_a p(a, b | \mathcal{A}_x, \mathcal{B}_y) = \sum_a p(a, b | \mathcal{A}_{x'}, \mathcal{B}_y) = p(b | \mathcal{B}_y) \forall b, x, x', y$  where  $x \neq x' \in \{0, 1\}$  and  $y \neq y' \in \{0, 1\}$ . Though the value of Bell-CHSH expression given in Eq.(1.29) *i.e.*  $B_{CHSH} = 4$  is allowed by a non-signalling correlation shown by Popescu and

Rohrlich [PR94], still quantum mechanics does not allow the measurement statistics on any quantum state to produce its value greater than  $2\sqrt{2}$ . The quantum mechanical violation of Bell's inequality certifies the presence of a certain correlation named Bell nonlocality between the pair of entangled particles. Several experiments were carried out to verify the Bell nonlocal correlation [FC72, AGR82].

### 1.3.3 Bell nonlocality measure

The set of joint probabilities for two binary inputs and two binary outputs for Alice and Bob respectively defines a correlation or a box. It is characterised by  $P(a, b | \mathcal{A}_x, \mathcal{B}_y) := \{p(a, b | \mathcal{A}_x, \mathcal{B}_y)\}_{a, b, x, y}$  or simply  $P(a, b | x, y)$ . In general, a correlation for bipartite qubit systems forms a  $4 \times 4$  matrix in 2-2-2 scenario. The non-signalling correlation has subsets of local and nonlocal correlations. Both the set of local and non-signalling correlations form a convex polytope [BLM<sup>+</sup>05]. Whereas some of the nonlocal correlations, allowed by quantum mechanics, are convex but do not form a polytope due to the presence of infinite number of extremal points. The minimum nonlocality present in a non-signalling correlation or the minimum distance of a given non-signalling correlation from the set of local correlations can be quantified by a Bell nonlocality measure, named Nonlocal cost.

#### 1.3.3.1 Nonlocal cost

Let us consider that, the binary measurements for Alice and Bob are denoted by  $x \in \{0, 1\}$  and  $y \in \{0, 1\}$  respectively. The binary outcomes  $a$  and  $b$  corresponding to Alice and Bob respectively are relabelled as  $+1 \mapsto 0$  and  $-1 \mapsto 1$  for both of them. The non-signalling correlations form a 8 dimensional convex polytope with 24 extremal points [BLM<sup>+</sup>05], out of which, 8 Popescu-Rohrlich(PR) correlations are expressed as,  $P(a, b | x, y) = \frac{1}{2} \delta_{a \oplus b, x \oplus \alpha x \oplus \beta y \oplus \gamma}$  where  $\alpha, \beta, \gamma \in \{0, 1\}$  and 16 local deterministic correlations are expressed as,  $P(a, b | x, y) = P(a | x) P(b | y) = \delta_{a, \alpha x \oplus \beta} \delta_{b, \gamma \oplus \epsilon}$  where  $\alpha, \beta, \gamma, \epsilon \in \{0, 1\}$  and  $\oplus$  implies the addition modulo 2. In binary input-output scenario, the 4 local deterministic (or certain) correlations for Alice correspond to  $\{p(a = 0 | x = 0) = 1, p(a = 1 | x = 0) = 0, p(a = 0 | x = 1) = 1, p(a = 1 | x = 1) = 0\}$ ,  $\{p(a = 0 | x = 0) = 1, p(a = 1 | x = 0) = 0, p(a = 0 | x = 1) = 0, p(a =$

$1|x=1)=1\}$ ,  $\{p(a=0|x=0)=0, p(a=1|x=0)=1, p(a=0|x=1)=1, p(a=1|x=1)=0\}$  and  $\{p(a=0|x=0)=0, p(a=1|x=0)=1, p(a=0|x=1)=0, p(a=1|x=1)=1\}$ . Similarly, the 4 local deterministic (or certain) correlations for Bob correspond to  $\{p(b=0|y=0)=1, p(b=1|y=0)=0, p(b=0|y=1)=1, p(b=1|y=1)=0\}$ ,  $\{p(b=0|y=0)=1, p(b=1|y=0)=0, p(b=0|y=1)=0, p(b=1|y=1)=1\}$ ,  $\{p(b=0|y=0)=0, p(b=1|y=0)=1, p(b=0|y=1)=1, p(b=1|y=1)=0\}$  and  $\{p(b=0|y=0)=0, p(b=1|y=0)=1, p(b=0|y=1)=0, p(b=1|y=1)=1\}$ . All the above correlations are invariant under Local Reversible Operations (LRO) defined by  $a \rightarrow a \oplus \alpha x \oplus \beta, b \rightarrow b \oplus \gamma y \oplus \varepsilon, x \rightarrow x \oplus 1, y \rightarrow y \oplus 1$  individually for Alice and Bob. But global operations may convert local correlation into a nonlocal one or vice-versa. The Bell-CHSH expression for local deterministic correlations has 8 different forms [Fin82], *i.e.*  $B_{\alpha\beta\gamma} = |(-1)^\gamma \langle \mathcal{A}_0 \mathcal{B}_0 \rangle + (-1)^{\beta \oplus \gamma} \langle \mathcal{A}_0 \mathcal{B}_1 \rangle + (-1)^{\alpha \oplus \gamma} \langle \mathcal{A}_1 \mathcal{B}_0 \rangle + (-1)^{\alpha \oplus \beta \oplus \gamma \oplus 1} \langle \mathcal{A}_1 \mathcal{B}_1 \rangle|$  (with  $\alpha, \beta, \gamma \in \{0, 1\}$ ) where  $B_{CHSH} = B_{000}$ .

According to Elitzur, Popescu and Rohrlich (EPR2) [EPR92], a correlation can be decomposed in terms of the local and the nonlocal part as

$$P(a, b|x, y) = p_{NL} P_{NL}(a, b|x, y) + (1 - p_{NL}) P_L(a, b|x, y) \quad (1.31)$$

where  $P_L(a, b|x, y)$  or  $P_L$  is a local correlation which is a single or convex sum of local-deterministic correlations and  $P_{NL}(a, b|x, y)$  or  $P_{NL}$  is a non-signalling correlation in general. Nonlocal cost [BCSS11] is defined by minimizing the weight of nonlocal part  $p_{NL}$  ( $0 \leq p_{NL} \leq 1$ ) considering all possible decompositions as given by Eq.(1.31), *i.e.*

$$C_{NL}(P) := \min_{\text{decompositions}} p_{NL} \in [0, 1] \quad (1.32)$$

The maximum value of the Bell-CHSH expression *i.e.* 4 is achieved by using one of the PR correlations for which  $C_{NL}(P_{NL}) = 1$  and the maximum quantum mechanical value of Bell-CHSH expression *i.e.*  $2\sqrt{2}$  is achieved when  $C_{NL}(P) = \sqrt{2} - 1$ . Nonlocal cost is a bonafide measure of nonlocality as it does not increase on average under local operations without communication between Alice and Bob.

### 1.3.4 Applications of Bell nonlocality

Bell nonlocality shows a way of instantaneous information transfer between spatially separated observers. But it is not a proxy for direct communication because of the restriction imposed by non-signalling theorem. Suppose that, Alice has a bit string  $\vec{x} = (x_1, x_2, \dots)$  and Bob has another bit string  $\vec{y} = (y_1, y_2, \dots)$  and they have no connection between them. Now Bob has to guess a function  $g(x, y)$  by using the information about the bit strings. For this, Alice can help Bob by making a number of bits of communication with Bob. The minimum number of bits required in this process is called the communication complexity. Cleve *et al* showed that [CB97], communication complexity can be reduced by using the presence of Bell nonlocal correlation between Alice and Bob. On the other hand, the task of genuine randomness generation can be executed by using Bell nonlocality [PAM<sup>+</sup>10]. The idea of local realism is based on the black box measurements on both the particles, where no restrictions are imposed on the measurement devices. Acín *et al* showed that [AGM06, ABG<sup>+</sup>07] the violation of Bell's inequality provides the secrecy for Quantum Key Distribution (QKD) protocol by certifying entanglement in a Device Independent (DI) scenario. The self-testing of the singlet state can be implied by the maximum quantum mechanical violation of Bell's inequality by using the method given by Mayers and Yao [MY04].

## 1.4 Quantum steering

The coinage of the term "steering" was initiated by Schrödinger [Sch35] in the context of EPR paradox in 1935 [EPR35] where he mentioned the possibility of steering Bob's system by Alice without having access to it. Quantum steering in the theory of quantum correlation suggests a task to be performed by Alice in order to convince Bob that they genuinely share an entangled state. It is based on an asymmetric scenario that Alice can measure only black box measurements whereas Bob has access to quantum measurements to be done on her quantum system resulting outcomes according to Born's rule. That is why from experimental perspective, quantum steering as a quantum correlation lies in-between

entanglement and Bell nonlocality [[WJD07](#), [JWD07](#)].

Let us consider that, Alice and Bob share a joint state  $\rho_{AB}$  where the particle  $A$  is possessed by Alice and the particle  $B$  is possessed by Bob. Now Bob asks Alice to steer his state in one of the preferred ensembles  $\{\mathcal{E}^{\mathcal{A}}\}$  by doing a measurement  $\mathcal{A}_x$  which yields outcome  $a$  governed by measurement operators  $M_{a|x} \in M_{\mathcal{A}}$ . After the announcement of Alice about her measurement, Bob will perform a quantum measurement  $\mathcal{B}_y$  on her subsystem to verify steerability through state tomography. Now depending on Alice's measurement, an unnormalized conditional state  $\sigma_{a|x} \in \boldsymbol{\sigma} := \{\sigma_{a|x}\}_{a,x}$  will be prepared at Bob's side, where  $\boldsymbol{\sigma}$  is called the assemblage. According to quantum mechanics

$$\sigma_{a|x} = p(a|A)\rho_{a|x} = \text{Tr}[(M_{a|x} \otimes \mathbb{1}_2) \rho_{AB}] \rho_{a|x} = \text{Tr}_A[(M_{a|x} \otimes \mathbb{1}_2) \rho_{AB}] \quad \forall a,x \quad (1.33)$$

where, the probability of getting normalised conditional state  $\rho_{a|x}$  at Bob's side after getting outcome  $a$  from Alice's measurement  $\mathcal{A}_x$  is given by  $p(a|A) = \text{Tr}[(M_{a|x} \otimes \mathbb{1}_2) \rho_{AB}]$ . However, Alice can cheat Bob by her knowledge about Bob's Local Hidden State(LHS) *i.e.*  $\rho_B^\lambda$  ( $\rho_B^\lambda \geq 0, \text{Tr}[\rho_B^\lambda] = 1$ ) at ontic space of  $\lambda$ . This strategy, being a probabilistic mapping between  $\lambda$  and  $a$ , may have the form [[WJD07](#), [JWD07](#)],

$$\sigma_{a|x} = \sum_{\lambda \in OS} p(\lambda) p(a|\mathcal{A}_x, \lambda) \rho_B^\lambda \quad (1.34)$$

The distribution of  $p(\lambda)$  in  $\lambda$ -space satisfies  $\sum_{\lambda \in OS} p(\lambda) = 1$  and  $p(a|\mathcal{A}_x, \lambda)$  is the probability of getting outcome  $a$  from the measurement  $\mathcal{A}_x$  depending on the hidden variable  $\lambda$ .

The alternative form of Eq.(1.34) is

$$p(a,b|\mathcal{A}_x, \mathcal{B}_y) = \sum_{\lambda \in OS} p(\lambda) p(a|\mathcal{A}_x, \lambda) p_Q(b|\mathcal{B}_y, \rho_B^\lambda) \quad (1.35)$$

where  $\sum_{\lambda \in OS} p(\lambda) = 1$ ,  $p_Q(b|\mathcal{B}_y, \rho_B^\lambda) = \text{Tr}[\Pi_{\mathcal{B}_y}^b \rho_B^\lambda]$ ,  $p(a,b|\mathcal{A}_x, \mathcal{B}_y) = \text{Tr}[\Pi_{\mathcal{B}_y}^b \sigma_{a|x}]$  and the subscript 'Q' stands for Bob's quantum system. The projector  $\Pi_{\mathcal{B}_y}^b$  corresponds to subsystem  $B$  only. By decomposing  $p(a|\mathcal{A}_x, \lambda)$  in terms of deterministic probability distributions at ontic level [[CS16](#)] and by decomposing a density matrix in terms of pure states,

one can represent Eq.(1.35) as [CFFW15],

$$p(a, b | \mathcal{A}_x, \mathcal{B}_y) = \sum_{\chi, \zeta} p(\chi, \zeta) \delta_{a, f(\mathcal{A}_x, \chi)} \langle \psi_\zeta | \Pi_{\mathcal{B}_y}^b | \psi_\zeta \rangle \quad (1.36)$$

where Alice obtains outcome  $a$  deterministically from the measurement  $\mathcal{A}_x$  by using a function  $f(\mathcal{A}_x, \chi)$  which depends on another ontic variable  $\chi$  for Alice and ontic variable  $\zeta$  determines the pure states  $|\psi_\zeta\rangle$  for Bob. The Eq.(1.35) or Eq.(1.36) is often termed as a hybrid LHV-LHS model or simply LHS model. The existence of Eq.(1.35) implies that, Alice can cheat Bob and from the comparison of the prepared assemblage with that of  $\mathcal{E}^{\mathcal{A}}$  Bob must know that, Alice can not actually steer Bob. Hence the set of correlations of the form  $P(a, b | \mathcal{A}_x, \mathcal{B}_y)$  or  $P(a, b | x, y) := \{p(a, b | \mathcal{A}_x, \mathcal{B}_y)\}_{a, b, x, y}$  obtained from Eq.(1.35) is convex and can be called as unsteerable correlations [CJWR09, CFFW15]. Whereas the non-existence of Eq.(1.35) gives rise to a correlation named quantum steering, which is, by definition, intermediate between entanglement and Bell nonlocality. Steerability is a performance-oriented correlation from untrusted to trusted party where Alice and Bob play the roles of untrusted and trusted party respectively. There exists no counterpart of it in classical physics [UCNG20].

## 1.4.1 Steering inequalities

The model of LHV-LHS at Bob's side can be constructed either from an uncertainty relation applicable for Bob's quantum system or from the convex set formulation of LHV-LHS correlations where mutually orthogonal measurements are performed at Bob's side. A steering inequality at the operational level can be constructed to capture a specific model and its violation implies the presence of quantum steerable correlations between the observers.

### 1.4.1.1 Utility of uncertainty relations

Uncertainty relations play a significant role in quantum mechanics. Through a mathematical inequality, it explains that, two non-commuting observables can not be measured

simultaneously with arbitrary precision. Uncertainty relations have a potential field of applications in the theory of quantum correlations. The existence of LHS for an observer say Bob can be expressed by the presence of an uncertainty principle corresponding to the LHS while its violation depending upon the measurements done by a spatially separated observer, say Alice implies quantum steering as a result of the non-existence of such model. Now there can be two types of steering inequalities based on two types of uncertainty relations, such as

- **Coarse-grained:** Here all the possible outcomes of two non-commuting observables are considered. There are coarse-grained uncertainty relations based on the variance of observables, for example, Heisenberg Uncertainty Relation(HUR) [Hei27], Heisenberg-Robertson Uncertainty Relation(HRUR) [Rob29], Sum Uncertainty Relation(SUR) [PS07, MP14] etc. Whereas the other forms of coarse-grained uncertainty relations are manifested by the Entropic Uncertainty Relations(EUR) [BBM75, MU88]. The steering inequality corresponding to HUR was first given by Reid [Rei89] and it is called as Reid criterion. The steering conditions from HRUR, SUR and EUR were respectively proved by Sasmal *et al* [SPHM18], Maity *et al* [MDM17] and Walborn *et al* [WSG<sup>+</sup>11].

1. **Application of HUR.** Let us define quadrature phase amplitudes of an electromagnetic field with a given quadrature angle  $\theta$  as  $\hat{X}_\theta = \frac{\hat{a}e^{-i\theta} + \hat{a}^\dagger e^{i\theta}}{\sqrt{2}}$  ( $i = \sqrt{-1}$ ) where annihilation and creation operators *i.e.*  $\hat{a} = \frac{\hat{x} + i\hat{p}}{\sqrt{2}}$  and  $\hat{a}^\dagger = \frac{\hat{x} - i\hat{p}}{\sqrt{2}}$  respectively obey the bosonic commutation relation  $[\hat{a}, \hat{a}^\dagger] = 1$ . Here  $\hat{x}$  and  $\hat{p}$  are position and momentum operators respectively. Now from HUR, it follows that

$$\Delta\hat{X}_{\theta_1}^2 \Delta\hat{X}_{\theta_2}^2 \geq \frac{1}{4} \quad (1.37)$$

Using Eq.(1.37), Reid derived the following steering inequality given by [Rei89]

$$\Delta_{\text{inf}}^2 \hat{X}_{\theta_1} \Delta_{\text{inf}}^2 \hat{X}_{\theta_2} \geq \frac{1}{4} \quad (1.38)$$

where, the inference variance of  $\hat{X}_\theta$  at Bob's side given the estimate of  $\hat{X}_\theta$  *i.e.*  $\hat{X}_\theta^{\text{est}}$  after Alice's measurement is given by  $\Delta_{\text{inf}}^2 \hat{X}_\theta = \langle (\hat{X}_\theta - \hat{X}_\theta^{\text{est}})^2 \rangle$ . The violation of inequality(1.38) suffices to demonstrate quantum steering from Alice to Bob. It was verified experimentally

by Ou *et al* [OPKP92].

2. **Application of SUR.** The sum uncertainty relation given by Pati and Sahu [PS07] can be represented in terms of quadrature phase amplitudes as,

$$\Delta(\hat{X}_{\theta_1} + \hat{X}_{\theta_2}) \leq \Delta\hat{X}_{\theta_1} + \Delta\hat{X}_{\theta_2} \quad (1.39)$$

Using the above inequality, Maity *et al* proved the sum steering inequality [MDM17] based on inference variances as given below.

$$\Delta(\hat{X}_{\theta_1} + \hat{X}_{\theta_2}) \leq \Delta_{\text{inf}}\hat{X}_{\theta_1} + \Delta_{\text{inf}}\hat{X}_{\theta_2} \quad (1.40)$$

The presence of steering for both the discrete and continuous variable systems are shown by the violation of inequality(1.40).

3. **Application of EUR.** Let us suppose that, the set of probabilities  $\{p_i\}_{i=1}^n$  ( $0 \leq p_i \leq 1, \sum_{i=1}^n p_i = 1$ ) are distributed for a set of outcomes  $i = \{1, 2, \dots, n\}$  corresponding to a measurement  $\mathfrak{P}$ . Then Shannon entropy can be defined as [Sha48a, Sha48b],  $H(\mathfrak{P}) = -\sum_{i=1}^n p_i \log p_i$  ( $0 \leq H(\mathfrak{P}) \leq 1$ ) where probability  $p_i = \{0, 1\}$  implies certainty with correspondence to  $H(\mathfrak{P}) = 0$  and the equiprobable distribution  $p_i = \frac{1}{n} \forall i$  implies maximum uncertainty with minimum information corresponding to  $H(\mathfrak{P}) = 1$ . There remains an uncertainty relation based on Shannon entropy between two non-commuting observables say,  $P$  and  $Q$  for Bob's quantum system and it can be expressed as [BBM75],

$$H(P) + H(Q) \geq \ln \pi e \quad (1.41)$$

Using Eq.(1.41), Walborn *et al* derived the following entropic steering inequality [WSG+11]

$$H(P_B|P_A) + H(Q_B|Q_A) \geq \ln \pi e \quad (1.42)$$

where the subscripts A and B indicates the measurements of Alice and Bob respectively. The conditional Shannon entropies of Bob's outcomes given Alice's measurements arise

from the distribution of conditional probabilities, e.g.  $p(b_{\mathcal{B}}|a_{\mathcal{A}}) = \sum_{\lambda \in OS} p(\lambda, b_{\mathcal{B}}|a_{\mathcal{A}}) = \sum_{\lambda \in OS} p(\lambda|a_{\mathcal{A}}) p(b_{\mathcal{B}}|\lambda) \forall a, b$  where Alice's measurement  $\mathcal{A}$  and Bob's measurement  $\mathcal{B}$  yield outcomes  $a$  and  $b$  respectively and it is computed over ontic space of  $\lambda$ . The violation of inequality(1.42) implies quantum steering from Alice to Bob and the correlation was investigated for continuous variable systems [CPMA14].

- **Fine-grained:** This type of uncertainty relation can be constructed depending upon a particular or a set of outcomes corresponding to non-commuting observables on discrete variable systems. Oppenheim and Wehner are the proponents of this inequality which is given for spin- $\frac{1}{2}$  particles as [OW10]

$$p(b|\mathcal{B}_0) + p(b|\mathcal{B}_1) \leq 1 + \frac{1}{\sqrt{2}} \quad \forall b \in \{-1, +1\} \quad (1.43)$$

Therefore a game can be imagined which can be won when Bob obtains either up or down outcome every time after measuring spin measurements from the set  $\{\mathcal{B}_1, \mathcal{B}_2\}$ . The equality in Eq.(1.43) is achieved when Bob's local state  $\rho_B^\lambda$  is one of the eigenstates of either  $\frac{\sigma_x + \sigma_z}{2}$  for up outcome or  $\frac{\sigma_x - \sigma_z}{2}$  for down outcome.

Now using the form of Eq.(1.35) for LHS model at Bob's side, it can be written that,

$$\begin{aligned} p(a_{\mathcal{A}_x}, b_{\mathcal{B}_y}) &= p(a_{\mathcal{A}_x})p(b_{\mathcal{B}_y}|a_{\mathcal{A}_x}) = \sum_{\lambda} p(\lambda)p(a_{\mathcal{A}_x}|\lambda)p_Q(b_{\mathcal{B}_y}|\rho_B^\lambda) \\ &\leq \max_{\lambda} p_Q(b_{\mathcal{B}_y}|\rho_B^\lambda) \sum_{\lambda} p(\lambda)p(a_{\mathcal{A}_x}|\lambda) \\ &= p_Q(b_{\mathcal{B}_y}|\rho_B^{\lambda_{\max}}) \sum_{\lambda} p(\lambda, a_{\mathcal{A}_x}) \\ &= p(a_{\mathcal{A}_x})p_Q(b_{\mathcal{B}_y}|\rho_B^{\lambda_{\max}}) \end{aligned} \quad (1.44)$$

where, the inequality follows from  $\sum_i x_i^1 x_i^2 \leq \max_i \{x_i^1\} \sum_i x_i^2$  ( $x_i^1 \geq 0, x_i^2 \geq 0 \forall i$ ). Hence by applying inequality(1.43) in inequality(1.44) for binary measurements denoted by  $y \in \{0, 1\}$  for Bob's side conditioned over binary measurements  $x \in \{0, 1\}$  at Alice's side, it

follows that,

$$p(b_{\mathcal{B}_0}|a_{\mathcal{A}_0}) + p(b_{\mathcal{B}_1}|a_{\mathcal{A}_1}) \leq p_Q(b|\mathcal{B}_0) + p_Q(b|\mathcal{B}_1) \leq 1 + \frac{1}{\sqrt{2}} \quad (1.45)$$

The inequality(1.45) is tight as the right hand side is maximized over all  $\lambda$  constructing the LHS  $\rho_B^{\lambda_{\max}}$  at Bob's side. Therefore the steering from Alice to Bob can be ascertained sufficiently by the violation of Bob's LHS model *i.e.* given by the inequality(1.45). The inequality(1.45) named as fine-grained steering inequality [PKM14] corresponds to the scenario (let us say, *Scenario I*) where Alice knows Bob's choice of measurement settings before starting the protocol.

If Alice lacks the knowledge of Bob's measurement settings, then Alice fixes the direction of  $\mathcal{B}_0$  along any axis on the Bloch sphere and takes the average of the left-hand side of Eq.(1.43) by considering all possible directions of  $\mathcal{B}_1$  on the Bloch sphere. The scenario can be considered as *Scenario II*, where the form of inequality(1.43) can be modified as

$$\bar{p}(b|\mathcal{B}_0) + \bar{p}(b|\mathcal{B}_1) = \frac{1}{4\pi} \int_0^{2\pi} \int_0^\pi [p(b|\mathcal{B}_0) + p(b|\mathcal{B}_1)] \sin \theta \, d\theta \, d\phi \leq \frac{3}{2} \quad \forall b \in \{-1, +1\} \quad (1.46)$$

Therefore the fine-grained steering inequality in this scenario can be altered as [PKM14]

$$\bar{p}(b_{\mathcal{B}_0}|a_{\mathcal{A}_0}) + \bar{p}(b_{\mathcal{B}_1}|a_{\mathcal{A}_1}) \leq \bar{p}_Q(b|\mathcal{B}_0) + \bar{p}_Q(b|\mathcal{B}_1) \leq \frac{3}{2} \quad (1.47)$$

The violation of inequality(1.47) implies quantum steering.

The steerable correlation from Alice-to-Bob and Bob-to-Alice are similar in nature. However, there are entangled states where steering is possible only in one-way [HES<sup>+</sup>12, CYW<sup>+</sup>13, BVQB14].

### 1.4.1.2 Analogous CHSH inequality

In a 2-2-2 scenario, the LHV-LHS correlations form a convex set where the elliptical profile of the convex hull can be obtained by the boundaries depending upon different bi-

nary measurements. 4-vector formalism can be adopted for the local deterministic correlation of Alice, for example,  $(p(a = +1|x = 0), p(a = -1|x = 0), p(a = +1|x = 1), p(a = -1|x = 1))^T := \{(1, 0, 1, 0)^T, (1, 0, 0, 1)^T, (0, 1, 1, 0)^T, (0, 1, 0, 1)^T\}$ . Whereas the eigenbasis of binary measurements at Bob's side can be characterised as,  $\mathcal{B}_0 := \{|0\rangle, |1\rangle\}$  and  $\mathcal{B}_1 := \{\sqrt{v}|0\rangle + \sqrt{1-v}e^{i\phi}|1\rangle, -\sqrt{1-v}|0\rangle + \sqrt{v}e^{i\phi}|1\rangle\}$  to act upon Bob's LHS with a generalised form of a qubit, given by  $|\psi_{(v', \phi')}\rangle = \sqrt{v'}|0\rangle + \sqrt{1-v'}e^{i\phi'}|1\rangle$ . In this scenario, the elliptical boundary of the convex hull of LHV-LHS correlations can be defined by the extremal points giving rise to  $\cos(\phi - \phi') = \pm 1$  with eccentricity  $v$ . After suitable reparametrizations, *i.e.*  $|\psi_{(v', \phi')}\rangle \mapsto |\psi_{\zeta}\rangle$ , the continuous probability vector for Bob becomes  $(p(b = +1|y = 0), p(b = -1|y = 0), p(b = +1|y = 1), p(b = -1|y = 1))^T := \{(\frac{1+\cos \zeta}{2}, \frac{1-\cos \zeta}{2}, \frac{1+\sin \zeta}{2}, \frac{1-\sin \zeta}{2})^T\}_{\zeta}$ . Now by employing Eq.(1.36) with  $\sum_{\zeta} \mapsto \int_{\zeta=0}^{2\pi} d\zeta$  as an LHV-LHS model, the joint expectation values can be expressed as,

$$\begin{aligned} \langle \mathcal{A}_x \mathcal{B}_y \rangle &= p(a = b | \mathcal{A}_x, \mathcal{B}_y) - p(a \neq b | \mathcal{A}_x, \mathcal{B}_y) \\ &= \sum_{\chi} \int_{\zeta} p(\chi, \zeta) (2p(a = +1|x, \chi) - 1) (2p(b = +1|y, \zeta) - 1) d\zeta \end{aligned} \quad (1.48)$$

By using four joint expectations for all combinations of  $x, y \in \{0, 1\}$  in the convex space of LHV-LHS correlations spanned by orthogonal basis  $\{(1, 1, 0, 0), (0, 0, 1, 1), (1, -1, 0, 0), (0, 0, 1, -1)\}$ , Cavalcanti *et al* showed that, steering can be demonstrated iff the following nonlinear inequality is violated [CFFW15].

$$\sqrt{(\langle (\mathcal{A}_0 + \mathcal{A}_1) \mathcal{B}_0 \rangle)^2 + (\langle (\mathcal{A}_0 + \mathcal{A}_1) \mathcal{B}_1 \rangle)^2} + \sqrt{(\langle (\mathcal{A}_0 - \mathcal{A}_1) \mathcal{B}_0 \rangle)^2 + (\langle (\mathcal{A}_0 - \mathcal{A}_1) \mathcal{B}_1 \rangle)^2} \leq 2 \quad (1.49)$$

The above necessary and sufficient criterion for quantum steering in 2-2-2 scenario can be called as analogous CHSH inequality or CFFW (Cavalcanti-Foster-Fuwa-Wiseman) inequality. It has been shown that, all LHV-LHS correlations in 2-2-2 scenario satisfies the inequality(1.49) and all the correlations satisfying inequality(1.49) are LHV-LHS. The state-based CFFW criterion [QZL<sup>+</sup>16, MDSM17] depending upon the maximization over all possible measurement settings can be written as  $2\sqrt{\mu + \mu'} \leq 2$  where  $\mu$  and  $\mu'$  are the two greatest eigenvalues of the unitary matrix  $TT^t$  with  $T$  as the correlation matrix corre-

sponding to Eq.(1.12) and  $T^t$  as the transpose of  $T$ . The maximum quantum mechanical violation of Eq.(1.49) *i.e.*  $2\sqrt{2}$  can be obtained by using all the Bell states. For example, using  $|\Phi^+\rangle_{AB}$  and measurement settings  $\mathcal{A}_0 = \frac{\sigma_x - \sigma_z}{\sqrt{2}}$ ,  $\mathcal{A}_1 = \frac{\sigma_x + \sigma_z}{\sqrt{2}}$ ,  $\mathcal{B}_0 = \sigma_z$  and  $\mathcal{B}_1 = \sigma_x$ , the left hand side of inequality(1.49) gives the maximum of  $2\sqrt{2}$ .

### 1.4.1.3 Criterion of $n$ -measurement settings per side

The steering inequalities as discussed up to now involve two measurements per side. Among several steering criteria, Cavalcanti *et al* provided an important  $n$ -measurement per side linear EPR-steering criterion based on uncertainty relation among non-commutating spin component observables for bipartite spin- $j$  particles [CJWR09]. For example, a spin- $\frac{1}{2}$  particle or a qubit satisfies  $\langle S_x \rangle_{\rho_B^\lambda} + \langle S_y \rangle_{\rho_B^\lambda} \leq \frac{\sqrt{2}}{2}$  where  $S_i = \frac{\sigma_i}{2}$ , hence the steering criterion of 2-measurement per side, involving Alice's spin component measurements parallel to that of Bob's, can be written as  $\langle S_x^A S_x^B \rangle + \langle S_y^A S_y^B \rangle \leq \frac{\sqrt{2}}{4}$ . Similarly, corresponding to the  $n$ -number of mutually orthogonal spin component measurements per side for bipartite spin- $j$  particles, the steering criterion can be generalized as,

$$\left| \sum_{i=1}^n \langle S_i^{\mathcal{A}} S_i^{\mathcal{B}} \rangle \right| \leq \sqrt{n} j^2 \quad (1.50)$$

Now by employing  $n$ -number of Pauli spinors per side for bipartite qubit systems, the steering criterion becomes

$$\frac{1}{\sqrt{n}} \left| \sum_{i=1}^n \langle \mathcal{A}_i \otimes \mathcal{B}_i \rangle \right| \leq 1 \quad (1.51)$$

where,  $\mathcal{A}_i = \vec{a}_i \cdot \vec{\sigma}$  ( $\vec{a}_i = (a_i^x, a_i^y, a_i^z) \in \mathbb{R}^3$ ),  $\mathcal{B}_i = \vec{b}_i \cdot \vec{\sigma}$  ( $\vec{b}_i = (b_i^x, b_i^y, b_i^z) \in \mathbb{R}^3$ ) and  $\vec{\sigma} = (\sigma_x, \sigma_y, \sigma_z)$ . The joint expectation values can be calculated from  $\rho_{AB} \in \mathbb{C}^2 \otimes \mathbb{C}^2$  as  $\langle \mathcal{A}_i \otimes \mathcal{B}_i \rangle = \text{Tr}[\rho_{AB}(\sigma_i \otimes \sigma_i)]$ . The sufficient criterion of steering given by the operational inequality(1.51) is known as CJWR (Cavalcanti-Jones-Wiseman-Reid) criterion. The state-based CJWR criterion for 3-measurement settings per side [PM20] can also be simplified as  $\sqrt{\text{Tr}[T^t T]} \leq 1$  where  $T$  is the correlation matrix corresponding to Eq.(1.12) and  $T^t$  is the transpose of  $T$ .

The detection of quantum steering does not always depend on the construction of

steering inequalities. Chen *et al* provided the *All-Versus-Nothing* proof to detect EPR-steering without inequalities [CYW<sup>+</sup>13] and its implications in one-way quantum cryptography [OB08].

## 1.4.2 Quantum steering measures

Quantum steering is a resource in several information processing tasks, like one-sided device-independent quantum key distribution(1s-DIQKD) protocols [BCW<sup>+</sup>12], one-sided randomness certification [LTBS14], sub-channel discrimination with one-way measurements [PW15] etc. which can not be achieved by any classical strategy using unsteerable correlations. Hence the set of unsteerable assemblages acts as the free states in the resource theory of quantum steering given by Gallego and Aolita [GA15]. Now a deterministic one-way LOCC(1w-LOCC) from trusted to untrusted party can be characterized as a CPTP map with a deterministic wiring map at the level of assemblages. The action of 1w-LOCCs as free operations in the resource theoretic formalism of quantum steering is discussed afterward. The quantification of quantum steering depends on the notion of assemblages without measurement specifications at the untrusted(Alice's) side.

Given an assemblage  $\sigma_{a|x}$ , a bonafide convex steering monotone  $\mathcal{S}(\sigma_{a|x})$  satisfies the following properties:

- **Faithfulness.**  $\mathcal{S}(\sigma_{a|x}) = 0 \forall \sigma_{a|x} \in \text{LHS}$ .
- **Monotonicity.**  $\mathcal{S}(\sigma_{a|x})$  is non-increasing, on average, under a deterministic 1w-LOCC given by a sum of subchannels  $\mathcal{M}_w \forall w$ , i.e.  $\sum_w \mathcal{T}_w \mathcal{S}(\frac{\mathcal{M}_w(\sigma_{a|x})}{\text{Tr}[\mathcal{M}_w(\sigma_{a|x})]}) \leq \mathcal{S}(\sigma_{a|x}) \forall \sigma_{a|x}$  where  $\mathcal{T}_w = \text{Tr}[\mathcal{M}_w(\sigma_{a|x})]$  ( $0 \leq \mathcal{T}_w \leq 1$  and  $\sum_w \mathcal{T}_w \leq 1$ ).
- **Convexity.** For a convex decomposition of an assemblage  $\sigma_{a|x} = p\sigma'_{a|x} + (1-p)\sigma''_{a|x} \forall a, x$  ( $0 \leq p \leq 1$ ) in terms of two other assemblages  $\sigma'_{a|x}$  and  $\sigma''_{a|x} \forall a, x$ , it holds that  $\mathcal{S}(\sigma_{a|x}) \leq p \mathcal{S}(\sigma'_{a|x}) + (1-p)\mathcal{S}(\sigma''_{a|x})$ .

Few important quantifiers are given below.

### 1.4.2.1 Steering weight

If an assemblage  $\sigma_{a|x}$  can be decomposed in terms of steerable part  $\sigma_{a|x}^S$  and unsteerable part  $\sigma_{a|x}^{US}$  as given by  $\sigma_{a|x} = p_S \sigma_{a|x}^S + (1 - p_S) \sigma_{a|x}^{US} \forall a, x$ , then the minimum weight of the steerable part ( $p_S \in \mathbb{R}$ ) considering all possible decompositions can be called as steering weight *i.e.*  $W_{\text{steer}}(\sigma_{a|x}) = \min_{\text{decompositions}} p_S$ . It is derived by Skrzypczyk *et al* [SNC14].

### 1.4.2.2 Robustness of steering

If an assemblage  $\sigma_{a|x}$  is mixed with any other assemblage  $\sigma'_{a|x}$  in a way that  $\sigma''_{a|x} = \frac{1}{1+r} \sigma_{a|x} + \frac{r}{1+r} \sigma'_{a|x} \forall a, x$ , then the minimum  $r \in \mathbb{R}$  for which the mixed assemblage  $\sigma''_{a|x}$  becomes unsteerable, is called as the robustness of steering for the assemblage  $\sigma_{a|x}$  *i.e.*  $R_{\text{steer}}(\sigma_{a|x}) = \min_{\text{decompositions}} r$ . It is proposed by Piani *et al* [PW15].

Besides these measures, Gallego and Aolita proved that relative entropy of steering is also a useful convex steering monotone [GA15].

## 1.4.3 Applications of quantum steering

The field of applications from steerable correlations originates from the applicability of entanglement. Unlike BB84 protocol in prepare and measure scenario where Alice prepares and sends the quantum states physically to Bob for measurement, there remains entanglement-based protocol for the generation of quantum secret key [Eke91]. It is impossible to generate distillable secrecy without entanglement [CLL04]. The verification of entanglement through the violation of Bell's inequality provides the device-independent security of a quantum key distribution (QKD) [ABG<sup>+</sup>07]. Whereas the violation of steering inequalities gives secure QKD in one-sided device-independent way. Branciard *et al* [BCW<sup>+</sup>12] solved the problem by using the protocol proposed by Bennett *et al* [BBM92]. On the other hand, by using the monogamy inequality of steerable correlations by involving an eavesdropper as a third party, it was shown that a lower bound of the secret key rate in 1s-DIQKD scenario has a one-to-one relationship with the violation of fine-grained steering inequalities [PKM14]. In the one-sided device-independent scenario, the randomness certification using EPR-steering [LTBS14] was demonstrated by various techniques

including semi-definite programming [PCSA15, CHK18]. Steering can also be employed to discriminate sub-channels or linear CPTP maps for evolution by computing probability with local measurements [PW15] and it can be implemented efficiently in experimental set-up [SYX<sup>+</sup>18]. Even steering has information-theoretic implications in the teleportation of continuous variable systems [HRZAR15].

## 1.5 Nonlocal advantage of quantum coherence

Quantum coherence is a property of quantum state which depends upon the basis representation of the density matrix. For example, the eigenstates of  $\sigma_z$ -basis have no coherence in  $\sigma_z$ -basis, whereas maximum coherence in  $\sigma_x$  or  $\sigma_y$ -basis. This leads to a situation where the precision of estimation of coherence differs with respect to basis. Quantum steering is a nonlocal correlation that contravenes the presence of a local hidden state for the trusted party. Hence nonlocality can also be manifested if it contradicts an equivalent model based on local quantum coherence for the trusted side. This gives rise to one of the strongest nonlocal resources named nonlocal advantage of quantum coherence (NAQC) [MPP17].

### 1.5.1 Coherence complementarity relations

Coherence depends on the basis representation of the density matrix. Generally, it is represented in a computational or  $\sigma_z$  eigenbasis. Let us consider that, the change of basis representation of a matrix  $M$  from old basis  $\{|o_i\rangle\}$  to the new basis  $\{|n_j\rangle\}$  is governed by the transition matrix  $T$ , *i.e.*  $T^{m \times n} : M_{\{|o_i\rangle\}}^{n \times n} \mapsto M_{\{|n_j\rangle\}}^{m \times m}$ . Then the transformation of matrix elements can be expressed as,  $M_{\{|o_i\rangle\}}^{pq} \rightarrow M_{\{|n_j\rangle\}}^{rs} = \sum_{p,q} \langle n_r | o_p \rangle M_{\{|o_i\rangle\}}^{pq} \langle o_q | n_s \rangle$ . Thus the density matrix of a qubit can also be represented in terms of different eigenbasis with different coherence. Hence there can be coherence complementarity relations among mutually orthogonal bases depending on different quantifiers of quantum coherence. For example, there are 3 mutually orthogonal bases in  $\mathbb{C}^2$ . Therefore these relations for a qubit or a

spin- $\frac{1}{2}$  particle  $\rho_B^\lambda$  can be written as [MPP17]

$$\sum_{i=\{x,y,z\}} C_i^g(\rho_B^\lambda) \leq \gamma^g \quad (1.52)$$

where,  $g = \{l_1, E, S\}$  correspond to  $\gamma^g = \{\sqrt{6}, 2.23, 2\}$  respectively and the definition of the quantifiers, namely  $l_1$ -norm ( $C^{l_1}$ ), relative entropy ( $C^E$ ) and skew-information ( $C^S$ ) of coherence are given by Eq.(1.5), Eq.(1.6) and Eq.(1.7) respectively.  $C_i^g$  represents the value of quantum coherence in  $i$ -th basis corresponding to one of the quantifiers  $g$ . Eq.(1.52) constitutes the LHS for Bob in the ontic space of hidden variable  $\lambda$ .

## 1.5.2 Coherence steering inequalities

The non-existence of an LHS model given by inequality(1.52) in terms of quantum coherence for Bob implies the failure of Alice to cheat Bob in the task of quantum steering considered for a joint state of spatially separated observers Alice and Bob. Here the absence of LHS model in terms of coherence results in a nonlocal correlation which is the steering of quantum coherence from Alice to Bob. It can be captured via steering inequalities constructed from inequalities(1.52) as [MPP17]

$$\frac{1}{2} \sum_{i,j,a} p(a|\mathcal{A}_{j \neq i}) C_i^g(\rho_{B|\Pi_{\mathcal{A}_{j \neq i}}^a}) \leq \gamma^g \quad (1.53)$$

where,  $i, j \in \{x, y, z\}$ ,  $a \in \{0, 1\}$ ,  $p(a|\mathcal{A}_j) = \text{Tr}[(\Pi_{\mathcal{A}_j}^a \otimes \mathbb{1}_2)\rho_{AB}]$  and  $\rho_{B|\Pi_{\mathcal{A}_j}^a} = \rho_{a|\mathcal{A}_j} = \frac{1}{p(a|\mathcal{A}_j)} \text{Tr}_A[(\Pi_{\mathcal{A}_j}^a \otimes \mathbb{1}_2)\rho_{AB}]$ . There can be three different inequalities for the initial joint state  $\rho_{AB}$  between Alice and Bob depending upon three quantifiers of quantum coherence, *i.e.*  $l_1$ -norm ( $C^{l_1}$ ), relative entropy ( $C^E$ ) and skew-information ( $C^S$ ) of coherence. The quantum correlation through the violation of these inequalities is generalized in the name of Nonlocal Advantage of Quantum Coherence(NAQC).

### 1.5.3 Applications of NAQC

The observable measure of quantum coherence [Gir14] imposes a speed limit on the evolution of quantum states under unitary evolution [MDS16, SAP17]. It was shown by using NAQC that, nonlocal feature of quantum speed limit can also be demonstrated with stronger resource states [MPP17]. Thus it has implications on the speed of quantum computation. Under spin chain models, including the Ising model, the footprints of quantum phase transition can also be implied by the steered states obtained by NAQC [HGF20].

## 1.6 Quantum discord

If  $H(A)$  and  $H(B)$  are the Shannon entropies [Sha48a, Sha48b] of two probability distributions pertaining to the classical variables  $A$  and  $B$  and  $H(A, B)$  is the Shannon entropy for the joint probability distribution, then the classical mutual information between variables  $A$  and  $B$  in terms of Shannon entropy can be expressed as,  $I_C(A : B) = H(A) + H(B) - H(A, B)$ . The quantum analog of mutual information for a joint state  $\rho_{AB}$  shared between Alice and Bob can be expressed in terms of Von-Neumann entropy [Neu55] as,  $I_Q(A : B) = I_Q(\rho_{AB}) = S(\rho_A) + S(\rho_B) - S(\rho_{AB}) = S(\rho_A) - S(\rho_{AB}|\rho_A)$  where  $S(\rho_A)$ ,  $S(\rho_B)$  and  $S(\rho_{AB})$  are the Von-Neumann entropies defined by Eq.(1.4) for the reduced density matrices  $\rho_A = \text{Tr}_B[\rho_{AB}]$ ,  $\rho_B = \text{Tr}_A[\rho_{AB}]$  and the joint state  $\rho_{AB}$  respectively. Fundamentally it is the total correlation contained in  $\rho_{AB}$  [GPW05, SW06]. Whereas the measurement induced quantum mutual information, which is extracted from the conditional Von Neumann entropy by measuring one of the subsystems, can be interpreted as the optimum classical correlation extractable from  $\rho_{AB}$  [OZ01, HV01]. For example, if positive operator valued measure elements  $E_i$  are applied upon Bob's subsystem, then classical correlation can be written as,  $C_B(\rho_{AB}) = \sup_{\{E_i\}} [S(\rho_A) - \sum_i p_i S(\rho_{i|A})]$  where  $\rho_{i|A} = \frac{1}{p_i} \times [(\mathbb{1}_2 \otimes E_i)\rho_{AB}(\mathbb{1}_2 \otimes E_i)]$  with  $p_i = \text{Tr}[(\mathbb{1}_2 \otimes E_i)\rho_{AB}(\mathbb{1}_2 \otimes E_i)]$  ( $0 \leq p_i \leq 1, \sum_i p_i = 1$ ). Similarly, by measuring on Alice's subsystem, classical correlation  $C_A(\rho_{AB})$  can be extracted. The difference between total and optimum classical correlation can be termed as quantum discord [OZ01], *i.e.*  $Q_A(\rho_{AB}) = I_Q(\rho_{AB}) - C_A(\rho_{AB})$  and  $Q_B(\rho_{AB}) = I_Q(\rho_{AB}) - C_B(\rho_{AB})$ . In general, the bipar-

tite states satisfying  $Q_A(\rho_{AB}) = 0$  or  $Q_B(\rho_{AB}) = 0$  are called as classically correlated state or zero discordant state [HV01]. But normally  $Q_A \neq Q_B$ . If any bipartite state satisfies  $Q_A = Q_B = 0$ , then it is a completely classically correlated state [OHHH02, MPS<sup>+</sup>10]. The analytical expression of quantum discord for a certain class of bipartite qubit states *i.e.* for Bell-diagonal states is given by Luo [Luo08].

### 1.6.1 Geometric measure

The geometric measure of quantum discord is given by the minimum distance of a bipartite qubit state( $\rho_{AB}$ ) from the nearest classically correlated state( $\eta_{AB}$ ) by using the trace distance of norm 2 in Hilbert-Schmidt space. It is given by [DacVB10]

$$\mathbb{D}^{(2)}(\rho_{AB}) = 2 \min_{\eta_{AB}} \|\rho_{AB} - \eta_{AB}\|^2 = 2 \min_{\eta_{AB}} \text{Tr}[\rho_{AB} - \eta_{AB}]^2 \quad (1.54)$$

Unlike the analytic measure of quantum discord, it is not monotonic under local operations.

### 1.6.2 Applications of discord

Quantum discord has a range of applications in quantum information theory [Str15] counting from entanglement distribution in multi-party set-up using the exchange of particles [SKB12, CMM<sup>+</sup>12] to the classical transmission of quantum states via LOCC [SZ13] etc. However, the most important application of the geometric measure of quantum discord is to produce the lower bound of a figure of merit, namely optimal average payoff function for the task of remote state preparation [DacLM<sup>+</sup>12] as described below. Experiments also confirm the successful manifestation of the task with finite quantum discord [DacLM<sup>+</sup>12].

#### 1.6.2.1 Remote state preparation

Quantum entanglement is the resource for the preparation of a remote state unknown to both the sender and receiver with the aid of 2 cbit of classical communication(CC) and 1 ebit of entanglement [BBC<sup>+</sup>93]. Whereas for the preparation of a qubit at a remote

place using optimal classical protocol without entanglement, at least 2.19 cbit of CC is required [CGM00]. Then it was shown by Pati and Bennett [Pat00, BDS<sup>+</sup>01] that, only 1 cbit of CC and 1 ebit of entanglement can be sufficient for the preparation of a remote state which is unknown to the receiver but known to the sender. This protocol is termed as remote state preparation(RSP). Let us assume that, Alice is the sender and Bob is the receiver and they possess a shared state given by Eq.(1.24) which can further be expanded as

$$|\Psi^-\rangle_{AB} = \frac{1}{\sqrt{2}}(|\psi\rangle|\psi_\perp\rangle - |\psi_\perp\rangle|\psi\rangle) \quad (1.55)$$

where  $|\psi\rangle = \cos(\frac{\theta}{2})|0\rangle + e^{i\phi} \sin(\frac{\theta}{2})|1\rangle$  and  $|\psi_\perp\rangle = -\sin(\frac{\theta}{2})|0\rangle + e^{i\phi} \cos(\frac{\theta}{2})|1\rangle$  ( $0 \leq \theta \leq \pi, 0 \leq \phi \leq 2\pi$ ) are any two mutually orthogonal states lying on the surface of the Bloch sphere ( $\{|0\rangle, |1\rangle\}$  is the computational basis,  $(\theta, \phi)$  represents the polar co-ordinate of a pure state on the Bloch sphere). Similar representations up to local unitaries also exist for the other Bell states in the scenario. Now if Alice wants to prepare  $|\psi\rangle$  at Bob's end, she measures her subsystem in the basis  $\{|\psi\rangle, |\psi_\perp\rangle\}$ . If the outcome is  $|\psi_\perp\rangle$ , then Alice communicates the result to Bob and without any action of Bob,  $|\psi\rangle$  is prepared at his end. If Alice obtains the outcome  $|\psi\rangle$ , then the state  $|\psi\rangle$  can be successfully prepared at Bob's side from  $|\psi_\perp\rangle$  with the application of unitary operator  $\sigma_z$  by Bob only when this desired remote state is chosen from the equatorial circle of the Bloch sphere ( $\theta = \frac{\pi}{2}$ ). Otherwise, the transformation  $|\psi_\perp\rangle \mapsto |\psi\rangle$  is forbidden for other circles on the Bloch sphere [BcvHW99] which thereby leads to 50% success of the protocol [BDS<sup>+</sup>01]. On the other hand, if  $\phi = 0$  (*i.e.* for the rebits), then 100% success of the protocol can be achieved depending upon the set of unitaries  $\{\mathbb{1}_2, \sigma_x \sigma_y\}$  at Bob's side. 100% success can also be achieved for the poles of the Bloch sphere depending upon identity and NOT operation at Bob's side [Pat00]. Hence 1 cbit of CC with 1 bit of entanglement can be sufficient for RSP. It was shown that a separable state with non-zero quantum discord can practically execute the task of RSP with a non-zero pay-off function (or with fidelity greater than that of random guess, *i.e.*  $\frac{1}{2}$ ) under a specific measurement scenario [DacLM<sup>+</sup>12].

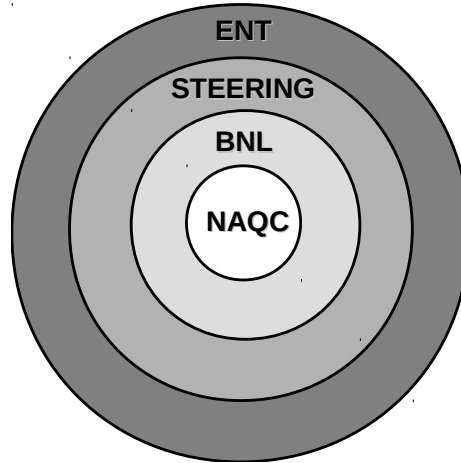


Figure 1.1: Hierarchy of quantum correlations, named after NAQC for Nonlocal Advantage of Quantum Coherence, BNL for Bell nonlocality, quantum steering and ENT for entanglement, are sketched. Additionally, the set of entangled states is comprised within the space of discordant states.

## 1.7 Hierarchy of quantum correlations

In the two-qubit scenario, there is an explicit hierarchical structure of spatial quantum correlations [CBA16, ABC16]. In this scenario, all bell nonlocal states form a strict subset of the set of steerable states, whereas all steerable states form a strict subset of the set of entangled(NPT) states [CA16, GA18]. This hierarchy also follows from operational symmetry in terms of measurements on both sides [WJD07, JWD07]. It is noteworthy that, all the entangled states form a subset of the set of quantum discordant states, which forms the global set of quantum correlations [ABC16]. Recently it was shown that the set of NAQC states forms a strict subset of Bell nonlocal states. Hence NAQC turns out as the strongest of all correlations [HWF18]. Bell nonlocality is a weaker form of quantum correlation than NAQC. Similarly, quantum steering is weaker than Bell nonlocality and entanglement is weaker than quantum steering. Quantum discord can be considered as the weakest form of quantum correlations. Whereas the classical correlations are even much weaker than the quantum correlations. The hierarchy of quantum correlations can be shown as the Venn diagram given in the Fig.1.1.

The hierarchical structure can simply be reproduced in terms of a class of bipartite qubit states. The generalized two-qubit state given by Eq.(1.12) can be reduced up to local unitary equivalence to a class of states with maximally mixed marginals, named as Bell-

diagonal states (of rank 3) [HH96, Luo08, VDD01], *i.e.*

$$\rho_{AB}^{BD} = \frac{1}{4}[\mathbb{1}_2 \otimes \mathbb{1}_2 + \sum_{i=1}^3 c_i(\sigma_i \otimes \sigma_i)] \quad (1.56)$$

The simplification from Eq.(1.12) requires  $|\vec{m}| = |\vec{n}| = \{t_{ij}|i \neq j\} = 0$  and  $t_{ii} = c_i$  ( $|c_i| \in [0, 1]$ )  $\forall i$ . The Bell diagonal states have great importance in quantum information theory [LC10, QZL<sup>+</sup>16]. Bell diagonal states given by Eq.(1.56) can be further simplified by taking  $c_1 = c_2 = c_3 = -c$  to obtain the well-known two-qubit Werner state given by [Wer89],

$$\rho_{AB}^W = c |\Psi^-\rangle_{AB}\langle\Psi^-| + \frac{1-c}{4}(\mathbb{1}_2 \otimes \mathbb{1}_2) \quad (1.57)$$

Werner states are the simplest (single parameter) rather the most powerful bipartite mixed states to act as a tool in quantum theory. The Werner parameter or the strength of visibility ( $0 \leq c \leq 1$ ) ranges from maximally mixed state with  $c = 0$  to maximally entangled singlet state (Eq.(1.24)) with  $c = 1$ . Using Eq.(1.57), one can show that, NAQC inequality(1.53) is optimally violated for  $l_1$ -norm of coherence when  $c > 0.816$  [MPP17], whereas Bell's inequality(1.29) is optimally violated when  $c > \frac{1}{\sqrt{2}} \simeq 0.707$  [HHH95] and quantum steering can be optimally achieved for steering inequality under  $n$ -measurement settings per side (with  $n \rightarrow \infty$ ) when  $c > \frac{1}{2} = 0.5$  [CJWR09]. On the other hand, Werner state is entangled with the quantum mechanical advantage of doing faithful teleportation when  $c > \frac{1}{3} \simeq 0.333$  [Per96] and has quantum discord when  $c > 0$  [Luo08] *i.e.* for states without having the product form. The range of Werner parameters clearly shows the hierarchical picture of the quantum correlations as discussed above. Except for these quantum correlations, there are temporal quantum correlations [KCL<sup>+</sup>18], which are beyond the scope of this thesis.

## 1.8 Generalized measurements

Quantum measurements play an integral role to display the features of quantum correlation between the spatially separated parties by reproducing different measurement statistics of

a joint system. When a physical system is measured by an observable, then some information can be gained at the expense of disturbing the state of the system. Von-Neumann measurement [Neu55] or strong measurement or sharp measurement are projective measurements (PVM) where the system is projected to one of the eigen subspaces of the observable. However, there exists Positive Operator Valued Measure (POVM) which maps a system to the mixed eigen subspaces. POVM can be realized when a projective measurement is performed on the joint space of the system with an ancilla up to global unitary operations [NC02, Per02]. Suppose that,  $\{E_i\}$  is a set of POVM acting on Hilbert space  $\mathcal{H}_S$  of dim.  $d_S$  and  $\{\Pi_i\}$  is a set of PVM acting on Hilbert space  $\mathcal{H}_{S'}$  of dim.  $d_{S'}$  ( $d_{S'} > d_S$ ), then there exists an isometry  $\mathcal{I} : \mathcal{H}_S \rightarrow \mathcal{H}_{S'}$  for which it holds that  $E_i = \mathcal{I}^\dagger \Pi_i \mathcal{I} \forall i$ . Thus a POVM is equivalent to a PVM in a Hilbert space of a higher dimension. Or in other words, a mixed state can be realized as a pure state in higher dimensional Hilbert space. It is the statement of Naimark's dilation theorem [Nai40].

Let us consider that,  $\{\mathfrak{M}_i\}$  is the set of measurement operators to be applied on a quantum system described by a density matrix  $\rho$ . The measurement operators are such that, they satisfy the relation  $\sum_i \mathfrak{M}_i^\dagger \mathfrak{M}_i = \mathbb{1}$ . The outcomes corresponding to the measurement operators are obtained with probabilities are governed by Born's rule as given by  $\text{Tr}[\mathfrak{M}_i^\dagger \mathfrak{M}_i \rho] = \text{Tr}[\mathfrak{M}_i \rho \mathfrak{M}_i^\dagger]$ . If  $\rho = |\psi\rangle\langle\psi|$  is a pure state, then the probabilities have the form,  $\langle\psi|\mathfrak{M}_i^\dagger \mathfrak{M}_i|\psi\rangle$ . Moreover, the state transforms post measurement as,  $\rho \rightarrow \left\{ \frac{\mathfrak{M}_i \rho \mathfrak{M}_i^\dagger}{\text{Tr}[\mathfrak{M}_i \rho \mathfrak{M}_i^\dagger]} \right\}$  or  $|\psi\rangle \rightarrow \left\{ \frac{\mathfrak{M}_i |\psi\rangle}{\sqrt{\langle\psi|\mathfrak{M}_i^\dagger \mathfrak{M}_i|\psi\rangle}} \right\}$  depending on the measurement operators for all outcomes. In this way, generalized measurements can be formulated. The elements  $E_i = \mathfrak{M}_i^\dagger \mathfrak{M}_i$  are called as POVM elements and the set of POVM elements constitute a complete POVM. Hence the probability of outcomes are given by  $\text{Tr}[E_i \rho]$ . A PVM is a special case of POVM where the measurement operators are idempotent, *i.e.* without changing the dimension of the Hilbert space  $E_i = \Pi_i \Pi_i = \Pi_i$ . Here we restrict the description of POVM to 2-dim. complex Hilbert space.

Let us briefly discuss the setup of quantum weak Von Neumann measurements. The idea was first introduced by Aharnov *et al* [AAV88, DSS89]. Spin component measurements on a qubit can be governed by the interaction of spin observables  $\vec{n} \cdot \vec{\sigma}$  ( $\vec{n} =$

$(\sin \theta \cos \phi, \sin \theta \sin \phi, \cos \theta)$ ,  $\vec{\sigma} = (\sigma_x, \sigma_y, \sigma_z)$ ,  $0 \leq \theta \leq \pi, 0 \leq \phi \leq 2\pi$ ) with momentum of the measuring device  $p$ . A particular choice of interaction Hamiltonian can be written as  $H_{\text{int}} = h(t)\vec{n} \cdot \vec{\sigma} \otimes p$  where we can choose the temporal function  $h(t) = \frac{1}{t}$  without loss of generality. Hence the unitary evolution of the joint state of the system and measuring device can be governed by the operator  $\hat{U} = e^{i\vec{n} \cdot \vec{\sigma} \otimes p}$  where  $i = \sqrt{-1}$ . In general for the weak interaction between the system and measuring device, the expansion of the unitary is restricted within the lower orders of temporal components. Assuming the continuous state of the pointer of the measuring device about the origin be  $|\Omega(q)\rangle$ , the pointer is considered to be shifted w.r.t. origin depending upon the eigenvalues of the spin component observables( $\vec{n} \cdot \vec{\sigma}$ ) either up or down. Hence by looking at the position of the pointer ( $q$ ), the outcome of the quantum measurement performed on the qubit system can be known. Here the weakness of the Von-Neumann measurement [SGGP15] lies within the limit  $0 \leq \langle \Omega(q-l) | \Omega(q-l') \rangle \leq 1 \forall l \neq l'$  depending upon the distinguishability of the pointer position corresponding to eigenvalues  $\{l, l'\}$  of the spin observable. The joint state of the system and measuring device can be transformed using the full expansion of the unitary as,

$$\begin{aligned}\hat{U}|\psi\rangle \otimes |\Omega(q)\rangle &= |\psi\rangle \otimes |\Omega(q-1)\rangle \\ \hat{U}|\psi_{\perp}\rangle \otimes |\Omega(q)\rangle &= |\psi_{\perp}\rangle \otimes |\Omega(q+1)\rangle\end{aligned}$$

due to the action of momentum operator as a generator of translation with a magnitude of the eigenvalues  $\{-1, +1\}$  of the spin observable  $\vec{n} \cdot \vec{\sigma}$  where  $\{|\psi\rangle, |\psi_{\perp}\rangle\}$  ( $|\psi\rangle = \cos(\frac{\theta}{2})|0\rangle + e^{i\phi} \sin(\frac{\theta}{2})|1\rangle, |\psi_{\perp}\rangle = -\sin(\frac{\theta}{2})|0\rangle + e^{i\phi} \cos(\frac{\theta}{2})|1\rangle, 0 \leq \theta \leq \pi, 0 \leq \phi \leq 2\pi$ ) are the eigenvectors of spin observable  $\vec{n} \cdot \vec{\sigma}$ . Thus by considering a pure state of the system,  $|\psi_1\rangle = a|\psi\rangle + b|\psi_{\perp}\rangle$  ( $|a|^2 + |b|^2 = 1$ ), the transformation of the joint state of the system and measuring device can be expressed as,

$$|\psi_1\rangle \otimes |\Omega(q)\rangle \rightarrow a|\psi\rangle \otimes |\Omega(q-1)\rangle + b|\psi_{\perp}\rangle \otimes |\Omega(q+1)\rangle \quad (1.58)$$

Whereas by considering the general density matrix  $\rho$  of the system, the transformation

takes the form,

$$\rho \otimes |\Omega(q)\rangle\langle\Omega(q)| \rightarrow \rho_{S-MD} = \sum_{x,y=0}^1 \Pi_x \rho \Pi_y \otimes |\Omega(q + (-1)^x)\rangle\langle\Omega(q + (-1)^y)| \quad (1.59)$$

where the projectors corresponding to up and down outcome labeled as 0 and 1 are given by  $\Pi_0 = |\psi\rangle\langle\psi|$  and  $\Pi_1 = |\psi_\perp\rangle\langle\psi_\perp|$  respectively. The post-measurement state of the system is the result of tracing the pointer state out of the joint state of the system and measuring device, *i.e.*  $\rho' = \sum_{x=0}^1 \langle\Omega(q + (-1)^x)|\rho_{S-MD}|\Omega(q + (-1)^x)\rangle = \Pi_0 \rho \Pi_0 + \Pi_1 \rho \Pi_1 + \Pi_0 \rho \Pi_1 \langle\Omega(q+1)|\Omega(q-1)\rangle + \Pi_1 \rho \Pi_0 \langle\Omega(q-1)|\Omega(q+1)\rangle$ . Complex functional can be assigned to the inner product as  $\langle\Omega(q+1)|\Omega(q-1)\rangle = F[\Omega]e^{i\Theta[\Omega]}$  ( $0 \leq F \leq 1, i = \sqrt{-1}$ ). If  $F = 0$ , then the measurement is called a strong or sharp measurement. Whereas for  $F = 1, \Theta = 0$ , the state of the system remains unaltered or undisturbed. The contribution of  $\Theta[\Omega]$  becomes insignificant under unitary operation because  $\rho' = U_S \rho'' U_S^\dagger$ , where  $\rho'' = F\rho + (1-F)(\Pi_0 \rho \Pi_0 + \Pi_1 \rho \Pi_1)$  and  $U_S = \Pi_0 + e^{i\Theta} \Pi_1$ . It can be seen easily from  $\rho''$  that, as  $F$  increases starting from 0, the disturbance to the system also increases. Hence  $F$  quantifies the disturbance corresponding to a weak Von Neumann measurement. Silva *et al* named  $F$  as the quality factor of a measurement [SGGP15].

The probability of getting up or down outcome from the measurement of spin observable on the qubit system can be reproduced by the probability of getting the pointer state shifted towards the right or left from the origin where the continuous state of the pointer is assumed to be symmetric about the origin. Hence the probability reproducibility conditions are  $p(\text{up}) = p(q > 0) = p(|\Omega(q-1)|^2 > |\Omega(q+1)|^2)$  and  $p(\text{down}) = p(q < 0) = p(|\Omega(q+1)|^2 > |\Omega(q-1)|^2)$  respectively, where the probability of getting the pointer shifted towards left(right) to the origin through weak quantum measurement is given by  $\langle\Omega(q \pm 1)|\Omega(q \pm 1)\rangle = |\Omega(q \pm 1)|^2$ . By tracing  $\rho_{S-MD}$  given by Eq.(1.59), we have  $p(\text{up(down)}) = \frac{1}{2}(1 \pm G[\Omega] \text{Tr}[(\vec{n} \cdot \vec{\sigma})\rho]) = G[\Omega] \times \text{probability of strong measurement} + (1 - G[\Omega]) \times \text{probability of random guess}$ , where the positive functional,  $G[\Omega] = \int_{-1}^{+1} |\Omega(q)|^2 dq$  quantifies the precision of measurement or the information gain by a measurement. Silva *et al* proved a trade-off between disturbance and information gain for a weak quantum measurement [SGGP15], *i.e.*  $F^2 + G^2 \leq 1$  where the equality holds for an optimal non-Gaussian

pointer state  $\Omega(q) \sim e^{\left(-\frac{c}{1-q^2}\right)}$  ( $c = \text{constant}$ ).

Under the standard scheme of Stern-Gerlach experiment, a single-parameter POVM can be implemented by denoting the spin observable for the qubit system as  $\Lambda(\vec{n} \cdot \vec{\sigma})$  where  $\Lambda$  ( $0 \leq \Lambda \leq 1$ ) is called the sharpness of the measurement.  $\Lambda = 1$  implies the measurement to be sharp or strong whereas  $\Lambda = 0$  implies null effect. Here the POVM elements or the effect operators can be expressed as  $E_{0(1)} = \Lambda \Pi_{0(1)} + \frac{1-\Lambda}{2} \mathbb{1}_2$  ( $E_0 + E_1 = \mathbb{1}_2$ ) and the post-measurement state by taking average over all possible outcomes becomes  $\rho'' = \sum_0^1 \sqrt{E_i} \rho \sqrt{E_i}$  from an initial qubit state  $\rho$  with  $F = \sqrt{1-\Lambda^2}$  according to non-selective Lüder's transformation [LÖ6], whereas for selective outcomes the normalised post-measurement state becomes  $\frac{\sqrt{E_i} \rho \sqrt{E_i}}{\text{Tr}[\sqrt{E_i} \rho \sqrt{E_i}]}$  corresponding to up ( $i = 0$ ) or down ( $i = 1$ ) outcomes respectively. Here the output states are mixed due to overlap in  $\{|\psi\rangle, |\psi_\perp\rangle\}$  basis. The probability of getting up or down outcome from this measurement can be represented as  $p(\text{up}(\text{down})) = \text{Tr}[E_{0(1)}\rho]$  with  $G = \Lambda$ . Therefore the formalism of unbiased unsharp measurement for the qubit systems always obeys the trade-off relation  $F^2 + G^2 = 1 \forall \Lambda \in [0, 1]$  [MMH16]. On the other hand, the biased unsharp measurement can be constructed by altering the effect operators as  $E'_{0(1)} = E_{0(1)} \pm \Gamma \mathbb{1}_2$  ( $E'_0 + E'_1 = \mathbb{1}_2$ ) where  $\Gamma$  ( $0 \leq \Gamma \leq 1$ ) is called the biasness of the measurement. For a given scheme of measurement, the following relation holds between the sharpness and the biasness parameters, *i.e.*  $|\Lambda| + |\Gamma| \leq 1$  [Bus09].

The weak measurement for a system can also be formalized by non-unitary evolution of the system corresponding to detection and non-detection of the system by the measuring device [KLKK12]. Under this measurement scheme, the system collapses towards one of the eigenstates of the measuring observable than the other. This technique is associated with the success rate of post-selecting the ensembles [ABL64]. It can be implemented with beam polarizers and wave plates for photonic qubits in optical set-up [LJKK11]. The reversal of a weak measurement is shown by Kim *et al* [KCRK09].

## 1.9 Quantum channels

The dynamics of quantum systems can not always be explained in terms of unitary evolution according to the basic postulates of quantum mechanics because the system practically remains open to the environment. Rather the unitary dynamics depend on the closed system comprising the system and environment. In this case, the evolution pertaining to the system only is governed by non-unitary operations. The general form of evolution for a quantum system,  $\rho$  can be expressed by a completely positive trace preserving (CPTP) map through operator-sum representation or Kraus representation as  $\rho \rightarrow \sum_{i=0}^{d_1 d_2 - 1} W_i \rho W_i^\dagger$  where  $\{W_i\}$  are called the Kraus operators and  $\{d_1, d_2\}$  are the dimension of Hilbert spaces corresponding to input and output quantum systems. For the mapping of a qubit into a qubit under the CPTP map, there can be utmost 4 number of Kraus operators. A positive map is a transformation between two positive operators, whereas a completely positive (CP) map, besides being positive, transforms a positive operator into a positive operator by taking its tensor product with ancillary  $\mathbb{1}_d$  (corresponding to  $d$ -dim. Hilbert space) also. CP maps can transform density operators into density operators only when it is trace-preserving (TP), *i.e.*  $\sum_i W_i^\dagger W_i = \mathbb{1}$  ( $d_1 \times d_2$  identity matrix). The environment or the ancilla is always considered to remain initially in the ground state  $|e_0\rangle$  and the CPTP map can be realised by an unitary evolution on the joint state of the system and ancilla accompanied by a partial trace on the ancilla, *i.e.*  $\rho \rightarrow \text{Tr}_{\text{ancilla}}[U(\rho \otimes |e_0\rangle\langle e_0|)U^\dagger]$  where  $W_i = \langle e_i | \rho | e_0 \rangle$  ( $\{|e_i\rangle\}$  span the Hilbert space of the environment). CPTP maps are often termed as quantum channels in quantum information theory, specifically, the irreversible interaction between the system and the environment is called as decoherence and the channels associated to it, are called as decoherence channels which generally destroy the quantum information by means of coherence of the density matrices thereby leading them asymptotically to maximally mixed states  $\frac{\mathbb{1}_{d_1}}{d_1}$  ( $d_1 = 2$  for qubit) with least information. The transformation of states under quantum channels may be compared with the formalism of generalized measurements without outcome statistics. In the theory of quantum correlations, both the decoherence channels and generalized measurements play a similar role in destroying quantum correlations under repeated applications [AdMHM<sup>+</sup>07, SGGP15, MMH16]. However, the tools can be cleverly

employed to restore the declining quantum correlations by using Zeno's paradox [MS77] or the technique of weak measurement and its reversal [KLKK12].

Among the many different decoherence channels [NC02], we discuss a few of them in the qubit state space spanned by computational basis  $\{|0\rangle, |1\rangle\}$  as given below.

- **Phase-flip channel:** This channel changes the phase of only  $|1\rangle$  to  $-|1\rangle$  with probability  $D$  and keeps the state unchanged with probability  $1 - D$ . The state transformation of a general qubit  $\rho$  is given by  $\rho \rightarrow D\sigma_z\rho\sigma_z + (1 - D)\rho$ . Hence the two Kraus operators associated with the phase-flip channel are  $W_0 = \sqrt{D}\sigma_z$  and  $W_1 = \sqrt{1 - D}\mathbb{1}_2$ .

- **Bit-flip channel:** Here the bit flips *i.e.*  $|0\rangle \rightarrow |1\rangle$  and  $|1\rangle \rightarrow |0\rangle$  occurs with probability  $D$  and the state remains unchanged with probability  $1 - D$ . The state transformation of  $\rho$  is given by  $\rho \rightarrow D\sigma_x\rho\sigma_x + (1 - D)\rho$ . The two Kraus operators associated with the bit-flip channel are  $W_0 = \sqrt{D}\sigma_x$  and  $W_1 = \sqrt{1 - D}\mathbb{1}_2$ .

- **Pauli channel:** The state transformation of  $\rho$  under Pauli channel is given by  $\rho \rightarrow D_x\sigma_x\rho\sigma_x + D_y\sigma_y\rho\sigma_y + D_z\sigma_z\rho\sigma_z + (1 - D_x - D_y - D_z)\rho$ . Hence the two Kraus operators associated with the phase-flip channel are  $W_0 = \sqrt{D_x}\sigma_x$ ,  $W_1 = \sqrt{D_y}\sigma_y$ ,  $W_2 = \sqrt{D_z}\sigma_z$  and  $W_3 = \sqrt{1 - D_x - D_y - D_z}\mathbb{1}_2$ . When  $D_x = D_y = D_z = \frac{D}{3}$ , then Pauli channels can be called as depolarizing channels. Under reparametrization  $D \rightarrow \frac{3D}{4}$ , the action of depolarizing channel can be expressed as  $\rho \rightarrow D\frac{\mathbb{1}_2}{2} + (1 - D)\rho$  *i.e.* mixing of  $\rho$  with white noise  $\frac{\mathbb{1}_2}{2}$  with probability  $D$ .

- **Amplitude damping channel:** Considering the initial state of the environment or ancilla as  $|e_0\rangle = |0\rangle$  and the basis  $\{|0\rangle, |1\rangle\}$  to span the Hilbert space of the environment, the amplitude damping channel characterizes the loss of photonic qubit while remaining in the excited state  $|1\rangle$  to the environment with probability  $D$  and the condition of being unaffected with probability  $1 - D$ . The global unitary map on the joint system-ancilla state is given by  $|0\rangle_{\text{system}} \otimes |0\rangle_{\text{ancilla}} \rightarrow |0\rangle_{\text{system}} \otimes |0\rangle_{\text{ancilla}}, |1\rangle_{\text{system}} \otimes |0\rangle_{\text{ancilla}} \rightarrow \sqrt{D}|0\rangle_{\text{system}} \otimes |1\rangle_{\text{ancilla}} + \sqrt{1 - D}|1\rangle_{\text{system}} \otimes |0\rangle_{\text{ancilla}}$ . The two Kraus operators associated with this channel are  $W_0 = \begin{pmatrix} 1 & 0 \\ 0 & \sqrt{1 - D} \end{pmatrix}$  and  $W_1 = \begin{pmatrix} 0 & \sqrt{D} \\ 0 & 0 \end{pmatrix}$ .

Except for these quantum channels, there exist entanglement-breaking channel [HSR03] useful in the theory of quantum correlations, Schumacher and Westmoreland qubit channel [SW97] useful in the theory of quantum communication within the classical capacity of the channel, erasure channel [GBP97] useful in error correction theory etc. As in quantum theory, the states are associated with density operators and quantum channels act on density operators, hence quantum channels can be recognized as superoperators. From the mathematical correspondence between the operators and the superoperators, Choi and Jamiołkowski proved that there exists one-to-one correspondence between the quantum states and the quantum channels. This correspondence is famously known as Choi-Jamiołkowski isomorphism [Cho75, Jam72] or the channel-state duality [JLF13].

## 1.10 Plan of the thesis

The existence of quantum mechanical resources in different forms of quantum correlations in bipartite qubit systems is discussed in the preceding sections. Every quantum correlation is associated with specific information theoretic applications, which are otherwise impossible to implement in the absence of such correlation. Characterization of quantum correlations enables the study of the strength of their nonlocal behavior. The formalism of measurements plays an important role in revealing such correlations via different statistical interpretations. It is practically impossible to neglect various modes of environmental interactions when quantum communication comes into play by utilizing the correlations shared between the quantum systems.

Among various quantum mechanical correlations, quantum steering [Sch35, Rei89] and NAQC [MPP17] are asymmetric in nature. Though steering, as a quantum correlation, has an intermediate kind of strength [WJD07, JWD07], NAQC performs as one of the strongest quantum correlations [HWF18]. Various aspects of asymmetric quantum correlations, present in bipartite qubit systems, including the mechanism of its protection against the environmental effect, the proper characterization of a measure for its detection in a given context, its shareability in multiple observer scenario etc are discussed in this thesis

driven by an empirical situation that, one of the two qubits has quantum description to reproduce the measurement statistics in order to test the presence of entanglement between them. Asymmetric quantum correlations are particularly important to certify cryptographic security in one-sided device-independent way [BCW<sup>+</sup>12]. Besides these, the processing of quantum information via RSP [Pat00] is another important facet of this thesis, where sharing of RSP in a multi-observer linear network is studied in light of several discordant pair of qubit systems.

In Chapter 2 [DGPM17], we explore the consequences of environmental interactions on the steerable correlations revealed by the violation of a fine-grained steering inequality [PKM14]. We show, in contrast to the behavior of teleportation fidelity [Ban02], that quantum steering and its analogous lower bound of quantum secret key rate in a one-sided device-independent quantum key distribution scenario diminish under the amplitude damping decoherence when acted on one or both the subsystems of a bipartite qubit system. However, the adverse effect of decoherence can be decelerated when the technique of weak measurement and its reversal [KLKK12] are plugged in respectively before and after the process of decoherence. Despite that, weak measurement is associated with the post-selection, our strategy can be applied surprisingly well to protect the steerable correlation even when the average is taken over the success and failure of the technique.

In Chapter 3 [DDJM18], we study a method to check and quantify quantum steering in a scenario, where binary black-box measurements are done on the untrusted side and binary projective qubit measurements in mutually unbiased bases are done on the trusted side of a bipartite qubit system. By decomposing a non-signalling correlation [BLM<sup>+</sup>05] in terms of extremal correlations in a steering scenario, we can detect the steerability of a correlation. Subject to such detection, quantum steering can be quantified through the optimization over all possible decompositions of correlations. Our steering quantifier *viz steering cost* is proved to be a convex steering monotone [GA15]. The relaxation of full tomographic knowledge of qubit assemblage to determine it causes it to be experimentally less demanding than the steering weight [SNC14]. We also show a mathematical relationship between the two measures by using the analogous CHSH inequality for quantum

steering [CFFW15]. We further illustrate our method to calculate the steering cost for two noted families of quantum correlations.

In Chapter 4 [DM18, DM19], we discuss the sequential sharing of NAQC correlations [MPP17] under the formalism of multiple POVMs [SGGP15, MMH16] without being restricted by the non-signalling theorem, where several untrusted observers at one half of the singlet state try to steer the local quantum coherence of a single trusted observer present at the other half of it. We show that not more than a single observer per side can demonstrate NAQC by using all the three quantifiers of quantum coherence. This result interestingly supports the inverse relationship between the bound on the number of observers under the given framework and the strength of quantum correlation, being shared.

Similar to the sharing of a quantum correlation, we investigate in Chapter 5 [DMPM21], whether a quantum information processing task can be shared under the multiple POVM framework [SGGP15, MMH16] in the presence of a single copy of a bipartite entangled state. The task of RSP for qubits by utilizing geometric quantum discord [DacLM<sup>+</sup>12] has remarkable operational advantages in the area of quantum communication protocols [CS12, JZLW19, NK08]. We first distinguish the classical and quantum strategies for such a task by designing a model without a quantum resource to obtain an optimal classical bound of the RSP-fidelity. Then we show that at most six sequential senders can remotely prepare qubits at a distant receiver with a non-classical advantage in terms of RSP-fidelity. By employing several class of bipartite entangled states, we demonstrate that the bound on the number of senders is optimum when a maximally entangled pure state is shared initially by the sender-receiver pair and the remote states from the equatorial great circle of the Bloch sphere are prepared during each course of action. We further show that the afore-said optimum bound gets lowered as the initial joint state shifts towards the non-maximally entangled pure or mixed states and/or the choice of remote states moves from the neighbourhood of the equatorial great circle towards the poles of the Bloch sphere.

Finally, in Chapter 6, the main results of this thesis are summarized and some prospects for future research are presented.

## Preservation of a quantum correlation

Quantum mechanical correlations between two or more quantum systems provide advantages in information processing tasks in many ways which can not be possible by using classical correlations [EPR35, Bel64, CHSH69]. However, the quantum correlations corresponding to the observed quantum systems become weakened due to the presence of non-negligible continuous interaction between the systems and the environment in reality. The most crucial task during the processing of quantum information is to protect the quantum correlations from the diminishing effect owing to the ubiquitous environment. Surprisingly, the generation of entanglement between two or more atoms happens to be possible [BKPV99, PH02, Bra02, DK03] when they consecutively interact with the common environment, called a cavity [KLAK02, KC04, GMN06]. The environmental interaction modeled by an amplitude damping channel (ADC) can enhance the fidelity of another information processing task, *i.e.* quantum teleportation [BmcHHH00] where for a certain class of bipartite states [Ban02, PM13], the teleportation fidelity is found to be raised from classical to quantum region. But in most of the cases, quantum correlation is destroyed because of the presence of an interacting environment.

The technique of weak measurements is very useful to protect the strength of quantum correlation, *e.g.* the fidelity of quantum teleportation, when the systems are interacting with the environment modeled by an amplitude damping channel [PM13, KU99, KJ06, KCRK09, LJJK11, KLKK12, MXA12, LX13]. The technique was originally proposed [AAV88, DSS89] on the basis of weak coupling between the observed system and the

measurement device, thereby making it possible for the measurement outcomes to be amplified compared to the eigenvalue spectrum of the original system, for the befitting post-selected ensembles. This technique has been implemented in many different ways, such as in the study of the spin Hall effect [HK08], superluminal propagation of light [SMC<sup>+</sup>04, BSW<sup>+</sup>04], wave-particle duality using cavity-QED experiments [Wis02], direct measurement of the quantum wave function [LSP<sup>+</sup>11], measurement of ultrasmall time delays of light [BS10, SB13], and observing Bohmian trajectories of photons [KBR<sup>+</sup>11, GMGS01].

This chapter is based on our work "*Preservation of a lower bound of quantum secret key rate in the presence of decoherence*", S. Datta, S. Goswami, T. Pramanik, and A. S. Majumdar, Phys. Lett. A, **381**, 897 (2017) [DGPM17]. Here we study the possibility of preservation of a lower bound of the quantum secret key rate for a bipartite state shared between Alice and Bob where Alice's system is not trusted as a quantum system. We frame the secrecy of the quantum key rate in a way that, such a lower bound becomes zero or negative under the attack of an eavesdropper. More specifically, we discuss a way to protect the one-sided device-independent quantum key distribution (1s-DIQKD) [TR11, BCW<sup>+</sup>12] scenario when the system interacts with the environment modeled by ADC. Here we analyze the secrecy of the 1s-DIQKD scenario which does not depend on a particular protocol used by the two observers, *i.e.* Alice and Bob to generate the secret key. Unlike the fidelity of quantum teleportation [BmcHHH00, Ban02], We observe that ADC cannot improve the optimal secret key rate in 1s-DIQKD under the fine-grained steering scenario [PKM14], which is based on the fine-grained uncertainty relation [OW10]. We show that improvement of the secret key rate becomes possible using the technique of weak measurement and its reversal, which may be used to vanquish the adverse effect of the ADC [KU99, KJ06, KCRK09, LJKK11, KLKK12, MXA12].

## 2.1 Technique of weak measurement plus ADC

The mechanism of amplitude damping channel(ADC) is discussed earlier. This work involves two subsystems( $S$ ) possessed by Alice and Bob. We denote Alice's subsystem as

$S = A$  and Bob's subsystem as  $S = B$ . The Kraus operators corresponding to subsystem  $S$  are represented as  $W_{S,i}$  ( $i = 0, 1$ ) with the strength of decoherence  $D_S$  ( $0 \leq D_S \leq 1$ ) as each subsystem is considered as a two-level system in photon number basis with zero photon state denoted by  $|0\rangle = \begin{pmatrix} 1 \\ 0 \end{pmatrix}$  and the excited or single photon state denoted by  $|1\rangle = \begin{pmatrix} 0 \\ 1 \end{pmatrix}$ . Alice and Bob are well separated, and the environments for  $A$  and  $B$  are completely disconnected. Hence we neglect the influence or the memory effect of the environments on the dynamics of each other. However, for the sake of simplicity, we take the same decoherence strength for both of them.

There are instances in the literature [KU99, KJ06, KCRK09, LJJK11, KLKK12] where the technique of weak measurement and its reverse are found to be useful for suppressing the environmental effect modeled by ADC on the system. We assume that the system is measured under a specified scheme of weak measurement having strength  $p_S$  before being open to the environment. More specifically, the non-unitary evolution of the system by tracing the state of the measurement device out of the joint state, involves two parts corresponding to the detection and the non-detection of the system. Physically the detector detects the system with probability  $p_S$  ( $0 \leq p_S \leq 1$ ) when it is in the state  $|1\rangle_S$  and does not affect otherwise. The Kraus operator corresponding to the detection of the system can be represented in the photon number basis as,

$$M_{S,1} = \begin{pmatrix} 0 & 0 \\ 0 & \sqrt{p_S} \end{pmatrix}, \quad (2.1)$$

which does not have any inverse. When a system is measured, then the entanglement of the system with other systems is broken completely. Hence, the operation of detection is irreversible. Whereas the Kraus operator, when the system is not detected, has the following form

$$M_{S,0} = \begin{pmatrix} 1 & 0 \\ 0 & \sqrt{1-p_S} \end{pmatrix}, \quad (2.2)$$

which is reversible, *i.e.* the application of its inverse restores the system to its initial state. The case corresponding to the detection of the system is discarded. Hence, the post-selection of the system by weak measurement is associated with a success probability.

After performing the weak measurement, the system is allowed to interact with the environment and at the end, a reverse weak measurement is performed to reduce the effect of the environment. The Kraus operator corresponding to the reversal of weak measurement when the system is not detected, can be written in the photon number basis as

$$N_{S,0} = \begin{pmatrix} \sqrt{1-q_S} & 0 \\ 0 & 1 \end{pmatrix}, \quad (2.3)$$

where  $q_S$  ( $0 \leq q_S \leq 1$ ) is the strength of the reverse weak measurement. In reality, no operation can completely restore the initial coherence of the state. So that, we assume  $p_S \neq q_S$ .

## 2.2 1s-DIQKD associated with steering

The security of quantum key distribution(QKD) in a given scenario depends on the demonstration of nonlocal correlations present in the joint state( $\rho_{AB}$ ) between two observers, say Alice( $A$ ) and Bob( $B$ ). For example, Bell nonlocality by the violation of Bell's inequality certifies the security of a QKD scenario, called as a fully device-independent QKD scenario, where none of the two parties are trusted. In a one-sided device-independent quantum key distribution(1s-DIQKD) scenario, the device of one of the two parties is not trusted, and hence the secrecy is directly connected with the demonstration of quantum steering. We employ, in this work, the optimal fine-grained steering criteria among others [Rei89, MDM17, WSG<sup>+</sup>11, SBW<sup>+</sup>13, CFFW15, CJWR09, Bus12, SJWP10] to study the quantum secret key rate of steerable states [PKM14].

To discuss fine-grained steering, let us consider the following game. Alice prepares a large number of bipartite quantum states  $\rho_{AB}$ . She then sends all the subsystems  $B$  to Bob

and keeps the subsystems  $A$  with her. Bob only trusts that the subsystem  $B$  is quantum, but agrees that the prepared state is entangled if and only if Alice has control over the state of subsystems  $B$ . In other words,  $\rho_{AB}$  is said to be steerable when it cannot be explained by a local hidden state(LHS) model [WJD07]. To check whether the state is steerable, Bob asks Alice to control or steer the state of his subsystem  $B$  in one of the eigenstates of the observable chosen randomly from the set  $\{\mathcal{B}_0 = \sigma_z, \mathcal{B}_1 = \sigma_x\}$ . Next, Alice measures a suitable observable chosen from the set  $\{\mathcal{A}_0, \mathcal{A}_1\}$  and communicates her choice and outcome. The shared state  $\rho_{AB}$  is steerable when the conditional probability distribution  $P(b_{\mathcal{B}_i}|a_{\mathcal{A}_i}) \forall i \in \{0, 1\}$  (where  $a \in \{0, 1\}$  and  $b \in \{0, 1\}$  are the outcomes corresponding to the measurements at Alice's and Bob's side) violates the relation [PKM14] reordered from Eq.(1.47) as

$$\frac{1}{2}[P(b_{\sigma_z}|a_{\mathcal{A}_0}) + P(b_{\sigma_x}|a_{\mathcal{A}_1})] \leq \frac{3}{4}. \quad (2.4)$$

It can be further shown that if the shared state  $\rho_{AB}$  between the subsystems  $A$  and  $B$  is maximally steerable, then none of the given subsystems can have quantum correlation or in our case, the steerability with any other (sub)system. This phenomenon is commonly called as the monogamy of steerable states. To elaborate, let us consider that,  $\rho_{ABC}$  is shared among the parties, *viz.* Alice( $A$ ), Bob( $B$ ) and Charlie( $C$ ) respectively. The monogamy relation is given by

$$\frac{1}{2}(\Sigma_{A,B} + \Sigma_{B,C}) \leq \frac{3}{4}, \quad (2.5)$$

where  $\Sigma_{A,B} = \frac{1}{2}[P(b_{\sigma_z}|a_{\mathcal{A}_0}) + P(b_{\sigma_x}|a_{\mathcal{A}_1})]$  and  $\Sigma_{B,C} = \frac{1}{2}[P(b_{\sigma_z}|c_{\mathcal{C}_0}) + P(b_{\sigma_x}|c_{\mathcal{C}_1})]$ . Here, Charlie measures the observable from the set  $\{\mathcal{C}_0, \mathcal{C}_1\}$  on his subsystem (labelled by  $C$ ) in order to steer Bob's subsystem in the preferred basis of  $\{\sigma_z, \sigma_x\}$ , and  $c \in \{0, 1\}$  is Charlie's measurement outcome. The relation given by Eq.(2.5) is derived under contradiction. When Alice and Bob share a steerable state  $\rho_{AB}$ , according to the monogamy relation given

by Eq.(2.5), one has

$$\Sigma_{A,B} = \frac{1}{2}[P(b_{\sigma_z}|a_{\mathcal{A}_0}) + P(b_{\sigma_x}|a_{\mathcal{A}_1})] = \frac{3}{4} + \delta, \quad (2.6)$$

where  $\delta$  ( $0 < \delta \leq \frac{1}{4}$ ) is the degree of violation of the steering inequality(2.4). The state shared by Bob and Charlie is unsteerable  $\forall \delta > 0$ , *i.e.*

$$\Sigma_{B,C} = \frac{1}{2}[P(b_{\sigma_z}|c_{\mathcal{C}_0}) + P(b_{\sigma_x}|c_{\mathcal{C}_1})] \leq \frac{3}{4} - \delta. \quad (2.7)$$

The shared correlation (measured by the aforesaid mutual information) between Alice and Bob is  $I(B : A) = H(B) - H(B|A)$ , where the Shannon entropy [Sha48a, Sha48b] of variable  $X$  with probability distribution  $\{p(x)|0 \leq p(x) \leq 1\}$  is given by,  $H(X) = -\sum_x p(x) \log_2 p(x)$  and the conditional Shannon entropy of variable  $X$  given variable  $Y$  with probability distribution  $\{p(y)|0 \leq p(y) \leq 1\}$  is given by,  $H(X|Y) = -\sum_{x,y} p(x,y) \log_2 \frac{p(x,y)}{p(y)} = -\sum_{x,y} p(x,y) \log_2 p(x|y)$  (the conditional probability of occurring  $x \in X$  given  $y \in Y$  is denoted by  $p(x|y)$ ). The Shannon entropy functions are defined here for the binary outcomes of an observable in  $\mathbb{C}^2$ . Similarly, the shared information between Bob and Charlie can be expressed by  $I(B : C) = H(B) - H(B|C)$ . The secret key rate between Alice and Bob under individual attack is then lower bounded by [CK78]

$$\begin{aligned} r &\geq I(B : A) - I(B : C) = H(B|C) - H(B|A) \\ &= \sum_{a,b} p(a,b) \log_2 p(b|a) - \sum_{a,b} p(b,c) \log_2 p(b|c) \\ &= \sum_{a,b,c} p(a,b,c) \log_2 p(b|a) - \sum_{a,b,c} p(a,b,c) \log_2 p(b|c) \\ &= \sum_{a,b,c} p(a,b,c) \log_2 \frac{p(b|a)}{p(b|c)}. \end{aligned} \quad (2.8)$$

where, the marginal probabilities  $p(a,b)$  and  $p(b,c)$  come from the joint probability  $p(a,b,c)$  as  $p(a,b) = \sum_c p(a,b,c)$  and  $p(b,c) = \sum_a p(a,b,c)$  respectively. In a given steering scenario,  $p(b|a)$  and  $p(b|c)$  can be replaced by  $\Sigma_{A,B}$  and  $\Sigma_{B,C}$  respectively.

Now by using Eq.(2.6) and the inequality(2.7), the above inequality becomes

$$r \geq \log_2 \left[ \frac{\frac{3}{4} + \delta}{\frac{3}{4} - \delta} \right]. \quad (2.9)$$

The above secret key rate is based on the maximum violation of the Fine-grained steering inequality(2.4) by the state  $\rho_{AB}$ , where one of the devices (here, the subsystem  $A$ ) is not trusted in the context of quantum steering. The violation of the steering inequality(2.4) amounts to  $\delta \in [0, \frac{1}{4}]$  which is maximum when one of the Bell states is shared and zero for an unsteerable bipartite state. Consequently, the lower bound of the secret key rate lies within  $0 \leq r \leq 1$ . The secret key rate given by the inequality(2.9), as derived above, is independent of the measurement device used by the untrusted party and hence it is associated with the 1s-DIQKD scenario. It is worth mentioning that, the lower bound of the secret key rate is not uniquely defined. For example, Branciard et al derived another lower bound of secret key rate in 1s-DIQKD scenario [BCW<sup>+</sup>12] by using the smooth entropic functions [TR11], where an EPR-steering inequality  $r \leq 0$  is manifested in terms of that lower bound.

## 2.3 Quantum secret key rate under ADC

We have discussed the connection of the secret key rate under individual attack with steerability. In our steering game, Alice needs to send the quantum system  $B$  to Bob through the environment. In the derivation of secret key rate represented by inequality(2.9), the interaction between the system and the environment is not considered. Now our aim is to study the effect of the environment on steerability and hence, on the secret key rate associated with 1s-DIQKD. Here, we discuss two different cases separately.

- **Case-I:** We consider the effect of the environment on the subsystem  $B$  when it is passing through the environment.
- **Case-II:** We consider the effect on the secret key rate when both the subsystems interact with the environment through amplitude damping decoherence.

In both the cases, we assume that Alice prepares the subsystems  $A$  and  $B$  initially in one of the maximally entangled states given by,

$$\begin{aligned} |\Psi^\pm\rangle &= \frac{|00\rangle \pm |11\rangle}{\sqrt{2}}, \\ |\Phi^\pm\rangle &= \frac{|01\rangle \pm |10\rangle}{\sqrt{2}}. \end{aligned} \quad (2.10)$$

which has the highest amount of concurrence (as defined by Eq.(1.19)), *i.e.* 1. Maximum entanglement comes up with the maximum violation of the Fine-grained steering inequality(2.4) and so the maximum value of the secret key rate, *i.e.*  $r = 1$ . Note that, once Alice chooses a particular form among the above four possibilities and all the subsequent operations are carried out based on the state, chosen initially.

### 2.3.1 Case-I: Single interaction

Here we discuss the environmental effect on the steerability when the system  $B$  interacts with the environment via ADC during the time of its passage. After environmental interaction, the shared state between Alice's system  $A$  and Bob's system  $B$  becomes

$$\rho'_{AB} = \sum_{i=0}^1 (\mathbb{1}_2 \otimes W_{B,i}) |\Psi^\pm\rangle \langle \Psi^\pm| (\mathbb{1}_2 \otimes W_{B,i}^\dagger), \quad (2.11)$$

when Alice prepares the initial state  $|\Psi^\pm\rangle$  given by Eq.(2.10), or

$$\sigma'_{AB} = \sum_{i=0}^1 (\mathbb{1}_2 \otimes W_{B,i}) |\Phi^\pm\rangle \langle \Phi^\pm| (\mathbb{1}_2 \otimes W_{B,i}^\dagger), \quad (2.12)$$

where Alice prepares the initial state  $|\Phi^\pm\rangle$  given by Eq.(2.10). The Kraus operators  $W_{B,0}$  and  $W_{B,1}$  are given by  $\begin{pmatrix} 1 & 0 \\ 0 & \sqrt{1-D_B} \end{pmatrix}$  and  $\begin{pmatrix} 0 & \sqrt{D_B} \\ 0 & 0 \end{pmatrix}$  respectively ( $\sum_{i=0}^1 W_{B,i}^\dagger W_{B,i} = \mathbb{1}_2$ ). The strength of the environmental interaction associated with the system  $B$  is  $D_B$  ( $0 \leq D_B \leq 1$ ).

Next, with the help of the inequalities(2.4) and (2.9), we study the effect of decoherence on the steerability and lower bound of the secret key rate of the state  $\rho'_{AB}$  ( $\sigma'_{AB}$ ). We

calculate the quantity  $\Sigma_{A,B}$  (left-hand side of Eq.(2.4)) by maximizing over Alice's choice of observables  $\mathcal{A}_0$  corresponding to spin measurement along the direction  $\vec{n}_0$ , and  $\mathcal{A}_1$  along the direction  $\vec{n}_1$ . For both the prepared states  $|\Psi^\pm\rangle$  and  $|\Phi^\pm\rangle$ , the above quantity becomes

$$\frac{1}{2}[P(b_{\sigma_z}|a_{\sigma_z}) + P(b_{\sigma_x}|a_{\sigma_x})] = \frac{3 + \sqrt{1 - D_B}}{4}, \quad (2.13)$$

where Alice's optimal measurement setting is spin measurement along the  $z$ -direction (or  $x$ -direction) when Bob measures along the same direction, *i.e.*  $\mathcal{A}_0 = \sigma_z$  and  $\mathcal{A}_1 = \sigma_x$  respectively. Using inequalities (2.9) and Eq. (2.13), the lower bound of quantum secret key rate corresponding to the aforementioned definition, when the subsystem  $B$  interacts with the environment, becomes

$$r_B = \log_2 \left[ \frac{3 + \sqrt{1 - D_B}}{3 - \sqrt{1 - D_B}} \right] \quad (2.14)$$

It can be easily checked that, the maximally entangled state with no decoherence gives rise to maximum amount of quantum secret key rate, *i.e.* 1 obtained by using decoherence strength,  $D_B = 0$  in Eq.(2.14) or by using  $\delta = \frac{1}{4}$  in Eq.(2.9). It can be easily checked that, as the strength of decoherence increases, the secret key rate in 1s-DIQKD gets reduced.

### 2.3.2 Case II: Double interaction

Here we consider that both the subsystems,  $A$  and  $B$  interact with the environment under amplitude damping decoherence. After environmental interaction of both subsystems, the shared state becomes either

$$\rho''_{AB} = \sum_{i=0}^1 (W_{A,i} \otimes \mathbb{1}_2) \rho'_{AB} (W_{A,i}^\dagger \otimes \mathbb{1}_2), \quad (2.15)$$

where  $\rho'_{AB}$  is given by Eq.(2.11), or

$$\sigma''_{AB} = \sum_{i=0}^1 (W_{A,i} \otimes \mathbb{1}_2) \sigma'_{AB} (W_{A,i}^\dagger \otimes \mathbb{1}_2), \quad (2.16)$$

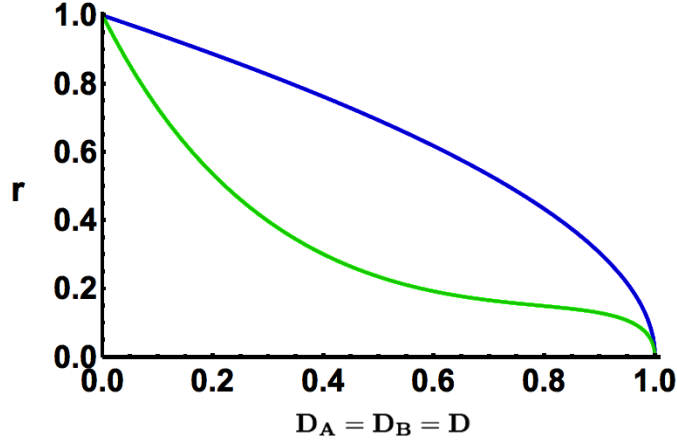


Figure 2.1: Lower bound of the quantum secret key rate for the initial Bell state  $|\Psi^\pm\rangle$  given by Eq.(2.10) is plotted versus the decoherence parameter  $D$ . The upper (blue) curve corresponds to Case-I (*i.e.* single interaction) while the lower (green) curve corresponds to Case-II (*i.e.* double interaction).

where  $\sigma'_{AB}$  is given by Eq.(2.12). Again, for both the states  $\rho''_{AB}$  and  $\sigma''_{AB}$ , the optimal set of measurement settings for Alice is  $\{\mathcal{A}_0 = \sigma_z, \mathcal{A}_1 = \sqrt{1-D^2}\sigma_x - D\sigma_z\}$ , where we consider, for simplicity, the interaction of both the subsystems  $A$  and  $B$  with the same environment, *i.e.*  $D_A = D_B = D$ . The left-hand side of Eq.(2.4) becomes

$$\frac{1}{2}[P(b_{\sigma_z}|a_{\mathcal{A}_0}) + P(b_{\sigma_x}|a_{\mathcal{A}_1})] = \frac{3 + D + 2D^2 + \sqrt{1-D^2}}{4 + 4D}, \quad (2.17)$$

when the shared state is  $\rho''_{AB}$ , and

$$\frac{1}{2}[P(b_{\sigma_z}|a_{\mathcal{A}_0}) + P(b_{\sigma_x}|a_{\mathcal{A}_1})] = \frac{3 + 3D + \sqrt{1-D^2}}{4 + 4D}, \quad (2.18)$$

when the shared state is  $\sigma''_{AB}$ .

In Fig.2.1 and Fig.2.2, we plot the respective secret key rates with the strength of decoherence,  $D$ . From these two figures, it is clear that the secret key rate when both subsystems interact with the environment is lower in comparison with the secret key rate when a single system interacts with environment, for all values of the environmental interaction strength  $D$ . It is worth mentioning that, for both the cases the lower bound of quantum secret key rate is inversely related to  $D$  and becomes zero when  $D = 1$ .

It is worth recounting here that for the amplitude damping channel, the teleportation fidelity can be improved between two parties when both of them are made to interact with

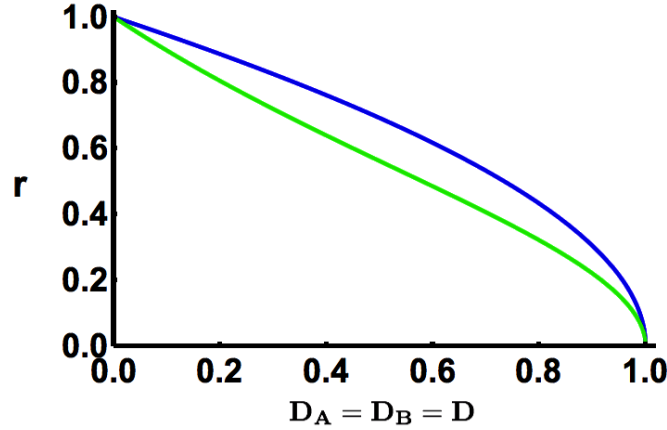


Figure 2.2: Lower bound of quantum secret key rate for the initial Bell state  $|\Phi^\pm\rangle$  given by Eq.(2.10) is plotted versus the decoherence parameter  $D$ . The upper (blue) curve corresponds to Case-I (*i.e.* single interaction) while the lower (green) curve corresponds to Case-II (*i.e.* double interaction).

the environment [BmcHHH00, Ban02, PM13]. Such a phenomenon occurs because the decoherence effect on both systems can improve the classical correlation between them, enhancing in turn the teleportation fidelity. However, no such effect occurs for the quantum secret key rate which is associated only with a quantum correlation *viz* steerability.

## 2.4 Improvement of quantum secret key rate

The technique of weak measurement and its reversal comes into effect for reducing the environmental effect represented by ADC in several contexts to protect quantum correlations [PM13, KU99, KJ06, KCRK09, LJKK11, KLKK12]. Unlike the case of preservation of teleportation fidelity [PM13], we investigate the preservation of quantum correlations in the form of steerability by using the technique of weak measurement and its reversal and we show its implication in quantum cryptography by protecting the secrecy of key rate in a 1s-DIQKD scenario, which is an important factor for secure processing of quantum information in the given scenario. In order to show improvement of quantum secret key rate under the action of weak measurement technique, we go for the two cases mentioned in the previous section, *i.e.* *Case-I* where the environment affects the subsystem  $B$  only during the time of traversal and *Case-II* where the environment affects both the subsystems.

### 2.4.1 Case-I: Single interaction

To neutralize the effect of decoherence, Alice makes a weak measurement with strength  $p_B$  on the subsystem  $B$  and considers the case when the system  $B$  is not detected. In this case, depending upon the chosen initial state  $|\Psi^\pm\rangle$  or  $|\Phi^\pm\rangle$  the combined state of the subsystems  $A$  and  $B$  becomes either

$$\rho_W = (\mathbb{1}_2 \otimes M_{B,0}) |\Psi^\pm\rangle \langle \Psi^\pm| (\mathbb{1}_2 \otimes M_{B,0}^\dagger), \quad (2.19)$$

or

$$\sigma_W = (\mathbb{1}_2 \otimes M_{B,0}) |\Phi^\pm\rangle \langle \Phi^\pm| (\mathbb{1}_2 \otimes M_{B,0}^\dagger), \quad (2.20)$$

where  $M_{B,0}$  is defined in Eq.(2.2) and  $\rho_W$  ( $\sigma_W$ ) is unnormalized because Alice discards the state when the subsystem  $B$  is detected. Hence, the success probability of generating the state  $\rho_W$  ( $\sigma_W$ ) by the method of post-selection is given by  $\text{Tr}[\rho_W] = \text{Tr}[\sigma_W] = 1 - \frac{p_B}{2}$ . Next, Alice sends the subsystem  $B$  to Bob through the environment. Due to environmental interaction via ADC, the shared state is transformed into either

$$\rho_E = \sum_{i=0}^1 (\mathbb{1}_2 \otimes W_{B,i}) \rho_W (\mathbb{1}_2 \otimes W_{B,i}^\dagger) \quad (2.21)$$

or

$$\sigma_E = \sum_{i=0}^1 (\mathbb{1}_2 \otimes W_{B,i}) \sigma_W (\mathbb{1}_2 \otimes W_{B,i}^\dagger) \quad (2.22)$$

After receiving the subsystem  $B$ , Bob applies a suitable reverse weak measurement with the Kraus operator given by Eq.(2.3). The final shared state thus becomes either

$$\rho_R = (\mathbb{1}_2 \otimes N_{B,0}) \rho_E (\mathbb{1}_2 \otimes N_{B,0}^\dagger), \quad (2.23)$$

or

$$\sigma_R = (\mathbb{1}_2 \otimes N_{B,0}) \sigma_E (\mathbb{1}_2 \otimes N_{B,0}^\dagger) \quad (2.24)$$

respectively. Now the strength of the reverse weak measurement  $q_B$ , in principle, can be chosen by Bob such that it maximizes the violation of the steering inequality (2.4) and hence, it maximizes the secret key rate associated with 1s-DIQKD as given by Eq.(2.9). The maximization plays an important role to restore the steerability, lost during the course of decoherence.

When Alice prepares the joint system of  $A$  and  $B$  either in the state  $|\Psi^\pm\rangle$  or in the state  $|\Phi^\pm\rangle$  given by Eq.(2.10), the left-hand side of the inequality(2.4) becomes

$$\frac{1}{2}[P(b_{\sigma_z}|a_{\mathcal{A}_0}) + P(b_{\sigma_x}|a_{\mathcal{A}_1})] = \frac{3}{4} + \frac{3}{4\sqrt{1+D_B-D_B p_B}}, \quad (2.25)$$

where Alice's measurement settings are the same as the measurement settings when the technique of weak measurement is not applied along with the decoherence, *i.e.*  $\{\mathcal{A}_0 = \sigma_z, \mathcal{A}_1 = \sigma_x\}$ , and the optimal strength of the reverse weak measurement is found to be  $q_B^O = \frac{2D_B + p_B - 2D_B p_B}{1 + D_B - D_B p_B}$ . Lower bound of the secret key rate is then given by

$$r_P^B = \log_2 \left[ \frac{\frac{3}{4} + \frac{3}{4\sqrt{1+D_B-D_B p_B}}}{\frac{3}{4} - \frac{3}{4\sqrt{1+D_B-D_B p_B}}} \right], \quad (2.26)$$

where the success probability of achieving this bound is the probability of sharing the state  $\rho_R$ , *i.e.*  $\text{Tr}[\rho_R] = (1 - D_B)(1 - p_B)$ .

In Fig.2.3, we compare the secret key rate given by Eq.(2.14) without using the technique of weak measurement with the secret key rate given by Eq.(2.26) when the technique of weak measurement and its reversal is used. It is clear from Fig.2.3 that, one can protect steerability and hence, the secret key rate in 1s-DIQKD scenario from the ill-effect of decoherence modeled by ADC through its enhancement caused by the action of weak measurement technique.

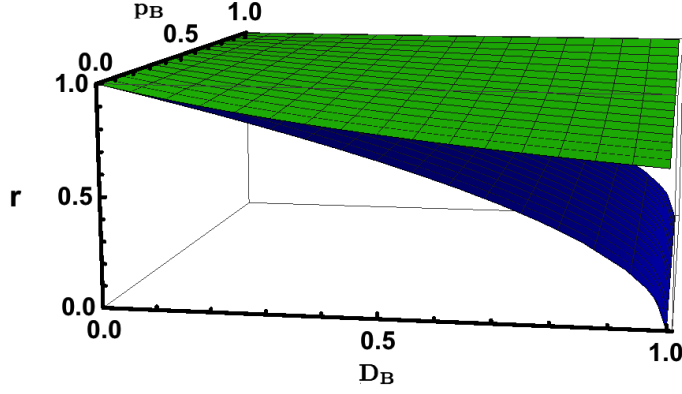


Figure 2.3: Lower bound of quantum secret key rate is plotted against the strength of decoherence  $D_B = D$  ( $x$ -axis) and the strength of weak measurement  $p_B$  ( $y$ -axis). The upper (green) surface is for the secret key rate given by Eq.(2.26) using the technique of weak measurement while the lower (blue) one is for the secret key rate given by Eq.(2.14) *i.e.* without using such technique.

## 2.4.2 Case-II: Double interaction

Here both the subsystems  $A$  and  $B$  interact with the environment via ADC. To protect the correlation from decoherence, Alice makes weak measurements on both subsystems. When both systems are not detected, the combined state of subsystems  $A$  and  $B$  becomes either

$$\rho'_W = (M_{A,0} \otimes M_{B,0}) |\Psi^\pm\rangle \langle \Psi^\pm| (M_{A,0} \otimes M_{B,0}^\dagger), \quad (2.27)$$

or

$$\sigma'_W = (M_{A,0} \otimes M_{B,0}) |\Phi^\pm\rangle \langle \Phi^\pm| (M_{A,0} \otimes M_{B,0}^\dagger). \quad (2.28)$$

depending upon the initial state  $|\Psi^\pm\rangle$  or  $|\Phi^\pm\rangle$  respectively. Next, Alice sends the subsystem  $B$  to Bob and allows both the subsystems to interact with the environment. Due to the environmental effect, the shared state becomes either

$$\rho'_E = \sum_{i=0}^1 \sum_{j=0}^1 (W_{A,i} \otimes W_{B,j}) \rho'_W (W_{A,i}^\dagger \otimes W_{B,j}^\dagger) \quad (2.29)$$

or

$$\sigma'_E = \sum_{i=0}^1 \sum_{j=0}^1 (W_{A,i} \otimes W_{B,j}) \sigma'_W (W_{A,i}^\dagger \otimes W_{B,j}^\dagger) \quad (2.30)$$

respectively. In the end, both of them apply reverse weak measurement having Kraus representation given by Eq.(2.3). The final shared state becomes either

$$\rho'_R = (N_{A,0} \otimes N_{B,0}) \rho'_E (N_{A,0} \otimes N_{B,0}^\dagger), \quad (2.31)$$

or

$$\sigma'_R = (N_{A,0} \otimes N_{B,0}) \sigma'_E (N_{A,0} \otimes N_{B,0}^\dagger). \quad (2.32)$$

Now, we study the steerability of the shared states  $\rho'_R$  ( $\sigma'_R$ ) after normalization. Let us consider that, Alice prepares the joint system comprising  $A$  and  $B$  in the state  $|\Psi^\pm\rangle$  and Alice's chosen set of observables is the same as that when both the subsystems interact with the environment without applying the technique of weak measurements, *i.e.*  $\{\mathcal{A}_0 = \sigma_z, \mathcal{A}_1 = \sqrt{1-D^2} \sigma_x - D\sigma_z\}$ . For computational simplicity, we adjust  $D_A = D_B = D$ ,  $p_A = p_B = p$  and  $q_A = q_B = q$  externally without the loss of our general assumption that, both the subsystems are detached and independent of each other. We numerically maximize the quantity  $\frac{1}{2}[P(b_{\sigma_z}|a_{\mathcal{A}_0}) + P(b_{\sigma_x}|a_{\mathcal{A}_1})]$  with respect to the strength of the reverse weak measurement  $q$ .

From Fig.2.4, the improvement of quantum secret key rate, by making use of the weak measurement technique, can be observed in contrast to its declination governed by the decoherence, when Alice prepares the subsystems in the state  $|\Psi^\pm\rangle$ . Whereas such improvement of the key rate using weak measurement is not possible for the initially prepared state  $|\Phi^\pm\rangle$ .

As this technique is associated with the post-selection of weak measurement, the success probability of sharing the final state  $\rho'_R$  ( $\sigma'_R$ ) is given by  $\max_q[\text{Tr}[\rho'_R]]$  ( $\max_q[\text{Tr}[\sigma'_R]]$ ). Hence it is interesting to calculate the average steerability of the state  $\rho'_R$ , where the aver-

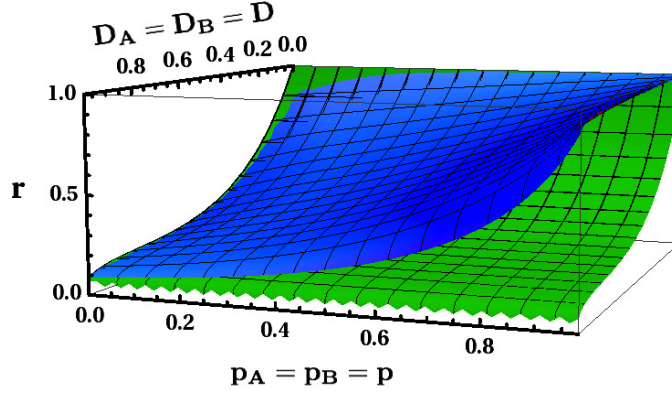


Figure 2.4: Lower bound of quantum secret key rate is plotted against the strength of decoherence  $D_A = D_B = D$  ( $x$ -axis) and the strength of weak measurement  $p_A = p_B = p$  ( $y$ -axis). The upper (blue) surface corresponds to the secret key rate associated with  $\rho'_R$  obtained successively from the initial state given by Eq.(2.10) where the technique of weak measurement is utilized and the lower (green) surface corresponds to the secret key rate associated with the state  $\rho''_{AB}$  given by Eq.(2.15) where the technique of weak measurement is not utilized.

age is taken over the success probability of sharing the state  $\rho'_R$ . It also takes the successful detection of the subsystems by the measuring device (during the weak measurement) into account where the entanglement between the subsystems is completely lost and the separable state optimally gives rise to  $\frac{3}{4}$  as the left-hand side of the inequality(2.4). Thus, the relevant quantity which provides lower bound of the secret key rate (or in other words, the average of secret key rate,  $r_{Av}$ ) corresponding to our framework, depending upon the success probability is given by  $\left[ [\text{Tr}[\rho'_R]] \frac{1}{2} [P(b_{\sigma_z}|a_{\mathcal{A}0}) + P(b_{\sigma_x}|a_{\mathcal{A}1})] + (1 - [\text{Tr}[\rho'_R]]) \frac{3}{4} \right]_{q=q^*}$ , where the reverse weak measurement parameter  $q^*$  maximizes the left-hand side of the steering inequality(2.4) corresponding to *Case-II* and  $\frac{3}{4}$  is the upper bound of the left-hand side of inequality(2.4) achievable for an unsteerable state with the help of an LHS model.

Fig.2.5 shows the improvement in the average of quantum secret key rate,  $r_{Av}$  corresponding to the shared state  $\rho'_R$ . We observe that such improvement in a notable region of parameter space is allowed by the technique of weak measurement compared to the secret key rate under ADC without employing the weak measurement technique. To quantify the above improvement in  $r_{Av}$  with respect to  $\rho'_R$ , we quantify the improvement factor as,

$$r_I = \frac{r_{Av}}{r_{\rho''_{AB}}}, \quad (2.33)$$

where  $r_{\rho''_{AB}}$  is the lower bound of the secret key rate obtained from the shared state  $\rho''_{AB}$  given

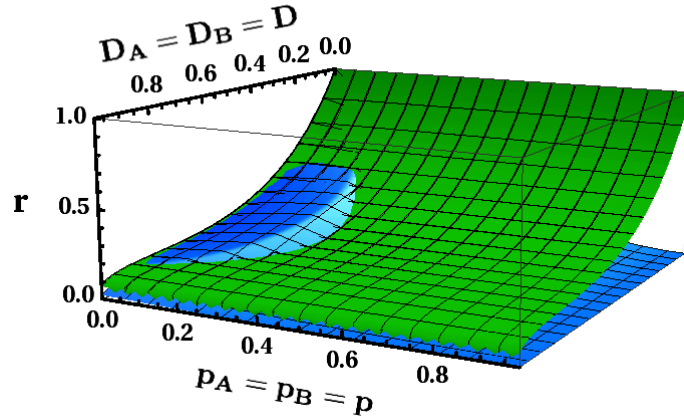


Figure 2.5: The average of quantum secret key rate,  $r_{Av}$  is plotted (blue surface) against the strength of decoherence  $D_A = D_B = D$  (x-axis) and the strength of weak measurement  $p_A = p_B = p$  (y-axis). The green surface corresponding to the case without weak measurement is the same as in Fig.2.4. It can be seen from the blue surface that, the improvement of the average secret key rate is possible for a certain range of values of the strength of decoherence and weak measurement.

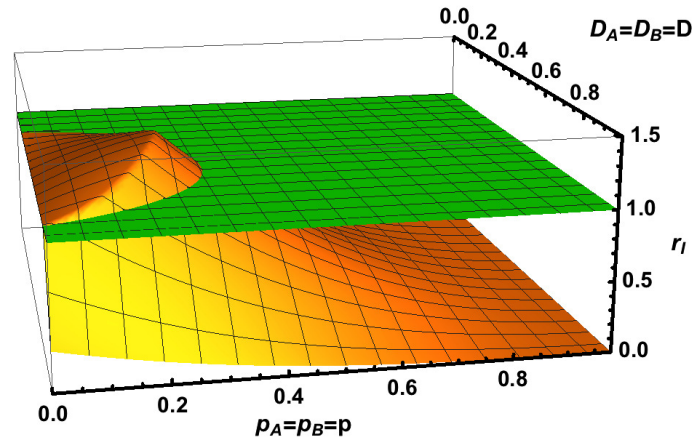


Figure 2.6: The improvement factor  $r_I$  (yellow surface) is plotted against the decoherence strength,  $D(= D_A = D_B)$  (x-axis) and the weak measurement strength,  $p(= p_A = p_B)$  (y-axis). By utilizing the weak measurement technique, the improvement of the given lower bound of the average secret key rate can be seen well above the green plane representing  $r_I = 1$  for a certain region in  $\{D, p\}$  space.

by Eq.(2.15). We plot  $r_I$  in Fig.2.6, where the region indicating  $r_I > 1$ , *i.e.*  $r_{Av} > r_{\rho_{AB}}''$ , is clearly demarcated. Therefore the technique of weak measurement and its reversal turns out to be effective for certain parametric regions even where the successful detection of the subsystems by the measuring device is not ignored.

## 2.5 Summary and Outlook

Quantum steering, as a quantum correlation, has a fundamental role in one-sided device-independent quantum cryptography, where the secrecy of key rate depends on the mag-

nitude of violation of a special kind of steering inequality, called as fine-grained steering inequality [PKM14]. It emerges from the aspect of monogamy of quantum steering. It is a challenge to isolate resourceful quantum systems from the surroundings, in practical situations, such that their implication in information processing tasks can be kept intact. In this chapter, we aim to protect quantum steering and its cryptographic utility by discussing the effect on steerability and the secret key rate in 1s-DIQKD scenario when the system possessed by one or both the parties interact with the environment via an amplitude damping channel. Here we indicate from the analogy of improvement of the teleportation fidelity under amplitude damping decoherence [Ban02, PM13] that, such enhancement may be associated with the classical correlation, because the secret key rate, whose lower bound is fixed by a quantum correlation *viz.*, the steerability of bipartite states, is found to be declining under the identical set-up of environmental coupling. It falls down in a non-linear way with the rise of the coupling strength where temporal memory of the evolution is abandoned.

Under the action of the weak measurement technique, we show that quantum steerability and the secret key rate can be preserved in the presence of amplitude damping decoherence. We show that for any maximally entangled initial state one can protect the secret key rate in 1s-DIQKD scenario with the help of weak measurement and its reversal when one of the parties of a bipartite system interacts with the environment. However, when both the subsystems interact with the environment, the technique of weak measurement can protect the secret key rate only for the prepared states of kind  $|\Psi^\pm\rangle$ . Similar to the case of improvement of the teleportation fidelity [PM13], the technique of weak measurement fails to protect the key rate for the prepared states of kind  $|\Phi^\pm\rangle$ . The technique of weak measurement is associated with a success probability, as it is implemented with post-selection by discarding the state when it is detected. We further show that considering even the successful detection of the system by the measuring device, the lower bound of the secret key rate under individual attack turns out to be higher than the case where the weak measurement technique is not applied, for a considerable region of the interaction parameters. It may be interesting to perform, in future studies, the effect of weak measure-

ment and its reversal on the key rate in the context of other decoherence channels such as bit-flip, phase-flip and depolarising channels.

## Cost of a quantum correlation

The preservation of a quantum correlation is discussed in the previous chapter. As quantum correlation acts as a resource in an information processing task, it is inevitably important to keep a record of its gain or loss in different practical situations. The presence of quantum entanglement can be certified from the statistics of measurement outcomes in different operational scenarios. For example, Bell nonlocal correlation via the violation of an LHV model does this in device-independent scenario [Bel64, BCP<sup>+</sup>14b], whereas another nonlocal correlation, *viz* quantum steering via the violation of an LHS model does this in one-sided device-independent scenario [Sch35, WJD07, Rei89, WSG<sup>+</sup>11, PKM14, CPMA14, CPM15]. Inequivalent operational scenarios have different applications in quantum information processing [QVC<sup>+</sup>15] and cost some amount of quantum correlations responsible for those applications. Therefore quantification of the strength of quantum correlations is another important aspect of quantum information theory, which is studied in this chapter.

Motivated by the question of how much quantum spatial nonlocal correlation *viz* quantum steerability can be demonstrated in a steering scenario, steering weight is defined in [SNC14] earlier with its quantitative characterization followed from the resource theoretic formulations proposed in [GA15, CBLC16]. The set of postulates for a bonafide quantifier of steering or more precisely, for a convex steering monotone are discussed in Sec.1.4.2 of Chapter 1. The usefulness of a quantifier depends on its operational advantage, hence we explore such a steering measure in this chapter by comparing its robustness with steering weight in a given scenario. This chapter embodies our work "*Cost of Einstein-Podolsky-*

"Rosen steering in the context of extremal boxes", D. Das, S. Datta, C. Jebaratnam, and A. S. Majumdar, Phys. Rev. A, **97**, 022110 (2018) [DDJM18].

The extremal points of a convex set of measurement correlations in the absence of a quantum correlation, particularly under consideration, make a significant contribution to construct the measures of this kind. For example, Brunner *et al* proposed nonlocal cost (as defined in Sec.1.3.3.1) in case of the Bell scenario with a finite number of settings per party and a finite number of outcomes per setting, where the set of correlations admitting LHV model forms a convex polytope [Fin82, PR94, BLM<sup>+</sup>05]. The nontrivial facet inequalities of this polytope are dubbed as Bell inequalities. Similarly, an LHV-LHS model producing correlations between the black-box side and the trusted side can be expressed as a convex mixture of the extremal points of the unsteerable set. EPR steering can thus be characterized by the exclusion of a quantum correlation or a family of quantum correlations from this convex set of unsteerable correlations [CFFW15]. In this work, we present a method to check EPR steering in the context of such extremal points in a steering scenario where Alice performs two black-box measurements and Bob performs projective qubit measurements corresponding to any two mutually unbiased bases (MUBs). We term the measure of quantum steering arising from this formulation as steering cost which is shown to be a convex steering monotone. We illustrate that this method can be used to check and quantify the steerability of two families of measurement correlations. We also discuss the experimental advantage of steering cost by comparing it with the steering weight.

### 3.1 Extremal non-signalling boxes

Let us recall from Sec.1.3.3.1 that, the set of joint probabilities for binary inputs and binary outputs can be called as a box or a correlation with a representation  $P(a, b|x, y) := \{p(a, b|\mathcal{A}_x, \mathcal{B}_y)\}_{a, b, x, y}$  or  $\{p(a, b|x, y)\}_{a, b, x, y}$ . The convex polytope of non-signalling boxes is composed of 24 extremal boxes [BLM<sup>+</sup>05], among which 8 PR boxes [PR94] can be

expressed as,

$$P_{PR}^{\alpha\beta\gamma}(a,b|x,y) = \begin{cases} \frac{1}{2}, & a \oplus b = x \cdot y \oplus \alpha x \oplus \beta y \oplus \gamma \\ 0, & \text{otherwise} \end{cases} \quad (3.1)$$

and 16 local-deterministic boxes can be written as,

$$P_D^{\alpha\beta\gamma\epsilon}(a,b|x,y) = \begin{cases} 1, & a = \alpha x \oplus \beta, b = \gamma y \oplus \epsilon \\ 0, & \text{otherwise.} \end{cases} \quad (3.2)$$

where,  $\alpha, \beta, \gamma, \epsilon \in \{0, 1\}$  and  $\oplus$  denotes addition modulo 2. All the deterministic boxes as the product of marginals for Alice and Bob can be written as,  $P_D^{\alpha\beta\gamma\epsilon}(a,b|x,y) = P_D^{\alpha\beta}(a|x)P_D^{\gamma\epsilon}(b|y)$ , where deterministic box at Alice's side is given by,

$$P_D^{\alpha\beta}(a|x) = \begin{cases} 1, & a = \alpha x \oplus \beta \\ 0, & \text{otherwise} \end{cases} \quad (3.3)$$

and deterministic box at Bob's side is given by,

$$P_D^{\gamma\epsilon}(b|y) = \begin{cases} 1, & b = \gamma y \oplus \epsilon \\ 0, & \text{otherwise.} \end{cases} \quad (3.4)$$

The 8 PR boxes and the 16 local-deterministic boxes are equivalent under local reversible operations(LRO). By using LRO Alice and Bob can convert a PR box into another PR box, or a local-deterministic box into another local-deterministic box. LRO is designed [BLM<sup>+</sup>05] under the relabelling of Alice's inputs  $x \rightarrow x \oplus 1$ , and her outputs  $a \rightarrow a \oplus \alpha x \oplus \beta$  subject to the inputs  $x$  and similarly under the relabelling of Bob's inputs and outputs.

### 3.2 Steering scenario in the context of extremal boxes

Let us consider a steering scenario where Alice and Bob share an unknown quantum system described by  $\rho_{AB} \in \mathcal{B}(\mathcal{H}_A \otimes \mathcal{H}_B)$ , with Alice performing a set of black-box measurements and the Hilbert-space dimension of Bob's subsystem is known. Such a scenario is called one-sided device-independent since Alice's measurement operators  $\mathbf{M}_{\mathcal{A}} := \{M_{a|x}\}_{a,x}$  corresponding to her black-box measuring device are unknown. The steering scenario is completely characterized by an assemblage [Pus13]  $\sigma := \{\sigma_{a|x}\}_{a,x}$  where each element of unnormalized conditional state at Bob's side is given by Eq.(1.33). Let  $\Sigma^S$  denote the set of all valid assemblages.

In the above scenario, Alice demonstrates steerability to Bob if the assemblage does not have a local hidden state (LHS) model given by Eq.(1.34). Let  $\Sigma^{US}$  denote the set of all unsteerable assemblages. Now  $p(a|\mathcal{A}_x, \lambda)$  or simply  $p(a|x, \lambda)$  can arise from the decomposition of deterministic probability distributions  $D(a|x, \chi)$  at the level of ontic variable  $\chi$  as  $p(a|x, \lambda) = \sum_{\chi} p(\chi|\lambda)D(a|x, \chi)$  where a particular outcome  $a$  corresponding to a measurement  $\mathcal{A}_x$  at Alice's side can be deterministically predicted from the function  $D(a|x, \chi) = \delta_{a, f(\mathcal{A}_x, \chi)}$  or  $\delta_{a, f(x, \chi)}$ . By using  $\sigma_{\chi} = \sum_{\lambda} p(\lambda)p(\chi|\lambda)\rho_B^{\lambda}$  in Eq.(1.34), an element of the given assemblage  $\sigma \in \Sigma^{US}$  can be decomposed as [Pus13, CS16],

$$\sigma_{a|x} = \sum_{\chi} D(a|x, \chi)\sigma_{\chi} = \sum_{\chi} \delta_{a, f(x, \chi)}\sigma_{\chi} = \sum_{\substack{\chi \\ f(x, \chi)=a}} \sigma_{\chi}, \quad (3.5)$$

where  $D(a|x, \chi)$  gives the single-partite extremal conditional probability for Alice determined at ontic space of variables  $\chi$  and  $\sigma_{\chi}$  satisfy  $\sigma_{\chi} \geq 0$  and  $\sum_{\chi} \text{Tr}[\sigma_{\chi}] = \sum_{\lambda, \chi} p(\lambda)p(\chi|\lambda) = 1$ .

A semi-definite programming (SDP) [VB96, Wat11] is a method to optimize a linear functional of a positive semi-definite self-adjoint matrix subject to some constraints on its linear functionals. A linear steering functional  $\mathcal{F} := \{\mathcal{F}_{a|x}\}_{a,x}$  can be defined such that it maps an unsteerable assemblage to a real number. If it is maximized over all possible descriptions of LHS via SDP, then it gives an upper bound of a linear steering inequality corresponding to that functional. The quantum mechanical violation of such an upper

bound demonstrates quantum steering. In the scenario mentioned above, the SDP can be written as [Pus13]

$$\begin{aligned} & \text{maximize} && \sum_{\chi} \text{Tr}[(\sum_x \mathcal{F}_{f(x,\chi)|x})\sigma_{\chi}] \\ & \text{subject to} && \sigma_{\chi} \geq 0 \\ & && \sum_{\chi} \text{Tr}[\sigma_{\chi}] = 1. \end{aligned}$$

which may be reduced to a feasibility problem as given in [CS16]. Hence the full interpretation of a steering scenario depends on the assemblage, acted upon by an observable.

Let us suppose that,  $\Pi_{\mathcal{B}_y}^b$  or  $\Pi_{b|y}$  represents a projective measurement corresponding to an observable  $\mathcal{B}_y$  at Bob's side which yields outcome  $b$ . The scenario, where Bob performs a set of projective measurements  $\mathbf{\Pi}_{\mathcal{B}} := \{\Pi_{b|y}\}_{b,y}$  on the given assemblage  $\sigma$ , is fully characterized by the set of measurement correlations which is a box shared by Alice and Bob,  $P(a, b|x, y) = \left\{ \text{Tr}[\Pi_{b|y}\sigma_{a|x}] \right\}_{a,b,x,y}$ . Let us denote the set of all correlations, that belongs to the given steering scenario, as  $\mathcal{N}_{\Sigma S}$ . The set of correlations, that admit a LHV-LHS model given by Eq.(1.35), is denoted by  $\mathcal{L}_{\Sigma US}$ , which forms a convex subset of  $\mathcal{N}_{\Sigma S}$  [CJWR09]. Such correlations can be called an unsteerable set. In particular, the decomposition of an LHV-LHS model given by Eq.(1.36) in terms of the extremal points of  $\mathcal{L}_{\Sigma US}$  can be simplified as [CFFW15],

$$\begin{aligned} p(a, b|x, y) &= \sum_{\chi, \zeta} p(\chi, \zeta) D(a|x, \chi) \langle \psi_{\zeta} | \Pi_{b|y} | \psi_{\zeta} \rangle \quad \forall a, b, x, y \\ &= \sum_{\chi, \zeta} p(\chi, \zeta) \delta_{a, f(x, \chi)} \langle \psi_{\zeta} | \Pi_{b|y} | \psi_{\zeta} \rangle \\ &= \sum_{\substack{\chi, \zeta \\ f(x, \chi) = a}} p(\chi, \zeta) \langle \psi_{\zeta} | \Pi_{b|y} | \psi_{\zeta} \rangle \end{aligned} \tag{3.6}$$

where the hidden variables  $\chi$  and  $\zeta$  correspond to Alice and Bob respectively.

### 3.3 Quantifying EPR steering

#### 3.3.1 Definition

The nonlocal cost was defined in the operational scenario of binary inputs and binary outputs [BCSS11]. In a similar fashion, steering cost of a box  $P(a, b|x, y) \in \mathcal{N}_{\Sigma S}$  can be defined. Analogous to EPR2 decomposition [EPR92] in Bell scenario, we first decompose the given box  $P(a, b|x, y)$  as a convex mixture of a steerable part and an unsteerable part, *i.e.*

$$P(a, b|x, y) = p_S P_S(a, b|x, y) + (1 - p_S) P_{US}(a, b|x, y), \quad (3.7)$$

where  $P_S(a, b|x, y)$  (or simply,  $P_S$ ) is a steerable box weighted by  $p_S$  ( $0 \leq p_S \leq 1$ ) and  $P_{US}(a, b|x, y)$  (or simply,  $P_{US}$ ) is an unsteerable box. If the weight of the steering part is minimized over all possible decompositions of the form given by Eq.(3.7), then the steering cost of the box  $P(a, b|x, y)$ , denoted by  $C_{\text{steer}}(P)$ , is defined as

$$C_{\text{steer}}(P) := \min_{\text{decompositions}} p_S. \quad (3.8)$$

where,  $0 \leq C_{\text{steer}}(P) \leq 1$  (since,  $0 \leq p_S \leq 1$ ). It follows that, for the optimal decomposition of a box, the steerable part  $P_S(a, b|x, y)$  has the maximum steering cost, *i.e.*  $C_{\text{steer}}(P_S) = 1$  since it is an extremal steerable box and can not be decomposed further. An extremal steerable box denoted by  $P_S^{\text{Ext}}(a, b|x, y)$ , without a convex decomposition of boxes in the set  $\mathcal{N}_{\Sigma S}$ , violates a steering inequality maximally in the given steering scenario.'

#### 3.3.2 Consistency with the resource theory of steering

To demonstrate that the steering cost  $C_{\text{steer}}(P)$  is a proper quantifier of steering, or it is a convex steering monotone [GA15], we introduce the following notations. A box  $P(a, b|x, y)$  which is obtained by Bob performing projective measurements  $\mathbf{\Pi}_{\mathcal{B}}$  on an assemblage  $\sigma$ , is denoted by  $P[\sigma]$  as it owns complete characterization in terms of assemblages. Here,  $P[\sigma] := P(a, b|x, y) = \left\{ \text{Tr} [\mathbf{\Pi}_{b|y} \sigma_{a|x}] \right\}_{a, b, x, y}$ . Now we consider the situation where deterministic *one-way local operations and classical communications* (1W-

LOCCs) [GA15] is allowed from the trusted party (*viz* Bob) to the untrusted party (*viz* Alice) before Bob measures on the assemblage. We define the deterministic 1W-LOCC, following from [HLL16], as a completely positive trace preserving (CPTP) map  $\mathcal{M}$  that transform an assemblage  $\sigma$  into a final assemblage  $\mathcal{M}(\sigma)$ , where

$$\mathcal{M}(\sigma) = \sum_{\omega} \mathcal{M}_{\omega}(\sigma) := \sum_{\omega} \mathcal{K}_{\omega} \mathcal{W}_{\omega}(\sigma) \mathcal{K}_{\omega}^{\dagger}, \quad (3.9)$$

with  $\mathcal{W}_{\omega}$ , being a deterministic wiring map transforms one assemblage  $\sigma = \{\sigma_{a|x}\}_{a,x}$  to another assemblage  $\tilde{\sigma} = \{\tilde{\sigma}_{a'|x'}\}_{a',x'}$  having different measurement setting  $\mathcal{A}_{x'}$  and outcome  $a'$  at Alice's side in the following way,

$$[\mathcal{W}_{\omega}(\sigma)]_{x'} := \tilde{\sigma}_{a'|x'} = \sum_{a,x} p(x|x', \omega) p(a'|x', a, x, \omega) \sigma_{a|x} \quad \forall a', x'. \quad (3.10)$$

Let us define

$$\mathcal{D}_{\omega}(\sigma) := \frac{\mathcal{M}_{\omega}(\sigma)}{\text{Tr}[\mathcal{M}_{\omega}(\sigma)]},$$

which is the set of normalized conditional states arising from the action of a subchannel  $\mathcal{M}_{\omega}$ , labeled by  $\omega$ , of the CPTP map  $\mathcal{M}$  on the assemblage  $\sigma$  at Bob's end. Here,  $\mathcal{T}(\omega) := \text{Tr}[\mathcal{M}_{\omega}(\sigma)]$  is the probability of transmitting the assemblage  $\sigma$  through the  $\omega$ -th subchannel of  $\mathcal{M}$  and  $\sum_{\omega} \mathcal{T}(\omega) \leq 1$ . Let us denote  $\mathcal{D}_{\omega}(\sigma) := \{[\mathcal{D}_{\omega}(\sigma)]_{a'|x'}\}_{a',x'}$ , where the normalized state  $[\mathcal{D}_{\omega}(\sigma)]_{a'|x'}$  denotes an element of  $\mathcal{D}_{\omega}(\sigma)$ . Hence, we can define  $P[\mathcal{D}_{\omega}(\sigma)]$  which is a box arising from any valid assemblage (steerable or unsteerable)  $\sigma \in \Sigma^S$  after the action of a map  $\mathcal{M}_{\omega}$  as follows,

$$P[\mathcal{D}_{\omega}(\sigma)] = P(a'b|x'y) := \left\{ p(a'|x') \text{Tr}[\Pi_{b|y}[\mathcal{D}_{\omega}(\sigma)]_{a'|x'}] \right\}_{a',b,x',y}, \quad (3.11)$$

where  $p(a'|x')$  is the conditional probability of obtaining the outcome  $a'$ , when Alice measures  $\mathcal{A}_{x'}$ , and is given by

$$p(a'|x') = \sum_{a,x} p(x|x', \omega) p(a'|x', a, x, \omega) p(a|x).$$

This can be obtained from Eq.(3.10) by expressing the elements of the assemblages *i.e.*  $\sigma_{a|x}$  and  $\tilde{\sigma}_{a'|x'}$  at Bob's side as  $p(a|x)\rho_{a|x}$  and  $p(a'|x')\tilde{\rho}_{a'|x'}$  respectively where  $p(a|x)$  and  $p(a'|x')$  are the conditional probabilities and  $\rho_{a|x}$  and  $\tilde{\rho}_{a'|x'}$  are normalized states at Bob's side and by taking the trace on both side of the Eq.(3.10). With the above notations, we show that  $C_{\text{steer}}(P[\sigma])$  fulfills all the following properties of a bonafide steering quantifier.

### 3.3.2.1 Faithfulness

An unsteerable correlation  $P_{US}(a,b|x,y) \in \mathcal{L}_{\Sigma^{US}}$  can not be decomposed into a steerable and an unsteerable part as given by Eq.(3.7) because the set of unsteerable correlations *i.e.*  $\mathcal{L}_{\Sigma^{US}}$  is convex. Thus the weight of the steerable part *i.e.*  $p_S$  reduces to zero for all possible convex decompositions of an unsteerable box in terms of other unsteerable boxes. Hence for all unsteerable assemblage *i.e.*  $\sigma \in \Sigma^{US}$ , the steering cost  $C_{\text{steer}}(P_{US}[\sigma]) = 0$ .

### 3.3.2.2 Monotonicity

$C_{\text{steer}}(P[\sigma])$  does not increase on average under deterministic 1W-LOCCs, *i.e.*

$$\sum_{\omega} \mathcal{T}(\omega) C_{\text{steer}}(P[\mathcal{D}_{\omega}(\sigma)]) \leq C_{\text{steer}}(P[\sigma]), \quad \forall \sigma \in \Sigma^S. \quad (3.12)$$

*Proof.* Let us consider the following decomposition of an arbitrary assemblage  $\sigma := \{\sigma_{a|x}\}_{a,x} \in \Sigma^S$ :

$$\sigma_{a|x} = p_S \sigma_{a|x}^S + (1 - p_S) \sigma_{a|x}^{US} \quad \forall a, x, \quad (3.13)$$

where  $\sigma_{a|x}^S$  is an element of a steerable assemblage  $\sigma^S$  and  $\sigma_{a|x}^{US}$  is an element of an unsteerable assemblage  $\sigma^{US} \in \Sigma^{US}$ . Now, one can write,

$$\text{Tr} [\Pi_{b|y} \sigma_{a|x}] = p_S \text{Tr} [\Pi_{b|y} \sigma_{a|x}^S] + (1 - p_S) \text{Tr} [\Pi_{b|y} \sigma_{a|x}^{US}] \quad \forall a, b, x, y. \quad (3.14)$$

From the analogy given above, the box  $P[\sigma]$  arising from assemblage  $\sigma$  can be decomposed

as,

$$P[\boldsymbol{\sigma}] = p_S P_S[\boldsymbol{\sigma}^S] + (1 - p_S) P_{US}[\boldsymbol{\sigma}^{US}]. \quad (3.15)$$

where,  $P_S[\boldsymbol{\sigma}^S]$  is a steerable box, produced from the steerable assemblage  $\boldsymbol{\sigma}^S$  and  $P_S[\boldsymbol{\sigma}^{US}]$  is an unsteerable box, produced from the unsteerable assemblage  $\boldsymbol{\sigma}^{US}$ . The steering cost of the box  $P[\boldsymbol{\sigma}]$ , *i.e.*  $C_{\text{steer}}(P[\boldsymbol{\sigma}])$  is obtained by minimizing  $p_S$  in Eq.(3.15) over all such possible decompositions. Now let the decomposition(3.15) be the optimal decomposition, for which  $p_S = C_{\text{steer}}(P[\boldsymbol{\sigma}])$ .

Let us come to the set of normalized states  $\mathcal{D}_\omega(\boldsymbol{\sigma})$ , where  $\mathcal{D}_\omega$  has been applied on the assemblage  $\boldsymbol{\sigma}$  which produces the box  $P[\boldsymbol{\sigma}]$  with the optimal decomposition given by Eq.(3.15) with  $p_S = C_{\text{steer}}(P[\boldsymbol{\sigma}])$ . From Eq.(3.13), we have,

$$\mathcal{D}_\omega(\boldsymbol{\sigma}) = \mathcal{D}_\omega\left(p_S \boldsymbol{\sigma}^S + (1 - p_S) \boldsymbol{\sigma}^{US}\right) = \frac{\mathcal{M}_\omega\left(p_S \boldsymbol{\sigma}^S + (1 - p_S) \boldsymbol{\sigma}^{US}\right)}{\text{Tr}[\mathcal{M}_\omega(\boldsymbol{\sigma})]}, \quad (3.16)$$

where

$$\mathcal{M}_\omega\left(p_S \boldsymbol{\sigma}^S + (1 - p_S) \boldsymbol{\sigma}^{US}\right) = \mathcal{K}_\omega \mathcal{W}_\omega\left(p_S \boldsymbol{\sigma}^S + (1 - p_S) \boldsymbol{\sigma}^{US}\right) \mathcal{K}_\omega^\dagger. \quad (3.17)$$

Now, we consider the assemblage,

$$\tilde{\boldsymbol{\sigma}} = \{\tilde{\boldsymbol{\sigma}}_{a'|x'}\}_{a',x'} = \mathcal{W}_\omega\left(p_S \boldsymbol{\sigma}^S + (1 - p_S) \boldsymbol{\sigma}^{US}\right). \quad (3.18)$$

From Eq. (3.10), it follows that each element in the above assemblage  $\tilde{\boldsymbol{\sigma}}$  has the following decomposition:

$$\begin{aligned} \tilde{\boldsymbol{\sigma}}_{a'|x'} &= \sum_{a,x} p(x|x', \omega) p(a'|x', a, x, \omega) \left( p_S \boldsymbol{\sigma}_{a|x}^S + (1 - p_S) \boldsymbol{\sigma}_{a|x}^{US} \right) \\ &= p_S \sum_{a,x} p(x|x', \omega) p(a'|x', a, x, \omega) \boldsymbol{\sigma}_{a|x}^S + (1 - p_S) \sum_{a,x} p(x|x', \omega) p(a'|x', a, x, \omega) \boldsymbol{\sigma}_{a|x}^{US} \quad \forall a', x', \end{aligned} \quad (3.19)$$

which implies that

$$\mathcal{W}_\omega(p_S \boldsymbol{\sigma}^S + (1 - p_S) \boldsymbol{\sigma}^{US}) = p_S \mathcal{W}_\omega(\boldsymbol{\sigma}^S) + (1 - p_S) \mathcal{W}_\omega(\boldsymbol{\sigma}^{US}). \quad (3.20)$$

Hence, from Eqs.(3.17) and (3.20), we obtain

$$\begin{aligned} \mathcal{M}_\omega(p_S \boldsymbol{\sigma}^S + (1 - p_S) \boldsymbol{\sigma}^{US}) &= \mathcal{K}_\omega [p_S \mathcal{W}_\omega(\boldsymbol{\sigma}^S) + (1 - p_S) \mathcal{W}_\omega(\boldsymbol{\sigma}^{US})] \mathcal{K}_\omega^\dagger \\ &= p_S \mathcal{K}_\omega [\mathcal{W}_\omega(\boldsymbol{\sigma}^S)] \mathcal{K}_\omega^\dagger + (1 - p_S) \mathcal{K}_\omega [\mathcal{W}_\omega(\boldsymbol{\sigma}^{US})] \mathcal{K}_\omega^\dagger \\ &= p_S \mathcal{M}_\omega(\boldsymbol{\sigma}^S) + (1 - p_S) \mathcal{M}_\omega(\boldsymbol{\sigma}^{US}) \end{aligned} \quad (3.21)$$

Now from Eqs.(3.16) and (3.21), we obtain

$$\begin{aligned} \mathcal{D}_\omega(\boldsymbol{\sigma}) &= \frac{p_S \mathcal{M}_\omega(\boldsymbol{\sigma}^S) + (1 - p_S) \mathcal{M}_\omega(\boldsymbol{\sigma}^{US})}{\text{Tr}[\mathcal{M}_\omega(\boldsymbol{\sigma})]} \\ &= p_S \mathcal{D}_\omega(\boldsymbol{\sigma}^S) \frac{\text{Tr}[\mathcal{M}_\omega(\boldsymbol{\sigma}^S)]}{\text{Tr}[\mathcal{M}_\omega(\boldsymbol{\sigma})]} + (1 - p_S) \mathcal{D}_\omega(\boldsymbol{\sigma}^{US}) \frac{\text{Tr}[\mathcal{M}_\omega(\boldsymbol{\sigma}^{US})]}{\text{Tr}[\mathcal{M}_\omega(\boldsymbol{\sigma})]}, \end{aligned} \quad (3.22)$$

which implies that each element of  $\mathcal{D}_\omega(\boldsymbol{\sigma})$  has the following decomposition:

$$[\mathcal{D}_\omega(\boldsymbol{\sigma})]_{a'|x'} = p_S [\mathcal{D}_\omega(\boldsymbol{\sigma}^S)]_{a'|x'} \frac{\text{Tr}[\mathcal{M}_\omega(\boldsymbol{\sigma}^S)]}{\text{Tr}[\mathcal{M}_\omega(\boldsymbol{\sigma})]} + (1 - p_S) [\mathcal{D}_\omega(\boldsymbol{\sigma}^{US})]_{a'|x'} \frac{\text{Tr}[\mathcal{M}_\omega(\boldsymbol{\sigma}^{US})]}{\text{Tr}[\mathcal{M}_\omega(\boldsymbol{\sigma})]} \quad \forall a', x'. \quad (3.23)$$

From Eq. (3.23), one can write,

$$\begin{aligned} p(a'|x') \text{Tr} \left[ \Pi_{b|y} [\mathcal{D}_\omega(\boldsymbol{\sigma})]_{a'|x'} \right] &= p_S \frac{\text{Tr}[\mathcal{M}_\omega(\boldsymbol{\sigma}^S)]}{\text{Tr}[\mathcal{M}_\omega(\boldsymbol{\sigma})]} p(a'|x') \text{Tr} \left[ \Pi_{b|y} [\mathcal{D}_\omega(\boldsymbol{\sigma}^S)]_{a'|x'} \right] \\ &\quad + (1 - p_S) \frac{\text{Tr}[\mathcal{M}_\omega(\boldsymbol{\sigma}^{US})]}{\text{Tr}[\mathcal{M}_\omega(\boldsymbol{\sigma})]} p(a'|x') \text{Tr} \left[ \Pi_{b|y} [\mathcal{D}_\omega(\boldsymbol{\sigma}^{US})]_{a'|x'} \right] \\ &\quad \forall a', b, x', y. \end{aligned} \quad (3.24)$$

Hence, from Eq. (3.24), we get the following decomposition for the box  $P[\mathcal{D}_\omega(\boldsymbol{\sigma})]$ :

$$P[\mathcal{D}_\omega(\boldsymbol{\sigma})] = p_S \frac{\text{Tr}[\mathcal{M}_\omega(\boldsymbol{\sigma}^S)]}{\text{Tr}[\mathcal{M}_\omega(\boldsymbol{\sigma})]} P[\mathcal{D}_\omega(\boldsymbol{\sigma}^S)] + (1 - p_S) \frac{\text{Tr}[\mathcal{M}_\omega(\boldsymbol{\sigma}^{US})]}{\text{Tr}[\mathcal{M}_\omega(\boldsymbol{\sigma})]} P[\mathcal{D}_\omega(\boldsymbol{\sigma}^{US})]. \quad (3.25)$$

Note that the assemblage  $\{p(a'|x')[\mathcal{D}_\omega(\boldsymbol{\sigma}^{US})]_{a'|x'}\}_{a',x'} \in \Sigma^{US}$  since the assemblage  $\boldsymbol{\sigma}^{US}$  is unsteerable [GA15]. This implies that the box  $P[\mathcal{D}_\omega(\boldsymbol{\sigma}^{US})]$  in the decomposition (3.25) is an unsteerable box. Now there are the following two cases to be checked in order to verify Eq.(3.12).

- (i) Suppose the assemblage  $\{p(a'|x')[\mathcal{D}_\omega(\boldsymbol{\sigma}^S)]_{a'|x'}\}_{a',x'}$  is unsteerable. Then from Eq. (3.25), it is clear that the box  $P[\mathcal{D}_\omega(\boldsymbol{\sigma})]$  is a convex mixture of two unsteerable boxes and hence unsteerable. Therefore in this case, the following inequality holds trivially.

$$\sum_{\omega} \mathcal{T}(\omega) C_{\text{steer}}(P[\mathcal{D}_\omega(\boldsymbol{\sigma})]) = 0 \leq C_{\text{steer}}(P[\boldsymbol{\sigma}]) \quad \forall \boldsymbol{\sigma} \in \Sigma^S. \quad (3.26)$$

- (ii) Suppose the assemblage  $\{p(a'|x')[\mathcal{D}_\omega(\boldsymbol{\sigma}^S)]_{a'|x'}\}_{a',x'}$  is steerable and the box  $P[\mathcal{D}_\omega(\boldsymbol{\sigma}^S)]$  in the decomposition (3.25) is a steerable box. Then, the decomposition (3.25) may not be the optimal decomposition (*i.e.* for which the weight of the steerable part being the minimum over all possible decompositions of the box  $P[\mathcal{D}_\omega(\boldsymbol{\sigma})]$ ). Hence, one has to minimize the weight of the steerable part  $p_S \frac{\text{Tr}[\mathcal{M}_\omega(\boldsymbol{\sigma}^S)]}{\text{Tr}[\mathcal{M}_\omega(\boldsymbol{\sigma})]}$  in Eq.(3.25) over all possible decompositions of the box  $P[\mathcal{D}_\omega(\boldsymbol{\sigma})]$  to obtain the steering cost  $C_{\text{steer}}(P[\mathcal{D}_\omega(\boldsymbol{\sigma})])$  of the box. Therefore, we have

$$C_{\text{steer}}(P[\mathcal{D}_\omega(\boldsymbol{\sigma})]) \leq p_S \frac{\text{Tr}[\mathcal{M}_\omega(\boldsymbol{\sigma}^S)]}{\text{Tr}[\mathcal{M}_\omega(\boldsymbol{\sigma})]} = C_{\text{steer}}(P[\boldsymbol{\sigma}]) \frac{\text{Tr}[\mathcal{M}_\omega(\boldsymbol{\sigma}^S)]}{\text{Tr}[\mathcal{M}_\omega(\boldsymbol{\sigma})]}. \quad (3.27)$$

The last equality holds as we have assumed that the decomposition (3.15) denotes the optimal decomposition of the box  $P[\boldsymbol{\sigma}]$ , *i.e.*  $p_S = C_{\text{steer}}(P[\boldsymbol{\sigma}])$ . As for all  $\omega$ ,  $\mathcal{T}(\omega) = \text{Tr}[\mathcal{M}_\omega(\boldsymbol{\sigma})] \geq 0$  and  $\sum_{\omega} \mathcal{T}(\omega) \leq 1$ , from Eq. (3.27) we get for deterministic 1W-

LOCCs,

$$\begin{aligned}
\sum_{\omega} \mathcal{T}(\omega) C_{\text{steer}}(P[\mathcal{D}_{\omega}(\boldsymbol{\sigma})]) &\leq \sum_{\omega} \mathcal{T}(\omega) C_{\text{steer}}(P[\boldsymbol{\sigma}]) \frac{\text{Tr}[\mathcal{M}_{\omega}(\boldsymbol{\sigma}^S)]}{\text{Tr}[\mathcal{M}_{\omega}(\boldsymbol{\sigma})]} \\
&= \sum_{\omega} C_{\text{steer}}(P[\boldsymbol{\sigma}]) \text{Tr}[\mathcal{M}_{\omega}(\boldsymbol{\sigma}^S)] \\
&= C_{\text{steer}}(P[\boldsymbol{\sigma}]) \sum_{\omega} \text{Tr}[\mathcal{M}_{\omega}(\boldsymbol{\sigma}^S)] \\
&\leq C_{\text{steer}}(P[\boldsymbol{\sigma}]), \quad \forall \boldsymbol{\sigma} \in \Sigma^S.
\end{aligned} \tag{3.28}$$

The last inequality holds, because  $\boldsymbol{\sigma}^S$  is the set of unnormalized conditional states and  $\mathcal{M}$  is a deterministic map, i.e.  $\sum_{\omega} \text{Tr}[\mathcal{M}_{\omega}(\boldsymbol{\sigma}^S)] \leq 1$ .

This completes the proof for the monotonicity of  $C_{\text{steer}}(P)$  on average, under 1W-LOCCs for all assemblages.  $\square$

### 3.3.2.3 Convexity

For all convex decompositions of

$$\boldsymbol{\sigma} = \mu \boldsymbol{\sigma}' + (1 - \mu) \boldsymbol{\sigma}'', \tag{3.29}$$

in terms of two other assemblages  $\boldsymbol{\sigma}'$  and  $\boldsymbol{\sigma}''$  ( $0 \leq \mu \leq 1$ ),

$$C_{\text{steer}}(P[\boldsymbol{\sigma}]) \leq \mu C_{\text{steer}}(P[\boldsymbol{\sigma}']) + (1 - \mu) C_{\text{steer}}(P[\boldsymbol{\sigma}'']) \quad \forall \boldsymbol{\sigma} \in \Sigma^S. \tag{3.30}$$

*Proof.* An arbitrary assemblage  $\boldsymbol{\sigma} := \{\sigma_{a|x}\}_{a,x} \in \Sigma^S$  for all possible convex decompositions given in Eq.(3.29) satisfies the following relation,

$$\text{Tr}[\Pi_{b|y} \sigma_{a|x}] = \mu \text{Tr}[\Pi_{b|y} \sigma'_{a|x}] + (1 - \mu) \text{Tr}[\Pi_{b|y} \sigma''_{a|x}] \quad \forall a, b, x, y, \tag{3.31}$$

which implies the following decomposition of the box  $P[\boldsymbol{\sigma}]$  arising from the assemblage

$\sigma$ ,

$$P[\sigma] = \mu P[\sigma'] + (1 - \mu)P[\sigma''], \quad (3.32)$$

where the box  $P[\sigma']$  arises from the assemblage  $\sigma' := \{\sigma'_{a|x}\}_{a,x}$  and the box  $P[\sigma'']$  arises from the assemblage  $\sigma'' := \{\sigma''_{a|x}\}_{a,x}$ . We write the optimal decompositions (with weight of the steerable part being the minimum over all the possible decompositions) for the two boxes in the above decomposition (3.32) as follows,

$$P[\sigma'] := C_{\text{steer}}(P[\sigma'])P_S^1 + (1 - C_{\text{steer}}(P[\sigma']))P_{US}^1, \quad (3.33)$$

where  $P_S^1$  and  $P_{US}^1$  are steerable and unsteerable boxes, respectively, and  $C_{\text{steer}}(P[\sigma']) \in [0, 1]$  is the steering cost of the box  $P[\sigma']$  and

$$P[\sigma''] := C_{\text{steer}}(P[\sigma''])P_S^2 + (1 - C_{\text{steer}}(P[\sigma'']))P_{US}^2, \quad (3.34)$$

where  $P_S^2$  and  $P_{US}^2$  are steerable and unsteerable boxes, respectively, and  $C_{\text{steer}}(P[\sigma'']) \in [0, 1]$  is the steering cost of the box  $P[\sigma'']$ . By writing the boxes given in the decomposition (3.32) in terms of the above two optimal decompositions, we obtain

$$\begin{aligned} P[\sigma] &= \mu \left[ C_{\text{steer}}(P[\sigma'])P_S^1 + (1 - C_{\text{steer}}(P[\sigma']))P_{US}^1 \right] \\ &\quad + (1 - \mu) \left[ C_{\text{steer}}(P[\sigma''])P_S^2 + (1 - C_{\text{steer}}(P[\sigma'']))P_{US}^2 \right] \end{aligned} \quad (3.35)$$

$$:= \nu \mathbb{P} + (1 - \nu)\mathbb{P}_{US}, \quad (3.36)$$

where

$$\nu := \mu C_{\text{steer}}(P[\sigma']) + (1 - \mu)C_{\text{steer}}(P[\sigma'']), \quad (3.37)$$

satisfies  $0 \leq \nu \leq 1$  and the box

$$\mathbb{P} := \frac{1}{\nu} \left[ \mu C_{\text{steer}}(P[\sigma'])P_S^1 + (1 - \mu)C_{\text{steer}}(P[\sigma''])P_S^2 \right], \quad (3.38)$$

may be either steerable or unsteerable and the box

$$\mathbb{P}_{US} := \frac{1}{1-\nu} \left[ \mu(1 - C_{\text{steer}}(P[\boldsymbol{\sigma}']))P_{US}^1 + (1-\mu)(1 - C_{\text{steer}}(P[\boldsymbol{\sigma}'']))P_{US}^2 \right], \quad (3.39)$$

is unsteerable due to the convex structure of the set of unsteerable boxes. Now there can be two possibilities, *e.g.*

- (i) If the box  $\mathbb{P}$  given by Eq.(3.38) is unsteerable, then from Eq.(3.36) it is clear that, the box  $P[\boldsymbol{\sigma}]$  is a convex mixture of two unsteerable boxes and hence unsteerable. Therefore, in this case the following inequality trivially holds for all possible convex decompositions as given in Eq.(3.29) for an arbitrary assemblage  $\boldsymbol{\sigma} \in \Sigma^S$ ,

$$C_{\text{steer}}(P[\boldsymbol{\sigma}]) = 0 \leq \nu = \mu C_{\text{steer}}(P[\boldsymbol{\sigma}']) + (1-\mu)C_{\text{steer}}(P[\boldsymbol{\sigma}''']). \quad (3.40)$$

- (ii) If the box  $\mathbb{P}$  (3.38) is steerable, then the decomposition (3.36) is not optimal for the nonzero weights of both the boxes  $P_S^1$  and  $P_S^2$  because an extremal steerable box in the set  $\mathcal{N}_{\Sigma^S}$  cannot be decomposed as a convex mixture of the other boxes in the set  $\mathcal{N}_{\Sigma^S}$ . Even if the weight of the box  $P_S^1$  or  $P_S^2$  is zero, then also decomposition (3.36) may not be the optimal one. To obtain the steering cost  $C_{\text{steer}}(P[\boldsymbol{\sigma}])$  of the box  $P[\boldsymbol{\sigma}]$ , the weight of the steerable part  $\nu$  over all such possible decompositions of the box  $P[\boldsymbol{\sigma}]$  has to be minimized. Hence by using Eq.(3.37) we have,

$$C_{\text{steer}}(P[\boldsymbol{\sigma}]) \leq \nu = \mu C_{\text{steer}}(P[\boldsymbol{\sigma}']) + (1-\mu)C_{\text{steer}}(P[\boldsymbol{\sigma}''']). \quad (3.41)$$

From Eq.(3.40) together with Eq.(3.41), we can conclude that the following relation holds for all possible convex decompositions given by Eq.(3.29) of an arbitrary assemblage  $\boldsymbol{\sigma} \in \Sigma^S$ , *i.e.*

$$C_{\text{steer}}(P[\boldsymbol{\sigma}]) \leq \mu C_{\text{steer}}(P[\boldsymbol{\sigma}']) + (1-\mu)C_{\text{steer}}(P[\boldsymbol{\sigma}''']). \quad (3.42)$$

□

It is evident from the above discussions that, the steering cost  $C_{\text{steer}}(P)$  for a box  $P$  satisfies all the properties of a bonafide quantum steering measure [GA15] and it is a convex steering monotone.

### 3.4 Illustrations

Here we show the detection and quantification of quantum steering by employing two families of correlations, useful in quantum cryptography. These are the well-known white-noise BB84 family and colored-noise BB84 family. Let us consider the steering scenario where Alice performs two black-box dichotomic measurements on her part of an unknown  $d \otimes 2$  quantum state shared with Bob, which produces the assemblage  $\{\sigma_{a|x}\}_{a,x}$  at Bob's side. Bob applies projective qubit measurements  $\{\Pi_{\mathcal{B}_y}^b\}_{b,y}$  or  $\{\Pi_{b|y}\}_{b,y}$  on the produced assemblage corresponding to any two mutually unbiased bases (MUBs), *i.e.*  $\mathcal{B}_0 \equiv \{|f_i\rangle\}_{i=1}^2$  and  $\mathcal{B}_1 \equiv \{|g_j\rangle\}_{j=1}^2$  such that,  $|\langle f_i|g_j\rangle|^2 = \frac{1}{2} \forall i, j$  (here,  $\{|f_i\rangle\}_{i=1}^2$  and  $\{|g_j\rangle\}_{j=1}^2$  are two sets of orthonormal basis). In the given scenario, the necessary and sufficient condition for quantum steering from Alice to Bob is given by Eq.(1.49), which is also called as the analogous CHSH inequality for quantum steering [CFFW15].

The white-noise BB84 and colored-noise BB84 families belong to the local polytope of the two-binary-inputs and two-binary-outputs Bell scenario. In order to find out the existence of an LHV-LHS model for the given local correlation, we consider a classical simulation model by using shared randomness as the classical resource, *i.e.* a local hidden variable(LHV) model with limited dimension [DW15]. Suppose a local box  $P_L(a, b|x, y) := \{p_L(a, b|x, y)\}_{a,b,x,y}$  admits the following decomposition:

$$p_L(a, b|x, y) = \sum_{\lambda=0}^{d_\lambda-1} p(\lambda) p(a|x, \lambda) p(b|y, \lambda) \quad \forall a, b, x, y. \quad (3.43)$$

where the dimension of the shared randomness is restricted to  $d_\lambda$  according to the classical simulation model.

The minimum dimension of the shared randomness, required to simulate a local  $n$ -partite correlation, is given by the classical Carathéodory number (*i.e.* *ontological com-*

pression) which is bounded in both ways by the different numbers in different scenarios (given in Appendix B of Ref. [DW15]). For example, in the bipartite Bell scenario with two-binary inputs and two-binary outputs *i.e.* in 2-2-2 Bell scenario, the classical Carathéodory number is 4. It implies that, the shared randomness of dimension  $d_\lambda = 4$  or the sharing of  $\log_2 d_\lambda = 2$  classical bits is sufficient to simulate any local box. As the simulation of measurement statistics from a local box gives a dimensional advantage by sharing a qubit (dim. 2) rather than classical randomness (dim. 4) with an observer (say, Bob) compared to another observer (say, Alice), so that the quantum advantage of such local correlations is called as *superlocality* [JAS17].

Our method to check the existence of an LHV-LHS model for the local correlations in terms of the extremal boxes of the given steering scenario goes as follows. We first decompose the given local correlation in the form of Eq.(3.43) where  $p(a|x, \lambda)$  are different deterministic distributions whereas  $p(b|y, \lambda)$  may be non-deterministic in order to minimize the dimension of the shared randomness. Then we check whether each of Bob's distributions in this decomposition has a quantum realization or not, in the context of the given steering scenario.

### 3.4.1 White-noise BB84 family

Let us consider the family of correlations defined as

$$P_{\text{BB84}}(a, b|x, y) = \frac{1 + (-1)^{a \oplus b \oplus x \cdot y} \delta_{x,y} c}{4}, \quad (3.44)$$

with marginal probabilities  $\frac{1}{2}$  for both Alice and Bob and the strength of visibility satisfies  $0 < c \leq 1$ . For  $c = 1$ , the above family of correlations corresponds to the BB84 correlation, mentioned in Sec.1.2.2.3, which satisfies  $p(a = b|x, y) = 1$  when  $x = y$  and  $p(a = b|x, y) = \frac{1}{2}$  when  $x \neq y$  (Note that,  $p(a = b|x, y) = p(0, 0|x, y) + p(1, 1|x, y)$ ) up to LRO [AGM06]. Hence Eq. (3.44) can be generalised as white-noise BB84 family. The white-noise BB84 family is local as it does not violate a Bell-CHSH inequality given by Eq.(1.29) for a set of measurement settings. This family of correlations arises from the two-qubit Werner

state given by Eq.(1.57) acted upon by the measurement settings  $\{\mathcal{A}_0 = -\sigma_z, \mathcal{A}_1 = \sigma_x\}$  at Alice's side and  $\{\mathcal{B}_0 = \sigma_z, \mathcal{B}_1 = \sigma_x\}$  at Bob's side. The Werner state is entangled iff  $c > \frac{1}{3}$  [Wer89].

The white noise BB84 family violates the analogous CHSH inequality for quantum steering given by Eq.(1.49) for  $c > \frac{1}{\sqrt{2}}$ . Hence, the white noise BB84 family cannot be decomposed as a convex mixture of the extremal points of the unsteerable set as given in Eq.(3.6) iff  $c > \frac{1}{\sqrt{2}}$  in the given steering scenario, *i.e.* where Alice performs two black-box dichotomic measurements and Bob performs projective qubit measurements corresponding to any two mutually unbiased bases (MUBs). In the following, we will demonstrate our procedure to find out in which range of  $c$ , the white noise BB84 family can be written as a convex mixture of the extremal points of the unsteerable set as written in Eq.(3.6) in the given steering scenario.

In the context of non-signalling polytope, the BB84 family can be decomposed as follows:

$$P_{\text{BB84}} = c \left( \frac{P_{PR}^{000} + P_{PR}^{110}}{2} \right) + (1 - c)P_N, \quad (3.45)$$

where  $P_N$  is the maximally mixed box, *i.e.*  $P_N(a, b|x, y) = \frac{1}{4}$ ,  $\forall a, b, x, y$  (*i.e.* white-noise BB84 correlation with  $c = 0$ ). Let us rewrite the above decomposition as follows,

$$P_{\text{BB84}} = c \left( \frac{1}{2}P_{PR}^{000} + \frac{1}{2}P_N \right) + c \left( \frac{1}{2}P_{PR}^{110} + \frac{1}{2}P_N \right) + (1 - 2c)P_N \quad (3.46)$$

By writing each box in the above decomposition in terms of the local deterministic boxes, we obtain the following decomposition which defines a classical simulation protocol with shared randomness of dimension 4.

$$P_{\text{BB84}}(a, b|x, y) = \frac{c}{8} \sum_{\alpha\beta\gamma} P_D^{\alpha\beta\gamma(\alpha\gamma\oplus\beta)}(a, b|x, y) + \frac{c}{8} \sum_{\alpha\beta\gamma} P_D^{\alpha\beta\gamma(\bar{\alpha}\bar{\gamma}\oplus\beta)}(a, b|x, y) + (1 - 2c)P_N \quad (3.47)$$

$$= \frac{1}{4} \sum_{\lambda=0}^3 P_\lambda(a|x) P_\lambda(b|y), \quad (3.48)$$

where  $p(\lambda) = \frac{1}{4} \forall \lambda$ ,  $\bar{\alpha} = \alpha \oplus 1$ ,  $\bar{\gamma} = \gamma \oplus 1$ ,  $P_\lambda(a|x) := \{p(a|x, \lambda)\}_{a,x} \forall \lambda$  is the set of con-

ditional probability distributions  $p(a|x, \lambda)$  for all possible  $a, x$  and  $P_\lambda(b|y) := \{p(b|y, \lambda)\}_{b,y}$  is the set of conditional probability distributions  $p(b|y, \lambda)$  for all possible  $b, y$ . In the LHV model given in Eq.(3.48), untrusted party, *viz* Alice uses deterministic strategies given by,

$$P_0(a|x) = P_D^{00}, P_1(a|x) = P_D^{01}, P_2(a|x) = P_D^{10}, P_3(a|x) = P_D^{11}, \quad (3.49)$$

while the trusted party, *viz* Bob uses non-deterministic strategies given by,

$$\begin{aligned} P_0(b|y) &= cP_D^{10} + (1-c) \left( \frac{P_D^{00} + P_D^{01} + P_D^{10} + P_D^{11}}{4} \right), \\ P_1(b|y) &= cP_D^{11} + (1-c) \left( \frac{P_D^{00} + P_D^{01} + P_D^{10} + P_D^{11}}{4} \right), \\ P_2(b|y) &= cP_D^{00} + (1-c) \left( \frac{P_D^{00} + P_D^{01} + P_D^{10} + P_D^{11}}{4} \right), \\ P_3(b|y) &= cP_D^{01} + (1-c) \left( \frac{P_D^{00} + P_D^{01} + P_D^{10} + P_D^{11}}{4} \right). \end{aligned} \quad (3.50)$$

Let us represent  $P_\lambda(b|y) = \{p(0|0, \lambda), p(0|1, \lambda), p(1|0, \lambda), p(1|1, \lambda)\} \forall \lambda \in \{0, 1, 2, 3\}$  in a vector form. Then we find that,  $P_0(b|y) = \{\frac{1+c}{2}, \frac{1-c}{2}, \frac{1-c}{2}, \frac{1+c}{2}\}$ ,  $P_1(b|y) = \{\frac{1-c}{2}, \frac{1+c}{2}, \frac{1+c}{2}, \frac{1-c}{2}\}$ ,  $P_2(b|y) = \{\frac{1+c}{2}, \frac{1-c}{2}, \frac{1+c}{2}, \frac{1-c}{2}\}$  and  $P_3(b|y) = \{\frac{1-c}{2}, \frac{1+c}{2}, \frac{1-c}{2}, \frac{1+c}{2}\}$  respectively.

We aim to find the range of  $c \in (0, 1]$  for which the BB84 family has a decomposition in terms of the extremal points of the unsteerable set as given in Eq.(3.6) derived from the decomposition given in Eq. (3.48). Now each non-deterministic strategy at Bob's side given by Eq.(3.50) can arise from a pure qubit state in the given steering scenario with the measurements  $\mathcal{B}_0$  and  $\mathcal{B}_1$  in two mutually unbiased bases (MUB). Hence Bob's non-deterministic strategies can be expressed as  $P_\lambda(b|y) = \langle \psi_\lambda | \mathbf{\Pi}_{\mathcal{B}} | \psi_\lambda \rangle \forall \lambda$  where  $\mathbf{\Pi}_{\mathcal{B}} := \{\mathbf{\Pi}_{\mathcal{B}_y}^b\}_{b,y}$  or  $\{\mathbf{\Pi}_{b|y}\}_{b,y}$  corresponds to two MUBs in  $\mathbb{C}^2$ , *i.e.*  $\mathcal{B}_0 \equiv \{|f_i\rangle\}_{i=1}^2$  and  $\mathcal{B}_1 \equiv \{|g_j\rangle\}_{j=1}^2$  such that,  $|\langle f_i | g_j \rangle|^2 = \frac{1}{2} \forall i, j$  holds for two sets of orthonormal basis  $\{|f_i\rangle\}_{i=1}^2$  and  $\{|g_j\rangle\}_{j=1}^2$  respectively. Therefore the pure states associated with the non-deterministic strategies turn out as,

$$|\psi_\lambda\rangle = \sqrt{\frac{1+(-1)^\lambda c}{2}} |f_1\rangle + e^{i\phi_\lambda} \sqrt{\frac{1-(-1)^\lambda c}{2}} |f_2\rangle, \quad \forall \lambda \in \{0, 1, 2, 3\} \quad (3.51)$$

where the polar angles of  $\{|\psi_\lambda\rangle\}_{\lambda=0}^3$  satisfy  $\theta_\lambda = \cos^{-1}((-1)^\lambda c) \forall \lambda$  ( $\{\theta_0, \theta_2\} \in [0, \frac{\pi}{2}]$  and  $\{\theta_1, \theta_3\} \in [\frac{\pi}{2}, \pi]$  analogous to  $c \in [0, 1]$ ) and the azimuthal angles of  $\{|\psi_\lambda\rangle\}_{\lambda=0}^3$  satisfy  $\cos \phi_0 = -\cos \phi_1 = -\cos \phi_2 = \cos \phi_3 = -\frac{c}{\sqrt{1-c^2}}$ . The physicality of LHS *i.e.*  $|\cos \phi_\lambda| \leq 1 \forall \{|\psi_\lambda\rangle\}_{\lambda=0}^3$  is satisfied when  $c \leq \frac{1}{\sqrt{2}}$ . Hence Eq.(3.48), for  $c \leq \frac{1}{\sqrt{2}}$  in the given steering scenario, can be recognised as a LHV-LHS decomposition limited by the dimension 4 of the shared randomness or hidden variable  $\lambda$  which corresponds to LHS *i.e.*  $\rho_B^\lambda = |\psi_\lambda\rangle\langle\psi_\lambda| \forall \lambda \in \{0, 1, 2, 3\}$  for Bob. It has been proved in Theorem 1 of Ref. [DBD<sup>+</sup>18] that, a dimension of the hidden variable lower than 4 can not execute such decomposition for an unsteerable box in the given 2-2-2 scenario. The measurement statistics from unsteerable correlations through joint probability distributions may arise by sharing either classical randomness or a qubit with Bob w.r.t. Alice. But the local Hilbert space dimension of qubit (*i.e.* 2) is lower than the minimum dimension of classical shared randomness (*i.e.* 4). This dimensional advantage by using a qubit than classical randomness from an operational perspective is termed as *superunsteerability* of the unsteerable correlations. Note that, in the given steering scenario, these pure states uniquely give rise to the non-deterministic probability distributions at Bob's side as given by Eq.(3.48). Thus we are in a position to say that, the decomposition given by Eq.(3.48) represents a convex mixture of the extremal points of the unsteerable set as shown in Eq.(3.6) iff the given steering scenario is restricted within  $c \leq \frac{1}{\sqrt{2}}$ .

**Theorem 3.1.** *The steering cost of the white-noise BB84 family is given by  $C_{steer}(P_{BB84}) = \max\{0, \frac{\sqrt{2}c-1}{\sqrt{2}-1}\}$  in the given steering scenario.*

*Proof.* Note that for  $\frac{1}{\sqrt{2}} \leq c \leq 1$ , the BB84 family can be decomposed as

$$P_{BB84} = \frac{\sqrt{2}c-1}{\sqrt{2}-1} P_S^{Ext} + \frac{\sqrt{2}(1-c)}{\sqrt{2}-1} P_{US}, \quad (3.52)$$

where

$$P_S^{Ext} = P_{BB84}|_{c=1} = \frac{1 + (-1)^{a \oplus b \oplus x \cdot y} \delta_{x,y}}{4} \quad (3.53)$$

is an extremal steerable box as it violates the steering inequality(1.49) maximally, and  $P_{US}$  is an unsteerable box which has a decomposition as given in Eq.(3.48) with  $c = \frac{1}{\sqrt{2}}$  in

terms of the extremal boxes of the given steering scenario. We see that the weight  $\frac{\sqrt{2c-1}}{\sqrt{2}-1}$  in the decomposition (3.52) is nonzero iff  $P_{\text{BB84}}$  demonstrates EPR-steering (in the region  $c > \frac{1}{\sqrt{2}}$ ). Therefore, the decomposition given in Eq.(3.52) is the optimal decomposition corresponding to the white-noise BB84 family for  $c \geq \frac{1}{\sqrt{2}}$ , because it is a convex mixture of the extremal steerable box (in the given steering scenario) and the convex sum of extremal unsteerable boxes causing the weight of the steerable part to be minimized. Hence the cost of EPR-steering for the entire family of white-noise BB84 correlations ( $0 \leq c \leq 1$ ) is given by  $C_{\text{steer}}(P_{\text{BB84}}) = \max\{0, \frac{\sqrt{2c-1}}{\sqrt{2}-1}\}$  which goes to zero iff the box is unsteerable (*i.e.* within  $0 \leq c \leq \frac{1}{\sqrt{2}}$ ).  $\square$

**Lemma 3.1.**  $C_{\text{steer}}(P_{\text{BB84}}) = \max\{0, \frac{\sqrt{2c-1}}{\sqrt{2}-1}\}$  is a convex roof measure.

*Proof.* From Eq.(1.33), we know that the assemblage  $\sigma|_{\rho_{AB}^W}$  arising from the state  $\rho_{AB}^W$  given in Eq.(1.57) can be decomposed as,

$$\begin{aligned} \sigma|_{\rho_{AB}^W} &= \text{Tr}_A(\mathbf{M}_{\mathcal{A}} \otimes \mathbb{1}_2 \rho_{AB}^W) \\ &= c \text{Tr}_A(\mathbf{M}_{\mathcal{A}} \otimes \mathbb{1}_2 |\Psi^-\rangle\langle\Psi^-|) + (1-c) \text{Tr}_A(\mathbf{M}_{\mathcal{A}} \otimes \mathbb{1}_2 \frac{\mathbb{1}_2 \otimes \mathbb{1}_2}{4}) \\ &= c \sigma|_{|\Psi^-\rangle} + (1-c) \sigma|_{\frac{\mathbb{1}_2 \otimes \mathbb{1}_2}{4}}. \end{aligned} \quad (3.54)$$

Here,  $\sigma|_{|\Psi^-\rangle}$  is the assemblage arising from the singlet state  $|\Psi^-\rangle$ , and  $\sigma|_{\frac{\mathbb{1}_2 \otimes \mathbb{1}_2}{4}}$  is the assemblage arising from the maximally mixed state  $\frac{\mathbb{1}_2 \otimes \mathbb{1}_2}{4}$ . We now observe that, the following relation is satisfied  $\forall c \in [0, 1]$ :

$$C_{\text{steer}}\left(P_{\text{BB84}}[\sigma|_{\rho_{AB}^W}]\right) \leq c C_{\text{steer}}\left(P[\sigma|_{|\Psi^-\rangle}]\right) + (1-c) C_{\text{steer}}\left(P[\sigma|_{\frac{\mathbb{1}_2 \otimes \mathbb{1}_2}{4}}]\right), \quad (3.55)$$

for the measurements that generate the white-noise BB84 family of correlations. Here  $C_{\text{steer}}\left(P_{\text{BB84}}[\sigma|_{\rho_{AB}^W}]\right) = \max\{0, \frac{\sqrt{2c-1}}{\sqrt{2}-1}\}$ ,  $C_{\text{steer}}\left(P[\sigma|_{|\Psi^-\rangle}]\right) = 1$  (since  $P[\sigma|_{|\Psi^-\rangle}]$  violates the steering inequality(1.49) maximally for the aforementioned measurement settings) and  $C_{\text{steer}}\left(P[\sigma|_{\frac{\mathbb{1}_2 \otimes \mathbb{1}_2}{4}}]\right) = 0$  (since the maximally mixed state is unsteerable in any scenario). Eq.(3.55) verifies the convexity property of the steering cost *i.e.*  $C_{\text{steer}}(P_{\text{BB84}}) \forall c \in [0, 1]$

defined for the family of white-noise BB84 correlations.  $\square$

In another way, we can conclude that, if the two boxes, *e.g.*  $P[\sigma]$  and  $P[\sigma']$  obey the following relation in the given steering scenario,

$$P[\sigma] = \eta P[\sigma'] + (1 - \eta)P_{US}, \quad (3.56)$$

where  $0 \leq \eta \leq 1$  and  $P_{US}$  is an unsteerable box, then  $P[\sigma']$  is more or equally steerable than  $P[\sigma]$ , analogous to that of Bell nonlocality as demonstrated by de Vicente in [dV14].

### 3.4.2 Colored-noise BB84 family

We now define the colored-noise BB84 family as

$$P_{\text{BB84}}^{\text{col}}(a, b|x, y) = \frac{1}{4} \left( 1 + (-1)^{a \oplus b \oplus x \cdot y} [\delta_{x,y} c + \frac{1-c}{2}] + (-1)^{a \oplus b \oplus x \oplus y} \frac{1-c}{2} \right), \quad (3.57)$$

where the visibility satisfies  $0 < c \leq 1$ . The above family of correlations demonstrates the BB84 correlation [AGM06] up to LRO. It can be obtained from the singlet state ( $|\Psi^-\rangle = \frac{1}{\sqrt{2}}(|01\rangle - |10\rangle)$ ) by mixing with the colored-noise, *i.e.*

$$\rho_{\text{col}} = c|\Psi^-\rangle\langle\Psi^-| + (1-c)\mathbb{1}_{\text{col}}, \quad (3.58)$$

where the noise  $\mathbb{1}_{\text{col}} = \frac{1}{2}(|01\rangle\langle 01| + |10\rangle\langle 10|)$  has a colored spectrum, and by using suitable binary dichotomic projective measurements. The colored-noise BB84 family is local as it does not violate a Bell-CHSH inequality(1.29).

The colored-noise BB84 family violates the analogous CHSH inequality for quantum steering given by Eq.(1.49) for  $c > 0$ . Hence, the colored-noise BB84 family cannot be decomposed as a convex mixture of the extremal points of the unsteerable set as given in Eq.(3.6) iff  $c > 0$  in the given steering scenario. Now by adopting our procedure, we determine the range of  $c$  for which the colored-noise BB84 family can be written as a convex mixture of the extremal points of the unsteerable set as given by Eq.(3.6) in the given steering scenario.

In the context of non-signalling polytope, the colored-noise BB84 family has the following decomposition,

$$P_{\text{BB84}}^{\text{col}} = c \left( \frac{P_{PR}^{000} + P_{PR}^{110}}{2} \right) + (1 - c)P_{US}. \quad (3.59)$$

where,

$$P_{US} := \frac{P_{PR}^{000} + P_{PR}^{110} + P_{PR}^{010} + P_{PR}^{100}}{4},$$

is an unsteerable box in the given steering scenario. There are many possible decompositions for the box  $P_{US}$  in terms of local deterministic boxes. However, all of them do not lead to convex mixtures of extremal boxes of the unsteerable set  $\mathcal{L}_{\Sigma US}$  in the given steering scenario for any two projective measurements  $\mathbf{\Pi}_{\mathcal{B}} := \{\mathbf{\Pi}_{b|y}\}_{b,y}$  in any two mutually unbiased bases (at Bob's side) in Hilbert space  $\mathbb{C}^2$ , *i.e.*  $\mathcal{B}_0 \equiv \{|f_i\rangle\}_{i=1}^2$  and  $\mathcal{B}_1 \equiv \{|g_j\rangle\}_{j=1}^2$  such that,  $|\langle f_i|g_j\rangle|^2 = \frac{1}{2} \forall i, j$  (Here  $\{|f_i\rangle\}_{i=1}^2$  and  $\{|g_j\rangle\}_{j=1}^2$  are two sets of orthonormal basis). To obtain such a convex mixture of extremal unsteerable boxes, we consider the following decomposition for the box  $P_{US}$ ,

$$\begin{aligned} P_{US} &= \frac{1}{4}P_D^{00} \frac{P_D^{00} + P_D^{10}}{2} + \frac{1}{4}P_D^{01} \frac{P_D^{01} + P_D^{11}}{2} + \frac{1}{4}P_D^{10} \frac{P_D^{00} + P_D^{10}}{2} + \frac{1}{4}P_D^{11} \frac{P_D^{01} + P_D^{11}}{2} \quad (3.60) \\ &:= \frac{1}{4}P_D^{00} \langle f_1 | \mathbf{\Pi}_{\mathcal{B}} | f_1 \rangle + \frac{1}{4}P_D^{01} \langle f_2 | \mathbf{\Pi}_{\mathcal{B}} | f_2 \rangle + \frac{1}{4}P_D^{10} \langle f_1 | \mathbf{\Pi}_{\mathcal{B}} | f_1 \rangle + \frac{1}{4}P_D^{11} \langle f_2 | \mathbf{\Pi}_{\mathcal{B}} | f_2 \rangle, \end{aligned} \quad (3.61)$$

which demonstrates an LHV-LHS model in terms of the extremal boxes of the unsteerable set.

By decomposing the first box in the decomposition (3.59), *i.e.* with co-efficient  $c$ , in terms of local deterministic boxes and by using the decomposition (3.60) for the second box (unsteerable), *i.e.* with co-efficient  $(1 - c)$ , in the decomposition (3.59), we obtain the following LHV model for the colored-noise BB84 family of correlations where the sufficient dimension of the shared randomness is 4.

$$P_{\text{BB84}}^{\text{col}}(a, b|x, y) = \frac{1}{4} \sum_{\lambda=0}^3 P_{\lambda}(a|x) P_{\lambda}(b|y), \quad (3.62)$$

where  $p(\lambda) = \frac{1}{4}$ , Alice uses deterministic strategies given by,

$$P_0(a|x) = P_D^{00}, P_1(a|x) = P_D^{01}, P_2(a|x) = P_D^{10}, P_3(a|x) = P_D^{11}, \quad (3.63)$$

and Bob uses non-deterministic strategies given by,

$$\begin{aligned} P_0(b|y) &= cP_D^{10} + (1-c)\frac{P_D^{00} + P_D^{10}}{2}, \\ P_1(b|y) &= cP_D^{11} + (1-c)\frac{P_D^{01} + P_D^{11}}{2}, \\ P_2(b|y) &= cP_D^{00} + (1-c)\frac{P_D^{00} + P_D^{10}}{2}, \\ P_3(b|y) &= cP_D^{01} + (1-c)\frac{P_D^{01} + P_D^{11}}{2}. \end{aligned} \quad (3.64)$$

Now we aim to decompose the colored-noise BB84 family in terms of the extremal points of the unsteerable set as given by Eq.(3.6) from the decomposition given by Eq.(3.62). To do this, we check whether each non-deterministic strategy at Bob's side given by Eq.(3.64) arises from a pure qubit state  $|\psi'_\lambda\rangle$  within certain parametric regime of the visibility  $c$  in the given steering scenario *i.e.* for the measurements  $\mathcal{B}_0$  and  $\mathcal{B}_1$  in two mutually unbiased bases (MUB). With this aim, we express each of Bob's non-deterministic strategies as,  $P_\lambda(b|y) = \langle \psi'_\lambda | \mathbf{\Pi}_{\mathcal{B}} | \psi'_\lambda \rangle$  (where  $\mathbf{\Pi}_{\mathcal{B}} := \{\Pi_{b|y}\}_{b,y}$  corresponds to the set projective qubit measurements at Bob's side in any two mutually unbiased bases:  $\mathcal{B}_0 \equiv \{|f_i\rangle\}_{i=1}^2$  and  $\mathcal{B}_1 \equiv \{|g_j\rangle\}_{j=1}^2$  as defined earlier), with the following pure states:

$$|\psi'_\lambda\rangle = \cos\left(\frac{\theta'_\lambda}{2}\right)|g_1\rangle + e^{i\frac{(-1)^\lambda}{\sqrt{1-c^2}}}\sin\left(\frac{\theta'_\lambda}{2}\right)|g_2\rangle, \quad \forall \lambda \{0, 1, 2, 3\} \quad (3.65)$$

where the polar angles of  $\{|\psi'_\lambda\rangle\}_{\lambda=0}^3$  satisfy  $\cos\theta'_0 = -\cos\theta'_1 = -\cos\theta'_2 = \cos\theta'_3 = -c$  ( $\{\theta_1, \theta_2\} \in [0, \frac{\pi}{2}]$  and  $\{\theta_0, \theta_3\} \in [\frac{\pi}{2}, \pi]$  analogous to  $c \in [0, 1]$ ) and the azimuthal angles of  $\{|\psi'_\lambda\rangle\}_{\lambda=0}^3$  satisfy  $\phi'_\lambda = \cos^{-1}\frac{(-1)^\lambda}{\sqrt{1-c^2}} \forall \lambda$ . The LHS denoted by  $\rho_B^\lambda = |\psi'_\lambda\rangle\langle\psi'_\lambda|$  is physical *i.e.*  $|\cos\phi'_\lambda| \leq 1 \forall \{|\psi'_\lambda\rangle\}_{\lambda=0}^3$  is satisfied when  $c = 0$ . This is an instance of *superunsteerability* where the shared randomness of dimension 4 suffices to represent a LHV-LHS decomposition of a bipartite qubit state. Note that, in the given steering scenario, the

above states are the only pure states which give rise to the non-deterministic probability distributions at Bob's side *i.e.* given by Eq.(3.62). Therefore we can conclude that, the decomposition (3.62) represents the convex mixture of the extremal points of the unsteerable set as given by Eq.(3.6) in the given steering scenario if and only if  $c = 0$ .

**Theorem 3.2.** *The steering cost of the colored-noise BB84 family is given by  $C_{steer}(P_{BB84}^{col}) = c$  in the given 2-2-2 steering scenario.*

*Proof.* The colored-noise BB84 family can be decomposed as,

$$P_{BB84}^{col} = c P_S^{Ext} + (1 - c) P_{US}, \quad (3.66)$$

where the extremal steerable box  $P_S^{Ext}$  given by Eq.(3.53) arises from Eq.(3.57) by using  $c = 1$  and  $P_{US}$  is the unsteerable box given by Eq.(3.61). Eq.(3.66) represents the optimal decomposition for the colored-noise BB84 family because it is a convex mixture of the extremal steerable box (in the given steering scenario) and the convex sum of the extremal unsteerable boxes with the weight of steerable part to be minimized. Hence the cost of EPR-steering for the entire family of colored-noise BB84 correlations can be represented by  $C_{steer}(P_{BB84}^{col}) = c$  which goes to zero iff the box is unsteerable (*i.e.* for  $c = 0$ ).  $\square$

**Lemma 3.2.**  *$C_{steer}(P_{BB84}^{col}) = c$  is a convex roof measure.*

*Proof.* The assemblage  $\sigma|_{\rho_{col}}$  arising from state  $\rho_{col}$  given in Eq.(3.58) can be decomposed as,

$$\begin{aligned} \sigma|_{\rho_{col}} &= \text{Tr}_A(\mathbf{M}_{\mathcal{A}} \otimes \mathbb{1} \rho_{col}) \\ &= c \text{Tr}_A(\mathbf{M}_{\mathcal{A}} \otimes \mathbb{1}_2 |\Psi^-\rangle\langle\Psi^-|) + (1 - c) \text{Tr}_A(\mathbf{M}_{\mathcal{A}} \otimes \mathbb{1}_2 \mathbb{1}_{col}) \\ &= c \sigma|_{|\Psi^-\rangle\langle\Psi^-|} + (1 - c) \sigma|_{\mathbb{1}_{col}}. \end{aligned} \quad (3.67)$$

where,  $\sigma|_{|\Psi^-\rangle}$  is the assemblage arising from the singlet state  $|\Psi^-\rangle$ , and  $\sigma|_{\mathbb{1}_{col}}$  is the assemblage arising from the noisy state  $\mathbb{1}_{col}$ . It can be easily checked that, the following

relation holds for  $c \in [0, 1]$ .

$$C_{\text{steer}}\left(P_{\text{BB84}}^{\text{col}}[\boldsymbol{\sigma}|\rho_{\text{col}}]\right) = c C_{\text{steer}}\left(P[\boldsymbol{\sigma}|\Psi^-]\right) + (1-c) C_{\text{steer}}\left(P[\boldsymbol{\sigma}|\mathbb{1}_{\text{col}}]\right), \quad (3.68)$$

For the measurements that generate the colored-noise BB84 family, it can be observed that,  $C_{\text{steer}}\left(P_{\text{BB84}}^{\text{col}}[\boldsymbol{\sigma}|\rho_{\text{col}}]\right) = c$ ,  $C_{\text{steer}}\left(P[\boldsymbol{\sigma}|\Psi^-]\right) = 1$  (since  $P[\boldsymbol{\sigma}|\Psi^-] = P_{\text{BB84}}^{\text{col}}|_{c=1} = P_S^{E,xt}$ , being an extremal steerable box violates the CFFW inequality(1.49) maximally) and  $C_{\text{steer}}\left(P[\boldsymbol{\sigma}|\mathbb{1}_{\text{col}}]\right) = 0$  (since  $\mathbb{1}_{\text{col}}$  is unsteerable). Therefore Eq.(3.68) verifies the convexity property of the steering cost defined for the family of colored-noise BB84 correlations, *i.e.*  $C_{\text{steer}}(P_{\text{BB84}}^{\text{col}})$ .  $\square$

### 3.5 Steering cost versus steering weight

The steering weight  $W_{\text{steer}}(\boldsymbol{\sigma})$  for a given assemblage  $\boldsymbol{\sigma}$  is quantified by Skrzypczyk *et al* [SNC14] and is described in Sec.1.4.2.1. Let us assume the following optimal decomposition of the given assemblage  $\boldsymbol{\sigma} = \{\sigma_{a|x}\}_{a,x}$  with the weight of the steerable part being minimized over all possible decompositions of the assemblage, *i.e.* the weight of the steerable part is equal to the steering weight  $W_{\text{steer}}(\boldsymbol{\sigma})$  of the assemblage  $\boldsymbol{\sigma}$ ,

$$\sigma_{a|x} = W_{\text{steer}}(\boldsymbol{\sigma}) \tilde{\sigma}_{a|x}^S + (1 - W_{\text{steer}}(\boldsymbol{\sigma})) \tilde{\sigma}_{a|x}^{US} \quad \forall a, x. \quad (3.69)$$

where  $\tilde{\sigma}_{a|x}^S$  is an element of a steerable assemblage  $\tilde{\boldsymbol{\sigma}}^S$  and  $\tilde{\sigma}_{a|x}^{US}$  is an element of an unsteerable assemblage  $\tilde{\boldsymbol{\sigma}}^{US}$ .

**Proposition 3.1.** *Depending upon a set of projective measurements  $\Pi_{\mathcal{B}} := \{\Pi_{b|y}\}_{b,y}$  performed by Bob on the assemblage  $\boldsymbol{\sigma} = \{\sigma_{a|x}\}_{a,x}$ , the following trade-off between our steering cost and the steering weight is satisfied.*

$$C_{\text{steer}}(P[\boldsymbol{\sigma}]) \leq W_{\text{steer}}(\boldsymbol{\sigma}), \quad (3.70)$$

where the box  $P[\boldsymbol{\sigma}] = P(a, b|x, y) = \left\{ \text{Tr} [\Pi_{b|y} \sigma_{a|x}] \right\}_{a,b,x,y}$  arises from the assemblage  $\boldsymbol{\sigma}$ .

*Proof.* Suppose Bob performs a set of projective measurements  $\Pi_{\mathcal{B}} := \{\Pi_{b|y}\}_{b,y}$  on  $\sigma$  given by the decomposition (3.69). Then one can write,

$$\text{Tr} [\Pi_{b|y} \sigma_{a|x}] = W_{\text{steer}}(\sigma) \text{Tr} [\Pi_{b|y} \tilde{\sigma}_{a|x}^S] + (1 - W_{\text{steer}}(\sigma)) \text{Tr} [\Pi_{b|y} \tilde{\sigma}_{a|x}^{US}], \quad \forall a, b, x, y. \quad (3.71)$$

Using Eq.(3.71), the following decomposition can be written for the box  $P[\sigma]$  arising from the assemblage  $\sigma$ ,

$$P[\sigma] = W_{\text{steer}}(\sigma) P_S[\tilde{\sigma}^S] + (1 - W_{\text{steer}}(\sigma)) P_{US}[\tilde{\sigma}^{US}]. \quad (3.72)$$

Here,  $P_S[\tilde{\sigma}^S]$  is a steerable box, produced from the steerable assemblage  $\tilde{\sigma}^S$  and  $P_{US}[\tilde{\sigma}^{US}]$  is an unsteerable box, produced from the unsteerable assemblage  $\tilde{\sigma}^{US}$ .

Now the weight  $W_{\text{steer}}(\sigma)$  of the steerable part in the decomposition (3.72) may not be the minimum weight over all possible decompositions of the correlation  $P[\sigma]$ . Since the steering cost of the correlation  $P[\sigma]$  is obtained by minimizing the weight of the steerable part over all possible decompositions of the correlation  $P[\sigma]$ , hence the steering cost  $C_{\text{steer}}(P[\sigma])$  of the correlation  $P[\sigma]$  is either less or equal to the weight  $W_{\text{steer}}(\sigma)$ . Thus the following trade-off holds between the two quantifiers of quantum steering, *i.e.*  $C_{\text{steer}}(P[\sigma]) \leq W_{\text{steer}}(\sigma)$ .  $\square$

### 3.5.1 Illustrations

Now we demonstrate the above proposition by comparing two examples. Note that, the steering cost of a correlation, unlike the steering weight of an assemblage, depends on Bob's set of measurements. So that the steering cost changes with the measurement settings chosen by Bob, while steering weight remains unchanged. Suppose that, Alice and Bob share the two-qubit Werner state  $\rho_{AB}^W$  with visibility parameter  $c \in [0, 1]$  given by Eq.(1.57) and Alice performs projective measurements corresponding to observables  $\mathcal{A}_0 = -\sigma_z$  and  $\mathcal{A}_1 = \sigma_x$ . The assemblage prepared at Bob's side is denoted by  $\sigma|_{\rho_{AB}^W}$ , which is steerable

iff  $c > \frac{1}{\sqrt{2}}$  [CJWR09, CS16]. Hence it can be decomposed for  $c \geq \frac{1}{\sqrt{2}}$  as follows,

$$\sigma_{a|x}|\rho_{AB}^W = \frac{\sqrt{2}c-1}{\sqrt{2}-1}\sigma_{a|x}|\Psi^-\rangle + \frac{\sqrt{2}(1-c)}{\sqrt{2}-1}\sigma_{a|x}|\rho_{AB}^W(c=\frac{1}{\sqrt{2}})\rangle \quad \forall a, x, \quad (3.73)$$

where  $\sigma_{a|x}|\Psi^-\rangle$  represents an element of the steerable assemblage arised at Bob's side depending upon Alice's measurements on the singlet state  $|\Psi^-\rangle$  and  $\sigma_{a|x}|\rho_{AB}^W(c=\frac{1}{\sqrt{2}})\rangle$  represents an element of the unsteerable assemblage arised at Bob's side depending upon Alice's measurements on the state  $\rho_{AB}^W$  (given by Eq.(1.57)) for  $c = \frac{1}{\sqrt{2}}$ , which is an element of unsteerable assemblage [CS16]. It can be checked that, for all  $a, x$ , each element of the steerable assemblage  $\sigma_{a|x}|\Psi^-\rangle$  is a pure state after normalization and hence, cannot be written as a convex combination of the steerable and unsteerable assemblage. So the weight of the steerable assemblage in the decomposition (3.73) cannot be reduced further. Moreover, the weight of the steerable part goes to zero iff the assemblage  $\sigma|\rho_{AB}^W$  is unsteerable (*i.e.* for  $c \leq \frac{1}{\sqrt{2}}$ ). The decomposition (3.73) thus comes out as the optimal decomposition for the assemblage  $\sigma|\rho_{AB}^W$ . This implies that the steering weight of the two-qubit Werner state  $\rho_{AB}^W$ , when Alice performs the aforementioned two measurements, is given by

$$W_{\text{steer}}(\sigma|\rho_{AB}^W) = \max\{0, \frac{\sqrt{2}c-1}{\sqrt{2}-1}\} = C_{\text{steer}}(P_{\text{BB84}}[\sigma]), \quad (3.74)$$

which is equal to the steering cost of the white-noise BB84 family (3.44) arose from this assemblage  $\sigma$  in the given steering scenario.

### 3.5.1.1 Example 1.

Let us consider the white-noise BB84 family of correlations, where Bob performs projective measurements corresponding to observables  $\mathcal{B}_0 = \sigma_z$  and  $\mathcal{B}_1 = \sigma_x$  on the assemblage  $\sigma|\rho_{AB}^W$ . The steering cost of the white-noise BB84 family produced from the two-qubit Werner state  $\rho_{AB}^W$  in the given 2-2-2 scenario is equal to the steering weight produced from the state  $\rho_{AB}^W$  for the same set of measurements at Alice's side. It is shown in Eq.(3.74).

### 3.5.1.2 Example 2.

Now we consider that, instead of performing the above measurements, Bob performs projective measurements corresponding to the observables  $\mathcal{B}_0 = \cos \frac{\pi}{5} \sigma_x + \sin \frac{\pi}{5} \sigma_y$  and  $\mathcal{B}_1 = \sigma_z$  on the assemblage  $\sigma|_{\rho_{AB}^W}$ . The produced correlation does not belong to the white-noise BB84 family and it violates the analogous CHSH inequality for quantum steering [CFFW15] given by Eq.(1.49) when  $c > \sqrt{\frac{2}{29}(11 - \sqrt{5})} \simeq 0.77$ . Hence, for  $0 < c \leq \sqrt{\frac{2}{29}(11 - \sqrt{5})}$ , the steering cost of the above correlation is 0. In the range  $\frac{1}{\sqrt{2}} < c \leq \sqrt{\frac{2}{29}(11 - \sqrt{5})}$ , with these measurements performed by Alice and Bob, we have  $C_{\text{steer}}(P[\sigma|_{\rho_{AB}^W}]) = 0$  whereas  $\max_c W_{\text{steer}}(P[\sigma|_{\rho_{AB}^W}]) = 0.24$ . Therefore the steering cost of the correlation arised from the assemblage  $\sigma|_{\rho_{AB}^W}$  is less than the steering weight of the same assemblage in the given 2-2-2 steering scenario.

From an experimental point of view, the determination of the steering weight in a steering scenario requires complete tomographic knowledge of the qubit assemblage prepared on the trusted side [JKMW01]. Whereas the steering cost, proposed by us, is determined from the observed correlations with restricted knowledge of the prepared assemblage for a given set of measurements on the trusted side. As the complete tomographic knowledge of the assemblage is dispensable for the determination of our steering cost, so that it is experimentally less demanding than the determination of the steering weight.

## 3.6 Summary and Outlook

The quantification of quantum correlations is an important aspect to observe the extent of its utility in an information processing task, where the quantum correlation acts as a resource. Moreover, if the context, in which the quantifier is defined, has an operational efficacy, then the applicable field of the quantifier becomes widened. In this chapter, we present a method to check one of the powerful quantum resources, *viz* steering for a scenario where Alice performs two black-box dichotomic measurements and Bob performs two arbitrary projective qubit measurements in mutually unbiased bases(MUBs). This method is based on the decompositions of the measurement correlations acted upon bipar-

tite qubit states, in the context of extremal boxes in the 2-2-2 steering scenario. The existence of an LHV-LHS model for a set of measurement correlations can be easily checked through this formulation. Then we come up with the proposition of a quantifier of steering called steering cost, which is a bonafide measure according to the resource theory of quantum steering. It can be proved that steering cost is a convex steering monotone. Quantum steering for two well-known families of measurement correlations in the theory of quantum information can be demonstrated by fixing their steering cost. We also show that the determination of our steering cost is experimentally less demanding than the determination of the steering weight.

Steering cost finds applications in the context of extremal non-signalling correlations. The security of a device-independent quantum key distribution protocol is shown [AGM06] by using the nonlocal correlations which arise from the two-qubit Werner states in the context of extremal non-signalling boxes. A similar investigation to study the security of a one-sided device-independent quantum key distribution(1s-DIQKD) protocol with the measurement correlations in the context of extremal boxes in a 2-2-2 steering scenario can make use of steering cost to manifest quantum steerable correlations. Further, it would be interesting to explore the implementation of steering cost in future studies. Note that, like steering cost to manifest quantum steering, *Schrödinger strength* is defined recently in [JDK<sup>+</sup>19] to quantify the *superunsteerability* of the unsteerable correlations by maximizing the weight of the steerable part of a box decomposition in the context of extremal non-signalling boxes, which is shown to be useful for the task of quantum random access codes(RACs).

## Sharing of a quantum correlation

The identifying feature of quantum correlation is that no classical description is adequate for its realization. The features of several quantum correlations, including entanglement, steering, Bell nonlocality etc, are discussed in Chapter 1. Then we show the ways to preserve and quantify a kind of quantum correlation, *viz* quantum steering [Sch35, Sch36] which surfaced from the famous EPR paradox [EPR35]. Quantum steering is a task, where an ensemble of states is remotely prepared at Bob's side by measuring on the subsystem of Alice while Alice and Bob share a bipartite entangled state,  $\rho_{AB}$ , by ruling out a local hidden state (LHS) model for Bob. As quantum coherence is an inherent property of a quantum state, so the steerable correlations may have implications through the steering of quantum coherence and vice-versa. The possibility of the task is discussed in Sec.1.5 via the demonstration of another space-like bipartite quantum correlation in  $\mathbb{C}^2 \otimes \mathbb{C}^2$  which is named as nonlocal advantage of quantum coherence or NAQC [MPP17]. It is based on basis-dependent quantifiers of quantum coherence, namely  $l_1$ -norm [BCP14a], relative entropy [BCP14a] and skew-information [Gir14, Luo03]. Steering of quantum state and steering of quantum coherence are two inequivalent features of quantum correlations. In this chapter we discuss whether a quantum correlation *viz* Nonlocal Advantage of Quantum Coherence (NAQC) can be shared by more than one observer in a sequence at the untrusted side.

Hu *et al* showed from geometrical analogy that [HWF18], NAQC is one of the strongest quantum correlations which forms a subset of Bell nonlocal correlations. The interplay be-

tween quantum steering and quantum coherence for higher dimensional states was further investigated in another paper [HF18]. The nonlocal feature of quantum coherence via complementarity between various coherence steering criteria has also been proposed [MK18]. The development of quantum coherence as a resource [SAP17] is another interesting aspect of quantum information theory. Quantum correlations satisfying non-signalling conditions are generally monogamous, and relaxation of non-signalling implies the violation of monogamy relations. In particular, non-signalling cannot be enforced in scenarios such as the case when half of an entangled pair of two particles is shared by one observer and another half is shared among several observers who measure the particle sequentially and independently of each other [SGGP15]. In this scenario, Bell nonlocality can be shared by two observers at one end [MMH16], whereas quantum steering can be shared by a number of observers ranging from two to infinitely many [SDMM18], depending on the number of settings per side for a steering inequality [CJWR09, CFFW15]. The results in the given scenario are also substantiated through experimental demonstrations [HZH<sup>+</sup>16, SCP<sup>+</sup>17]. Even entanglement can be detected by more than or equal to 6 number of observers in this scenario [BMSS18, SMSS21], by using a different experimental set-up.

This chapter is written by comprising our work, "*Sharing of nonlocal advantage of quantum coherence by sequential observers*", S. Datta and A. S. Majumdar, Phys. Rev. A, **98**, 042311 (2018); Phys. Rev. A **99**, 019902(E) (2019) [DM18, DM19]. In this chapter, we investigate the sharing of NAQC, which is stronger than other quantum correlations, including even Bell nonlocality [HWF18], by employing multiple observers on one wing. In light of the above studies, we are also motivated by the question of whether the number of observers who share quantum correlations sequentially depends on the strength of that correlation. In particular, we consider the scenario where multiple Alices share half of an entangled pair of qubits and perform self-contained unbiased unsharp measurements sequentially, whereas a single Bob computes quantum coherence in one of the mutually unbiased basis at the other end. This scenario is compatible with the description of the LHS model considered in [MPP17]. Here we show that not more than a single Alice can share NAQC with a single Bob.

## 4.1 NAQC under unsharp measurement formalism

The non-existence of a local hidden state(LHS) model given by Eq.(1.34) or Eq.(1.35) at the trusted side (here Bob) demonstrates steering from the untrusted side (here Alice) to the trusted side (Bob) [WJD07, JWD07]. This implies that, Bob does not hold an ensemble  $\{p(\lambda), \rho_B^\lambda\}_\lambda$ , where LHS is characterised by  $\rho_B^\lambda$  with  $\lambda$  as a hidden variable occurring with probability  $p(\lambda) \in [0, 1]$  ( $\sum_\lambda p(\lambda) = 1$ ). As the demonstration of steerability in terms of quantum state does not necessarily imply the steerability in terms of quantum coherence of that state, hence we assume the dimension of the hidden variables in the ontic space to be arbitrary to describe an LHS model.

The LHS model at Bob's side can be demonstrated by Alice's cheating strategy given by Eq.(1.34). However, the strategy can be recast in terms of local quantum coherence at Bob's side by determining the coherence of the unnormalized conditional state  $\sigma_{a|x}$  and local hidden qubit state  $\rho_B^\lambda \forall \lambda$ . Now by using coherence complementarity relations given by inequalities(1.52), one can derive the following coherence steering inequalities, better known as NAQC inequalities [MPP17],

$$N^{l_1} = \frac{1}{2} \sum_{i,j,a} p(a|\mathcal{A}_{j \neq i}) C_i^{l_1}(\rho_{B|\Pi_{\mathcal{A}_{j \neq i}}^a}) \leq \sqrt{6} \quad (4.1)$$

$$N^E = \frac{1}{2} \sum_{i,j,a} p(a|\mathcal{A}_{j \neq i}) C_i^E(\rho_{B|\Pi_{\mathcal{A}_{j \neq i}}^a}) \leq 2.23 \quad (4.2)$$

$$N^S = \frac{1}{2} \sum_{i,j,a} p(a|\mathcal{A}_{j \neq i}) C_i^S(\rho_{B|\Pi_{\mathcal{A}_{j \neq i}}^a}) \leq 2 \quad (4.3)$$

where the coherence of a qubit at Bob's side is computed in one of the mutually unbiased basis in  $\mathbb{C}^2$ , *i.e.*  $i \in \{x, y, z\}$  depending upon Alice's measurement  $\mathcal{A}_j$  in the  $j$ -th direction ( $j \in \{x, y, z\}$ ) and its corresponding outcome  $a \in \{0, 1\}$ . The above inequalities are derived for projective measurements  $\Pi_{\mathcal{A}_j}^a$  at Alice's side. If Alice and Bob share a joint state  $\rho_{AB}$ , then the normalised conditional state at Bob's side, *i.e.*  $\rho_{B|\Pi_{\mathcal{A}_j}^a} = \frac{\text{Tr}_A[(\Pi_{\mathcal{A}_j}^a \otimes \mathbb{1}_2)\rho_{AB}]}{p(a|\mathcal{A}_j)}$  occurs with probability  $p(a|\mathcal{A}_j) = \text{Tr}[(\Pi_{\mathcal{A}_j}^a \otimes \mathbb{1}_2)\rho_{AB}]$ . The quantifiers of quantum coherence, *e.g.*  $l_1$ -norm, relative entropy and skew-information are defined by Eq.(1.5), Eq.(1.6) and Eq.(1.7) respectively. Note that, each quantifier of quantum coherence satisfies the basic

axioms of the resource theory for quantum coherence [BCP14a, SAPI17].  $\rho_{AB}$  demonstrates NAQC if it violates any of the three form of inequalities given by Eq.(4.1),(4.2),(4.3) respectively. Now it can be easily shown that Alice's choice of measurement is optimal when it is complementary to the basis chosen by Bob. NAQC describes the nonlocal feature of a quantum correlation because it violates the *locality* assumption of EPR-theorem given in Sec.1.3.1 in a way that, Alice's choice of measurements affects the quantum coherence of Bob's subsystem (qubit) separated by a distance. Hence the task of NAQC is that Bob wants the quantum coherence of her subsystem to be steered completely in a preferred eigenbasis and according to that, Alice measures her subsystem along a particular direction and an assemblage is prepared at Bob's lab. By determining the quantum coherence of the prepared assemblage at Bob's side, the steerability of quantum coherence by Alice can be certified through the violation of one of the NAQC inequalities. Eq.(4.1), Eq.(4.2) and Eq.(4.3) represent the sufficient criteria to achieve NAQC from the untrusted side, *i.e.* Alice to the trusted side, *i.e.* Bob. Therefore NAQC is a task that is operationally asymmetric to manifest nonlocal quantum correlations present between a pair of particles. Similarly, the reverse task of NAQC from Bob to Alice can be demonstrated and it requires one-way classical communication from Alice to Bob. Hu *et al* showed the presence of a strict hierarchy between Bell nonlocal correlations and NAQC [HWF18]. The concept of NAQC has also recently been extended to the steered quantum coherence for the qudits [HF18]. However, we restrict to NAQC for the qubits in this chapter.

Now we briefly recall the unsharp measurement scheme introduced in Section 1.8. Here we consider the standard framework of Von-Neumann measurement [Neu55] analogous to weak measurement formalism discussed in [SGGP15]. Let us rewrite the POVM in a dichotomic unsharp Von-Neumann measurement formalism, which is defined by the effect operators  $E_{\pm}^{\Lambda}$  ( $0 \leq E_{\pm}^{\Lambda} \leq \mathbb{1}_2$ ,  $\sum_{+,-} E_{\pm}^{\Lambda} = \mathbb{1}_2$ ) as follows,

$$E_{\pm}^{\Lambda} = \Lambda \Pi_{\pm} + \frac{1-\Lambda}{2} \mathbb{1}_2 \quad (4.4)$$

where  $\Lambda$  ( $0 \leq \Lambda \leq 1$ ) is the sharpness parameter,  $\Pi_{\pm}$  (*i.e.* either  $\Pi_{\mathcal{A}}^0$  or  $\Pi_{\mathcal{A}}^1$ ) is a projective measurement operator corresponding to up or down outcome and  $\mathbb{1}_2$  is  $2 \times 2$  identity

matrix. Now by performing unsharp measurement  $\{E_{\pm}^{\Lambda}\}$  in one of the eigenbasis  $\{x, y, z\}$  on the initial state  $\rho_{AB}$  shared between Alice and Bob, the normalized conditional state at Bob's side becomes,

$$\rho_{B|E_{\pm}^{\Lambda}} = \frac{\text{Tr}_A[(\sqrt{E_{\pm}^{\Lambda}} \otimes \mathbb{1}_2) \rho_{AB} (\sqrt{E_{\pm}^{\Lambda}} \otimes \mathbb{1}_2)]}{\text{Tr}[(\sqrt{E_{\pm}^{\Lambda}} \otimes \mathbb{1}_2) \rho_{AB} (\sqrt{E_{\pm}^{\Lambda}} \otimes \mathbb{1}_2)]} \quad (4.5)$$

where, the state  $\rho_{B|E_{\pm}^{\Lambda}}$  occurs with probability

$$\begin{aligned} p_{\pm} &= \text{Tr}[(\sqrt{E_{\pm}^{\Lambda}} \otimes \mathbb{1}_2) \rho_{AB} (\sqrt{E_{\pm}^{\Lambda}} \otimes \mathbb{1}_2)] \\ &= \text{Tr}[(E_{\pm}^{\Lambda} \otimes \mathbb{1}_2) \rho_{AB}] \\ &= \Lambda \text{Tr}[(\Pi_{\pm} \otimes \mathbb{1}_2) \rho_{AB}] + \frac{1 - \Lambda}{2}. \end{aligned} \quad (4.6)$$

In general, if the outcome of the unsharp measurement is non-selective, then the transformation of the input state  $\rho_{AB}$  to the average state  $\rho'_{AB}$  under the rule of Lüder transformation, can be expressed by tracing out the state of the apparatus as

$$\begin{aligned} \rho_{AB} \rightarrow \rho'_{AB} &= \sum_{+,-} (\sqrt{E_{\pm}^{\Lambda}} \otimes \mathbb{1}_2) \rho_{AB} (\sqrt{E_{\pm}^{\Lambda}} \otimes \mathbb{1}_2) \\ &= \sqrt{1 - \Lambda^2} \rho_{AB} + (1 - \sqrt{1 - \Lambda^2}) \sum_{+,-} (\Pi_{\pm} \otimes \mathbb{1}_2) \rho_{AB} (\Pi_{\pm} \otimes \mathbb{1}_2) \end{aligned} \quad (4.7)$$

Thus in comparison with weak measurement formalism proposed by Silva *et al* [SGGP15], Mal *et al* showed that [MMH16], for unsharp qubit measurements, the *quality factor* of the measurement can be given as  $F = \sqrt{1 - \Lambda^2}$  ( $0 \leq F \leq 1$ ) which quantifies the extent to which the system remain unaffected after the measurement. Whereas the *precision* of the unsharp qubit measurement can be given as  $G = \Lambda$  ( $0 \leq G \leq 1$ ) which implies the gain of information through the measurement. It is also shown in [MMH16] through numerical analysis of various apparatus models that, for unsharp measurement on qubits, the following trade-off is strictly satisfied.

$$F^2 + G^2 = 1 \quad \forall \Lambda \in [0, 1]$$

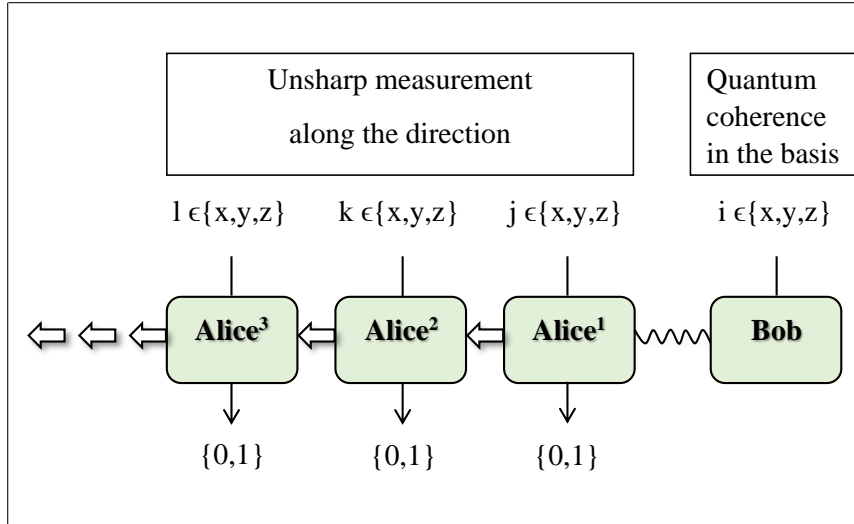


Figure 4.1: Schematic diagram of sharing the task of NAQC by sequential Alices in order to steer the local quantum coherence of Bob's subsystem.

It implies an optimal measurement which provides the maximum precision for a given quality factor. A strong or sharp measurement entails  $F = 0$  and  $G = 1$ , which implies  $\Lambda = 1$ .

We now describe a scenario introduced in [MMH16], where the non-signalling constraint is no longer applicable. We assume that half of the initial state is possessed by Bob and the other half is sequentially accessed by several Alices (say,  $Alice^1, Alice^2, \dots$ ) at Alice's side. Initially the first Alice or  $Alice^1$  shares a singlet state  $\rho_{A_1B} = |\Psi^-\rangle\langle\Psi^-|$  with Bob where  $|\Psi^-\rangle = \frac{1}{\sqrt{2}}(|01\rangle - |10\rangle)$  and  $\{|0\rangle, |1\rangle\}$  form the eigenbasis of  $\sigma_z$ . There are say,  $n$  number of Alices who perform dichotomic unsharp measurements during their individual turn of possessing half of the entangled pair of particles, in order to achieve NAQC by steering the local quantum coherence of Bob. Now after performing her unsharp version of measurement along the  $j$ -th direction,  $Alice^1$  passes the particle to  $Alice^2$  who, after performing unsharp measurement along the  $k$ -th direction on the particle of her possession, transmits the particle to  $Alice^3$ , and so on and so forth. Here except the  $n$ -th Alice, the rest  $(n - 1)$  of them can not perform sharp measurements so that the entanglement between the pair of particles can not be instantly destroyed. Every Alice is independent of each other and is ignorant about the measurement chosen by the previous Alices. Therefore, any Alice has to take the average effect of all possible settings chosen by the previous Alices into account. In this scenario, the sequential unsharp measurements performed by the Alices

are unbiased in one of the possible directions of  $\{x, y, z\}$  and hence equally probable. All Alices and Bob know beforehand that, the probability of choosing a measurement setting from the complement set of the given set of measurement directions is zero. Finally, at the end of every step of demonstrating NAQC through unsharp measurements by the Alices, Bob determines the quantum coherence of his subsystem in one of the mutually unbiased basis *i.e.*,  $i \in \{x, y, z\}$  in  $\mathbb{C}^2$ . The entire scheme of sequential sharing of NAQC irrespective of different quantifiers of quantum coherence by employing several Alices at one side and one Bob at the other side of an entangled state is pictorially demonstrated in Fig.4.1. Here our aim is to find the last Alice up to whom NAQC can be achieved with Bob.

## 4.2 Sharing of $l_1$ -norm of NAQC

The singlet state (*i.e.*  $\rho_{A_1B}$ ) maximally violates Eq.(4.1) when sharp measurements are performed by the untrusted party and the QM maximum of  $N^{l_1}$  gives its algebraic maximum *i.e.* 3. It occurs for all the maximally entangled bipartite qubit states irrespective of the untrusted party being Alice or Bob.

### 4.2.1 Alice<sup>1</sup> in the given scenario

When Alice<sup>1</sup> performs unsharp measurements corresponding to the POVM along  $x$ ,  $y$  and  $z$  directions with sharpness  $\Lambda = \lambda_1 \in [0, 1]$  by using Eq.(4.4), then depending upon Bob's estimation of his local quantum coherence, the function at the left hand side of Eq.(4.1) becomes

$$N_{A_1B}^{l_1} = \frac{1}{2} \sum_{i,j,a} p(a|E_{a|j \neq i}^{\lambda_1}) C_i^{l_1}(\rho_{B|E_{a|j \neq i}^{\lambda_1}}) = 3\lambda_1 \quad (4.8)$$

where  $i$  denotes the basis chosen by Bob in order to estimate the local quantum coherence and  $j$  denotes the direction along which Alice<sup>1</sup> performs unsharp measurement by using the effect operator  $E_{a|j}^{\lambda_1}$  applied on the singlet state  $\rho_{A_1B}$  ( $i, j \in \{x, y, z\}$ ). Alice<sup>1</sup>'s measurement yields outcome either  $a = 0$  (*i.e.* up or +) or  $a = 1$  (*i.e.* down or -). After that, Bob determines the  $l_1$ -norm of quantum coherence for the normalized conditional state

$\rho_{B|E_{a|j \neq i}^{\lambda_1}}$  obtained from  $\rho_{A_1B}$  by using Eq.(4.5). We find that,  $C_i^{l_1}(\rho_{B|E_{a|j \neq i}^{\lambda_1}}) = \lambda_1 \forall i, j, a$ . The probability of getting either up (*i.e.* + or  $a = 0$ ) or down (*i.e.* - or  $a = 1$ ) outcome from Alice<sup>1</sup>'s measurement on the joint state  $\rho_{A_1B}$  by employing Eq.(4.6) can be identified as  $p(\pm|E_{\pm|j}^{\lambda_1})$  or simply  $p_{\pm|j} \forall j$ . Note that, the singlet state with maximally mixed marginals satisfies  $p_{a|j} = \frac{1}{2} \forall j, a$ . The NAQC function given by Eq.(4.8) is found to violate Eq.(4.1) when Alice<sup>1</sup>'s sharpness of measurement, *i.e.*  $\lambda_1 > \sqrt{\frac{2}{3}} \simeq 0.82$ . Alice<sup>1</sup>'s ability to achieve NAQC in a feasible region of  $\lambda_1$  leaves scope for Alice<sup>2</sup> to implement the steerability of local quantum coherence at Bob's side to some extent.

### 4.2.2 Alice<sup>2</sup> in the given scenario

Alice<sup>2</sup> enters into the given scenario of sequentially realizing the task of NAQC with Bob when Alice<sup>1</sup> sends the particle to Alice<sup>2</sup> after carrying out an unsharp measurement at her side. Due to Alice<sup>2</sup>'s lack of knowledge about the outcome of the measurement previously performed by Alice<sup>1</sup>, the average pre-measurement state between Alice<sup>2</sup> and Bob depending upon the settings chosen by Alice<sup>1</sup> *i.e.*  $E_{\pm|j}^{\lambda_1} \forall j \in \{x, y, z\}$  (outcomes  $\pm$  correspond to  $a = \{0, 1\}$  respectively), transforms as,

$$\rho_{A_1B} \rightarrow \{\rho_{A_2B}^j = \sqrt{1 - \lambda_1^2} \rho_{A_1B} + (1 - \sqrt{1 - \lambda_1^2}) \sum_{+,-} (\Pi_{\pm|j} \otimes \mathbb{1}_2) \rho_{A_1B} (\Pi_{\pm|j} \otimes \mathbb{1}_2)\}_j \quad (4.9)$$

Here,  $\Pi_{\pm|j}$  indicates the set of projectors  $\{\Pi_j^+, \Pi_j^-\}$  along the direction  $j \in \{x, y, z\}$ .

Now Alice<sup>2</sup> performs unsharp measurements  $E_{\pm|k}^{\lambda_2}$  along direction  $k \in \{x, y, z\}$  with unsharpness parameter  $\Lambda = \lambda_2 \in [0, 1]$  on the joint state  $\rho_{A_2B}^j \forall j$ . By taking the average over all possible choices of Alice<sup>1</sup>, the NAQC function for Alice<sup>2</sup> and Bob turns out as,

$$\overline{N_{A_2B}^{l_1}} = \sum_j P_j^{A_1} N_{A_2B}^{l_1} = \frac{1}{2} \sum_{i,j,k,a} P_j^{A_1} P^j(a|E_{a|k \neq i}^{\lambda_2}) C_i^{l_1}(\rho_{B|E_{a|k \neq i}^{\lambda_2}}) \quad (4.10)$$

where,  $i$  denotes the basis chosen by Bob and the indices  $j$  and  $k$  denote the directions of measurements chosen by Alice<sup>1</sup> and Alice<sup>2</sup> respectively ( $i, j, k \in \{x, y, z\}$ ). The corresponding outcomes of Alice<sup>2</sup> is represented by  $\pm$  or  $a \in \{0, 1\}$  respectively. The normalized

conditional states,  $\{\rho_{B|E_{a|k \neq i}}^{j \lambda_2}\}_{j=x,y,z}$  can be obtained from  $\{\rho_{A_2B}^j\}_{j=x,y,z}$  by using Eq.(4.5) depending upon the measurement,  $E_{\pm|k}^{\lambda_2} \forall k \in \{x,y,z\}$  done by Alice<sup>2</sup>. Here Bob determines the  $l_1$ -norm of quantum coherence of the qubit  $\rho_{B|E_{a|k \neq i}}^{j \lambda_2}$  in the  $i$ -th basis ( $i \in \{x,y,z\}$ ). It can be easily shown that,  $C_i^{l_1}(\rho_{B|E_{a|k \neq i}}^{j \lambda_2}) = \sqrt{1 - (1 - \delta_{jk})\lambda_1^2 \lambda_2} \forall i, a$  where  $\delta_{jk}$  is the Kronecker delta. Moreover,  $p^j(\pm|E_{\pm|k}^{\lambda_2})$  or simply  $p_{\pm|k}^j \forall j, k \in \{x,y,z\}$  represents the probability of obtaining either up (denoted by  $+$  or  $a = 0$ ) or down (denoted by  $-$  or  $a = 1$ ) outcome from the measurement  $E_{\pm|k}^{\lambda_2} \forall k$  performed by Alice<sup>2</sup> by using the pre-measurement shared state  $\rho_{A_2B}^j$  after the action  $E_{\pm|j}^{\lambda_1} \forall j$  done by Alice<sup>1</sup>. Now by following Eq.(4.6), we have  $p_{a|k}^j = \frac{1}{2} \forall j, k, a$  due to the maximally mixed marginals of the states  $\rho_{A_2B}^j \forall j$ . Note that,  $\rho_{A_2B}^j \forall j \in \{x,y,z\} \equiv \{x^\vartheta\}_{\vartheta=1}^3$  has the form of Bell-diagonal states given by Eq.(1.56) with the co-efficients  $c_{i'}^j \equiv c_{i'}^{x^\vartheta} = -\sqrt{1 - (1 - \delta_{i'\vartheta})\lambda_1^2} \forall j$  (where  $i' \in \{1,2,3\}$ ,  $\delta_{i'\vartheta}$  is the Kronecker delta and  $0 \leq |c_{i'}^j| \leq 1 \forall i', j$ ). Since we assume unbiased input settings for every Alice in our work, so that the possible measurement settings chosen by the previous Alice are equally probable, *i.e.* the probability of selecting a particular measurement setting among the three mutually exclusive choice of measurement settings corresponding to Alice<sup>1</sup> is  $p_j^{A_1} = \frac{1}{3} \forall j \in \{x,y,z\}$  ( $\sum_j p_j^{A_1} = 1$ ). From Eq.(4.10), we get

$$\overline{N_{A_2B}^{l_1}} = \lambda_2(1 + 2\sqrt{1 - \lambda_1^2}) \quad (4.11)$$

If we consider the effect of NAQC up to Alice<sup>2</sup> in the given scenario, we have to consider sharp measurement for Alice<sup>2</sup>, *i.e.*  $\lambda_2 = 1$ . Hence to satisfy  $\overline{N_{A_2B}^{l_1}} > \sqrt{6}$  so that, Alice<sup>2</sup> can also be able to achieve NAQC with Bob, it is observed that  $\lambda_1 < 0.69$ . Therefore no viable region of  $\lambda_1$  within  $[0,1]$  can be found such that both Alice<sup>1</sup> and Alice<sup>2</sup> can achieve NAQC sequentially with Bob using the  $l_1$ -norm of quantum coherence. Rather it can be seen that whenever  $\lambda_1 > 0.82$ , the 2nd Alice attains the quantum mechanical maximum of  $\overline{N_{A_2B}^{l_1}} = 2.15$  which is much less than  $\sqrt{6}$ , or in other words, can not violate inequality (4.1). It occurs when Alice<sup>1</sup> has the least capability to achieve NAQC through the violation of Eq.(4.1). Therefore, it is redundant to introduce Alice<sup>3</sup> into the given scenario. Precisely, at most one Alice can execute NAQC with a Bob successfully. It can

also be checked that Alice<sup>2</sup> and Bob can reveal NAQC subject to the relaxation of the restriction imposed by Alice<sup>1</sup> on the precisions of  $\lambda_1$ . Therefore Alice, who is the only one to accomplish the task with Bob, may not uniquely be Alice<sup>1</sup>, rather be some other Alice. We can say in another way that, the task of sharing  $l_1$ -norm of NAQC with a Bob with quantum mechanical advantage, can never be achieved by more than one Alice under the given framework.

### 4.3 Sharing of relative entropy of NAQC

We now focus on sharing of NAQC using the relative entropy as a coherence measure demonstrated by the violation of Eq.(4.2). We ask whether the bound on the number of Alices who can independently steer the relative entropy of coherence of Bob in the foregoing scenario is similar to that of the previous case utilizing the  $l_1$ -norm of coherence. Keeping the possible choices of measurement settings for all Alices and the single Bob unchanged, the singlet state ( $\rho_{A_1B} = |\Psi^-\rangle\langle\Psi^-|$ ) like other Vell states in  $\mathbb{C}^2 \otimes \mathbb{C}^2$  gives the maximum quantum mechanical violation of Eq.(4.2) *i.e.*  $N^E(\rho_{A_1B}) = 3$  achieves the algebraic maximum.

#### 4.3.1 Alice<sup>1</sup> in the given scenario

When Alice<sup>1</sup> performs unsharp measurement with effect operators  $E_{a|j}^{\lambda_1}$  along direction  $j \in \{x, y, z\}$  with binary outcomes  $a \in \{0, 1\}$  satisfying Eq.(4.4) with  $\Lambda = \lambda_1$ , then the NAQC function at the left hand side of Eq.(4.2) becomes,

$$\begin{aligned} N_{A_1B}^E &= \frac{1}{2} \sum_{i,j,a} p(a|E_{a|j}^{\lambda_1}) C_i^E(\rho_{B|E_{a|j}^{\lambda_1}}) \\ &= 3[1 - H(\frac{1 - \lambda_1}{2})] \\ &= 3 \log_2(e) \lambda_1 \tanh^{-1}(\lambda_1) + \frac{3}{2} \log_2(1 - \lambda_1^2) \end{aligned} \quad (4.12)$$

where  $i \in \{x, y, z\}$ ,  $C_i^E(\cdot)$  denotes relative entropy of quantum coherence in the  $i$ -th eigenbasis and  $H(\cdot)$  represents the binary Shannon entropy function given as  $H(p) = -p \log_2 p -$

$(1-p)\log_2(1-p)$ . The other notations have their usual meaning as mentioned previously. We observe that,  $C_i^E(\rho_{B|E_{a|j \neq i}}^{\lambda_1}) = 1 - H(\frac{1-\lambda_1}{2}) \forall i, j, a$  in terms of binary Shannon entropy function. By applying  $N_{A_1B}^E$ , Eq.(4.2) is violated when  $\lambda_1 \gtrsim 0.91$ . In this region, Alice<sup>2</sup> has the possibility to achieve NAQC with Bob.

### 4.3.2 Alice<sup>2</sup> in the given scenario

Now Alice<sup>2</sup> comes into the scenario and measures  $E_{\pm|k}^{\lambda_2}$  ( $k \in \{x, y, z\}$ ) with precision  $\Lambda = \lambda_2$  on the average pre-measurement states given by Eq.(4.9). The NAQC function between Alice<sup>2</sup> and Bob, by taking the average over all possible settings of Alice<sup>1</sup>, becomes

$$\overline{N_{A_2B}^E} = \sum_j p_j^{A_1} N_{A_2B}^E = \frac{1}{2} \sum_{i,j,k,a} p_j^{A_1} p^j(a|E_{a|k \neq i}^{\lambda_2}) C_i^E(\rho_{B|E_{a|k \neq i}}^{\lambda_2}) \quad (4.13)$$

where  $i, j, k \in \{x, y, z\}$ ,  $a \in \{0, 1\}$  and Bob measures the relative entropy of coherence of the conditional state given by  $\rho_{B|E_{a|k \neq i}}^j \forall j$  in the  $i$ -th basis. The meaning of other notations remains the same as that mentioned before. It can be checked from the given scenario that, Bob's relative entropy of quantum coherence (in the  $i$ -th basis) depending upon Alice<sup>2</sup>'s unsharp measurement becomes  $C_i^E(\rho_{B|E_{a|k \neq i}}^j) = 1 - H\left(\frac{1 - \sqrt{1 - (1 - \delta_{jk})\lambda_1^2} \lambda_2}{2}\right) \forall i, a$  ( $H(\cdot)$  being the binary Shannon entropy function and  $\delta_{jk}$  being the Kronecker delta), the probability of measurement statistics for Alice<sup>2</sup>, i.e.  $p_{a|k}^j = \frac{1}{2} \forall j, k, a$  corresponding to the maximally mixed marginals of the Bell-diagonal states  $\rho_{A_2B}^j \forall j$  and  $p_j^{A_1} = \frac{1}{3} \forall j$  as per the unbiased or equiprobable measurement settings considered for Alice<sup>1</sup>.

Hence we obtain from Eq.(4.13) that,

$$\begin{aligned} \overline{N_{A_2B}^E} &= 3 - H\left(\frac{1 - \lambda_2}{2}\right) - 2H\left(\frac{1 - \sqrt{1 - \lambda_1^2} \lambda_2}{2}\right) \\ &= \log_2(e) \lambda_2 \tanh^{-1}(\lambda_2) + \frac{1}{2} \log_2(1 - \lambda_2^2) \\ &\quad + 2 \log_2(e) \sqrt{1 - \lambda_1^2} \lambda_2 \tanh^{-1}(\sqrt{1 - \lambda_1^2} \lambda_2) + \log_2(1 - (1 - \lambda_1^2) \lambda_2^2) \quad (4.14) \end{aligned}$$

where  $H(\cdot)$  is the binary Shannon entropy function.

It can be checked that, Alice<sup>2</sup> and Bob can not achieve NAQC in the range  $\lambda_1 \gtrsim$

0.91  $\forall \lambda_2 \in [0, 1]$ . The quantum mechanical maximum of  $\overline{N_{A_2B}^E}$  is 1.24 which is much smaller than the upper bound given in Eq.(4.2), *i.e.* 2.23, and can be attainable when Alice<sup>1</sup> and Bob demonstrate negligible violation of Eq.(4.2) and Alice<sup>2</sup> measures as sharp as possible. Let us consider that,  $\lambda_2 = 1$ . Then  $\overline{N_{A_2B}^E} > 2.23$  occurs when  $\lambda_1 < 0.53$ . Thus it is impossible to imagine a value of  $\lambda_1 \in [0, 1]$  for which both Alice<sup>1</sup> and Alice<sup>2</sup> can achieve NAQC sequentially with Bob. Hence just one Alice can be able to share NAQC with a single unaffected Bob when relative entropy is considered instead of  $l_1$ -norm as a coherence measure in the framework of multiple POVMs. It is needless to say that there is no need to bring Alice<sup>3</sup> in the given scenario.

## 4.4 Sharing of skew-information of NAQC

Now we investigate the sharing of NAQC by applying skew-information as the quantifier of quantum coherence. The correlation can be viewed through the quantum mechanical violation of Eq.(4.3). We enquire in the given scenario as to how many Alices can independently exhibit NAQC with a single Bob. The possible choices of settings for Alices and Bob are the kept same as before. The singlet state,  $\rho_{A_1B}$  (*i.e.*  $|\Psi^-\rangle\langle\Psi^-|$ ) provides the maximum quantum mechanical violation of Eq.(4.3), *i.e.*  $N_{A_1B}^S = 3$  by using sharp measurements at Alice<sup>1</sup>'s side. It is the algebraic maximum as well.

### 4.4.1 Alice<sup>1</sup> in the given scenario

If Alice<sup>1</sup> chooses to perform unsharp measurement ( $E_{a|j}^{\lambda_1}$ ) along the direction  $j$  with sharpness of measurement  $\Lambda = \lambda_1$ , then the left hand side of the inequality(4.3) turns out as

$$N_{A_1B}^S = \frac{1}{2} \sum_{i,j,a} p(a|E_{a|j}^{\lambda_1}) C_i^S(\rho_{B|E_{a|j}^{\lambda_1}}) = 3(1 - \sqrt{1 - \lambda_1^2}) \quad (4.15)$$

where  $i, j \in \{x, y, z\}$ ,  $a \in \{0, 1\}$  and the meaning of other notations remains unchanged. We obtain by using skew-information as the notion of quantum coherence that,  $C_i^S(\rho_{B|E_{a|j}^{\lambda_1}}) = 1 - \sqrt{1 - \lambda_1^2} \forall i, j, a$ . Eq.(4.15) violates the upper bound of Eq.(4.3) when  $\lambda_1 > \frac{2\sqrt{2}}{3} \simeq 0.94$ ,

where Alice<sup>2</sup> can operate to achieve NAQC with Bob.

#### 4.4.2 Alice<sup>2</sup> in the given scenario

Next, we consider that Alice<sup>2</sup> does dichotomic unsharp measurement along  $k$ -th direction with unsharpness parameter  $\Lambda = \lambda_2$  by considering the bipartite pre-measurement states given by Eq.(4.9). As Alice<sup>2</sup> has no knowledge about the choice of setting of the previous Alice, the correlation function of NAQC between Alice<sup>2</sup> and Bob is taken by averaging over all possible choices by Alice<sup>1</sup>, and can be expressed as,

$$\overline{N_{A_2B}^S} = \sum_j p_j^{A_1} N_{A_2B}^S = \frac{1}{2} \sum_{i,j,k,a} p_j^{A_1} p^j(a|E_{a|k \neq i}^{\lambda_2}) C_i^S(\rho_{B|E_{a|k \neq i}}^j) \quad (4.16)$$

where  $i, j, k \in \{x, y, z\}$ ,  $a \in \{0, 1\}$  keeping the rest of the notations unaltered with their usual meaning. Depending upon Alice<sup>2</sup>'s unsharp measurement along  $k$ -th direction, the skew-information of quantum coherence for the normalised conditional states  $\rho_{B|E_{a|k \neq i}}^j \quad \forall j$  in the  $i$ -th eigenbasis becomes  $C_i^S(\rho_{B|E_{a|k \neq i}}^j) = 1 - \sqrt{1 - [1 - (1 - \delta_{jk})\lambda_1^2]\lambda_2^2} \quad \forall i, a$  where  $\delta_{jk}$  is the Kronecker delta. Furthermore,  $p_{a|k}^j = \frac{1}{2} \quad \forall j, k, a$  corresponding the Bell-diagonal states  $\rho_{A_2B}^j \quad \forall j$  and  $p_j^{A_1} = \frac{1}{3} \quad \forall j$  corresponding to the unbiased framework of measurement settings pertaining to Alice<sup>1</sup>.

Now from Eq.(4.16), we get

$$\overline{N_{A_2B}^S} = 3 - \sqrt{1 - \lambda_2^2} - 2\sqrt{1 - (1 - \lambda_1^2)\lambda_2^2} \quad (4.17)$$

We see that the Alice<sup>2</sup>-Bob pair is unable to reveal NAQC when Alice<sup>1</sup> shows the correlation of NAQC with Bob, *i.e.* in the range of  $\lambda_1 \in (0.94, 1)$ . Rather the quantum mechanical maximum of  $\overline{N_{A_2B}^S}$  *i.e.* 1.11 occurs when Alice<sup>1</sup>-Bob pair marginally violates Eq.(4.3) and by performing sharp qubit measurements at Alice<sup>2</sup>'s side. Now we assume that,  $\lambda_2 = 1$  (*i.e.* sharp measurement by Alice<sup>2</sup>). In this case,  $\overline{N_{A_2B}^S} = 3 - 2\lambda_1 > 2$  occurs when  $\lambda_1 < \frac{1}{2}$ . So that, no physical value of  $\lambda_1 \in [0, 1]$  can imply the sequential realization of NAQC at Bob's side by both the untrusted parties Alice<sup>1</sup> and Alice<sup>2</sup>. Hence without in-

roducing Alice<sup>3</sup> in the given scenario, we can conclude that, skew-information of NAQC, like other forms of NAQC, can be shared by at most one Alice at the untrusted side and one Bob at the trusted side in the given set-up.

## 4.5 Summary and Outlook

Sequential sharing of nonlocal quantum correlations could be of relevance in practical information theoretic protocols involving secret key generation among multiple parties, and randomness certification [PAM<sup>+</sup>10, CJA<sup>+</sup>17]. In the present chapter, we investigate the sequential sharing of nonlocal advantage of quantum coherence (NAQC) [MPP17] which is a quantum correlation even stronger than Bell nonlocality in bipartite qubit scenario [HWF18, HF18]. We consider a bipartite entangled state in the  $\mathbb{C}^2 \otimes \mathbb{C}^2$  Hilbert space where multiple Alices perform sequential POVMs on half of the entangled pair, and a single Bob measures coherence on the other half in a particular basis. As maximally entangled states give rise to maximum quantum mechanical advantage to manifest NAQC, so by employing the singlet state, we show that at most one Alice can demonstrate NAQC with Bob. Our result is uniformly befitted to all kinds of measures of quantum coherence, including  $l_1$ -norm, relative entropy and skew-information despite of the qualitative differences among the three measures as interpreted by Rana *et al* in [RPWL17]. This stems from the relationship among them, *i.e.*  $C_i^{l_1}(\rho) \geq C_i^E(\rho) \geq C_i^S(\rho)$  in the  $i$ -th basis for a qubit  $\rho$ , in general. Moreover, our analysis displays the monogamy of NAQC in an alternative way without restricting the correlation by non-signalling theorem. On the other hand, our study is not specific for NAQC from Alice to Bob, rather it is from an observer to another observer, without a loss of generality.

It is known from the earlier results that, bipartite entanglement can be witnessed by 6 or more number of observers at one side depending upon the given framework [BMSS18, SMSS21], Bell-CHSH nonlocality can be shared between at most two observers at one end [SGGP15, MMH16, HZH<sup>+</sup>16, SCP<sup>+</sup>17], whereas quantum steering has been conjectured to be demonstrated with at most  $n$ -number of observers at one end when a steering

inequality with  $n$ -measurement settings per party is employed [SDMM18] viz three observers corresponding to 3-settings steering inequality. Based on these results, it might be expected that the bound on the number of observers is inherently connected to the strength of the nonlocal correlation, with an increase in the strength of the correlation causing the number of observers being able to share it to be decreased. Our present analysis supports such an intuition, without a proof, to the extent that, all three forms of NAQC can only be shared by one observer with another observer on the other side. Recently, our results are extended by involving higher dimensional quantum states within the multi-observer framework [HWF22], where it is shown that, the bound on the number of observers can not be improved if the biasness of the measurements on the untrusted observers is taken into consideration. However, it may be possible to improve the bound by considering the different effects of the POVMs along the different directions of the measurements for the untrusted observers, as shown in the case of Bell nonlocal correlations [BC20]. Finally, it may be interesting to implement sequential measurements together with nonlocal advantage of quantum coherence in various protocols, in the future, to certify unbounded randomness in one-sided device-independent scenario [CHK18], as well as to enhance the security of certain quantum cryptographic protocols [MDSK19].

## Sharing of an information processing task

The facets of quantum correlations have significant implications in quantum information processing tasks, such as quantum cryptography, quantum communication at a long distance etc. A secure quantum key distribution scenario has been discussed in Chapter 2. Quantum communication is another important task in quantum technologies where it is required to transfer secret information between distant locations within the capacity of quantum channels. One way is to teleport [BBC<sup>+</sup>93] an unknown quantum state by using a quantum channel without physically transporting the system. By engaging quantum repeaters network [BDCZ98] with the help of entanglement-swapping [idZZHE93], it is now possible to teleport an unknown qubit over a distance of more than a hundred kilometers [SSdRG11]. It is known for teleporting a two-level quantum system that, the protocol requires Bell-state measurement [PCL<sup>+</sup>12], 1 ebit of entanglement and 2 cbits of classical communication from the sender to the receiver. Whereas Cerf *et al* showed that [CGM00], the shared local randomness by relaxing the requirement of entanglement can teleport an unknown state classically with the aid of 2.19 cbits under the effect of projective measurements only. However, the quantum mechanical advantage, demonstrated by the protocol of Remote State Preparation (RSP) [Pat00, BDS<sup>+</sup>01], needs only 1 cbit along with the 1 ebit. The task of RSP is to prepare a remote state known to the sender but unknown to the receiver and can yet be generalized in several ways as given in the literature [LS03, BS03], and can be realized in magnetic [PZF<sup>+</sup>03] as well as optical systems by means of using single-mode photonic qubit [BBL04], polarised photons [LWO<sup>+</sup>07] via spontaneous para-

metric down-conversion, decoherent channels [XLYG05] etc. RSP has found several applications in the field of quantum information such as deterministic creation of single-photon states [CS12], preparation of single-photon hybrid entanglement [JZLW19], initializing atomic quantum memory [RBV<sup>+</sup>07], preparing qubits in quantum nodes [NK08] etc.

Despite the implementation of RSP being similar to that of teleportation [PCB03] in quantum information processing, entanglement does not act as a quantum resource for the RSP unlike teleportation for two-level systems. However, geometric quantum discord [DacLM<sup>+</sup>12, LF10] or in other way, the simultaneous correlation between mutually unbiased bases [KKJH18] plays such a role in the context of RSP. Even though the correlations remaining in the separable states can perform RSP with non-zero fidelity, it can not outperform, in terms of the strength of communication, than that corresponding to the entangled states [HTMH14, BDS<sup>+</sup>17]. The non-classicality of RSP can be further revealed in terms of steerable features of dynamical processes [CKL<sup>+</sup>20]. Additionally, it has recently been shown that similar to the spin systems, two-component Bose-Einstein condensates [CFIO<sup>+</sup>21] and single-photon beams with two degrees of freedom [WYG21, CCS<sup>+</sup>21] can be remotely prepared in different optical arrangements.

The present chapter is based on our work, "*Remote qubit state preparation by multiple observers using a single copy of a two-qubit entangled state*", S. Datta, S. Mal, A. K. Pati, and A. S. Majumdar, arXiv:2109.03682 [quant-ph] (2021) [DMPM21]. Here we investigate the possibility of implementing RSP at the receiver's (*viz* Alice's) lab by multiple distant senders (*viz* Bobs) who act sequentially and independently of each other. Alice owns half of a single copy of an entangled state while the other half is shared sequentially by several Bobs. Each Bob individually wants to convey a message to Alice by preparing a particular state at Alice's lab up to some prefixed level of tolerance. Any pure state of a qubit is represented by a point on the Bloch sphere, which is characterized by two parameters, *i.e.* polar angle *viz*  $\theta$  and azimuthal angle *viz*  $\phi$ . Before starting the protocol, the value of  $\theta$  is pre-agreed between Alice and the Bobs, *i.e.* from which circle the state would be prepared, so that Alice can apply a suitable unitary to obtain the desired state. At any instant, a particular Bob remains ignorant about the encoding activities of the previous Bobs.

In this framework of multiple observers (compatible with the description given in chapter 4), now the pertinent question is: how many Bobs can reliably convey the message to Alice within some error tolerance? In an ideal scenario, the sender, through projective measurements, can deterministically prepare the desired remote qubit [HHH03] at the receiver's end with the expense of a complete breakdown of the entanglement. However, in order to accomplish RSP by multiple senders in our case, all the Bobs (except the last one) have to measure weakly so that some amount of quantum correlation is left to be shared by the subsequent Bob and Alice. In other words, the disturbance caused due to the measurement by the Bobs has to be such that, there remains a possibility of information gained from the shared state by the subsequent Bob, as well [SGGP15, MMH16]. Motivated by the task described above, the unsharp measurements [Bus86, BLM96] are employed as Bobs' local activity such that they can prepare a remote state at Alice's lab with non-classical fidelity.

The framework of sharing of quantum correlations was investigated earlier in the context of Bell-nonlocality [SGGP15, MMH16] with experimental demonstrations [SCP<sup>+</sup>17, HZH<sup>+</sup>18, FRT<sup>+</sup>20]. Studies in different directions, including Bell-type nonlocality [DGS<sup>+</sup>19, Cab21], bipartite [SDMM18, SHDH<sup>+</sup>19], and tripartite steerability [GMD<sup>+</sup>21], nonlocal advantage of quantum coherence(NAQC) [DM18, DM19], entanglement witness [BMSS18, SMSS21], quantum teleportation [RBM<sup>+</sup>21], unbounded randomness [CJA<sup>+</sup>17] etc has been reported in succession. In all the above cases, each observer at the clustered side implements unbiased and unsharp measurements for all chosen observables. A modified framework with altered sharpness for measurements of different observables shows the possibility of realizing a quantum correlation with an unbounded number of observers [BC20, ZF21, SPS22].

In the backdrop of the above studies, here we first compute the classical limit of fidelity to prepare a remote state unknown to the receiver, without utilizing any quantum resource in the given scenario, where 1 cbit of information is allowed to be transferred from the sender (*viz* Bob) to the receiver (*viz* Alice) via a classical channel. It is calculated by taking the average of input states over a particular circle on the Bloch sphere and turns out to be different from  $\frac{2}{3}$ , found as optimal for the standard scheme of quantum teleporta-

tion [MP95]. Then we show that the maximum number of observers who can successfully realize RSP with non-classical fidelity, depends upon the choice of a plane on the Bloch sphere. Considering a singlet state shared initially, we show here that, at most 6 Bobs become successful in this task if the state to be prepared is selected from the equator of the Bloch sphere. Whereas if the chosen remote state shifts from the equatorial circle towards the poles of the Bloch sphere, then the maximum number of Bobs demonstrating the quantum advantage of RSP reduces, until zero at the two poles. It is also observed that the upper bound on the number of Bobs becomes lower than 6 when the initial state is non-maximally entangled pure or mixed.

## 5.1 Recapitulation of RSP

Let us consider the framework of RSP given in Sec.1.6.2.1 in the other way round, *i.e.* in the direction of Bob (the sender) to Alice (the receiver). If two spin- $\frac{1}{2}$  particles are prepared in a singlet state given by Eq.(1.24), where the first particle is possessed by Bob and the second particle is possessed by Alice, then from the rotational invariance under local unitary operation, it can also be represented as,

$$|\Psi^-\rangle = \frac{1}{\sqrt{2}}(|\psi^j\rangle |\psi_\perp^j\rangle - |\psi_\perp^j\rangle |\psi^j\rangle), \quad (j = 1, 2, 3, \dots) \quad (5.1)$$

where  $|\psi^j\rangle = \cos(\frac{\theta}{2})|0\rangle + \exp(i\phi_j)\sin(\frac{\theta}{2})|1\rangle$  and  $|\psi_\perp^j\rangle = -\sin(\frac{\theta}{2})|0\rangle + \exp(i\phi_j)\cos(\frac{\theta}{2})|1\rangle$ , ( $0 \leq \theta \leq \pi, 0 \leq \phi_j \leq 2\pi$ ) are two complementary pure states lying on the surface of a Bloch sphere. Now Bob selects either  $|\psi^j\rangle$  or  $|\psi_\perp^j\rangle$  which he intends to remotely prepare at Alice's side. As the state is known to Bob, he performs projective measurement from the basis  $\{|\psi^j\rangle, |\psi_\perp^j\rangle\}$  on his particle. If the outcome is  $|\psi_\perp^j\rangle$ , then he will communicate the output of his measurement to Alice through some classical channel. Hence, without transferring the particle physically, an unknown qubit will be simulated at Alice's end. Similarly, depending upon the outcome  $|\psi^j\rangle, |\psi_\perp^j\rangle$  will be prepared at Alice's end. This occurs due to the consumption of 1 ebit and 1 cbit of classical communication(CC). Let us call the CC corresponding to  $|\psi^j\rangle$  as 'up' and the CC corresponding to  $|\psi_\perp^j\rangle$  as 'down'. This require-

ment cannot be further reduced, no matter, how strong the quantum resource is [Pat00]. If Bob wants to prepare  $|\psi^j\rangle$  at Alice's lab, then he will be successful for half of the time with certainty, whereas Alice can regenerate  $|\psi^j\rangle$  from  $|\psi_\perp^j\rangle$  for the other half of the times by applying  $\sigma_z$  locally when  $|\psi^j\rangle$  is chosen only from the equatorial circle of the Bloch sphere (*i.e.*  $\theta = \frac{\pi}{2}$ ). Physically, the universal operation of complementarity on an unknown qubit is impossible to perform [BcvHW99]. Therefore, for chosen states other than the equator of the Bloch sphere, the process can not be more than 50% successful [BDS<sup>+</sup>01].

The preparation of a remote state  $|\psi^j\rangle$  at Alice's lab by using singlet state  $|\Psi^-\rangle$  shared between Alice and Bob depends on the representation of  $|\Psi^-\rangle$  in terms of two complementary pure states  $|\psi^j\rangle$  and  $|\psi_\perp^j\rangle$  as given by Eq.(5.1). However, similar representations for the other three Bell states exist [Pat00]. These are as follows,

$$|\Psi^+\rangle = \frac{1}{\sqrt{2}}(|01\rangle + |10\rangle) = -\frac{1}{\sqrt{2}}[\sigma_z|\psi_\perp^j\rangle|\psi^j\rangle - \sigma_z|\psi^j\rangle|\psi_\perp^j\rangle], \quad (5.2)$$

$$|\Phi^+\rangle = \frac{1}{\sqrt{2}}(|00\rangle + |11\rangle) = \frac{1}{\sqrt{2}}[i\sigma_y|\psi_\perp^j\rangle|\psi^j\rangle - i\sigma_y|\psi^j\rangle|\psi_\perp^j\rangle] \quad (5.3)$$

and

$$|\Phi^-\rangle = \frac{1}{\sqrt{2}}(|00\rangle - |11\rangle) = \frac{1}{\sqrt{2}}[\sigma_x|\psi_\perp^j\rangle|\psi^j\rangle - \sigma_x|\psi^j\rangle|\psi_\perp^j\rangle] \quad (5.4)$$

where  $\sigma_x$ ,  $\sigma_y$  and  $\sigma_z$  are Pauli matrices in x-, y- and z- basis respectively. Bob performs projective measurement in the basis  $\{|\psi^j\rangle, |\psi_\perp^j\rangle\}$  and communicates the result to Alice. If Bob obtains  $|\psi_\perp^j\rangle$ , then Alice applies local unitaries  $\sigma_z$ ,  $i\sigma_y$  and  $\sigma_x$  for shared states  $|\Psi^+\rangle$ ,  $|\Phi^+\rangle$  and  $|\Phi^-\rangle$  respectively, instead of  $\mathbb{1}_2$  for singlet state  $|\Psi^-\rangle$  so that  $|\psi^j\rangle$  is remotely prepared at Alice's lab. On the other hand, if Bob obtains  $|\psi^j\rangle$ , then Alice applies local unitaries  $\mathbb{1}_2$ ,  $i\sigma_z\sigma_y$  and  $\sigma_z\sigma_x$  for shared states  $|\Psi^+\rangle$ ,  $|\Phi^+\rangle$  and  $|\Phi^-\rangle$  respectively, instead of  $\sigma_z$  for singlet state  $|\Psi^-\rangle$  so that a state  $|\psi^j\rangle$  from the equatorial circle of the Bloch sphere is remotely prepared at Alice's lab. Therefore Alice's operation is invariant under local unitary for deterministic preparation of an unknown remote state at Alice's side when distinct Bell states are shared initially.

If the state is prepared with certainty, then the measure of fidelity between the target

state and the prepared state will be 1. Consider for a particular bipartite state, the prepared state is  $\rho^p$  and the pure state,  $|\psi^d\rangle$  is desired to be prepared, then by definition, the generally symmetric fidelity function between these two quantum states can be written as [Pop94],

$$f(\rho^p, \rho^d) = f(\rho^d, \rho^p) = \left( \text{Tr} \left[ \sqrt{\sqrt{\rho^d} \cdot \rho^p \cdot \sqrt{\rho^d}} \right] \right)^2 = \langle \psi^d | \rho^p | \psi^d \rangle$$

where  $\rho^d = |\psi^d\rangle\langle\psi^d|$ . The local unitary operation on Alice, *i.e.* from the set  $\{\mathbb{1}_2, \sigma_z\}$ , is not uniquely considered for the equator of the Bloch sphere due to the rotational freedom of choosing the desired state by the sender accompanied by the similar rotation on the prepared state by the receiver, *i.e.*  $f(\rho^p, \rho^d) = f(U\rho^p U^\dagger, U\rho^d U^\dagger)$  for all unitary operators  $U$ . For a singlet state with projective measurements performed on Bob's particle, a remote state can be prepared at Alice's lab perfectly such that  $f = 1$ . This is the condition for deterministic RSP [WLCL10]. Since Alice has no information available to her about the state to be prepared, the average fidelity can be calculated by considering all input states from the circle on the Bloch sphere (taking single infinity of bits *i.e.*  $\phi_i$  ( $i = 1, 2, 3, \dots$ ) into account) as,

$$f_{av} = \frac{1}{2\pi} \int_0^{2\pi} f(\rho^p, \rho^d) d\phi_i, \quad \forall i \quad (5.5)$$

The above expression is general in the sense that, it depends on the way the plane on the Bloch sphere is chosen and the way  $\rho^p$  is obtained at the receiver's end. It is obvious that the result differs for the classical, quantum and post-quantum strategies.

## 5.2 Optimal classical strategy

Let us suppose that, the sender, *viz* Bob wants to prepare a pure qubit state  $|\psi^d\rangle = \cos(\frac{\theta}{2})|0\rangle + e^{i\phi^d} \sin(\frac{\theta}{2})|1\rangle$  ( $0 \leq \theta \leq \pi, 0 \leq \phi^d \leq 2\pi$ ) in the receiver's *viz* Alice's lab, which is unknown to her, without transferring the particle physically. Here, Bob is not allowed to exploit any shared quantum resource except a classical channel by which he can send 1 cbit of information to Alice, and Alice is free to prepare a qubit up to local unitary operations.

If the prepared state in Alice's lab is  $\rho^p$ , then the closeness between the desired state and the prepared state is  $\langle \psi^d | \rho^p | \psi^d \rangle$ , which takes the form  $|\langle \psi^d | \psi^p \rangle|^2$  for pure states, *i.e.*  $\rho^p = |\psi^p\rangle\langle\psi^p|$ . The classical fidelity can be calculated by averaging the closeness over infinitely many runs where in each run Bob is given different  $|\psi^d\rangle$  from a certain plane of the Bloch sphere (*i.e.* with  $\theta$  fixed in advance). The scenario is consistent with the protocol of RSP.

If classical communication (CC) is not allowed from Bob to Alice, then Alice has to randomly guess the desired state which will either match or does not match with the desired state. Hence, the fidelity becomes  $\frac{1}{2}$  which is the lower bound of classical fidelity in any circumstances. Whereas if CC is allowed from Bob to Alice, then Bob measures a dichotomic observable  $\vec{n}_B \cdot \vec{\sigma}$  where  $\vec{n}_B = (\sin \theta_B \cos \phi_B, \sin \theta_B \sin \phi_B, \cos \theta_B)$  with  $0 \leq \theta_B \leq \pi, 0 \leq \phi_B \leq 2\pi$  and sends the outcome (either up or down) to Alice by a classical channel. The probability of getting up(down) outcome is given by  $\langle \psi^d | \frac{\mathbb{1}_2 \pm \vec{n}_B \cdot \vec{\sigma}}{2} | \psi^d \rangle = \text{Tr}[\frac{\mathbb{1}_2 \pm \vec{n}_B \cdot \vec{\sigma}}{2} \cdot |\psi^d\rangle\langle\psi^d|]$ . Now Alice can prepare either  $|\psi_1^p\rangle$  or  $|\psi_2^p\rangle$  depending upon the outcomes either up or down. As the input state is unknown to Alice, hence by taking the average over all the input states  $|\psi^d\rangle$  from the specified circle of the Bloch sphere (with  $\theta$  fixed), the fidelity expression for a classical strategy (described above) can be computed as

$$f_{cl} = \frac{1}{2\pi} \int_0^{2\pi} \left( \langle \psi^d | \frac{\mathbb{1}_2 + \vec{n}_B \cdot \vec{\sigma}}{2} | \psi^d \rangle \langle \psi^d | \psi_1^p \rangle \langle \psi_1^p | \psi^d \rangle + \langle \psi^d | \frac{\mathbb{1}_2 - \vec{n}_B \cdot \vec{\sigma}}{2} | \psi^d \rangle \langle \psi^d | \psi_2^p \rangle \langle \psi_2^p | \psi^d \rangle \right) d\phi^d \quad (5.6)$$

The classical fidelity *i.e.*  $f_{cl}$  can be optimized with respect to the measurement parameters chosen by Bob and the parameters of the states prepared by Alice. The optimum classical fidelity in terms of different state preparations considered by Alice can be classified as follows:

### 5.2.1 Case I

Let us consider here that, Alice chooses  $|\psi_2^p\rangle = \cos(\frac{\theta}{2})|0\rangle + e^{i\phi_2^p} \sin(\frac{\theta}{2})|1\rangle$  ( $0 \leq \phi_2^p \leq 2\pi$ ) and applies either  $\sigma_z$  or  $\mathbb{1}_2$  locally depending upon the outcome either up or down respec-

tively. Here  $|\psi_1^p\rangle\langle\psi_1^p| = \sigma_z \cdot |\psi_2^p\rangle\langle\psi_2^p| \cdot \sigma_z$  because unitary evolution preserves the purity of  $|\psi_1^p\rangle$ . Alice fixes the polar angle same as that of Bob using the information known beforehand and single infinity bits of information remain unknown to her. Corresponding to this condition, it can be easily seen that,

$$f_{cl} = \frac{3}{4} + \frac{1}{4}[\cos 2\theta - \cos(\phi_B - \phi_2^p) \sin^3 \theta \sin \theta_B] \leq \frac{3}{4} + \frac{\cos 2\theta + \sin^3 \theta}{4}, \quad (5.7)$$

where the inequality comes from the maximization over  $\theta_B, \phi_B, \phi_2^p$  and the equality holds for  $\theta_B = \frac{\pi}{2}, \phi_B - \phi_2^p = \pm\pi$ .

### 5.2.2 Case II

Here Alice, without applying a rotation on a certain state, chooses  $|\psi_1^p\rangle = \cos(\frac{\theta}{2})|0\rangle + e^{i\phi_1^p} \sin(\frac{\theta}{2})|1\rangle$  ( $0 \leq \phi_1^p \leq 2\pi$ ) and  $|\psi_2^p\rangle = \cos(\frac{\theta}{2})|0\rangle + e^{i\phi_2^p} \sin(\frac{\theta}{2})|1\rangle$  ( $0 \leq \phi_2^p \leq 2\pi$ ) randomly from the specified circle corresponding to the fixed polar angle of the Bloch sphere depending upon the outcomes up and down respectively. By averaging over the unknown bits of information *i.e.*  $\phi^d$ , the given condition yields that,

$$f_{cl} = \frac{3}{4} + \frac{\cos 2\theta}{4} + \frac{\sin^3 \theta \sin \theta_B}{8} [\cos(\phi_B - \phi_1^p) - \cos(\phi_B - \phi_2^p)] \leq \frac{3}{4} + \frac{\cos 2\theta + \sin^3 \theta}{4} \quad (5.8)$$

The last inequality comes by maximizing over  $\theta_B, \phi_B, \phi_1^p, \phi_2^p$  and the equality holds for  $\theta_B = \frac{\pi}{2}, \phi_B - \phi_1^p = 0$  or  $2\pi, \phi_B - \phi_2^p = \pm\pi$ .

Thus by considering both the cases, the classical upper limit of fidelity for preparing an unknown state becomes  $f_{cl}^{\max} = \frac{3}{4} + \frac{\cos 2\theta + \sin^3 \theta}{4}$  which rises above  $\frac{1}{2}$  by utilizing 1 cbit of information. It can be easily checked that, this limit can not be improved by using a Positive Operator Valued Measurement (POVM) instead of a projective measurement at Bob's side because POVM gives less information than that of projective measurements. Unlike the standard scheme of teleportation [MP95], the protocol of RSP achieves higher optimal limit of classical fidelity, *i.e.*  $\frac{3}{4} \leq f_{cl}^{\max} \leq 1$  compared to Eq.(1.23) by considering all possible circles of latitude, *i.e.*  $0 \leq \theta \leq \pi$ , on the Bloch sphere. For example, when the

equatorial circle with  $\theta = \frac{\pi}{2}$  is considered, then  $f_{cl}^{\max} = \frac{3}{4}$ , when one of the non-equatorial circles with  $\theta = \frac{\pi}{4}$  or  $\frac{3\pi}{4}$  is considered, then  $f_{cl}^{\max} = 0.838$ , and when one of the two poles with  $\theta = 0$  or  $\pi$  is considered, then  $f_{cl}^{\max} = 1$ . The choice of states from the two poles of the Bloch sphere leaves no uncertainty in predicting the state classically because these correspond to two particular states whose polar angles are already pre-shared between Alice and Bob.

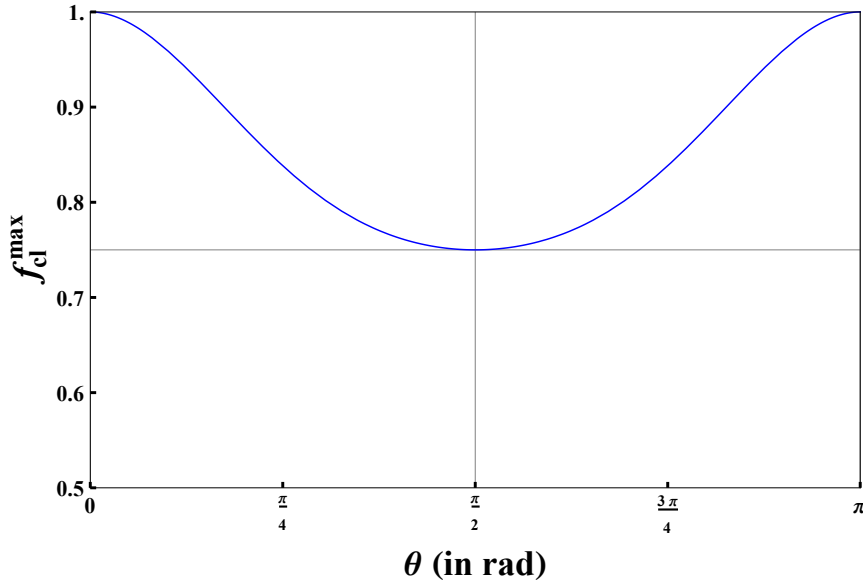


Figure 5.1: The optimum classical bound on the RSP-fidelity, *i.e.*  $f_{cl}^{\max}$  is plotted against the polar angle  $\theta$  of a fixed circle on the Bloch sphere from where Bob chooses a state to prepare at Alice's side remotely.

$f_{cl}^{\max}$  under the framework of RSP for the choice of different circles of the Bloch sphere are plotted in Fig.5.1 where it is seen that  $f_{cl}^{\max}(\theta)$  is an even function of  $\theta$  w.r.t.  $\theta = \frac{\pi}{2}$ .  $f_{cl}^{\max}$  is symmetrically distributed on either side of the equatorial circle of the Bloch sphere and gets amplified as the size of the non-equatorial circle contracts over the Bloch sphere. Any shared state without making use of quantum resources can achieve such fidelity.

### 5.3 RSP under unsharp measurement formalism

Let us recall the scenario of unsharp measurements done by sequential observers mentioned in Sec.4.1. Here we discuss the sharing of an information processing task *viz* the preparation of remote qubits at Alice's side under the formalism of sequential POVMs done by multiple Bobs. We consider that, an entangled state, for example, the singlet state,

$\rho^1 = |\Psi^-\rangle\langle\Psi^-|$ , given by Eq.(5.1), is initially shared between Alice and Bob<sup>1</sup>. The CC from Bob<sup>1</sup>, contingent upon the projective or sharp measurement on the basis known to him, can prepare the desired state at Alice's lab with certainty. Whereas unsharp measurement may result in further utilization of the state as all the entangled states are discordant [CBA16]. In this case, a CC from Bob<sup>1</sup> triggers Alice to apply a specific local unitary operation from  $\{\mathbb{1}_2, \sigma_z\}$  on her subsystem in order to obtain the desired state from the equatorial circle of the Bloch sphere with finite average RSP-fidelity.

If the chosen state is not from the equatorial circle of the Bloch sphere, then Alice allows the state without rotation depending upon the down outcome and rejects the state corresponding to the up outcome. When Alice rejects the state to consider for RSP without altering her subsystem, then she only takes the optimal classical strategy (by picking random pure states from the same non-equatorial circle of the Bloch sphere as given in case 5.2.2) to count the fidelity of preparing an unknown state from a non-equatorial circle of the Bloch sphere (*i.e.*  $f_{cl}^{\max}(\theta \neq \frac{\pi}{2})$ ). Alice rejects the system because she knows that, RSP can never be implemented deterministically corresponding to the up outcome and she takes the classical strategy because she does not know beforehand, whether Bob<sup>1</sup> and she share a quantum channel or not, without calculating the average RSP-fidelity by considering all the possible outcomes. Whereas the down outcome corresponding to the sharp measurement at Bob<sup>1</sup>'s side implies the possibility for the deterministic RSP where making use of Alice's subsystem (unknown to her) for the estimation of RSP-fidelity is no different than choosing an unknown pure state randomly from the non-equatorial plane of the Bloch sphere. In most of the cases, the occurrence of selecting or rejecting the state by Alice is random and is associated with success probability  $\frac{1}{2}$  (*i.e.* for  $\theta \neq \frac{\pi}{2}$ ). It comes out to be true for all the cases considered in our work. Hence this is linked with RSP which is successful for 50% times.

Now to restore the shared state to be reused by the next Bob for the same task, Alice can reverse her previous unitary operation by further applying  $\sigma_z$  if her previous operation was  $\sigma_z$  (in the case of remote states from the equatorial circle of the Bloch sphere), and doing nothing if it was  $\mathbb{1}_2$ . The reverse operation is redundant for the remote states chosen from

a non-equatorial circle of the Bloch sphere. Otherwise, the one-to-one correspondence between 1-cbit of communication from the sender and local unitary transformation by the receiver will be lost. Up to now, the set of operations is compatible with the framework of RSP solely.

Next, we come to the general framework of sharing a task sequentially. We assume that there are utmost  $n$ -number of Bobs at the sender wing of the initial entangled state who want to prepare qubits sequentially at the other wing occupied by a remotely placed receiver, called Alice. Following the successful intervention, Bob<sup>1</sup> passes the particle of his possession to Bob<sup>2</sup> such that, Bob<sup>2</sup> can prepare a remote state at Alice's lab. Since Bob<sup>2</sup> is independent of Bob<sup>1</sup>, he considers the average effect of all probable choices of basis by Bob<sup>1</sup>. Bob<sup>2</sup> performs an unsharp measurement on the resultant state and makes a CC to Alice. Similarly, depending upon the outcome and the chosen plane from the Bloch sphere (with known  $\theta$ ), Alice applies a suitable unitary operation so that average RSP-fidelity can be determined from the prepared state. Here also the procedure of post-selection corresponding to the non-equatorial plane of the Bloch sphere is applicable for Alice with Bob<sup>2</sup> in the scenario. Alice again performs the reverse operation, *i.e.*  $\{\mathbb{1}_2, \sigma_z\}$  for the remote state chosen from the equatorial circle of the Bloch sphere to restore the state to be re-utilized by Bob<sup>3</sup>.

Then Bob<sup>2</sup> sends his particle to Bob<sup>3</sup> and Bob<sup>3</sup> repeats the same task with different sharpness of measurement. In this way, all independent  $n$ -number of Bobs can sequentially access the particle depending upon the encryptions of previous Bobs [MMH16] and can prepare remote qubit at Alice's end by making use of a single copy of the initial entangled state. Fig.5.2 depicts the protocol in this scenario. The process continues as long as Bobs are able to perform the task of RSP with average non-classical fidelity which attains maximum value if only the last Bob in the sequence performs sharp measurement. Our aim in this chapter is to find the bound on the optimum number of Bobs in the framework of RSP mentioned above.

In general, an unsharp measurement which is a class of POVM, is characterized by the effect operators [BLM96], given by Eq.(4.4) where the outcomes are indicated as  $\{+, -\}$

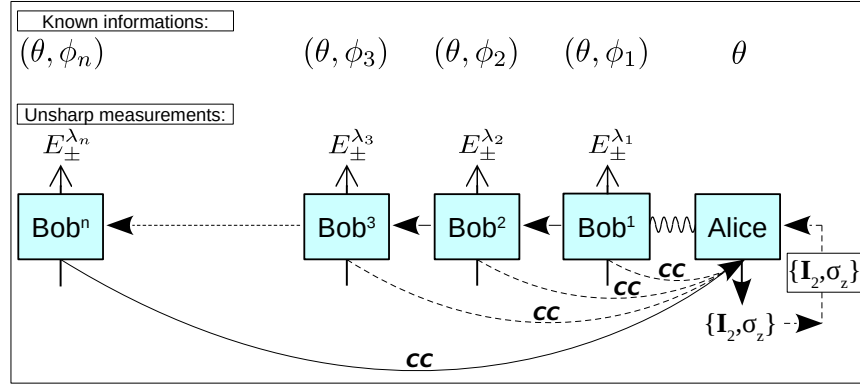


Figure 5.2: Schematic diagram of remote state preparation at Alice's lab by multiple Bobs. The local unitary operations,  $\{\mathbb{I}_2, \sigma_z\}$  and their reverse are applicable for remote states chosen from the equatorial circle of the Bloch sphere.

and  $\Lambda = \lambda_i$  corresponds to the sharpness of measurement performed by Bob<sup>*i*</sup>. The choice of measurements corresponding to projectors,  $\Pi_+^i = |\psi^i\rangle\langle\psi^i|$  and  $\Pi_-^i = |\psi_-^i\rangle\langle\psi_-^i|$  are considered to be distinct for each Bob. Depending on the outcome  $a$ , *i.e.* {up(+)} or down(-)} of the unsharp measurement done by Bob<sup>*i*</sup>, the normalised conditional state at Alice's side becomes,

$$\rho_{A|E_a^{\lambda_i}}^i = \frac{\text{Tr}_{\text{Bob}^i} \left[ \left( \mathbb{1}_2 \otimes \sqrt{E_a^{\lambda_i}} \right) \rho^i \left( \mathbb{1}_2 \otimes \sqrt{E_a^{\lambda_i}} \right) \right]}{\text{Tr} \left[ \left( \mathbb{1}_2 \otimes \sqrt{E_a^{\lambda_i}} \right) \rho^i \left( \mathbb{1}_2 \otimes \sqrt{E_a^{\lambda_i}} \right) \right]}, \quad (i = 1, 2, 3, \dots) \quad (5.9)$$

The probability of getting such state is given by,  $p_a^i = \text{Tr}[(\mathbb{1}_2 \otimes \sqrt{E_a^{\lambda_i}}) \rho^i (\mathbb{1}_2 \otimes \sqrt{E_a^{\lambda_i}})]$  (here,  $\Lambda = \lambda_i, a \in \{+, -\}$ ). Now Bob<sup>*i*</sup> communicates the outcome of his measurement to Alice through some classical channel and Alice applies a suitable unitary operation on her conditional state. Hence the average RSP-fidelity of Alice's state prepared by Bob<sup>*i*</sup>, considering all input states from a circle of the Bloch sphere chosen by Bob<sup>*i*</sup>, irrespective of outcomes, can be computed as

$$f_{av}^{AB^i} = \frac{1}{2\pi} \int_0^{2\pi} \langle \psi_-^i | \rho_{A|E_+^{\lambda_i}}^i | \psi_-^i \rangle d\phi_i = \frac{1}{2\pi} \int_0^{2\pi} \langle \psi^i | \rho_{A|E_-^{\lambda_i}}^i | \psi^i \rangle d\phi_i, \quad (i = 1, 2, 3, \dots) \quad (5.10)$$

The above general expression can be utilized to reckon RSP-fidelity averaged over all possible outcomes (binary outcomes corresponding to  $\mathbb{C}^2$ ) under suitable unitary operation for

the equatorial great circle of the Bloch sphere or under a suitable post-selection method applied for non-equatorial circles of the Bloch sphere. The first and second equality corresponds to the cases where each Bob desires to prepare  $|\psi_{\perp}^i\rangle$  or  $|\psi^i\rangle$  from the chosen circle of the Bloch sphere respectively.

When Bob<sup>*i*</sup> sends his particle to Bob<sup>*i+1*</sup> to perform the task of RSP, Bob<sup>*i+1*</sup> being completely uninformed about the choice made by Bob<sup>*i*</sup> before his measurement, considers the state shared with Alice as an average over all possible input states chosen by Bob<sup>*i*</sup> and all possible measurement outcomes. As Alice's operation is reversible, hence according to non-selective Lüder transformation (in a similar fashion to Eq.(4.7)), the shared state between Alice and Bob<sup>*i+1*</sup> becomes,

$$\rho^{i+1} = \frac{1}{2\pi} \int_0^{2\pi} \sum_{a=+,-} \left( \mathbb{1}_2 \otimes \sqrt{E_a^{\lambda_i}} \right) \rho^i \left( \mathbb{1}_2 \otimes \sqrt{E_a^{\lambda_i}} \right) d\phi_i, \quad (i = 1, 2, 3, \dots) \quad (5.11)$$

This is true even for non-equatorial circles (*i.e.*  $\theta \neq \frac{\pi}{2}$ ), when Alice discards the state without rotating and does not consider for the task of RSP corresponding to the up outcome (*i.e.* for the desirable remote state  $|\psi^i\rangle$ ) and similarly corresponding to the down outcome for the desirable remote state  $|\psi_{\perp}^i\rangle$ ) obtained by the last Bob in the sequence (*i.e.* Bob<sup>*i*</sup>) as the independence of each Bob with others and the ignorance of Bob<sup>*i+1*</sup> about the choice and outcome of the measurements done by the previous Bobs are also applicable here. By using the shared state  $\rho^{i+1}$ , Bob<sup>*i+1*</sup> completes his task, resulting in the conditional state given by Eq.(5.9) with  $i = i + 1$ .

The above steps are recursive. For the *n*-th Bob,  $f_{av}^{AB^n}$  ( $n = 1, 2, 3, \dots$ ) happens to be a function of all  $\lambda_i$  ( $i \leq n$ ). The entire process stops when the average fidelity goes below the classical limit of fidelity for all physical ranges of  $\lambda_i \in [0, 1]$ s compatible for successful remote state preparations up to previous Bob.

## 5.4 Sequential RSP with maximally entangled pure state

According to the previously mentioned formalism, here we explore the bound on the number of Bobs who can sequentially prepare remote state, picked from the different circles of

a Bloch sphere, at Alice's side. Primarily, we assume the initial state between Alice and Bob<sup>1</sup> to be one of the maximally entangled states, *i.e.* the singlet state, since the resource in terms of quantum geometric discord is maximum (*i.e.* 1) for such a state [DacLM<sup>+</sup>12, Luo08, LF10]. Note that, all the maximally entangled states produce similar results as they are invariant under local unitary operations. Now, instead of performing the sharp measurement, Bob<sup>1</sup> chooses to perform  $\{E_{\pm}^{\lambda_1}\}$ , and by communicating the output classically, he wants to prepare states from  $\{|\psi^1\rangle, |\psi_{\perp}^1\rangle\}$  at Alice's side.

**Lemma 5.1.** *The fidelity of preparing any pure state to Alice subject to unsharp measurement by Bob<sup>1</sup> with sharpness  $\lambda_1$  while sharing a Bell state is  $\frac{1+\lambda_1}{2}$ .*

*Proof.* We consider the initial state  $\rho^1 = |\Psi^-\rangle\langle\Psi^-|$ . Depending upon the outcome  $\{+, -\}$  obtained by Bob<sup>1</sup>, the state produced at Alice becomes either

$$\rho_{A|E_+}^{1\lambda_1} = \lambda_1 |\psi_{\perp}^1\rangle\langle\psi_{\perp}^1| + \frac{1-\lambda_1}{2} \mathbb{1}_2, \quad \forall \theta, \phi_1 \quad (5.12)$$

or

$$\rho_{A|E_-}^{1\lambda_1} = \lambda_1 |\psi^1\rangle\langle\psi^1| + \frac{1-\lambda_1}{2} \mathbb{1}_2, \quad \forall \theta, \phi_1 \quad (5.13)$$

Therefore, it follows that,  $f^{AB^1} = \langle\psi_{\perp}^1|\rho_{A|E_+}^{1\lambda_1}|\psi_{\perp}^1\rangle = \langle\psi^1|\rho_{A|E_-}^{1\lambda_1}|\psi^1\rangle = \frac{1+\lambda_1}{2}$ ,  $\forall \theta, \phi_1$ .  $\square$

Corresponding to the completely successful preparation of remote states  $\{|\psi^1\rangle\}_{\phi_1}$  from the equatorial circle of the Bloch sphere (*i.e.* with  $\theta = \frac{\pi}{2}$ ), the average RSP-fidelity,  $f_{av}^{AB^1} = \frac{1}{2\pi} \int_0^{2\pi} (p_+^1 \langle\psi^1|\sigma_z \cdot \rho_{A|E_+}^{1\lambda_1} \cdot \sigma_z |\psi^1\rangle + p_-^1 \langle\psi^1|\rho_{A|E_-}^{1\lambda_1} |\psi^1\rangle) d\phi_1 = \frac{1+\lambda_1}{2} > \frac{3}{4}$  occurs when  $\lambda_1 > \frac{1}{2}$ . Here, the probability of getting  $\rho_{A|E_{\pm}}^{1\lambda_1}$ , *i.e.*  $p_{\pm}^1$  satisfies  $p_+^1 = p_-^1 = \frac{1}{2} \forall \phi_1, \lambda_1$ . The result is unaltered for the choice of remote states  $\{|\psi_{\perp}^1\rangle\}_{\theta=\frac{\pi}{2}, \phi_1}$ .

On the other hand, corresponding to the 50% successful preparation of remote states  $\{|\psi^1\rangle\}_{\phi_1}$  from any non-equatorial circle of the Bloch sphere (*i.e.* with  $\theta \neq \frac{\pi}{2}$ ), the average RSP-fidelity, by considering both the outcomes, becomes  $f_{av}^{AB^1} = \frac{1}{2\pi} \int_0^{2\pi} (p_+^1 f_{cl}^{\max} + p_-^1 \langle\psi^1|\rho_{A|E_-}^{1\lambda_1} |\psi^1\rangle) d\phi_1 = \frac{f_{cl}^{\max}}{2} + \frac{1+\lambda_1}{4}$  where  $p_+^1 = p_-^1 = \frac{1}{2} \forall \theta, \phi_1, \lambda_1$ . This is because Alice post-selects the state corresponding to the down outcome at Bob<sup>1</sup>'s side and dis-

cards the state without considering it for the task of RSP corresponding to the up outcome at Bob<sup>1</sup>'s side and the fidelity can achieve the classical upper bound  $f_{cl}^{\max} = \frac{3}{4} + \frac{\cos 2\theta + \sin^3 \theta}{4}$  when Alice discards the state. Therefore  $f_{av}^{AB^1} = \frac{f_{cl}^{\max}}{2} + \frac{1+\lambda_1}{4} > f_{cl}^{\max}$  occurs when  $\lambda_1 > \frac{1+\cos 2\theta + \sin^3 \theta}{2}$  (see Fig.5.5). By applying similar arguments for the remote states  $\{|\psi_{\perp}^1\rangle\}_{\theta \neq \frac{\pi}{2}, \phi_1}$ , the result remains unchanged. Hence for this region of  $\lambda_1$ , the Bell states remain useful for further utilization in the task of RSP.

After a suitable reversible operation done by Alice, Bob<sup>1</sup> can now send his particle to Bob<sup>2</sup> for the next round of the protocol. From now onwards, we discuss the task of sharing by several Bobs in two different ways based on their choice of circles from the Bloch sphere.

#### 5.4.1 RSP from equatorial great circle

Here we fix, a priori, the remote states from the equatorial circle of the Bloch sphere, *i.e.*  $\theta = \frac{\pi}{2}$ , which is known to all the Bobs and Alice as well via a public channel. As per the formalism, Alice has no access to  $\phi_i$ s, *i.e.* single infinity bits of information about the state to be prepared remains unknown to her.

**Lemma 5.2.** *For every step of remote qubit preparation at Alice's side, the average state remains discordant for the subsequent Bob.*

*Proof.* From Bob<sup>2</sup> onwards, the pre-measurement state between Alice and Bob<sup>*i*</sup> can be obtained from Eq.(5.11) by using the singlet state as the initial state and by averaging over all input states from the equatorial great circle of the Bloch sphere and the measurement outcomes chosen by previous Bob. It takes the form of a Bell-diagonal state as given by Eq.(1.56) with different state parameters corresponding to different numbers of Bobs at a particular stage of the protocol. For instance, the average state between Alice and Bob<sup>*i*</sup> (up to *i*-number of Bobs in a given scenario) becomes,

$$\rho^i = \frac{1}{4} \left( \mathbb{1}_2 \otimes \mathbb{1}_2 + \sum_{j=1}^3 c_{ij} \sigma_j \otimes \sigma_j \right), \quad (i \geq 2) \quad (5.14)$$

where,  $\{\sigma_j\}_{j=1}^3$  are Pauli spin matrices (for a spin- $\frac{1}{2}$  particle) and the state co-efficients

( $0 \leq |c_{ij}| \leq 1 \forall i, j$ ) turn out to be,

$$c_{i1} = c_{i2} = -\frac{1}{2^{i-1}} \prod_{k=1}^{i-1} \left(1 + \sqrt{1 - \lambda_k^2}\right), \quad c_{i3} = -\prod_{k=1}^{i-1} \sqrt{1 - \lambda_k^2}, \quad (i \geq 2) \quad (5.15)$$

Note that, by using singlet state  $\rho^1$  and unsharp measurements  $E_a^{\lambda_1} \forall a$ , the form of  $\rho^2$  can be obtained from Eq.(5.11). Now  $E_{\pm}^{\lambda_1}$  depends on either  $|\psi^i\rangle$  or  $|\psi_{\perp}^i\rangle$  which is a function of azimuthal angle  $\phi_i$  by fixing polar angle  $\theta = \frac{\pi}{2}$ . Then  $\rho^2$  takes the form of a Bell-diagonal state given by Eq.(5.14) by using  $i = 2$ . Similarly, by using  $\rho^2$  and unsharp measurements  $E_{\pm}^{\lambda_2}$ , Eq.(5.11) can further be employed to obtain  $\rho^3$ , which has the form of Eq.(5.14) with  $i = 3$ . Thus Eq.(5.14) is a generalized form of shared state between Alice and subsequent Bobs with having the state co-efficients given by Eq.(5.15).

The correlation matrix  $M^i$  corresponding to  $\rho^i$ , which is constructed by the elements  $\{M_{pq}^i | M_{pq}^i = \text{Tr}[(\sigma_p \otimes \sigma_q) \rho^i]\}_{p,q=1}^3$ , has eigenvalues  $\{c_{i1}, c_{i2}, c_{i3}\}$ . It is easy to check that two of the eigenvalues,  $c_{i1} = c_{i2} \neq 0 \forall \lambda_k \in [0, 1], (k = 1, \dots, i)$ . Hence, the geometric discord of the state is always non-zero [DacLM<sup>+</sup>12]. This implies that the average state remains resourceful for the next round of RSP.  $\square$

Note that, when Alice and Bob<sup>*i*</sup> ( $i \geq 2$ ) share the joint state  $\rho^i$ , belonging to the family of Bell-diagonal states with maximally mixed marginals [HH96, Luo08], then Bob<sup>*i*</sup> performs an unsharp measurement on his subsystem in the basis  $\{|\psi^i\rangle, |\psi_{\perp}^i\rangle\}$  and sends the result to Alice via CC. Depending upon the outcome, the normalised conditional state at Alice's side becomes either  $\rho_{A|E_{+}^{\lambda_i}}^i$  or  $\rho_{A|E_{-}^{\lambda_i}}^i$ . If Bob<sup>*i*</sup> wants to prepare  $|\psi^i\rangle$  or  $|\psi_{\perp}^i\rangle$  chosen from a given circle with polar angle  $\theta$  on the Bloch sphere, then the average fidelity between the prepared and the desired state becomes  $f_{av} = \frac{1}{2\pi} \int_0^{2\pi} \langle \psi^i | \rho_{A|E_{-}^{\lambda_i}}^i | \psi^i \rangle d\phi_i = \frac{1}{2\pi} \int_0^{2\pi} \langle \psi_{\perp}^i | \rho_{A|E_{+}^{\lambda_i}}^i | \psi_{\perp}^i \rangle d\phi_i = \frac{1}{2} - \frac{\lambda_i}{4} [(c_{i1} + c_{i2}) \sin^2 \theta + 2c_{i3} \cos^2 \theta]$ . It corresponds to either less than or nearly 50% successful RSP when  $\theta \in (0, \frac{\pi}{2}) \cup (\frac{\pi}{2}, \pi)$ . Whereas for completely successful RSP with  $\theta = \frac{\pi}{2}$ , the fidelity, averaged over all input states and measurement

outcomes, becomes

$$\begin{aligned}
f_{av}^{ABi} &= \frac{1}{2\pi} \int_0^{2\pi} (p_+^i \langle \Psi^i | \sigma_z \cdot \rho_{A|E_+}^i \cdot \sigma_z | \Psi^i \rangle + p_-^i \langle \Psi^i | \rho_{A|E_-}^i | \Psi^i \rangle) d\phi_i \\
&= \frac{1}{2\pi} \int_0^{2\pi} \langle \Psi^i | \rho_{A|E}^i | \Psi^i \rangle d\phi_i \\
&= \frac{1}{2} - \frac{\lambda_i(c_{i1} + c_{i2})}{4},
\end{aligned} \tag{5.16}$$

where  $p_+^i = p_-^i = \frac{1}{2} \forall c_{ij}, \phi_i, \lambda_i$ . Now  $\rho^i$  reduces to the well-known Werner state [Wer89] with  $c_{i1} = c_{i2} = c_{i3} = -c$ , *i.e.* given by Eq.(1.57) where  $0 \leq c \leq 1$ . By using  $\rho_{AB}^W$  and projective (sharp) measurements (*i.e.*  $\Lambda = \lambda_i = 1$ ) at Bob's side, we have the average RSP-fidelity as

$$f_{av}(\rho_{AB}^W) = \frac{1+c}{2}, \tag{5.17}$$

which yields the quantum advantage at its best when  $\theta = \frac{\pi}{2}$ . Hence the non-classicality of average RSP-fidelity corresponding to input states from the equatorial plane of the Bloch sphere is achieved for the initially shared Werner state when  $c > \frac{1}{2}$ . Whenever the shared state between Alice and Bob is discordant with maximally mixed marginals, it has the average RSP-fidelity  $\frac{1}{2} < f_{av} \leq 1$ . It can be easily checked that, the fidelity is 1 for the maximally entangled or Bell states, whereas it goes to  $\frac{1}{2}$  iff the shared state is maximally mixed. In fact, the average RSP-fidelity lowers as the mixedness of the shared state increases as shown in [DacLM<sup>+</sup>12].

#### 5.4.1.1 Geometric discord vs concurrence

Geometric quantum discord of a joint state  $\rho_{AB} = \rho^i$  can be computed by minimizing the trace distance of  $\rho^i$  from the set of zero-discord states or the classical states ( $\eta_{AB}$ ) [DacVB10, DacLM<sup>+</sup>12] as given by Eq.(1.54). Thus we have,

$$\mathbb{D}^{(2)}(\rho^i) = \frac{1}{2}(c_{i1}^2 + c_{i2}^2 + c_{i3}^2 - \max\{c_{i1}^2, c_{i2}^2, c_{i3}^2\}) \tag{5.18}$$

Corresponding to Bob<sup>*i*</sup>, we have  $c_{i1}^2 = c_{i2}^2 \geq c_{i3}^2$  for all  $i \geq 2$  by using Eq.(5.15). Hence  $\mathbb{D}^{(2)}(\rho^{i \geq 2}) = \frac{1}{2}(c_{i1}^2 + c_{i3}^2)$ . Let us consider for Bob<sup>1</sup>,  $\mathbb{D}^{(2)}(|\Psi^-\rangle\langle\Psi^-|) = 1$ . Bob<sup>*i*</sup> ( $i \geq 2$ )

in order to perform the task of RSP, can utilize  $\max_{\{\lambda_k\}_{k=1}^{i-1}} \mathbb{D}^{(2)}(\rho^i)$  amount of quantum resource maximally.

On the other hand, a non-zero measure of concurrence implies the entanglement of a bipartite qubit state [HW97, Woo98] as demonstrated by Eq.(1.19). Concurrence is maximum for Bell states, e.g.  $\mathcal{E}_C(|\Psi^-\rangle\langle\Psi^-|) = 1$ , whereas for a Bell diagonal state  $\rho^i$  ( $i \geq 2$ ), we can construct a matrix  $\mathbb{R} = \sqrt{\sqrt{\rho^i} (\rho^i)^* \sqrt{\rho^i}}$  which has the same eigenspectrum as that of  $\rho^i$ . Let us call the largest eigenvalue of  $\rho^i$  as  $\tau^i$ . Therefore the concurrence function [QZL<sup>+</sup>16] can be expressed as,

$$\mathcal{E}_C(\rho^i) = \max\{0, 2\tau^i - 1\} \quad (5.19)$$

In the given scenario, we obtain

$$\tau^i = \frac{1}{4} \left[ 1 + \prod_{k=1}^{i-1} \sqrt{1 - \lambda_k^2} + \frac{1}{2^{i-2}} \prod_{k=1}^{i-1} \left( 1 + \sqrt{1 - \lambda_k^2} \right) \right], \quad (i \geq 2) \quad (5.20)$$

The optimum resource in terms of entanglement between Alice and Bob<sup>*i*</sup> ( $i \geq 2$ ) becomes,  $\max_{\{\lambda_k\}_{k=1}^{i-1}} \mathcal{E}_C(\rho^i)$ . The maximization of the resources, whether it is geometric discord or entanglement w.r.t. the  $\lambda_k$  values, is done such that, the state remains useful for RSP beyond the classical domain considering all the previous Bobs. In other words, the maximum resource remaining for Bob<sup>*i*</sup> is such that, all Bobs from Bob<sup>1</sup> up to Bob<sup>*i-1*</sup> are successful in the task of RSP. We emphasize that this is not equivalent to sharing of resource in terms of geometric discord or entanglement among multiple observers at one side.

$i \hat{=} \text{Bob}^i$	$\max_{\{\lambda_k\}_{k=1}^{i-1}} \mathbb{D}^{(2)}(\rho^i)$	$\max_{\{\lambda_k\}_{k=1}^{i-1}} \mathcal{E}_C(\rho^i)$
1	1	1
2	0.810	0.866
3	0.637	0.726
4	0.481	0.578
5	0.342	0.418
6	0.219	0.239
7	0.109	0.021

Table 5.1: The leftover amount of geometric discord and concurrence, that can be maximally utilized by different numbers of Bobs in the given scenario where each Bob prepares remote state from the equatorial great circle of the Bloch sphere by making use of the singlet state as the initial quantum resource.

The residual amount of available resources in terms of both geometric discord and concurrence, after every successful step of RSP, gets diminished after subsequent measurements of Bobs. In each case we have to calculate the maximum utilizable resource present in the shared state to know whether the state can be further used for RSP or not. For instance, we have to calculate the maximum discord that remains in the state  $\rho^i$  shared between Alice and Bob<sup>*i*</sup> after the measurements performed by Bobs successful for RSP up to Bob<sup>*i*-1</sup> such that, Bob<sup>*i*</sup>'s ability to perform RSP by using  $\rho^i$  can be known. The maximization depends on the ability of all Bobs up to Bob<sup>*i*-1</sup> to perform RSP specified by the range of sharpness parameters shown subsequently in Table 5.2 where the remote states are prepared from the equatorial great circle of the Bloch sphere. Similarly, the concurrence as a measure of entanglement for the states  $\rho^i$  is maximized. We show the leftover quantum resources numerically for different number of Bobs in Table 5.1.

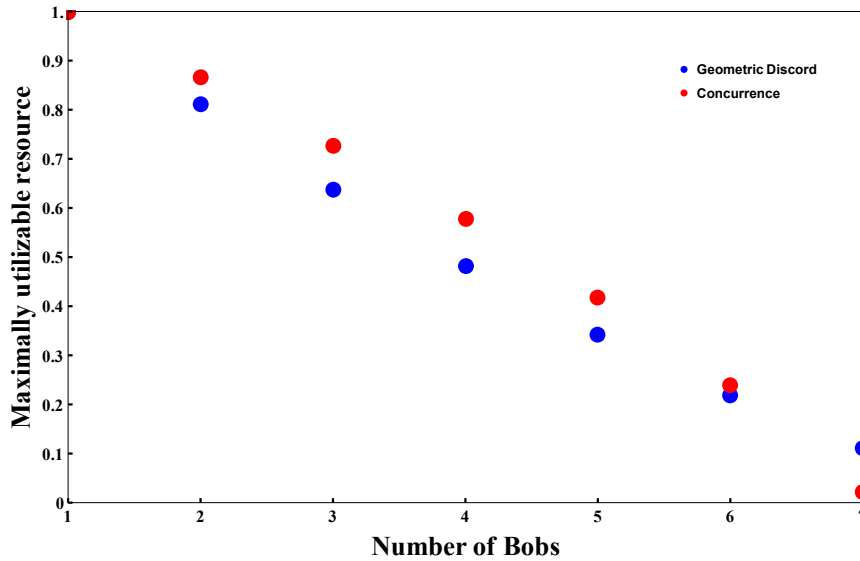


Figure 5.3: The optimally available geometric discord and concurrence for different number of Bobs is presented whenever the implementation of RSP is achievable upto its previous Bobs with non-classical advantage at Alice's side.

We can thus plot in Fig.5.3 the geometric discord and concurrence with the set of data points given in Table 5.1, which the Bobs can maximally utilize in the successive steps to perform RSP. We observe that, after the success of Bob<sup>6</sup> in the task of RSP, both the geometric quantum discord and the concurrence remains positive and the possibility remains for the 7-th Bob to perform RSP as well. From Table 5.2, we can easily predict that  $\lambda_7$  is no less than 0.859 and for such value of  $\lambda_7$ , the concurrence vanishes while the

geometric discord still remains positive.

**Theorem 5.1.** *At most 6 number of Bobs can share the task of preparing remote state chosen from the equatorial circle of the Bloch sphere at Alice's side when a maximally entangled state is initially shared between Alice and Bob<sup>1</sup>.*

*Proof.* Suppose that, Bob<sup>i</sup> wishes to prepare remote state and he communicates the result of his unsharp measurements  $E_{\pm}^{\lambda_i}$  to Alice via CC. According to Eq.(5.9), the conditional state prepared from the states  $\rho^i$  as given by Eq.(5.14) at Alice's side, becomes either corresponding to the outcome (+) as,

$$\begin{aligned} \rho_{A|E_+}^i &= \frac{\lambda_i}{2^{i-1}} \prod_{k=1}^{i-1} \left(1 + \sqrt{1 - \lambda_k^2}\right) |\psi_{\perp}^i\rangle\langle\psi_{\perp}^i| \\ &+ \frac{1}{2} \left[1 - \frac{\lambda_i}{2^{i-1}} \prod_{k=1}^{i-1} \left(1 + \sqrt{1 - \lambda_k^2}\right)\right] \mathbb{1}_2, \quad (i \geq 2) \end{aligned} \quad (5.21)$$

or corresponding to the outcome (-) as,

$$\begin{aligned} \rho_{A|E_-}^i &= \frac{\lambda_i}{2^{i-1}} \prod_{k=1}^{i-1} \left(1 + \sqrt{1 - \lambda_k^2}\right) |\psi^i\rangle\langle\psi^i| \\ &+ \frac{1}{2} \left[1 - \frac{\lambda_i}{2^{i-1}} \prod_{k=1}^{i-1} \left(1 + \sqrt{1 - \lambda_k^2}\right)\right] \mathbb{1}_2, \quad (i \geq 2) \end{aligned} \quad (5.22)$$

Finally depending upon the CC made by Bob<sup>i</sup>, Alice applies a local unitary operation chosen from the set  $\{\mathbb{1}_2, \sigma_z\}$  to obtain the maximum RSP-fidelity. The average RSP-fidelity can be derived from Eq.(5.10) by considering all the input states and all the measurement outcomes with the help of Eq.(5.21) and Eq.(5.22) as follows.

When Bob<sup>i</sup> obtains up(+) outcome, then the conditional state given by Eq.(5.21) is prepared at Alice's side and Alice applies  $\sigma_z$  rotation to attain the desired state  $|\psi^i\rangle = \frac{1}{\sqrt{2}}(|0\rangle + \exp(i\phi_i)|1\rangle)$ . Hence after the rotation, the state becomes  $\sigma_z \cdot \rho_{A|E_+}^i \cdot \sigma_z$ . So the RSP-fidelity by taking the average over all the desired states from the equatorial great circle of the Bloch sphere becomes,

$$f_+^{AB^i} = \frac{1}{2\pi} \int_0^{2\pi} \langle\psi^i|\sigma_z \cdot \rho_{A|E_+}^i \cdot \sigma_z|\psi^i\rangle d\phi_i, \quad (i \geq 2) \quad (5.23)$$

Now by applying  $\sigma_z \cdot |\psi_\perp^i\rangle\langle\psi_\perp^i| \cdot \sigma_z = |\psi^i\rangle\langle\psi^i|$  for  $\theta = \frac{\pi}{2}$  on Eq.(5.21), Eq.(5.23) becomes,

$$\begin{aligned} f_+^{AB^i} &= \left[ \frac{\lambda_i}{2^{i-1}} \prod_{k=1}^{i-1} \left( 1 + \sqrt{1 - \lambda_k^2} \right) \right] \frac{1}{2\pi} \int_0^{2\pi} \langle\psi^i|\psi^i\rangle\langle\psi^i|\psi^i\rangle d\phi_i \\ &\quad + \frac{1}{2} \left[ 1 - \frac{\lambda_i}{2^{i-1}} \prod_{k=1}^{i-1} \left( 1 + \sqrt{1 - \lambda_k^2} \right) \right] \frac{1}{2\pi} \int_0^{2\pi} \langle\psi^i|\sigma_z^2|\psi^i\rangle d\phi_i \\ &= \frac{1}{2} + \frac{\lambda_i}{2^i} \prod_{k=1}^{i-1} \left( 1 + \sqrt{1 - \lambda_k^2} \right), \quad (i \geq 2) \end{aligned} \quad (5.24)$$

In a similar fashion, when Bob<sup>i</sup> obtains down(-) outcome, then the conditional state given by Eq.(5.22) is prepared at Alice's side and Alice applies  $\mathbb{1}_2$  to obtain the desired state  $|\psi^i\rangle$ . Therefore the RSP-fidelity becomes,

$$\begin{aligned} f_-^{AB^i} &= \frac{1}{2\pi} \int_0^{2\pi} \langle\psi^i|\mathbb{1}_2 \cdot \rho_{A|E_-}^i \cdot \mathbb{1}_2|\psi^i\rangle d\phi_i, \\ &= \left[ \frac{\lambda_i}{2^{i-1}} \prod_{k=1}^{i-1} \left( 1 + \sqrt{1 - \lambda_k^2} \right) \right] \frac{1}{2\pi} \int_0^{2\pi} \langle\psi^i|\psi^i\rangle\langle\psi^i|\psi^i\rangle d\phi_i \\ &\quad + \frac{1}{2} \left[ 1 - \frac{\lambda_i}{2^{i-1}} \prod_{k=1}^{i-1} \left( 1 + \sqrt{1 - \lambda_k^2} \right) \right] \frac{1}{2\pi} \int_0^{2\pi} \langle\psi^i|\psi^i\rangle d\phi_i \\ &= \frac{1}{2} + \frac{\lambda_i}{2^i} \prod_{k=1}^{i-1} \left( 1 + \sqrt{1 - \lambda_k^2} \right), \quad (i \geq 2) \end{aligned} \quad (5.25)$$

On the other hand, if the desired state at Alice's side is  $|\psi_\perp^i\rangle = \frac{1}{\sqrt{2}}(|0\rangle - \exp(i\phi_i)|1\rangle)$ , then depending upon Alice's unitaries  $\{\mathbb{1}_2, \sigma_z\}$  corresponding to Bob<sup>i</sup>'s outcomes  $\{+, -\}$ , the RSP-fidelities turn out as,

$$\begin{aligned} f_\pm^{AB^i} &= \frac{1}{2\pi} \int_0^{2\pi} \langle\psi_\perp^i|\mathbb{1}_2 \cdot \rho_{A|E_\pm}^i \cdot \mathbb{1}_2|\psi_\perp^i\rangle d\phi_i, \\ &= \frac{1}{2\pi} \int_0^{2\pi} \langle\psi_\perp^i|\sigma_z \cdot \rho_{A|E_\pm}^i \cdot \sigma_z|\psi_\perp^i\rangle d\phi_i, \\ &= \frac{1}{2} + \frac{\lambda_i}{2^i} \prod_{k=1}^{i-1} \left( 1 + \sqrt{1 - \lambda_k^2} \right), \quad (i \geq 2) \end{aligned} \quad (5.26)$$

Thus the average RSP-fidelity considered upto Bob<sup>i</sup>, by taking all the input states from the equatorial great circle of the Bloch sphere and all the possible measurement outcomes

in different contexts into account, has the following representation,

$$\begin{aligned}
f_{av}^{AB^i} &= \frac{1}{2\pi} \int_0^{2\pi} (p_+^i \langle \psi^i | \sigma_z \cdot \rho_{A|E_+}^i \cdot \sigma_z | \psi^i \rangle + p_-^i \langle \psi^i | \mathbb{1}_2 \cdot \rho_{A|E_-}^i \cdot \mathbb{1}_2 | \psi^i \rangle) d\phi_i \\
&= \frac{1}{2\pi} \int_0^{2\pi} (p_+^i \langle \psi_\perp^i | \mathbb{1}_2 \cdot \rho_{A|E_+}^i \cdot \mathbb{1}_2 | \psi_\perp^i \rangle + p_-^i \langle \psi_\perp^i | \sigma_z \cdot \rho_{A|E_-}^i \cdot \sigma_z | \psi_\perp^i \rangle) d\phi_i \\
&= \frac{f_+^{AB^i} + f_-^{AB^i}}{2} = f_{\pm}^{AB^i} \\
&= \frac{1}{2} + \frac{\lambda_i}{2^i} \prod_{k=1}^{i-1} \left(1 + \sqrt{1 - \lambda_k^2}\right), \quad (i \geq 2)
\end{aligned} \tag{5.27}$$

where the probabilities of finding the conditional states  $\rho_{A|E_{\pm}}^i$  (i.e.  $p_{\pm}^i$ ) satisfy  $p_+^i = p_-^i = \frac{1}{2} \forall \phi_i, \lambda_i$  ( $i \geq 1$ ).

Eq.(5.27) can also be reproduced by plugging Eq.(1.56) into Eq.(5.16). Furthermore, it can easily be checked from the following observation that,  $\{\mathbb{1}_2, \sigma_z\}$  is eventually the optimal set of unitaries, which gives rise to Eq.(5.27). Let us consider that, Alice applies a general  $2 \times 2$  unitary matrix having the form,  $\mathcal{U} = \begin{pmatrix} \cos(\frac{\zeta}{2}) e^{i(\frac{\iota+\kappa}{2})} & \sin(\frac{\zeta}{2}) e^{-i(\frac{\iota-\kappa}{2})} \\ -\sin(\frac{\zeta}{2}) e^{i(\frac{\iota-\kappa}{2})} & \cos(\frac{\zeta}{2}) e^{-i(\frac{\iota+\kappa}{2})} \end{pmatrix}$  next to her prefixed set of unitaries  $\{\mathbb{1}_2, \sigma_z\}$ . Then the average fidelity in the given scenario between Alice and Bob<sup>*i*</sup> ( $i \geq 2$ ) transforms as,  $\langle \psi_\perp^i | \rho_{A|E_+}^i | \psi_\perp^i \rangle = \langle \psi^i | \rho_{A|E_-}^i | \psi^i \rangle = \frac{1}{2} + \frac{\lambda_i}{2^i} \prod_{k=1}^{i-1} (1 + \sqrt{1 - \lambda_k^2}) [\cos^2(\frac{\zeta}{2}) \cos(\iota + \kappa) - \sin^2(\frac{\zeta}{2}) \cos(\iota - \kappa - 2\phi_i)]$ , which becomes maximum when  $\zeta = \iota = \kappa = 0$  or  $2\pi$ , i.e.  $\mathcal{U} = \mathbb{1}_2$ .

The success of Bob<sup>*i*</sup> is indicated by  $f_{av}^{AB^i} > \frac{3}{4}$ , and there can be found a range of  $\lambda_i$ , ( $i \geq 1$ ) in each iteration ( $i$ ) for which such fidelity can be achieved. Using the range of  $\lambda_j$ , ( $j < i$ ) corresponding to all the previous Bobs up to Bob<sup>*j*</sup>  $\forall j \in \{1, 2, \dots, i-1\}$ , being capable of performing RSP at Alice's side, a new range of  $\lambda_i$  can be specified for the  $i$ -th Bob. Proceeding in this way, we can obtain the particular ranges of sharpness parameters given in Table 5.2, for which quantum fidelity of RSP is achieved up to the corresponding Bobs.

As the number of Bobs increases, the last Bob in the sequence has to perform sharper measurements in order to prepare remote state at Alice's side with average fidelity  $> \frac{3}{4}$ . The condition to achieve the task of RSP for Bob<sup>*i*</sup>, depending upon the ability of all the previous Bobs upto Bob<sup>*i-1*</sup> to do the same task in their turn, determines the minimum sharpness of measurement for Bob<sup>*i*</sup>. For example, Bob<sup>1</sup> is able to accomplish the task

of RSP when  $\frac{1}{2} < \lambda_1 \leq 1$ . Next, Bob<sup>2</sup> prepares remote states from the equatorial great circle of the Bloch sphere with average RSP-fidelity given by Eq.(5.27) with  $i = 2$ . Now,  $f_{av}^{AB^2} > \frac{3}{4}$  implies that,  $\frac{1}{1+\sqrt{1-\lambda_1^2}} < \lambda_2 \leq 1$  under the restriction of Bob<sup>1</sup>'s ability to perform the task of RSP, *i.e.* within the limit  $\frac{1}{2} < \lambda_1 \leq 1$ . Hence, the numerical minimum of  $\lambda_2$  occurs when  $\lambda_1$  tends to  $\frac{1}{2}$ , *i.e.*  $\lim_{\lambda_1 \rightarrow \frac{1}{2}^+} \frac{1}{1+\sqrt{1-\lambda_1^2}} = 0.536$ . In this way, the minimum sharpness of measurements for all the subsequent Bobs to perform RSP are calculated and the ranges of sharpness parameters are shown in Table 5.2.

$i \triangleq \text{Bob}^i$	Range of $\lambda_i$
1	(0.5,1]
2	(0.536,1]
3	(0.581,1]
4	(0.641,1]
5	(0.725,1]
6	(0.859,1]

Table 5.2: The domain of sharpness of measurements for which 6 subsequent Bobs can altogether attain the average fidelity  $> \frac{3}{4}$  for preparing remote qubits from the equatorial plane of the Bloch sphere when a single copy of the initially shared state is one among the maximally entangled pure states.

It can be verified that, after the 6-th Bob accomplishing the task of RSP, even a sharp measurement by Bob<sup>7</sup> can achieve a maximum of 0.72 as the merit of average RSP-fidelity. This shows that it is not possible for Bob<sup>7</sup> onwards to execute the task with the required quantum fidelity. Hence, at most 6 Bobs are able to independently and sequentially manifest the task of RSP under the given framework.  $\square$

It may be noted that the average fidelity of the  $i$ -th state produced by Bob <sup>$i$</sup>  at Alice's side reduces with the sharpness of the  $i$ -th measurement. The minimum of  $\lambda_i \forall i$  is required to obtain the maximum number of possible Bobs in the given framework, which we aim to figure out in different contexts. If one considers sharpness parameters higher than the minimum value, then the number of Bobs sharing the task of RSP will be lower than the maximum number of Bobs derived in this chapter. The range of sharpness parameters, *i.e.*  $(\lambda_i)_{\min} < \lambda_i \leq 1$  are defined corresponding to the range of average RSP-fidelity  $\frac{3}{4} < f_{av}^{AB^i} \leq 1$  for the remote states prepared from the equatorial great circle of the Bloch sphere. The minimum of sharpness parameters,  $(\lambda_i)_{\min}$  correspond to  $f_{av}^{AB^i}$  tending to  $f_{cl}^{\max}$  or at this

position  $\frac{3}{4}$ . Hence, by fixing  $f_{av}^{AB^i}$  at a higher value, the minimum of  $\lambda_i$  will be higher, and a lesser number of Bobs can be able to accomplish RSP with non-classical fidelity.

### 5.4.2 RSP from non-equatorial circles

Now we study the preparation of remote states at Alice's side from any circle with a fixed polar angle( $\theta$ ) on the Bloch sphere. Here Alice keeps the state when a CC from Bob contains the down outcome and rejects the state otherwise while preparing  $|\psi^i\rangle$ . Her action is reversed while preparing  $|\psi_{\perp}^i\rangle$ . We know that, Alice can never transform  $|\psi_{\perp}^i\rangle \Leftrightarrow |\psi^i\rangle$  from both the ways when  $\theta \neq \frac{\pi}{2}$  ( $0 < \theta < \pi$ ). However, the measurement statistics of the desired state can still be reproduced from the CC containing up outcome, if she assumes the transformation (up  $\rightarrow$  down) and (down  $\rightarrow$  up) for her outcomes, *a priori*. In order to determine the average RSP-fidelity of the prepared state at Alice's side, we consider that the fidelity equals the classical bound, *i.e.*  $f_{cl}^{\max}$  corresponding to the up outcome (while preparing  $|\psi^i\rangle$ ) obtained by the last Bob in the queue who sends the CC to Alice. Hence, remote state from any circle of a Bloch sphere can be reliably prepared at Alice's side with a success rate of 50% provided that a single infinity bits of information of the choice, *i.e.*  $\theta$ , is known to all the senders and the receiver. This implies that, once a particular  $\theta$  is fixed at the beginning of the procedure, it remains the same throughout the procedure. While the azimuthal angle of the state remains secret to the receiver, the sender in each iteration completely knows the state to be prepared. Here we keep  $\theta$  to be arbitrary, *i.e.* the remote state may come from any non-equatorial circle on the surface of the Bloch sphere.

As shown in Fig.5.4, for a particular azimuthal angle  $\phi_i$ , the remote states  $|\psi^i\rangle$  and  $|\psi_{\perp}^i\rangle$  are diametrically opposite to each other, *i.e.* they lie on a particular equatorial plane. But when we fix the polar angle,  $\theta \neq \frac{\pi}{2}$  and evaluate the average over all  $\phi_i$ s, the vector  $|\psi^i\rangle$  or its complement precess over the curved surface of the right-circular cone thus formed with its apex pointing at the center of the Bloch sphere. Choosing the remote states for a fixed  $\theta$  ( $0 \leq \theta \leq \pi$ ) indicates the choice of a circle from the Bloch sphere. Taking the initial state as one of the bipartite maximally entangled state *viz* singlet state, the following observations can be made.

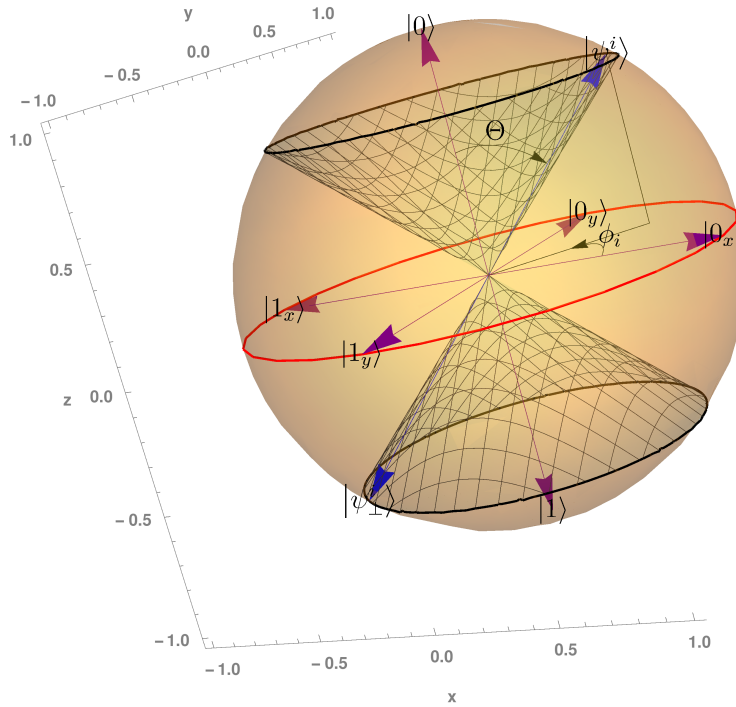


**Figure 5.4:** Schematic diagram of a Bloch sphere.  $\{|0\rangle, |1\rangle\}$  forms the computational basis, whereas  $\{|0_{x(y)}\rangle, |1_{x(y)}\rangle\}$  are the basis corresponding to  $x(y)$  direction.  $\{|\psi^i\rangle, |\psi_\perp^i\rangle\}$  are two mutually orthogonal states with a polar angle  $\theta$ . Traversing over all azimuthal angles  $\phi_i \in [0, 2\pi]$  implies, in effect, the precession over the curved surface of the double cone.

**Theorem 5.2.** *The maximum number of Bobs sharing the task of RSP at Alice's side from a circle of the Bloch sphere with  $\theta \neq \frac{\pi}{2}$ , is less than or equal to 6 when Alice shares a maximally entangled state with Bob<sup>1</sup> initially. As the choice of the circle moves from the neighbourhood of the equatorial plane towards the poles of the Bloch sphere in either direction, the maximum number of Bobs reduces gradually to zero.*

*Proof.* Here we choose a plane on the Bloch sphere by fixing the polar angle,  $\theta$  randomly. At this moment, the average pre-measurement states ( $\rho^i$ ) between Alice and Bob <sup>$i$</sup>  in the subsequent iterations ( $i \geq 2$ ), computed over all inputs and measurement outputs obtained by the previous Bobs, retain the form of Bell-diagonal states with maximally mixed marginals *i.e.* given by Eq.(5.14). Corresponding to Bob <sup>$i$</sup> , the co-efficients of

$\rho^i$  are given by,  $\{-\prod_{k=1}^{i-1}[\sqrt{1-\lambda_k^2} + \frac{1}{2}(1-\sqrt{1-\lambda_k^2})\sin^2\theta], -\prod_{k=1}^{i-1}[\sqrt{1-\lambda_k^2} + \frac{1}{2}(1-\sqrt{1-\lambda_k^2})\sin^2\theta], -\prod_{k=1}^{i-1}[1-(1-\sqrt{1-\lambda_k^2})\sin^2\theta]\}$ . The correlation matrix corresponding to it has two non-zero eigenvalues  $\forall\theta, \{\lambda_k\}_{k=1}^{i-1}$ . In the next iteration, subject to unsharp measurement done by the next Bob, the average RSP-fidelity can be determined by using the conditional state at Alice's side with a pre-condition that it is no less than  $f_{cl}^{\max}$  corresponding to the up outcome at Bob's side as Alice post-selects the state to consider for RSP corresponding to the down outcome at Bob's side while preparing  $|\psi^i\rangle$  at Alice's side. Therefore the average RSP-fidelity by applying Eq.(5.10) eventually becomes a function of all  $\lambda_i$ s ( $i \geq 2$ ) and  $\theta$ , as well. The average fidelity of the conditional state at Alice's side for preparing remote states  $\{|\psi^i\rangle\}_{\theta \neq \frac{\pi}{2}, \phi_i}$  from a circle with polar angle  $\theta$  on the Bloch sphere, contingent upon the possible choices and outcomes of the unsharp measurement done by Bob<sup>*i*</sup>, becomes

$$\begin{aligned} f_{av}^{AB^i} &= \frac{1}{2\pi} \int_0^{2\pi} (p_+^i f_{cl}^{\max} + p_-^i \langle \psi^i | \rho_{A|E_-}^i | \psi^i \rangle) d\phi_i \\ &= \frac{f_{cl}^{\max}}{2} + \frac{1}{4} + \frac{\lambda_i}{4} \left[ \cos^2\theta \prod_{k=1}^{i-1} (\cos^2\theta + \sin^2\theta \sqrt{1-\lambda_k^2}) \right. \\ &\quad \left. + \frac{\sin^2\theta}{2^{i-1}} \prod_{k=1}^{i-1} (\sin^2\theta + (\cos^2\theta + 1)\sqrt{1-\lambda_k^2}) \right], \quad (i \geq 2) \end{aligned} \quad (5.28)$$

where  $p_+^i = p_-^i = \frac{1}{2} \forall \theta, \phi_i, \lambda_i$  ( $i \geq 1$ ).

Similar expressions for the preparation of remote states  $\{|\psi_\perp^i\rangle\}_{\theta \neq \frac{\pi}{2}, \phi_i}$  can also be found with  $f_{cl}^{\max}$  as the optimal fidelity corresponding to the down outcome at Bob's side, *i.e.*  $f_{av}^{AB^i} = \frac{1}{2\pi} \int_0^{2\pi} (p_+^i \langle \psi_\perp^i | \rho_{A|E_+}^i | \psi_\perp^i \rangle + p_-^i f_{cl}^{\max}) d\phi_i$ . In this case, Alice rejects the state corresponding to the down outcome communicated by the last Bob in the queue. Let us illustrate the average RSP-fidelity between Alice and Bob<sup>2</sup>, *i.e.*  $f_{av}^{AB^2} = \frac{f_{cl}^{\max}}{2} + \frac{1}{4} + \frac{\lambda_2}{64} [(9 + 7\sqrt{1-\lambda_1^2}) + (1 - \sqrt{1-\lambda_1^2})(4\cos 2\theta + 3\cos 4\theta)]$ . Now  $f_{av}^{AB^2} > f_{cl}^{\max}$  is achieved when  $\lambda_2 > \frac{16+12\sin\theta+16\sin 2\theta-4\sin 3\theta}{18+8\cos 2\theta+6\cos 4\theta+(14-8\cos 2\theta-6\cos 4\theta)s(\theta)}$  where  $s(\theta) = \sqrt{1 - \frac{(1+\cos 2\theta+\sin^3\theta)^2}{4}}$  under the constraint  $\lambda_1 > \frac{1+\cos 2\theta+\sin^3\theta}{2}$  imposed by Bob<sup>1</sup>. Similarly, we can find the minimum sharpness parameters for subsequent Bobs (*i.e.*  $(\lambda_i)_{\min}$ ) as functions of  $\theta$ .

We plot minimum  $\lambda_i$ s as a function of  $\theta$  in subsequent iterations (see Fig.5.5) such that,

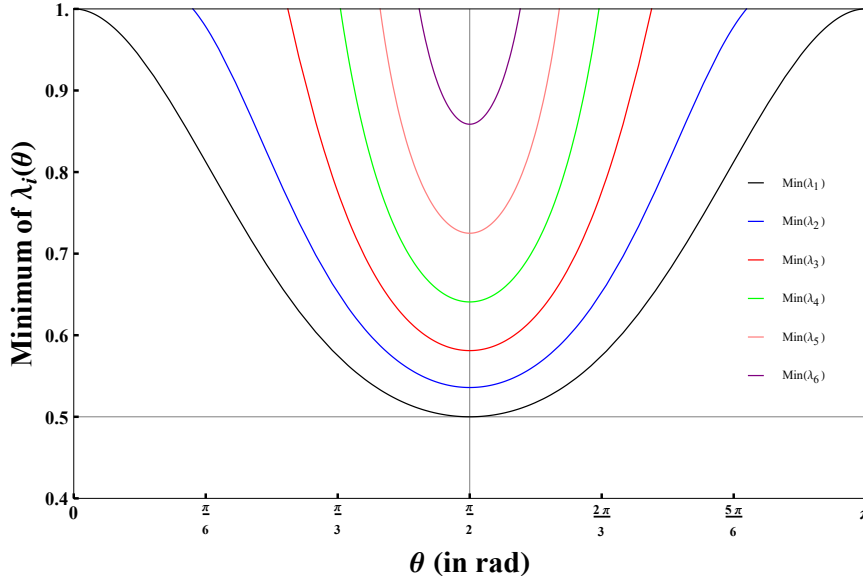


Figure 5.5: The minimum sharpness of measurements *i.e.*  $\{(\lambda_i)_{\min}\}_1^6$  specified by the respective Bobs are plotted against different polar angles of the remote state ( $\theta$ ) such that, the average RSP-fidelities can attain the non-classical values for  $(\lambda_i)_{\min} < \lambda_i \leq 1 \forall i$ , while the singlet state is shared initially and the sharpness of measurements, manifested by the previous Bobs (up to  $\text{Bob}^{i-1}$ ), are maintained with the corresponding non-classical region of average RSP-fidelities.

the classical limit of RSP-fidelity can be outdone. We observe that there can not be more than 6 number of Bobs who can sequentially and independently prepare remote states at Alice's side from a circle with polar angle  $\theta$  ( $\forall \theta \in [0, \pi]$ ). It can be seen from Fig.5.5 that,  $(\lambda_i)_{\min}(\theta) \forall i$  is an even function w.r.t.  $\theta = \frac{\pi}{2}$ . It can also be seen that,  $(\lambda_i)_{\min}(\theta)$  has minima at  $\theta = \frac{\pi}{2} \forall i \leq 6$  in order to attain  $f_{av}^{AB^i} > f_{cl}^{\max}$ . Thus the highest number of Bobs ( $n = 6$ ) can be employed for sharing the task of RSP within the permissible region of  $\lambda_i \in ((\lambda_i)_{\min}, 1] \forall i \leq n$  when the remote states are prepared from the equatorial circle of the Bloch sphere ( $\theta = \frac{\pi}{2}$ ). The permissible regions of  $\lambda_i$  is displayed earlier in Table 5.2.

For non-equatorial circles in the neighbourhood of  $\theta = \frac{\pi}{2}$ , the maximum number of Bobs remains 6, whereas it gradually becomes less than 6 as the chosen circle on the Bloch sphere progresses towards the poles of the Bloch sphere with  $\theta = 0$  or  $\pi$ . At the poles, we find that  $(\lambda_1)_{\min} = 1$ , and hence, there is no quantum advantage of RSP even by a single Bob. The maximum number of Bobs sharing the task of RSP gradually lowers towards the poles of the Bloch sphere because, as the perimeter of the chosen circle on the Bloch sphere shrinks, the possible number of input states becomes lower which, in turn, makes the probability of guessing the remote state higher for Alice. It is evident from Fig.5.1

that the classical fidelity limit increases to 1 as the chosen circle moves from the equatorial plane toward the poles of the Bloch sphere. Therefore it becomes more and more difficult for the subsequent Bobs to gain quantum advantage through the violation of the classical fidelity limit within  $(\lambda_i)_{\min} < \lambda_i \leq 1$ . Table 5.3 shows the maximum number of Bobs,  $n$  ( $i \leq n$ ) who share the task of RSP for a given  $\theta$  such that  $\lambda_{n+1}$  for Bob $^{n+1}$  exceeds the allowed range  $\lambda_{n+1} < 1$ .

$n$	Range of $\theta$ (in rad)
1	$(0, 0.472] \cup [2.669, \pi)$
2	$(0.472, 0.849] \cup [2.292, 2.669)$
3	$(0.849, 1.058] \cup [2.084, 2.292)$
4	$(1.058, 1.215] \cup [1.926, 2.084)$
5	$(1.215, 1.370] \cup [1.771, 1.926)$
6	$(1.370, 1.771)$

Table 5.3: At most  $n$ -number of Bobs can sequentially prepare the remote states having a fixed polar angle  $\theta$  on the surface of the Bloch sphere such that every Bob attains the average RSP-fidelity greater than  $f_{cl}^{\max}$  by utilizing the singlet state initially.

**Corollary 5.2.1.** *No Bob is able to achieve quantum advantage when the remote state at Alice's side is picked from one of the poles of the Bloch sphere with the polar angles given by  $\theta = \{0, \pi\}$ .*

*Proof.* By using Eq.(5.9), the conditional state produced at Alice's side, depending upon the outcomes  $\{\pm\}$  of the unsharp measurement performed by Bob $^i$ , becomes either,

$$\rho_{A|E_+}^i = \lambda_i |\psi_{\perp}^i\rangle\langle\psi_{\perp}^i| + \frac{1-\lambda_i}{2} \mathbb{1}_2, \quad (i \geq 1) \quad (5.29)$$

or,

$$\rho_{A|E_-}^i = \lambda_i |\psi^i\rangle\langle\psi^i| + \frac{1-\lambda_i}{2} \mathbb{1}_2, \quad (i \geq 1) \quad (5.30)$$

Hence, the average RSP-fidelity corresponding to Bob $^i$  becomes,

$$f_{av}^{AB^i} = \frac{1+\lambda_i}{2}, \quad (i \geq 1) \quad (5.31)$$

which is independent of all unsharp measurements performed by the previous Bobs. Eq.(5.31) can be easily derived from Eq.(5.28) by using  $\theta = \{0, \pi\}$  with an exception that, the RSP-protocol is 100% successful here without the need for post-selection. The transformation  $|0\rangle \rightarrow |1\rangle$  or vice-versa is allowed under the application of a NOT gate [Pat00]. Now,  $f_{cl}^{\max}|_{\theta=0,\pi} = 1$ . Thus  $f_{av}^{AB^i} \not\geq 1 \forall \lambda_i \in [0,1](i \geq 1)$ . Note that  $\theta = 0$  or  $\pi$  corresponds to a specific remote state,  $|\psi^i\rangle \forall (i \geq 1)$  to be either  $|0\rangle$  or  $|1\rangle$  (see Fig.5.4) which Alice can completely recognize by using the shared knowledge of  $\theta$  beforehand without using any quantum resource. Thus no Bob can successfully implement RSP with a non-classical fidelity for the two poles of the Bloch sphere.  $\square$

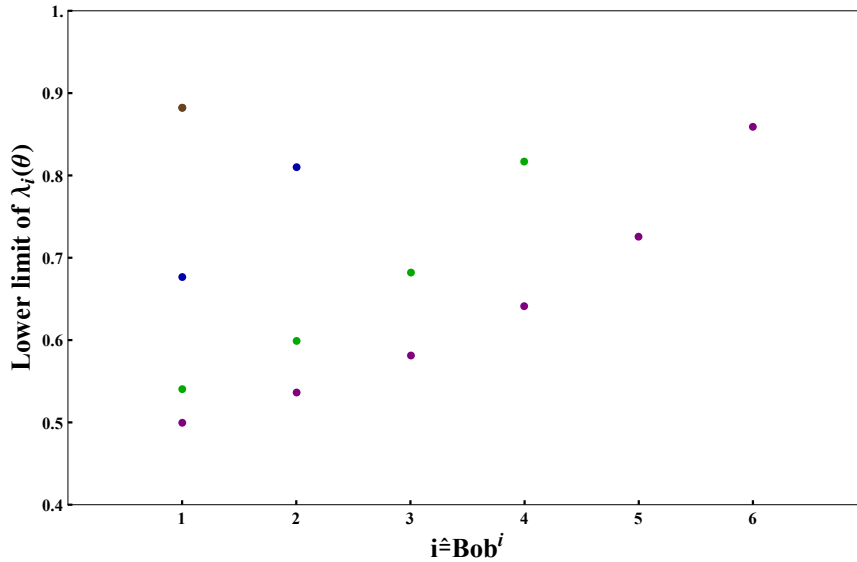


Figure 5.6: The data points corresponding to the minimum sharpness of measurements, *i.e.*  $(\lambda_i)_{\min}(\theta)$  to attain the non-classical advantage of the average RSP-fidelities are plotted w.r.t. the number of Bobs ( $i \leq n$ ) while sharing the singlet state initially and the remote states are prepared every time from a non-equatorial circle (with a fixed polar angle,  $\theta$ ) of the Bloch sphere such that, corresponding to  $\text{Bob}^{n+1}$  in the given scenario  $(\lambda_{n+1})_{\min} > 1$ . Purple, green, blue, brown data points represent  $\theta = \frac{\pi}{2}, \frac{3\pi}{8}, \frac{\pi}{4}$  and  $\frac{\pi}{8}$  respectively. The total number of data points for a given  $\theta$  is indicated by  $n$ .

We now choose a few circles of the Bloch sphere with polar angles restricted by  $0 < \theta < \frac{\pi}{2}$  from where the remote states are to be prepared. In Fig.5.6 we show that, the maximum number of Bobs sharing RSP with Alice reduces with  $\theta$  as compared to 6 for  $\theta = \frac{\pi}{2}$ . For instance, the bound ( $n$ ) is 4 for  $\theta = \frac{3\pi}{8}$ , 2 for  $\theta = \frac{\pi}{4}$  and 1 for  $\theta = \frac{\pi}{8}$ . Therefore in our scenario,  $n$  ranges from 0 to 6 as the chosen circle on the Bloch sphere varies from the poles to the equator of the Bloch sphere.  $\square$

### 5.4.2.1 Illustration: RSP with $\theta = \frac{\pi}{2} \pm (\frac{\pi}{2} - \tan^{-1} \sqrt{2})$

Now we discuss explicitly the sequential sharing of RSP for an example of non-equatorial circle of the Bloch sphere by using the maximally entangled singlet state between Alice and Bob<sup>1</sup>.

**Result 5.1.** *There can be at most 3 Bobs who sequentially prepare the remote states in Alice's lab by choosing from a circle with polar angle ( $\theta$ ) either  $\tan^{-1} \sqrt{2}$  or  $(\pi - \tan^{-1} \sqrt{2})$  (in radian) on the Bloch sphere when Alice and Bob<sup>1</sup> share a maximally entangled state initially.*

*Proof.* The average fidelity of preparing remote state at Alice's side by Bob<sup>*i*</sup> at the end of the *i*-th step of performing the task of RSP with success probability  $\frac{1}{2}$ , as  $\theta \in (0, \pi)$ , is given by,

$$f_{av}^{AB^i} = \frac{1}{2} f_{cl}^{\max} |_{\theta=\frac{\pi}{2} \pm (\frac{\pi}{2} - \tan^{-1} \sqrt{2})} + \frac{1}{4} \left[ 1 + \frac{\lambda_i}{3^{i-1}} \prod_{k=1}^{i-1} \left( 1 + 2\sqrt{1 - \lambda_k^2} \right) \right], \quad (i \geq 2) \quad (5.32)$$

where  $f_{cl}^{\max} |_{(\theta=\tan^{-1} \sqrt{2})} = f_{cl}^{\max} |_{(\theta=\pi - \tan^{-1} \sqrt{2})} = 0.803$ .

There exists a finite range of  $\lambda_i$  in each step upto Bob<sup>*i*</sup> ( $i \geq 2$ ), for which non-classical advantage through RSP-fidelity can be gained *i.e.*  $f_{av}^{AB^i} > 0.803$ . It is in accordance with the possible range of sharpness parameters  $\lambda_j$ , ( $j < i$ ) employed by all the previous Bobs up to Bob<sup>*j*</sup>  $\forall j \in \{1, 2, \dots, i-1\}$  to achieve RSP at Alice's side with quantum average fidelity. This is demonstrated in Table 5.4.

$i \hat{=} \text{Bob}^i$	Range of $\lambda_i$
1	(0.605, 1]
2	(0.701, 1]
3	(0.866, 1]

Table 5.4: The range of sharpness parameters  $\lambda_i \in ((\lambda_i)_{\min}, 1]$  for which 3 Bobs can independently prepare the remote states with polar angle  $\theta = \frac{\pi}{2} \pm (\frac{\pi}{2} - \tan^{-1} \sqrt{2})$  at Alice's side with average fidelity  $f_{av}^{AB^i} > 0.803$  by using the singlet state initially.

Corresponding to the 4-th Bob, there exists no region of  $\lambda_4 \in [0, 1]$  for which Bob<sup>4</sup> can be successful in preparing remote state at Alice's side whenever all the Bobs choose a circle with polar angle either  $\tan^{-1} \sqrt{2}$  or  $(\pi - \tan^{-1} \sqrt{2})$  from the Bloch sphere. Bob<sup>4</sup>

achieves optimum average RSP-fidelity, *i.e.* 0.733 even by doing a projective measurement. Therefore, at most 3 independent Bobs are able to exhibit the task of RSP, being successful half of the time, in the given scenario.  $\square$

## 5.5 Sequential RSP with non-maximally entangled pure state

Until now, we have discussed the scenario by considering a maximally entangled state as the initial state, which is also a maximally discordant state [Luo08, LF10]. As the requirement of entanglement is not essential for the preparation of remote states [DacLM<sup>+</sup>12], hence, it is interesting to consider a non-maximally entangled pure initial state of the form,

$$|\psi\rangle = \cos \xi |01\rangle - \sin \xi |10\rangle, \quad (0 \leq \xi \leq \frac{\pi}{2}). \quad (5.33)$$

between Alice and Bob<sup>1</sup>, where  $\rho^1(\xi) = |\psi\rangle\langle\psi|$ . If Bob<sup>1</sup> performs unsharp measurement with sharpness parameter  $\lambda_1$ , the fidelity of preparing remote states from the equatorial circle of the Bloch sphere ( $\theta = \frac{\pi}{2}$ ) takes the form,  $f_{av}^{AB^1} = \frac{1}{2}(1 + \lambda_1 \sin 2\xi)$ , which is maximum when  $\xi = \frac{\pi}{4} \forall \lambda_1 \in [0, 1]$ . Note that, when Bob<sup>1</sup> performs sharp measurement (*i.e.* with  $\Lambda = \lambda_1 = 1$ ), then  $f_{av}^{AB^1} \neq 1$  except  $\xi = \frac{\pi}{4}$ . It implies that non-maximally entangled states can not achieve 100% success in the RSP-protocol due to the lack of rotational invariance in terms of the basis representation as given by Eq.(5.1). However, our interest in this chapter is to find the region of  $\lambda_1$  for which the average RSP-fidelity,  $f_{av}^{AB^1}$  provides the non-classical advantage. Here we find that, Bob<sup>1</sup> achieves non-classical RSP-fidelity *i.e.* greater than  $\frac{3}{4}$  by using unsharp measurement when  $\lambda_1 > \frac{1}{2} \csc(2\xi)$ , enabling subsequent Bobs to repeat the task of RSP.

**Theorem 5.3.** *The maximum number of Bobs who sequentially share the task of preparing remote state at Alice's end from the equatorial circle,  $\theta = \frac{\pi}{2}$ , of the Bloch sphere, reduces gradually from six to zero as the initially shared pure state varies from a maximally entangled state towards a pure product state.*

*Proof.* Corresponding to Bob<sup>i</sup> in the *i*-th iteration, the average pre-measurement state takes the form of a two-qubit *X*-state whose correlation matrix has the non-zero eigenvalues  $\{-\prod_{k=1}^{i-1} \sqrt{1-\lambda_k^2}, -\frac{1}{2^{i-1}} \prod_{k=1}^{i-1} (1+\sqrt{1-\lambda_k^2}) \sin 2\xi, -\frac{1}{2^{i-1}} \prod_{k=1}^{i-1} (1+\sqrt{1-\lambda_k^2}) \sin 2\xi\}$  for all  $i \geq 2, \xi \in (0, \frac{\pi}{2})$ . It implies that the state remains resourceful for use in the subsequent iterations. The average fidelity of the conditional state at Alice's side, contingent upon the unsharp measurement done by Bob<sup>i</sup>, becomes

$$\begin{aligned} f_{av}^{AB^i} &= \frac{1}{2\pi} \int_0^{2\pi} (p_+^i \langle \psi^i | \sigma_z \cdot \rho_{A|E_+}^i \cdot \sigma_z | \psi^i \rangle + p_-^i \langle \psi^i | \mathbb{1}_2 \cdot \rho_{A|E_-}^i \cdot \mathbb{1}_2 | \psi^i \rangle) d\phi_i \\ &= \frac{1}{2\pi} \int_0^{2\pi} (p_+^i \langle \psi_\perp^i | \mathbb{1}_2 \cdot \rho_{A|E_+}^i \cdot \mathbb{1}_2 | \psi_\perp^i \rangle + p_-^i \langle \psi_\perp^i | \sigma_z \cdot \rho_{A|E_-}^i \cdot \sigma_z | \psi_\perp^i \rangle) d\phi_i \\ &= \frac{1}{2} + \frac{\lambda_i}{2^i} \sin 2\xi \prod_{k=1}^{i-1} (1 + \sqrt{1 - \lambda_k^2}), \quad (i \geq 2) \end{aligned} \quad (5.34)$$

where  $p_+^i = p_-^i = \frac{1}{2} \forall \xi, \phi_i, \lambda_i$ . As a result, the RSP-fidelity is maximum for the maximally entangled initial state, *i.e.*  $\xi = \frac{\pi}{4}$  for all the cases. The quantum supremacy of the protocol can be achieved when  $f_{av}^{AB^i} > f_{cl}^{\max}|_{\theta=\frac{\pi}{2}} = \frac{3}{4}$  which is analogous to obtaining  $(\lambda_i)_{\min}(\xi) < \lambda_i \leq 1$  for all the Bob<sup>i</sup>'s ( $i \geq 2$ ). For example, Bob<sup>2</sup> can successfully prepare a remote state from the equatorial circle of the Bloch sphere at Alice's side when  $\lambda_2 > 4 \sin 2\xi (1 - \sqrt{1 - \frac{\csc^2 2\xi}{4}})$ .

We plot in Fig.5.7 the minimum of  $\lambda_i$  as a function of the parameter  $\xi \in [0, \frac{\pi}{2}]$  of the initially shared non-maximally entangled state for which average RSP-fidelity achieves the non-classicality. It is observed that,  $(\lambda_i)_{\min}(\xi)$  is an even function w.r.t.  $\xi = \frac{\pi}{4}$  and has minima at  $\xi = \frac{\pi}{4}$  for all Bob<sup>i</sup> ( $i \leq 6$ ). It thus follows that, the highest number of Bobs, *i.e.*  $n = 6$  can achieve the quantum fidelity of RSP for  $\xi = \frac{\pi}{4}$ , in the allowed range of  $(\lambda_i)_{\min}(\xi) < \lambda_i \leq 1 \forall i \leq n$  (see Table 5.2). As  $\xi$  moves from the neighbourhood of  $\xi = \frac{\pi}{4}$  towards  $\xi = 0$  or  $\frac{\pi}{2}$  corresponding to the pure product states  $\{|01\rangle, |10\rangle\}$ , the bound on the number of Bobs ( $n$ ) sharing RSP with an Alice diminishes gradually from 6 to 0. As the entanglement of the initial state decreases, its utility to provide quantum supremacy of the RSP-protocol in terms of  $n$  also decreases. Table 5.5 shows the bound  $n$  corresponding to the region of  $\xi$  of the initial state so that  $\lambda_{n+1} \not\leq 1$ .

Note that, the initially shared state between Alice and Bob<sup>1</sup> given by Eq.(5.33) has the

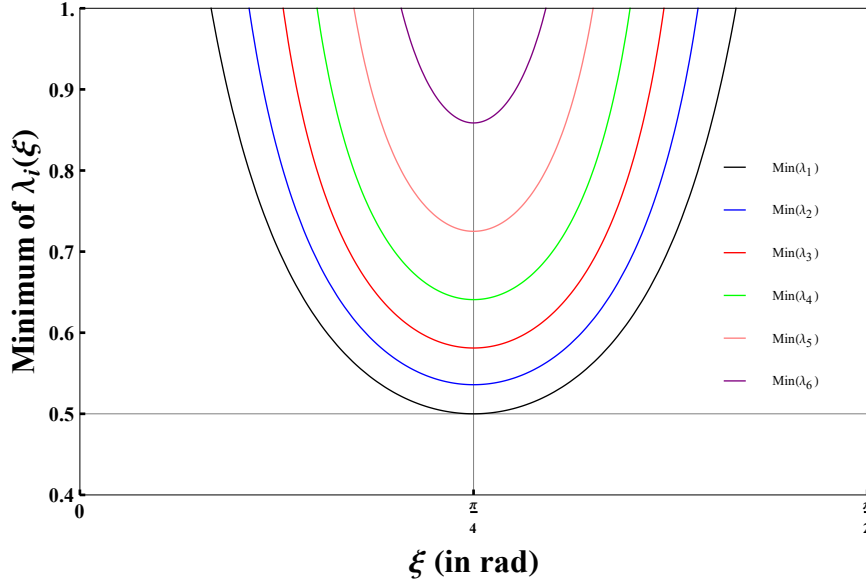


Figure 5.7: The minimum sharpness of measurements, *i.e.*  $\{(\lambda_i)_{\min}\}_1^6$  to achieve the quantum mechanical advantage of average RSP-fidelities are plotted against the state parameter  $\xi$  of the initially shared non-maximally entangled pure state where the remote states from the equatorial great circle ( $\theta = \frac{\pi}{2}$ ) of the Bloch sphere are chosen to be prepared by each Bob up to Bob<sup>*i*</sup>.

$n$	Range of $\xi$ (in rad)
0	$[0, \frac{\pi}{12}] \cup [\frac{5\pi}{12}, \frac{\pi}{2}]$
1	$(\frac{\pi}{12}, 0.337] \cup [1.233, \frac{5\pi}{12})$
2	$(0.337, 0.405] \cup [1.165, 1.233)$
3	$(0.405, 0.473] \cup [1.098, 1.165)$
4	$(0.473, 0.547] \cup [1.024, 1.098)$
5	$(0.547, 0.641] \cup [0.929, 1.024)$
6	$(0.641, 0.929)$

Table 5.5: At most  $n$ -number of Bobs can sequentially prepare the remote states from the equatorial circle ( $\theta = \frac{\pi}{2}$ ) of the Bloch sphere such that, every Bob up to Bob<sup>*n*</sup> attains the average RSP-fidelity  $> \frac{3}{4}$  whenever a single copy of the non-maximally entangled pure state is shared initially.

concurrence  $\mathcal{E}_C(\rho^1(\xi)) = \sin 2\xi$ . From Eq.(5.34), it is evident that as  $\mathcal{E}_C$  increases, the average RSP-fidelity for subsequent Bobs  $\forall i$  also increases linearly. The Bell states with  $\xi = \frac{\pi}{4}$  achieve the maximum of the average RSP-fidelity given by Eq.(5.27). For the pure product states ( $\xi = 0$  or  $\frac{\pi}{2}$ ), the average RSP-fidelity is merely the fidelity of random guess, *i.e.*  $f_{av}^{AB^i} = \frac{1}{2} \forall i$ . The neighbourhood of  $\xi = \{0, \frac{\pi}{2}\}$ , *i.e.*  $\xi \in [0, \frac{\pi}{12}] \cup [\frac{5\pi}{12}, \frac{\pi}{2}]$  corresponds to  $\mathcal{E}_C(\rho^1(\xi)) \leq \frac{1}{2}$  where the initial state is not useful for the implementation of RSP at Alice's side even with a single Bob.

Now we fix a number of initial states with  $\xi \in (0, \frac{\pi}{4})$  by taking into account the symmetry of Fig.5.8 w.r.t.  $\xi = \frac{\pi}{4}$  which yields similar results for the parameters  $\xi$  and  $\frac{\pi}{2} - \xi$ . We

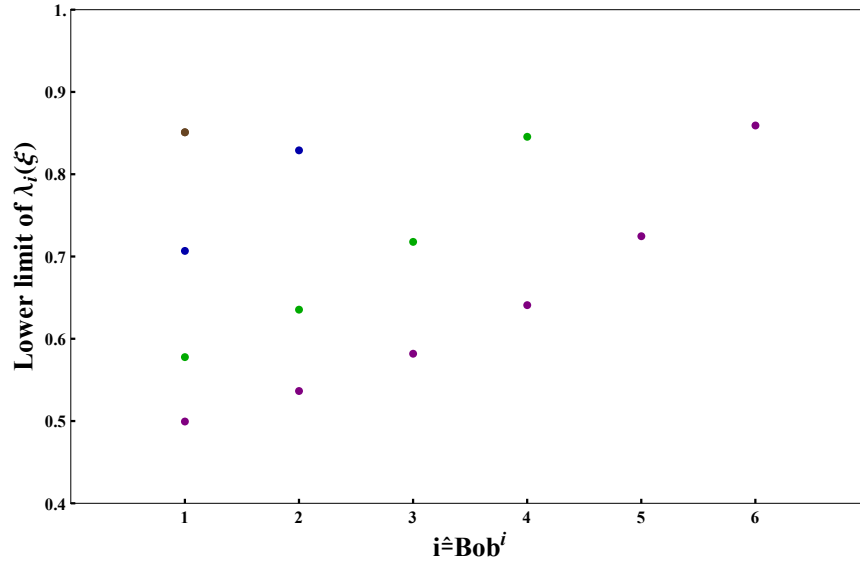


Figure 5.8: The data points corresponding to the minimum sharpness of measurements, *i.e.*  $(\lambda_i)_{\min}(\xi)$  to achieve the quantum advantage of the RSP-protocol are plotted w.r.t. the number of Bobs ( $i \leq n$ ) such that, for Bob <sup>$n+1$</sup>  in the given scenario  $(\lambda_{n+1})_{\min} > 1$  while a non-maximally entangled pure state with parameter  $\xi$  is shared initially and a remote state from the equatorial great circle of the Bloch sphere is prepared every time. Hence by fixing  $\theta = \frac{\pi}{2}$ , purple, green, blue and brown colored data points correspond to the initial states with  $\xi = \frac{\pi}{4}, \frac{\pi}{6}, \frac{\pi}{8}$  and  $\frac{\pi}{10}$  respectively. The total number of data points for a given  $\xi$  implies the optimal bound on the number of Bobs ( $n$ ).

show in Fig.5.8 that, the maximum number of Bobs ( $n$ ) sharing RSP with Alice decreases with  $\xi$  as compared to 6 obtained for  $\xi = \frac{\pi}{4}$ . For instance,  $n$  is found to be reduced to 4 for  $\xi = \frac{\pi}{6}$ , to 2 for  $\xi = \frac{\pi}{8}$  and to 1 for  $\xi = \frac{\pi}{10}$ .  $\square$

As seen above, pertaining to the equatorial great circle of the Bloch sphere, *i.e.*  $\theta = \frac{\pi}{2}$ , the bound on the number of observers, achieving the non-classicality of the RSP-protocol, is not improved for non-maximally entangled pure states as compared to the maximally entangled initial states. Similar results, with suitable post-selection on the outcomes of the subsequent Bobs (giving rise to an RSP-protocol with a success rate less than 50%), can be shown to hold for the choice of remote qubits from the other circles on the Bloch sphere with the polar angles fixed to  $\theta \neq \frac{\pi}{2}$  ( $0 < \theta < \pi$ ), where the transformation  $|\psi_{\perp}^i\rangle \leftrightarrow |\psi^i\rangle$  is forbidden  $\forall i$ . Therefore, we conjecture, in general, that the bound is less for non-maximally entangled pure states in comparison with the maximally entangled states for a pre-determined circle on the Bloch sphere.

## 5.6 Sequential RSP with mixed entangled state

In a practical environment, the initial singlet state can be mixed with the white noise to form the Werner state [Wer89] given by Eq.(1.57) with visibility parameter  $c$  ( $0 \leq c \leq 1$ ). At this moment, we investigate the formalism of multiple POVMs at Bobs' side to prepare remote states sequentially at Alice's side by employing the simplest example of the mixed entangled states, *i.e.* the Werner state, shared initially by the Alice-Bob<sup>1</sup> pair.

**Theorem 5.4.** *The maximum number of Bobs preparing remote states sequentially at Alice's side is upper bounded by six when Alice shares the Werner state with Bob<sup>1</sup> initially. As the mixedness of the initial state increases, the maximum number of Bobs reduces to zero gradually.*

*Proof.* We suppose here that, the initial state  $\rho^1 = \rho_{AB}^W$  as specified in Eq.(1.57), has the mixedness, quantified by the linear entropy [PWK04] as  $S_L(\rho_{AB}^W) = \frac{4}{3}(1 - \text{Tr}[(\rho_{AB}^W)^2]) = 1 - c^2$  where  $c$  is called the Werner parameter ( $0 \leq c \leq 1$ ). Bobs at one half of the Werner state want to sequentially prepare the remote states from the equatorial circle of the Bloch sphere (*i.e.*  $\theta = \frac{\pi}{2}$ ) to the other half of  $\rho^1$ , where Alice is present. For the RSP protocol in the given scenario, the average RSP-fidelity corresponding to Bob<sup>1</sup> becomes

$$f_{av}^{AB^1} = \frac{1 + c\lambda_1}{2} = \frac{1 + \sqrt{1 - S_L(\rho_{AB}^W)}\lambda_1}{2} \quad (5.35)$$

which can not produce 100% success of the protocol (*i.e.*  $f_{av}^{AB^1} \neq 1$ ) even by applying the sharp measurement at Bob<sup>1</sup>'s side (*i.e.*  $\Lambda = \lambda_1 = 1$ ) until the initial state is the singlet state with  $c = 1$  as given by Eq.(5.1). Here  $f_{av}^{AB^1}$  is higher than the classical fidelity bound *i.e.*  $\frac{3}{4}$  when  $\frac{1}{2c} < \lambda_1 \leq 1$ . Hence  $(\lambda_1)_{\min} = \frac{1}{2\sqrt{1 - S_L(\rho_{AB}^W)}}$  which increases with the mixedness and is the lowest when  $c = 1$  *i.e.* for the singlet state. When  $\rho^1$  is the maximally mixed state ( $c = 0$ ), then  $f_{av}^{AB^1} = \frac{1}{2}$  (that is equivalent to the fidelity of random guess) and is not capable of doing RSP with quantum advantage even by employing a single Bob. And the allowed range of  $(\lambda_1)_{\min} < 1$  is analogous to  $c > \frac{1}{2}$ . Therefore no Bob can prepare remote states from the equatorial plane of the Bloch sphere to Alice's side whenever  $0 \leq c \leq \frac{1}{2}$ .

For subsequent Bobs ( $i \geq 2$ ), the average RSP-fidelity, by using  $p_+^i = p_-^i = \frac{1}{2} \forall c, \phi_i, \lambda_i$ , becomes

$$f_{av}^{AB^i} = \frac{1}{2} + \frac{c\lambda_i}{2^i} \prod_{k=1}^{i-1} \left(1 + \sqrt{1 - \lambda_k^2}\right), \quad (i \geq 2) \quad (5.36)$$

which is larger than  $\frac{3}{4}$  when  $(\lambda_i)_{\min} < \lambda_i \leq 1$ . For instance,  $(\lambda_2)_{\min} = 4c - 2\sqrt{4c^2 - 1}$ . We plot in Fig.5.9  $(\lambda_i)_{\min}$  for all the iterations  $i \leq n$  within the allowed region of  $\lambda_i \forall i$  (such that  $\lambda_{n+1} > 1$ ) and show that there can not be more than 6 number of Bobs who can sequentially and independently share RSP with Alice for the initially shared Werner state. It can be observed from Fig.5.9 that,  $(\lambda_i)_{\min} \forall i \leq n = 6$  is inversely proportional to  $c$ . Thus as the mixedness of the initial state increases,  $(\lambda_i)_{\min} \forall i$  becomes larger and it becomes difficult for more number of Bobs to gain success in the RSP protocol and as a consequence, the optimum bound on the number of Bobs (*i.e.*  $n$ ) decreases.

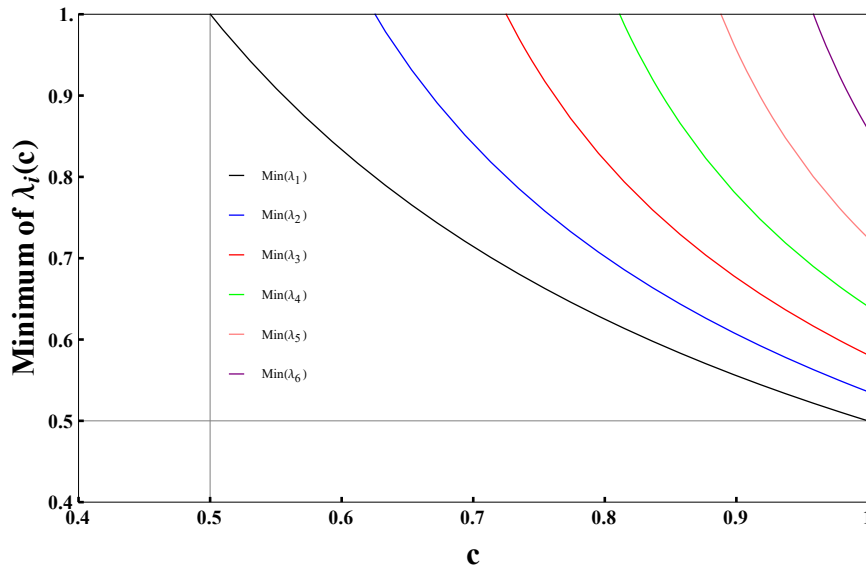


Figure 5.9: The minimum sharpness of measurements, *i.e.*  $\{(\lambda_i)_{\min}\}_1^6$  are plotted against the Werner state parameter  $c$  of the initial state where the remote states are picked from the equatorial great circle ( $\theta = \frac{\pi}{2}$ ) of the Bloch sphere in order to obtain the non-classical value of the average RSP-fidelity corresponding to Bob<sup>*i*</sup>.

The bound,  $n$  is maximum, *i.e.* 6 for the pure initial (singlet) state with  $c = 1$ , whereas it gradually decreases with the mixedness of the initial state and becomes zero for  $c \leq \frac{1}{2}$  or the linear entropy  $S_L(\rho_{AB}^W) \geq \frac{3}{4}$ . In Table 5.6, we demonstrate the bound on the successful Bobs ( $n$ ) corresponding to the regions of Werner parameters corresponding to  $\rho_{AB}^W$ .

If the remote states are chosen from the non-equatorial circles (*i.e.*  $\theta \neq \frac{\pi}{2}$ ) of the Bloch

$n$	Range of $c$
0	$[0, \frac{1}{2}]$
1	$(\frac{1}{2}, 0.625]$
2	$(0.625, 0.725]$
3	$(0.725, 0.811]$
4	$(0.811, 0.888]$
5	$(0.888, 0.959]$
6	$(0.959, 1]$

Table 5.6: At most  $n$ -number of Bobs can sequentially prepare the remote states from equatorial circle ( $\theta = \frac{\pi}{2}$ ) of the Bloch sphere such that every Bob up to Bob <sup>$n$</sup>  are capable of doing RSP with average RSP-fidelity  $> \frac{3}{4}$  by sharing Werner state initially.

sphere, then corresponding to Bob<sup>1</sup>,

$$f_{av}^{AB^1} = \frac{f_{cl}^{\max}}{2} + \frac{1 + c\lambda_1}{4} \quad (5.37)$$

where  $p_{\pm}^1 = \frac{1}{2}$  and  $f_{av}^{AB^1} > f_{cl}^{\max}$  occurs when  $\lambda_1 > \frac{1 + \cos 2\theta + \sin^3 \theta}{2c}$  which increases with mixedness and becomes the smallest for the singlet state. No Bob is able to prepare remote states from non-equatorial circles of the Bloch sphere to Alice's side when the initial state is mixed maximally. On the other hand, corresponding to subsequent Bobs ( $i \geq 2$ ), the average fidelity of preparing remote states from the non-equatorial circles of the Bloch sphere ( $\theta \neq \frac{\pi}{2}$ ,  $\theta \in (0, \pi)$ ) under the method of post-selection, by applying  $p_+^i = p_-^i = \frac{1}{2} \forall c, \theta, \phi_i, \lambda_i$ , becomes

$$f_{av}^{AB^i} = \frac{f_{cl}^{\max}}{2} + \frac{1}{4} + \frac{c\lambda_i}{4} \left[ \cos^2 \theta \prod_{k=1}^{i-1} \left( \cos^2 \theta + \sin^2 \theta \sqrt{1 - \lambda_k^2} \right) + \frac{\sin^2 \theta}{2^{i-1}} \prod_{k=1}^{i-1} \left( \sin^2 \theta + (\cos^2 \theta + 1) \sqrt{1 - \lambda_k^2} \right) \right], \quad (i \geq 2) \quad (5.38)$$

which decreases as the mixedness of the initial state increases, therefore it becomes higher than the classical fidelity bound for the lesser number of eligible Bobs in the sequence from the analogy of the previous discussion. Note that, RSP-protocol for the non-equatorial circles of the Bloch sphere can achieve success with less than 50% rate in the case of Werner state as the initial state. As a whole, we summarize that no more than 6 Bobs can share the task of RSP with an Alice when the Werner state is shared at the beginning and

the bound on the optimum number of Bobs changes inversely with the mixedness of the Werner state.  $\square$

Therefore we deduce that the bound on the number of observers sharing RSP corresponding to the mixed entangled states gets reduced than that for the singlet state. In fact, no Bob can even reliably prepare remote state at Alice's side corresponding to the maximally mixed initial state and its neighbouring states.

## 5.7 Summary and Outlook

Quantum correlations are deeply associated with their information-theoretic implications in the area of space-like communication and networking. The loss of information from an unknown quantum system during its physical transfer can be nullified by using quantum correlations, which empower the transfer of information more rapidly and securely. One of its noteworthy applications is the preparation of qubits at remote places by virtue of a quantum correlation *viz* geometric quantum discord. In this chapter, we explore the sharing of such an information processing task of RSP, implemented by multiple observers (Bobs) at one side, who act sequentially and independently of each other to achieve non-classicality in terms of RSP-fidelity. The resource utilized for remote preparation of qubits at the other side (Alice) in this scenario comprises only a single copy of a bipartite entangled state which is shared by Alice on one hand, and all the Bobs sequentially, on the other. Efficient utilization of a resource is a daunting task and has become more significant in the present context for devising quantum networks. The action of multiple observers in preparing remote qubits through the help of a single copy of a bipartite entangled state represents a possible protocol for re-utilization of the resource. The scheme of remote state preparation is itself experimentally viable in various other physical domains of quantum information processing [PZF<sup>+</sup>03, LWO<sup>+</sup>07, RWasidZB13], leaving a promising testable ground for multiple observer scenarios [HZH<sup>+</sup>18, CJA<sup>+</sup>17].

In this chapter, we first figure out the classical limit of fidelity for RSP by relaxing the requirement of quantum resource and show that such limit may vary from  $\frac{3}{4}$  to as high as

1 depending upon the population of states on the chosen plane of the Bloch sphere from where the desired remote state is picked. We demonstrate that, if the single copy of a singlet state is shared initially, then for a remote state chosen every time from the equatorial circle of the Bloch sphere, utmost 6 observers can be able to share the task. For other circles giving rise to 50% successful RSP, the bound reduces from 6 to zero as the chosen circle shifts from the neighbourhood of the equatorial circle to the poles of the Bloch sphere. It may be noted here that, the singlet state is not unique, and our scheme works equally well for any of the maximally entangled Bell states which are connected by local unitary operations. The bound on the number of observers does depend upon the choice of the circle on the Bloch sphere. As we are interested in the average of RSP-fidelity, where the average is taken over a circle of the Bloch sphere, the hemispheres on either side of the equator contribute equally and the population of states corresponding to a given circle plays the key role in determining the optimal bound on the number of senders.

Moreover, the non-classical preparation of a remote qubit from a pre-fixed circle on the Bloch sphere can also be achieved when the single copy of a non-maximally entangled pure state is pre-shared, but here the bound on the maximum number of observers gets reduced, as we have discussed. Even further reduction is shown to ensue when the initial states are mixed with the white noise. As the visibility of the initially shared Werner state reduces, the bound on the number of senders also reduces from 6 to zero slowly, because RSP-fidelity and the mixedness follow an inverse relation with each other [DacLM<sup>+</sup>12]. Since the optimum bound on the number of observers is implicitly connected with the quantum resource being employed, it is interesting to have a comparative view of different information processing tasks utilizing different quantum correlations. It is interesting to note that, remote state preparation in spite of being implementable by distinct quantum resource [CBA16], still furnishes a similar bound on the number of senders as probed for the task of quantum teleportation [RBM<sup>+</sup>21], *i.e.* six under the multiple observer framework.

The framework can be extended further to the remote preparation of qudits in the context of multiple observers. Additional investigations on collective remote state preparation [AK08] by using multipartite states can also be done as a consequence. Besides, there

---

are various CPTP maps [XLYG05, YL17] which can represent the scenario of RSP more practically. It may be worthwhile to present, in the future, the quantitative analysis of the trade-off between the cost of a quantum correlation accessed and the size of a population enacting an information processing task by utilizing the quantum correlation in such multiple observer scenarios.

## Concluding remarks

The transfer and decryption of secure quantum information, that remains inhered within the sub-atomic particles, depends upon the efficacy of quantum mechanics rather than its classical counterpart. Entanglement is a kind of the most salient signatures of the quantum theory which overpowers the classical worldview [HHHH09]. Even the inequivalence between the quantum mechanics and the classical realism persists in a macroscopic domain [HM95, MDH16] where the quantum-classical boundary seems to be vanished [Zur03]. The framework of quantum mechanical correlations present within the space-like separated systems has fundamental implications in the fields of quantum cryptography, quantum computing etc [ABC16]. In this thesis, different facets of spatial quantum correlations present in the bipartite qubit states are studied, which are not otherwise possible by a classical strategy. The freezing of a quantum correlation in a noisy environment, the quantification of that correlation in an operationally effective approach and the apportioning of another quantum correlation in a multiple observer scenario, by and large, form the backbone of this thesis. The association of quantum correlations with the one-sided device-independent cryptographic protocols and information processing tasks like remote state preparation are discussed. The sharing of such task among a group of observers and the role of quantum correlations behind its occurrence are thoroughly investigated here as well.

The mathematical framework of quantum theory has been constructed to explain counter-intuitive features of nature. Pioneering developments in the fields of microelectronics tech-

nology, lasers, masers etc have come into existence with the progress of quantum theory. The techniques to isolate and control the simplest quantum systems *viz* qubits have been used for encoding and processing information perfectly with sizeable strength of computation. The new trends of quantum information theory have now become the epitome of possibilities for reaching new heights in technological advancements. The journey started originally with the seminal paper by Einstein *et al* [EPR35] where entanglement was used as a tool to prove quantum theory incomplete in terms of the paradoxical arguments presented there. Schrödinger analysed Einstein's *spooky action at a distance* as a magical quantum phenomenon called *steering* [Sch35], by which one can influence the measurement statistics of a party separated by a distance. Bell showed that nonlocality is the essence of quantum theory and can not be explained by the classical assumptions [Bel64]. Nonlocality was later regarded as an axiom of quantum theory [PR94]. The coinage of the term *steering*, in its true sense, returned with the pioneering work by Reid [Rei89], to characterize the nonlocality in quantum theory accommodating the intermediate kind of strength. Stronger nonlocal behaviour can be observed when the steering phenomenon is extended further for quantum coherence [MPP17]. However, nonlocality in the aforementioned scenarios is described with the help of entanglement. However, Bennett *et al* showed that certain classes of separable states can even show nonlocality by means of their discrimination under global operation rather than local operation and classical communication (LOCC) [BDF<sup>+</sup>99]. Surprisingly, it is now known that quantum correlation between spatially separated parties can exist without both the nonlocality and entanglement, for instance, quantum discord [Luo08, LF10], superlocality [DW15, JAS17, DBD<sup>+</sup>18] etc.

We mainly focus on the steerable correlations (in terms of both the assemblage and coherence) present in the two-qubit states in this thesis. In the Chapter 2 [DGPM17], the fundamental connection between the quantum steering and the secret key rate under 1s-DIQKD scenario has been presented with the help of monogamy of steerable correlations. Here the sufficient criterion of bipartite quantum steering manifested by the fine-grained steering inequality [PKM14] has been applied to detect quantum steering. Then the adverse effect of amplitude damping decoherence on the steerability has been analysed. Sub-

sequently, we show a method, by introducing the technique of weak measurement and its reversal [KLKK12], to preserve the steerability of a state shared by two distant parties under decoherence. The method is also useful to protect steerability and the associated secret key rate by reducing the adverse effect of decoherence even when the method of post-selection under the technique of weak measurement is ignored. It would be interesting to explore the action of different quantum channels (as discussed in Sec.1.9) with and without memory [BCC<sup>+</sup>10, MP02, DMM18] on the steerable correlations in future.

The utilization of quantum nonlocal resources depends on the unconditional secrecy of the message being conveyed [Eke91, AGM06]. Depending upon the quantum mechanical advantages by making use of quantum correlations, the resource theories have been developed [BLM<sup>+</sup>05], such as the resource theory of quantum steering [GA15]. Under this framework, a quantifiable and activation-based measure for the steerable resource has been presented in Chapter 3 [DDJM18], which is named as *steering cost*. The definition of steering cost depends on the decomposition of a correlation in terms of the extremal non-signalling boxes [PR94, BLM<sup>+</sup>05] by taking into account the non-increasing behaviour of quantum steering under 1W-LOCC [GA15]. The measure can successfully detect the steerability of two well-known families of correlations in quantum information theory [AGM06]. At the same time, we demonstrate that it has less complexity and better operational advantage than the other measures [SNC14]. Similar to Leggett-Garg inequality [LG85] as a test for *macroscopic realism*, the notion of temporal steering [CLL<sup>+</sup>14, LCL<sup>+</sup>15, KTDR15] and channel steering [Pia15] has been introduced to certify temporal quantum correlations. It has been shown that steering weight [SNC14] has implications in quantifying temporal correlations and the strong non-Markovianity of the evolution [CBLC16]. So that it would be fascinating to explore the advantages of our steering cost in certifying the temporal correlations. Further, there is a scope to study steering cost in the context of POVMs employed for both the types of correlations. Moreover, quantum steering finds another application in a quantum information processing task, *i.e. sub-channel discrimination*, by which, different parts of a quantum evolution can be distinguished [PW15, SYX<sup>+</sup>18]. It may be absorbing to link the cost of EPR-steering with

the competence of such task as done in the literature by using the robustness of steering [PW15, GA15].

The idea of steerability depends on the characterization of the assemblages [GA15]. The steerability in terms of shared bipartite quantum states can be detected by the violation of numerous steering inequalities [SBW<sup>+</sup>13, CFFW15, CJWR09, MDM17, PKM14] which actually arises from the assumption of assemblages in the local hidden state space. On the other hand, Mondal *et al* showed the existence of steering in terms of quantum coherence [MPP17] within the structure of the state space. It was shown later that, this gives rise to a quantum correlation, called NAQC, which is even stronger than Bell nonlocality [HWF18]. In Chapter 4 [DM18, DM19], NAQC is encountered under the formalism of multiple POVMs, originated from the work of Silva *et al* [SGGP15]. We show that NAQC of different forms can uniformly be shared by utmost one observer per side despite the fundamental differences among the measures of quantum coherence [BCP14a, Gir14]. Interestingly, non-signalling theorem can be skipped to derive such monogamy of correlations. We also conjecture that the number of observers has an inverse relationship with the strength of correlations that are shared. Our analysis, however, lacks the mathematical proof to construct a trade-off between them, which can be an important direction for future research. There has been recent progress in the applicable areas of NAQC correlations especially in the authentication protocol [MDSK19], quantum phase transition [HGF20] etc, where the multiple observer framework may come into play.

The embodiment of multiple POVMs for sharing quantum correlations [SGGP15, MMH16] can be extended to the sharing of an information processing task which is feasible subject to the presence of an underlying quantum correlation initially connected between two spatially separated observers. For example, the sharing of entanglement [BMSS18, SMSS21] and the sharing of the task of quantum teleportation [RBM<sup>+</sup>21] are separate courses of action, although entanglement acts as a resource for quantum teleportation [BBC<sup>+</sup>93]. In Chapter 5 [DMPM21], we consider the sharing of an information processing task, namely remote state preparation(RSP) [Pat00, BDS<sup>+</sup>01] for qubit states where geometric discord acts a resource [DacLM<sup>+</sup>12]. Firstly, a single copy of an entangled state, *e.g.* maximally

or non-maximally entangled pure or mixed state, is shared by a number of senders at one end and a single receiver at the other. The senders can access one of the subsystems one-by-one independently so that, they can prepare the qubits, they desire, at the receiver's end with a fidelity, which can not be achievable by a classical strategy. In this way, the process continues until the non-classical advantage through RSP-fidelity can be gained. This is important in a scenario where multiple senders want to convey a secret message to a receiver at a remote location without making its physical transfer by using a quantum channel. We demonstrate in this chapter that, there is an upper bound for a classical strategy to prepare a remote state, unknown to only the receiver, which is drawn from a particular circular region of the Bloch sphere in  $\mathbb{C}^2$ . We find that, such upper bound fits with different values corresponding to different circular regions on the surface of the Bloch sphere. Subsequently, we show that the population of the observers at the senders' side can not exceed the number 6 in order to have the quantum mechanical advantage by considering several classes of well-known bipartite entangled states. This bound on the number of observers can be obtained when one of the Bell states is shared initially and the remote states are chosen from the equatorial great circle of the Bloch sphere. We further proved that, as the initial state deviates from the Bell states in terms of entanglement and purity and/or the chosen circle of the Bloch sphere shifts from the neighbourhood of the equatorial great circle towards the two poles of the Bloch sphere, the bound on the number of senders reduces from 6 up until zero. Surprisingly, our bound matches with the bound derived for quantum teleportation [RBM<sup>+</sup>21] where a different mechanism is applied for preparing remote states.

Quantum algorithm unfolds the potential for rapid computation[Gro97, Sho97] and secure communication [HBcvB99, SP13, Kim08] compared to its classical analogue. The probabilistic behaviour of remote state preparation requires less amount of classical resources than the other form of quantum communication, *i.e.* quantum teleportation [Pat00]. However, if the more classical resource is employed, then there arises the deterministic behaviour of RSP [NCNK11] for remote states chosen from the circles other than the equatorial great circle of the Bloch sphere. Furthermore, the various schemes re-

---

lated to joint [NK08, STP17], controlled [WLZZ09] and collective remote state preparation [AK08] in the multipartite scenario have been proposed, where our scheme, described in the previous chapter, may have possible implications. Nonetheless, it is worth mentioning that, our results are restricted to bipartite sharing of the qubit states. Also, there are shreds of evidence that substantiate RSP experimentally by using photon polarization [PBG<sup>+</sup>05], single-mode photonic beams [BBL04], nuclear magnetic imaging [PZF<sup>+</sup>03], via light-matter interaction [RBV<sup>+</sup>07] etc.

This thesis investigates some directions of studies within the plethora of bipartite quantum correlations. Quantum correlations vastly contribute in numerous fields of applications, including quantum state merging [HOW07], redistribution of entanglement [DY08], quantum metrology [FPAG16, MCWV11] etc in the multipartite network of quantum systems [GHZ89, DVC00, HHHH09, BCP<sup>+</sup>14b, CS16, UCNG20]. Apart from the several other utilizations [ABC16], the presence of quantum correlations among nanoscale systems plays a significant role in the recently emerging ground of quantum thermodynamic processes [OHHH02, MX16, GHR<sup>+</sup>16] and thermodynamic heat engine cycles [QLSN07, Qua09] where the thermal as well as quantum fluctuations amount to be significant.

# References

- [AAV88] Y. Aharonov, D. Z. Albert, and L. Vaidman. How the result of a measurement of a component of the spin of a spin-1/2 particle can turn out to be 100. *Phys. Rev. Lett.*, 60:1351–1354, Apr 1988.
- [ABC16] G. Adesso, T. R. Bromley, and M. Cianciaruso. Measures and applications of quantum correlations. *J. Phys. A: Math. Theor.*, 49(47):473001, nov 2016.
- [ABG<sup>+</sup>07] A. Acín, N. Brunner, N. Gisin, S. Massar, S. Pironio, and V. Scarani. Device-independent security of quantum cryptography against collective attacks. *Phys. Rev. Lett.*, 98:230501, Jun 2007.
- [ABL64] Y. Aharonov, P. G. Bergmann, and J. L. Lebowitz. Time symmetry in the quantum process of measurement. *Phys. Rev.*, 134:B1410–B1416, Jun 1964.
- [AdMHM<sup>+</sup>07] M. P. Almeida, F. de Melo, M. Hor-Meyll, A. Salles, S. P. Walborn, P. H. Souto Ribeiro, and L. Davidovich. Environment-induced sudden death of entanglement. *Science*, 316(5824):579–582, 2007.
- [AGM06] A. Acín, N. Gisin, and L. Masanes. From bell’s theorem to secure quantum key distribution. *Phys. Rev. Lett.*, 97:120405, Sep 2006.
- [AGR82] A. Aspect, P. Grangier, and G. Roger. Experimental realization of einstein-podolsky-rosen-bohm gedankenexperiment: A new violation of bell’s inequalities. *Phys. Rev. Lett.*, 49:91–94, Jul 1982.
- [AK08] N. Ba An and J. Kim. Collective remote state preparation. *Int. J. Quant. Info.*, 06(05):1051, 2008.
- [Ban02] S. Bandyopadhyay. Origin of noisy states whose teleportation fidelity can be enhanced through dissipation. *Phys. Rev. A*, 65:022302, Jan 2002.

- [BB84] C. H. Bennett and G. Brassard. Quantum cryptography: Public key distribution and coin tossing. *Proc. IEEE Int. Conf. Comp. Sys. Sig. Proc., New York*, 175:8, Dec 1984.
- [BBC<sup>+</sup>93] C. H. Bennett, G. Brassard, C. Crépeau, R. Jozsa, A. Peres, and W. K. Wootters. Teleporting an unknown quantum state via dual classical and einstein-podolsky-rosen channels. *Phys. Rev. Lett.*, 70:1895–1899, Mar 1993.
- [BBDM<sup>+</sup>98] D. Boschi, S. Branca, F. De Martini, L. Hardy, and S. Popescu. Experimental realization of teleporting an unknown pure quantum state via dual classical and einstein-podolsky-rosen channels. *Phys. Rev. Lett.*, 80:1121–1125, Feb 1998.
- [BBL04] S. A. Babichev, B. Brezger, and A. I. Lvovsky. Remote preparation of a single-mode photonic qubit by measuring field quadrature noise. *Phys. Rev. Lett.*, 92:047903, Jan 2004.
- [BBM75] I. Białyński-Birula and J. Mycielski. Uncertainty relations for information entropy in wave mechanics. *Comm. Math. Phys.*, 44:129–132, May 1975.
- [BBM92] C. H. Bennett, G. Brassard, and N. D. Mermin. Quantum cryptography without bell’s theorem. *Phys. Rev. Lett.*, 68:557–559, Feb 1992.
- [BC20] P. J. Brown and R. Colbeck. Arbitrarily many independent observers can share the nonlocality of a single maximally entangled qubit pair. *Phys. Rev. Lett.*, 125:090401, Aug 2020.
- [BCC<sup>+</sup>10] M. Berta, M. Christandl, R. Colbeck, J. M. Renes, and R. Renner. The uncertainty principle in the presence of quantum memory. *Nature Physics*, 6:659–662, Jul 2010.
- [BCP14a] T. Baumgratz, M. Cramer, and M. B. Plenio. Quantifying coherence. *Phys. Rev. Lett.*, 113:140401, Sep 2014.
- [BCP<sup>+</sup>14b] N. Brunner, D. Cavalcanti, S. Pironio, V. Scarani, and S. Wehner. Bell nonlocality. *Rev. Mod. Phys.*, 86:419–478, Apr 2014.
- [BCSS11] N. Brunner, D. Cavalcanti, A. Salles, and P. Skrzypczyk. Bound nonlocality and activation. *Phys. Rev. Lett.*, 106:020402, Jan 2011.
- [BcvHW99] V. Bužek, M. Hillery, and R. F. Werner. Optimal manipulations with qubits: Universal-not gate. *Phys. Rev. A*, 60:R2626–R2629, Oct 1999.

- [BCW<sup>+</sup>12] C. Branciard, E. G. Cavalcanti, S. P. Walborn, V. Scarani, and H. M. Wiseman. One-sided device-independent quantum key distribution: Security, feasibility, and the connection with steering. *Phys. Rev. A*, 85:010301(R), Jan 2012.
- [BDCZ98] H.-J. Briegel, W. Dür, J. I. Cirac, and P. Zoller. Quantum repeaters: The role of imperfect local operations in quantum communication. *Phys. Rev. Lett.*, 81:5932–5935, Dec 1998.
- [BDF<sup>+</sup>99] C. H. Bennett, D. P. DiVincenzo, C. A. Fuchs, T. Mor, E. Rains, P. W. Shor, J. A. Smolin, and W. K. Wootters. Quantum nonlocality without entanglement. *Phys. Rev. A*, 59:1070–1091, Feb 1999.
- [BDS<sup>+</sup>01] C. H. Bennett, D. P. DiVincenzo, P. W. Shor, J. A. Smolin, B. M. Terhal, and W. K. Wootters. Remote state preparation. *Phys. Rev. Lett.*, 87:077902, Jul 2001.
- [BDS<sup>+</sup>17] A. Bera, T. Das, D. Sadhukhan, S. Singha Roy, A. Sen(De), and U. Sen. Quantum discord and its allies: a review of recent progress. *Rep. Prog. Phys.*, 81(2):024001, dec 2017.
- [BDSW96] C. H. Bennett, D. P. DiVincenzo, J. A. Smolin, and W. K. Wootters. Mixed-state entanglement and quantum error correction. *Phys. Rev. A*, 54:3824–3851, Nov 1996.
- [Bel64] J. S. Bell. On the einstein podolsky rosen paradox. *Physics Physique Fizika*, 1:195–200, Nov 1964.
- [BG13] M. Banik and Md. R. Gazi. Classical communication and non-classical fidelity of quantum teleportation. *Quant. Info. Proc.*, 12:3607–3615, Nov 2013.
- [BKPV99] S. Bose, P. L. Knight, M. B. Plenio, and V. Vedral. Proposal for teleportation of an atomic state via cavity decay. *Phys. Rev. Lett.*, 83:5158–5161, Dec 1999.
- [BLM96] P. Busch, P. J. Lahti, and P. Mittelstaedt. *The Quantum Theory of Measurement*. Springer: Berlin, Germany, 1996.
- [BLM<sup>+</sup>05] J. Barrett, N. Linden, S. Massar, S. Pironio, S. Popescu, and D. Roberts. Nonlocal correlations as an information-theoretic resource. *Phys. Rev. A*, 71:022101, Feb 2005.

- [BmcHHH00] P. Badziag, M. Horodecki, P. Horodecki, and R. Horodecki. Local environment can enhance fidelity of quantum teleportation. *Phys. Rev. A*, 62:012311, Jun 2000.
- [BMSS18] A. Bera, S. Mal, A. Sen(De), and U. Sen. Witnessing bipartite entanglement sequentially by multiple observers. *Phys. Rev. A*, 98:062304, Dec 2018.
- [Bra02] D. Braun. Creation of entanglement by interaction with a common heat bath. *Phys. Rev. Lett.*, 89:277901, Dec 2002.
- [BS03] D. W. Berry and B. C. Sanders. Optimal remote state preparation. *Phys. Rev. Lett.*, 90:057901, Feb 2003.
- [BS10] N. Brunner and C. Simon. Measuring small longitudinal phase shifts: Weak measurements or standard interferometry? *Phys. Rev. Lett.*, 105:010405, Jul 2010.
- [BSW<sup>+</sup>04] N. Brunner, V. Scarani, M. Wegmüller, M. Legré, and N. Gisin. Direct measurement of superluminal group velocity and signal velocity in an optical fiber. *Phys. Rev. Lett.*, 93:203902, Nov 2004.
- [Bus86] P. Busch. Unsharp reality and joint measurements for spin observables. *Phys. Rev. D*, 33:2253, Apr 1986.
- [Bus09] P. Busch. On the sharpness and bias of quantum effects. *Found. Phys.*, 39:712–730, July 2009.
- [Bus12] F. Buscemi. All entangled quantum states are nonlocal. *Phys. Rev. Lett.*, 108:200401, May 2012.
- [BVQB14] J. Bowles, T. Vértesi, M. T. Quintino, and N. Brunner. One-way einstein-podolsky-rosen steering. *Phys. Rev. Lett.*, 112:200402, May 2014.
- [BW92] C. H. Bennett and S. J. Wiesner. Communication via one- and two-particle operators on einstein-podolsky-rosen states. *Phys. Rev. Lett.*, 69:2881–2884, Nov 1992.
- [CA16] A. C. S. Costa and R. M. Angelo. Quantification of einstein-podolsky-rosen steering for two-qubit states. *Phys. Rev. A*, 93:020103, Feb 2016.
- [Cab21] A. Cabello. Bell nonlocality between sequential pairs of observers. *arXiv:2103.11844 [quant-ph]*, 2021.

- [CB97] R. Cleve and H. Buhrman. Substituting quantum entanglement for communication. *Phys. Rev. A*, 56:1201–1204, Aug 1997.
- [CBA16] A.C.S. Costa, M.W. Beims, and R.M. Angelo. Generalized discord, entanglement, einstein–podolsky–rosen steering, and bell nonlocality in two-qubit systems under (non-)markovian channels: Hierarchy of quantum resources and chronology of deaths and births. *Phys. A: Stat. Mech. App.*, 461:469–479, 2016.
- [CBLC16] S.-L. Chen, C. Budroni, Y.-C. Liang, and Y.-N. Chen. Natural framework for device-independent quantification of quantum steerability, measurement incompatibility, and self-testing. *Phys. Rev. Lett.*, 116:240401, Jun 2016.
- [CCS<sup>+</sup>21] A. R. Cameron, S. W. L. Cheng, S. Schwarz, C. Kapahi, D. Sarenac, M. Grabowecky, D. G. Cory, T. Jennewein, D. A. Pushin, and K. J. Resch. Remote state preparation of single-photon orbital-angular-momentum lattices. *Phys. Rev. A*, 104:L051701, Nov 2021.
- [CFFW15] E. G. Cavalcanti, C. J. Foster, M. Fuwa, and H. M. Wiseman. Analog of the clauser-horne-shimony-holt inequality for steering. *J. Opt. Soc. Am. B*, 32(4):A74–A81, Apr 2015.
- [CFIO<sup>+</sup>21] M. Chaudhary, M. Fadel, E. O. Ilo-Okeke, A. N. Pyrkov, V. Ivannikov, and T. Byrnes. Remote state preparation of two-component bose-einstein condensates. *Phys. Rev. A*, 103:062417, Jun 2021.
- [CGM00] N. J. Cerf, N. Gisin, and S. Massar. Classical teleportation of a quantum bit. *Phys. Rev. Lett.*, 84:2521–2524, Mar 2000.
- [CHK18] B. Coyle, M. J. Hoban, and E. Kashefi. One-sided device-independent certification of unbounded random numbers. In M. Cuffaro and P. Papayannopoulos, editors, Proceedings of the 9th International Workshop on *Physics and Computation*, Fontainebleau, France, 26 June 2018, volume 273 of *Electronic Proceedings in Theoretical Computer Science*, pages 14–26. Open Publishing Association, 2018.
- [Cho75] M.-D. Choi. Completely positive linear maps on complex matrices. *Linear Algebra and its Applications*, 10(3):285–290, 1975.
- [CHSH69] J. F. Clauser, M. A. Horne, A. Shimony, and R. A. Holt. Proposed experiment to test local hidden-variable theories. *Phys. Rev. Lett.*, 23:880–884, Oct 1969.

- [Cir80] B. S. Cirel'son. Quantum generalizations of bell's inequality. *Lett. Math. Phys.*, 4:93–100, Feb 1980.
- [CJA<sup>+</sup>17] F. J. Curchod, M. Johansson, R. Augusiak, M. J. Hoban, P. Wittek, and A. Acín. Unbounded randomness certification using sequences of measurements. *Phys. Rev. A*, 95:020102, Feb 2017.
- [CJWR09] E. G. Cavalcanti, S. J. Jones, H. M. Wiseman, and M. D. Reid. Experimental criteria for steering and the einstein-podolsky-rosen paradox. *Phys. Rev. A*, 80:032112, Sep 2009.
- [CK78] I. Csiszàr and J. Körner. Broadcast channels with confidential messages. *IEEE Trans. Inf. Theory*, 24(3):339–348, May 1978.
- [CKL<sup>+</sup>20] S-H. Chen, Y-C. Kao, N. Lambert, F. Nori, and C-M. Li. Nonclassical preparation of quantum remote states. *arXiv:2008.06238 [quant-ph]*, 2020.
- [CKW00] V. Coffman, J. Kundu, and W. K. Wootters. Distributed entanglement. *Phys. Rev. A*, 61:052306, Apr 2000.
- [CLL04] M. Curty, M. Lewenstein, and N. Lütkenhaus. Entanglement as a precondition for secure quantum key distribution. *Phys. Rev. Lett.*, 92:217903, May 2004.
- [CLL<sup>+</sup>14] Y.-N. Chen, C.-M. Li, N. Lambert, S.-L. Chen, Y. Ota, G.-Y. Chen, and F. Nori. Temporal steering inequality. *Phys. Rev. A*, 89:032112, Mar 2014.
- [CLM<sup>+</sup>14] E. Chitambar, D. Leung, L. Mančinska, M. Ozols, and A. Winter. Everything you always wanted to know about locc (but were afraid to ask). *Comm. in Math. Phys.*, 328:303–326, Mar 2014.
- [CMM<sup>+</sup>12] T. K. Chuan, J. Maillard, K. Modi, T. Paterek, M. Paternostro, and M. Piani. Quantum discord bounds the amount of distributed entanglement. *Phys. Rev. Lett.*, 109:070501, Aug 2012.
- [CPM15] P. Chowdhury, T. Pramanik, and A. S. Majumdar. Stronger steerability criterion for more uncertain continuous-variable systems. *Phys. Rev. A*, 92:042317, Oct 2015.
- [CPMA14] P. Chowdhury, T. Pramanik, A. S. Majumdar, and G. S. Agarwal. Einstein-podolsky-rosen steering using quantum correlations in non-gaussian entangled states. *Phys. Rev. A*, 89:012104, Jan 2014.

- [CS12] A. Christ and C. Silberhorn. Limits on the deterministic creation of pure single-photon states using parametric down-conversion. *Phys. Rev. A*, 85:023829, Feb 2012.
- [CS16] D. Cavalcanti and P. Skrzypczyk. Quantum steering: a review with focus on semidefinite programming. *Rep. Prog. Phys.*, 80(2):024001, dec 2016.
- [CYW<sup>+</sup>13] J.-L. Chen, X.-J. Ye, C. Wu, H.-Y. Su, A. Cabello, L. C. Kwek, and C. H. Oh. All-versus-nothing proof of einstein-podolsky-rosen steering. *Sci. Rep.*, 3:2143, July 2013.
- [DacLM<sup>+</sup>12] B. Dakić, Y. O. Lipp, X. Ma, M. Ringbauer, S. Kropatschek, S. Barz, T. Paterek, V. Vedral, A. Zeilinger, Č. Brukner, and P. Walther. Quantum discord as resource for remote state preparation. *Nat. Phys.*, 8:666–670, Aug 2012.
- [DacVB10] B. Dakić, V. Vedral, and Č. Brukner. Necessary and sufficient condition for nonzero quantum discord. *Phys. Rev. Lett.*, 105:190502, Nov 2010.
- [DBD<sup>+</sup>18] D. Das, B. Bhattacharya, C. Datta, A. Roy, C. Jebaratnam, A. S. Majumdar, and R. Srikanth. Operational characterization of quantumness of unsteerable bipartite states. *Phys. Rev. A*, 97:062335, Jun 2018.
- [DDJM18] D. Das, S. Datta, C. Jebaratnam, and A. S. Majumdar. Cost of einstein-podolsky-rosen steering in the context of extremal boxes. *Phys. Rev. A*, 97:022110, Feb 2018.
- [DGPM17] S. Datta, S. Goswami, T. Pramanik, and A. S. Majumdar. Preservation of a lower bound of quantum secret key rate in the presence of decoherence. *Phys. Lett. A*, 381(10):897–902, 2017.
- [DGS<sup>+</sup>19] D. Das, A. Ghosal, S. Sasmal, S. Mal, and A. S. Majumdar. Facets of bipartite nonlocality sharing by multiple observers via sequential measurements. *Phys. Rev. A*, 99:022305, Feb 2019.
- [Die82] D. Dieks. Communication by epr devices. *Phys. Lett. A*, 92(6):271–272, 1982.
- [DK03] L.-M. Duan and H. J. Kimble. Efficient engineering of multiatom entanglement through single-photon detections. *Phys. Rev. Lett.*, 90:253601, Jun 2003.
- [DM18] S. Datta and A. S. Majumdar. Sharing of nonlocal advantage of quantum coherence by sequential observers. *Phys. Rev. A*, 98:042311, Oct 2018.

- [DM19] S. Datta and A. S. Majumdar. Erratum: Sharing of nonlocal advantage of quantum coherence by sequential observers [phys. rev. a 98, 042311 (2018)]. *Phys. Rev. A*, 99:019902, Jan 2019.
- [DMM18] S. Datta, S. Mal, and A. S. Majumdar. Protecting temporal correlations of two-qubit states using quantum channels with memory. *arXiv:1808.10345 [quant-ph]*, 2018.
- [DMPM21] S. Datta, S. Mal, A. K. Pati, and A. S. Majumdar. Remote state preparation by multiple observers using a single copy of a two-qubit entangled state. *arXiv:2109.03682 [quant-ph]*, 2021.
- [DSS89] I. M. Duck, P. M. Stevenson, and E. C. G. Sudarshan. The sense in which a "weak measurement" of a spin- $\frac{1}{2}$  particle's spin component yields a value 100. *Phys. Rev. D*, 40:2112–2117, Sep 1989.
- [dV14] J. I de Vicente. On nonlocality as a resource theory and nonlocality measures. *J. Phys. A: Math. Theor.*, 47(42):424017, oct 2014.
- [DVC00] W. Dür, G. Vidal, and J. I. Cirac. Three qubits can be entangled in two inequivalent ways. *Phys. Rev. A*, 62:062314, Nov 2000.
- [DW15] J. M. Donohue and E. Wolfe. Identifying nonconvexity in the sets of limited-dimension quantum correlations. *Phys. Rev. A*, 92:062120, Dec 2015.
- [DY08] I. Devetak and J. Yard. Exact cost of redistributing multipartite quantum states. *Phys. Rev. Lett.*, 100:230501, Jun 2008.
- [Eke91] A. K. Ekert. Quantum cryptography based on bell's theorem. *Phys. Rev. Lett.*, 67:661–663, Aug 1991.
- [EPR35] A. Einstein, B. Podolsky, and N. Rosen. Can quantum-mechanical description of physical reality be considered complete? *Phys. Rev.*, 47:777–780, May 1935.
- [EPR92] A. C. Elitzur, S. Popescu, and D. Rohrlich. Quantum nonlocality for each pair in an ensemble. *Phys. Lett. A*, 162(1):25–28, 1992.
- [Fan83] U. Fano. Pairs of two-level systems. *Rev. Mod. Phys.*, 55:855–874, Oct 1983.
- [FC72] S. J. Freedman and J. F. Clauser. Experimental test of local hidden-variable theories. *Phys. Rev. Lett.*, 28:938–941, Apr 1972.

- [Fin82] A. Fine. Hidden variables, joint probability, and the bell inequalities. *Phys. Rev. Lett.*, 48:291–295, Feb 1982.
- [FPAG16] A. Farace, A. De Pasquale, G. Adesso, and V. Giovannetti. Building versatile bipartite probes for quantum metrology. *New J. Phys.*, 18(1):013049, jan 2016.
- [FRT<sup>+</sup>20] T. Feng, C. Ren, Y. Tian, M. Luo, H. Shi, J. Chen, and X. Zhou. Observation of nonlocality sharing via not-so-weak measurements. *Phys. Rev. A*, 102:032220, Sep 2020.
- [FZF<sup>+</sup>00] X. Fang, X. Zhu, M. Feng, X. Mao, and F. Du. Experimental implementation of dense coding using nuclear magnetic resonance. *Phys. Rev. A*, 61:022307, Jan 2000.
- [GA15] R. Gallego and L. Aolita. Resource theory of steering. *Phys. Rev. X*, 5:041008, Oct 2015.
- [GA18] V. S. Gomes and R. M. Angelo. Nonanomalous measure of realism-based nonlocality. *Phys. Rev. A*, 97:012123, Jan 2018.
- [GBP97] M. Grassl, Th. Beth, and T. Pellizzari. Codes for the quantum erasure channel. *Phys. Rev. A*, 56:33–38, Jul 1997.
- [GHR<sup>+</sup>16] J. Goold, M. Huber, A. Riera, L. del Rio, and P. Skrzypczyk. The role of quantum information in thermodynamics—a topical review. *J. Phys. A: Math. Theor.*, 49(14):143001, feb 2016.
- [GHZ89] D. M. Greenberger, M. A. Horne, and A. Zeilinger. Going beyond bell’s theorem bell’s theorem, quantum theory and conceptions of the universe ed m kafatos. *Dordrecht: Kluwer*, 69:69–72, 1989.
- [Gir14] D. Girolami. Observable measure of quantum coherence in finite dimensional systems. *Phys. Rev. Lett.*, 113:170401, Oct 2014.
- [GKR<sup>+</sup>01] S. Ghosh, G. Kar, A. Roy, A. Sen(De), and U. Sen. Distinguishability of bell states. *Phys. Rev. Lett.*, 87:277902, Dec 2001.
- [GMD<sup>+</sup>21] S. Gupta, A. G. Maity, D. Das, A. Roy, and A. S. Majumdar. Genuine einstein-podolsky-rosen steering of three-qubit states by multiple sequential observers. *Phys. Rev. A*, 103:022421, Feb 2021.
- [GMGS01] P. Ghose, A. S. Majumdar, S. Guha, and J. Sau. Bohmian trajectories for photons. *Phys. Lett. A*, 290(5):205–213, 2001.

- [GMN06] B. Ghosh, A. S. Majumdar, and N. Nayak. Environment-assisted entanglement enhancement. *Phys. Rev. A*, 74:052315, Nov 2006.
- [GPW05] B. Groisman, S. Popescu, and A. Winter. Quantum, classical, and total amount of correlations in a quantum state. *Phys. Rev. A*, 72:032317, Sep 2005.
- [Gro97] L. K. Grover. Quantum mechanics helps in searching for a needle in a haystack. *Phys. Rev. Lett.*, 79:325–328, Jul 1997.
- [HBcvB99] M. Hillery, V. Bužek, and A. Berthiaume. Quantum secret sharing. *Phys. Rev. A*, 59:1829–1834, Mar 1999.
- [Hei27] W. Heisenberg. Über den anschaulichen inhalt der quantentheoretischen kinematik und mechanik. *Z. Physik.*, 43:172–198, Mar 1927.
- [HES<sup>+</sup>12] V. Händchen, T. Eberle, S. Steinlechner, A. Samblowski, T. Franz, R. F. Werner, and R. Schnabel. Observation of one-way einstein–podolsky–rosen steering. *Nature Photonics*, 6:596–599, Aug 2012.
- [HF18] M.-L. Hu and H. Fan. Nonlocal advantage of quantum coherence in high-dimensional states. *Phys. Rev. A*, 98:022312, Aug 2018.
- [HGF20] M.-L. Hu, Y.-Y. Gao, and H. Fan. Steered quantum coherence as a signature of quantum phase transitions in spin chains. *Phys. Rev. A*, 101:032305, Mar 2020.
- [HH96] R. Horodecki and M. Horodecki. Information-theoretic aspects of inseparability of mixed states. *Phys. Rev. A*, 54:1838–1843, Sep 1996.
- [HHH95] R. Horodecki, P. Horodecki, and M. Horodecki. Violating bell inequality by mixed spin-1/2 states: necessary and sufficient condition. *Phys. Lett. A*, 200(5):340–344, 1995.
- [HHH96] M. Horodecki, P. Horodecki, and R. Horodecki. Separability of mixed states: necessary and sufficient conditions. *Phys. Lett. A*, 223(1):1–8, 1996.
- [HHH03] A. Hayashi, T. Hashimoto, and M. Horibe. Remote state preparation without oblivious conditions. *Phys. Rev. A*, 67:052302, May 2003.
- [HHHH09] R. Horodecki, P. Horodecki, M. Horodecki, and K. Horodecki. Quantum entanglement. *Rev. Mod. Phys.*, 81:865–942, Jun 2009.

- [HHT01] P. M. Hayden, M. Horodecki, and B. M. Terhal. The asymptotic entanglement cost of preparing a quantum state. *Journal of Physics A: Mathematical and General*, 34(35):6891–6898, aug 2001.
- [HK08] O. Hosten and P. Kwiat. Observation of the spin hall effect of light via weak measurements. *Science*, 319(5864):787–790, 2008.
- [HLL16] C.-Y. Hsieh, Y.-C. Liang, and R.-K. Lee. Quantum steerability: Characterization, quantification, superactivation, and unbounded amplification. *Phys. Rev. A*, 94:062120, Dec 2016.
- [HM95] D. Home and A. S. Majumdar. Incompatibility between quantum mechanics and classical realism in the “strong” macroscopic limit. *Phys. Rev. A*, 52:4959–4962, Dec 1995.
- [Hol73] A. S. Holevo. Bounds for the quantity of information transmitted by a quantum communication channel. *Problems Inform. Transmission*, 9:177–183, 1973.
- [HOW07] M. Horodecki, J. Oppenheim, and A. Winter. Quantum state merging and negative information. *Comm. Math. Phys.*, 269:107–136, Jan 2007.
- [HRZAR15] Q. He, L. Rosales-Zárate, G. Adesso, and M. D. Reid. Secure continuous variable teleportation and einstein-podolsky-rosen steering. *Phys. Rev. Lett.*, 115:180502, Oct 2015.
- [HSR03] M. Horodecki, P. W. Shor, and M. B. Ruskai. Entanglement breaking channels. *Rev. Math. Phys.*, 15(06):629–641, 2003.
- [HTMH14] P. Horodecki, J. Tuziemski, P. Mazurek, and R. Horodecki. Can communication power of separable correlations exceed that of entanglement resource? *Phys. Rev. Lett.*, 112:140507, Apr 2014.
- [HV01] L. Henderson and V. Vedral. Classical, quantum and total correlations. *Journal of Physics A: Mathematical and General*, 34(35):6899–6905, aug 2001.
- [HW97] S. A. Hill and W. K. Wootters. Entanglement of a pair of quantum bits. *Phys. Rev. Lett.*, 78:5022–5025, Jun 1997.
- [HWF18] M.-L. Hu, X.-M. Wang, and H. Fan. Hierarchy of the nonlocal advantage of quantum coherence and bell nonlocality. *Phys. Rev. A*, 98:032317, Sep 2018.

- [HWF22] M.-L. Hu, J.-R. Wang, and H. Fan. Limits on sequential sharing of non-local advantage of quantum coherence. *Sci. China Phys. Mech. Astron.*, 65:260312, Apr 2022.
- [HZH<sup>+</sup>16] M.-J. Hu, Z.-Y. Zhou, X.-M. Hu, C.-F. Li, G.-C. Guo, and Y.-S. Zhang. Observation of nonlocality sharing among three observers with one entangled pair via optimal weak measurement. *arXiv:1609.01863 [quant-ph]*, 2016.
- [HZH<sup>+</sup>18] M.-J. Hu, Z.-Y. Zhou, X.-M. Hu, C.-F. Li, G.-C. Guo, and Y.-S. Zhang. Observation of non-locality sharing among three observers with one entangled pair via optimal weak measurement. *npj Quant. Info.*, 4(1):63, 2018.
- [idZZHE93] M. Żukowski, A. Zeilinger, M. A. Horne, and A. K. Ekert. "event-ready-detectors" bell experiment via entanglement swapping. *Phys. Rev. Lett.*, 71:4287–4290, Dec 1993.
- [idZZHW98] M. Żukowski, A. Zeilinger, M. A. Horne, and H. Weinfurter. Quest for ghz states. *Acta Phys. Pol. A*, 93:187–195, 1998.
- [Jam72] A. Jamiolkowski. Linear transformations which preserve trace and positive semidefiniteness of operators. *Rep. Math. Phys.*, 3(4):275–278, 1972.
- [JAS17] C. Jebaratnam, S. Aravinda, and R. Srikanth. Nonclassicality of local bipartite correlations. *Phys. Rev. A*, 95:032120, Mar 2017.
- [JDK<sup>+</sup>19] C. Jebarathinam, D. Das, S. Kanjilal, R. Srikanth, D. Sarkar, I. Chattopadhyay, and A. S. Majumdar. Superunsteerability as a quantifiable resource for random access codes assisted by bell-diagonal states. *Phys. Rev. A*, 100:012344, Jul 2019.
- [JKMW01] D. F. V. James, P. G. Kwiat, W. J. Munro, and A. G. White. Measurement of qubits. *Phys. Rev. A*, 64:052312, Oct 2001.
- [JLF13] M. Jiang, S. Luo, and S. Fu. Channel-state duality. *Phys. Rev. A*, 87:022310, Feb 2013.
- [JWD07] S. J. Jones, H. M. Wiseman, and A. C. Doherty. Entanglement, einstein-podolsky-rosen correlations, bell nonlocality, and steering. *Phys. Rev. A*, 76:052116, Nov 2007.
- [JZLW19] X.-F. Jiao, P. Zhou, S.-X. Lv, and Z.-Y. Wang. Remote preparation for single-photon two-qubit hybrid state with hyperentanglement via linear-optical elements. *Sc. Rep.*, 9:4663, Mar 2019.

- [KBR<sup>+</sup>11] S. Kocsis, B. Braverman, S. Ravets, M. J. Stevens, R. P. Mirin, L. K. Shalm, and A. M. Steinberg. Observing the average trajectories of single photons in a two-slit interferometer. *Science*, 332:1170, Jun 2011.
- [KC04] B. Kraus and J. I. Cirac. Discrete entanglement distribution with squeezed light. *Phys. Rev. Lett.*, 92:013602, Jan 2004.
- [KCL<sup>+</sup>18] H.-Y. Ku, S.-L. Chen, N. Lambert, Y.-N. Chen, and F. Nori. Hierarchy in temporal quantum correlations. *Phys. Rev. A*, 98:022104, Aug 2018.
- [KCRK09] Y.-S. Kim, Y.-W. Cho, Y.-S. Ra, and Y.-H. Kim. Reversing the weak quantum measurement for a photonic qubit. *Opt. Express*, 17(14):11978–11985, Jul 2009.
- [Kim08] H. J. Kimble. The quantum internet. *Nature*, 453(7198):1023–1030, Jun 2008.
- [KJ06] A. N. Korotkov and A. N. Jordan. Undoing a weak quantum measurement of a solid-state qubit. *Phys. Rev. Lett.*, 97:166805, Oct 2006.
- [KKJH18] S. Kanjilal, A. Khan, C. Jebarathinam, and D. Home. Remote state preparation using correlations beyond discord. *Phys. Rev. A*, 98:062320, Dec 2018.
- [KLAK02] M. S. Kim, J. Lee, D. Ahn, and P. L. Knight. Entanglement induced by a single-mode heat environment. *Phys. Rev. A*, 65:040101, Apr 2002.
- [KLKK12] Y.-S. Kim, J.-C. Lee, O. Kwon, and Y.-H. Kim. Protecting entanglement from decoherence using weak measurement and quantum measurement reversal. *Nat. Phys.*, 8:117–120, Feb 2012.
- [KTDR15] H. S. Karthik, J. P. Tej, A. R. U. Devi, and A. K. Rajagopal. Joint measurability and temporal steering. *J. Opt. Soc. Am. B*, 32(4):A34–A39, Apr 2015.
- [KU99] M. Koashi and M. Ueda. Reversing measurement and probabilistic quantum error correction. *Phys. Rev. Lett.*, 82:2598–2601, Mar 1999.
- [L06] G. Lüders. Concerning the state-change due to the measurement process. *Annalen der Physik*, 15(9):663–670, 2006.
- [LC10] M. D. Lang and C. M. Caves. Quantum discord and the geometry of bell-diagonal states. *Phys. Rev. Lett.*, 105:150501, Oct 2010.

- [LCL<sup>+</sup>15] C.-M. Li, Y.-N. Chen, N. Lambert, C.-Y. Chiu, and F. Nori. Certifying single-system steering for quantum-information processing. *Phys. Rev. A*, 92:062310, Dec 2015.
- [LF10] S. Luo and S. Fu. Geometric measure of quantum discord. *Phys. Rev. A*, 82:034302, Sep 2010.
- [LG85] A. J. Leggett and A. Garg. Quantum mechanics versus macroscopic realism: Is the flux there when nobody looks? *Phys. Rev. Lett.*, 54:857–860, Mar 1985.
- [LJKK11] J.-C. Lee, Y.-C. Jeong, Y.-S. Kim, and Y.-H. Kim. Experimental demonstration of decoherence suppression via quantum measurement reversal. *Opt. Express*, 19(17):16309–16316, Aug 2011.
- [LS03] D. W. Leung and P. W. Shor. Oblivious remote state preparation. *Phys. Rev. Lett.*, 90:127905, Mar 2003.
- [LSP<sup>+</sup>11] J. S. Lundeen, B. Sutherland, A. Patel, C. Stewart, and C. Bamber. Direct measurement of the quantum wavefunction. *Nature*, 474:188, Jun 2011.
- [LTBS14] Y. Z. Law, Le P. Thinh, J.-D. Bancal, and V. Scarani. Quantum randomness extraction for various levels of characterization of the devices. *J. Phys. A: Math. Theor.*, 47(42):424028, oct 2014.
- [Luo03] S. Luo. Wigner-yanase skew information and uncertainty relations. *Phys. Rev. Lett.*, 91:180403, Oct 2003.
- [Luo08] S. Luo. Quantum discord for two-qubit systems. *Phys. Rev. A*, 77:042303, Apr 2008.
- [LWO<sup>+</sup>07] W.-T. Liu, W. Wu, B.-Q. Ou, P.-X. Chen, C.-Z. Li, and J.-M. Yuan. Experimental remote preparation of arbitrary photon polarization states. *Phys. Rev. A*, 76:022308, Aug 2007.
- [LX13] Y.-L. Li and X. Xiao. Recovering quantum correlations from amplitude damping decoherence by weak measurement reversal. *Quant. Info. Proc.*, 12:3067, Sep 2013.
- [MCWV11] K. Modi, H. Cable, M. Williamson, and V. Vedral. Quantum correlations in mixed-state metrology. *Phys. Rev. X*, 1:021022, Dec 2011.
- [MDH16] S. Mal, D. Das, and D. Home. Quantum mechanical violation of macrorealism for large spin and its robustness against coarse-grained measurements. *Phys. Rev. A*, 94:062117, Dec 2016.

- [MDM17] A. G. Maity, S. Datta, and A. S. Majumdar. Tighter einstein-podolsky-rosen steering inequality based on the sum-uncertainty relation. *Phys. Rev. A*, 96:052326, Nov 2017.
- [MDS16] D. Mondal, C. Datta, and Sk Sazim. Quantum coherence sets the quantum speed limit for mixed states. *Phys. Lett. A*, 380(5):689–695, 2016.
- [MDSK19] D. Mondal, C. Datta, J. Singh, and D. Kaszlikowski. Authentication protocol based on collective quantum steering. *Phys. Rev. A*, 99:012312, Jan 2019.
- [MDSM17] S. Mal, D. Das, S. Sasmal, and A. S. Majumdar. Necessary and sufficient state condition for two-qubit steering using two measurement settings per party and monogamy of steering. *arXiv:1711.00872 [quant-ph]*, 2017.
- [MHS<sup>+</sup>12] X.-S. Ma, T. Herbst, T. Scheidl, D. Wang, S. Kropatschek, W. Naylor, B. Wittmann, A. Mech, J. Kofler, E. Anisimova, V. Makarov, T. Jennewein, R. Ursin, and A. Zeilinger. Quantum teleportation over 143 kilometres using active feed-forward. *Nature*, 489:269–273, Sep 2012.
- [MK18] D. Mondal and D. Kaszlikowski. Complementarity relations between quantum steering criteria. *Phys. Rev. A*, 98:052330, Nov 2018.
- [MMH16] S. Mal, A. S. Majumdar, and D. Home. Sharing of nonlocality of a single member of an entangled pair of qubits is not possible by more than two unbiased observers on the other wing. *Mathematics*, 4(3), 2016.
- [MP95] S. Massar and S. Popescu. Optimal extraction of information from finite quantum ensembles. *Phys. Rev. Lett.*, 74:1259–1263, Feb 1995.
- [MP02] C. Macchiavello and G. M. Palma. Entanglement-enhanced information transmission over a quantum channel with correlated noise. *Phys. Rev. A*, 65:050301, Apr 2002.
- [MP14] L. Maccone and A. K. Pati. Stronger uncertainty relations for all incompatible observables. *Phys. Rev. Lett.*, 113:260401, Dec 2014.
- [MPP17] D. Mondal, T. Pramanik, and A. K. Pati. Nonlocal advantage of quantum coherence. *Phys. Rev. A*, 95:010301(R), Jan 2017.
- [MPS<sup>+</sup>10] K. Modi, T. Paterek, W. Son, V. Vedral, and M. Williamson. Unified view of quantum and classical correlations. *Phys. Rev. Lett.*, 104:080501, Feb 2010.

- [MS77] B. Misra and E. C. G. Sudarshan. The zeno's paradox in quantum theory. *J. Math. Phys.*, 18(4):756–763, 1977.
- [MU88] H. Maassen and J. B. M. Uffink. Generalized entropic uncertainty relations. *Phys. Rev. Lett.*, 60:1103–1106, Mar 1988.
- [MWKZ96] K. Mattle, H. Weinfurter, P. G. Kwiat, and A. Zeilinger. Dense coding in experimental quantum communication. *Phys. Rev. Lett.*, 76:4656–4659, Jun 1996.
- [MX16] J. Millen and A. Xuereb. Perspective on quantum thermodynamics. *New J. Phys.*, 18(1):011002, jan 2016.
- [MXA12] Z.-X. Man, Y.-J. Xia, and N. Ba An. Enhancing entanglement of two qubits undergoing independent decoherences by local pre- and postmeasurements. *Phys. Rev. A*, 86:052322, Nov 2012.
- [MY04] D. Mayers and A. Yao. Self testing quantum apparatus. *Quantum Info. Comput.*, 4(4):273–286, jul 2004.
- [Nai40] M. A. Naimark. About second-kind self-adjoint extensions of symmetrical operator. *Izv. Akad. Nauk USSR, Ser. Mat*, 4:53–104, 1940.
- [NC02] M. A Nielsen and I. Chuang. *Quantum computation and quantum information (Cambridge Univ. Press, 2000)*. American Association of Physics Teachers, 2002.
- [NCNK11] B. A. Nguyen, T. B. Cao, V. D. Nung, and J. Kim. Remote state preparation with unit success probability. *Adv. Nat. Sci.: Nanosci. Nanotechnol.*, 2(3):035009, jul 2011.
- [Neu55] J. von Neumann. *Mathematical Foundations of Quantum Mechanics*. Princeton University Press, 1955.
- [NK08] B. A. Nguyen and J. Kim. Joint remote state preparation. *J. Phys. B: Atom. Mol. Opt. Phys.*, 41(9):095501, apr 2008.
- [OB08] M. K. Olsen and A. S. Bradley. Bright bichromatic entanglement and quantum dynamics of sum frequency generation. *Phys. Rev. A*, 77:023813, Feb 2008.
- [OH02] J. Oppenheim, M. Horodecki, P. Horodecki, and R. Horodecki. Thermodynamical approach to quantifying quantum correlations. *Phys. Rev. Lett.*, 89:180402, Oct 2002.

- [OPKP92] Z. Y. Ou, S. F. Pereira, H. J. Kimble, and K. C. Peng. Realization of the einstein-podolsky-rosen paradox for continuous variables. *Phys. Rev. Lett.*, 68:3663–3666, Jun 1992.
- [OW10] J. Oppenheim and S. Wehner. The uncertainty principle determines the nonlocality of quantum mechanics. *Science*, 330(6007):1072–1074, 2010.
- [OZ01] H. Ollivier and W. H. Zurek. Quantum discord: A measure of the quantumness of correlations. *Phys. Rev. Lett.*, 88:017901, Dec 2001.
- [PAM<sup>+</sup>10] S. Pironio, A. Acín, S. Massar, A. Boyer de la Giroday, D. N. Matsukevich, P. Maunz, S. Olmschenk, D. Hayes, L. Luo, T. A. Manning, and C. Monroe. Random numbers certified by bell’s theorem. *Nature*, 464:1021–1024, Apr 2010.
- [Pat00] A. K. Pati. Minimum classical bit for remote preparation and measurement of a qubit. *Phys. Rev. A*, 63:014302, Dec 2000.
- [PBG<sup>+</sup>05] N. A. Peters, J. T. Barreiro, M. E. Goggin, T.-C. Wei, and P. G. Kwiat. Remote state preparation: Arbitrary remote control of photon polarization. *Phys. Rev. Lett.*, 94:150502, Apr 2005.
- [PCB03] M. G. A. Paris, M. Cola, and R. Bonifacio. Remote state preparation and teleportation in phase space. *J. Opt. B: Quantum and Semiclassical Optics*, 5(3):S360, jun 2003.
- [PCL<sup>+</sup>12] J-W. Pan, Z-B. Chen, C-Y. Lu, H. Weinfurter, A. Zeilinger, and M. Żukowski. Multiphoton entanglement and interferometry. *Rev. Mod. Phys.*, 84:777, May 2012.
- [PCSA15] E. Passaro, D. Cavalcanti, P. Skrzypczyk, and A. Acín. Optimal randomness certification in the quantum steering and prepare-and-measure scenarios. *New Journal of Physics*, 17(11):113010, oct 2015.
- [Per96] A. Peres. Separability criterion for density matrices. *Phys. Rev. Lett.*, 77:1413–1415, Aug 1996.
- [Per02] A. Peres. *Quantum theory: concepts and methods*. Springer, 2002.
- [PH02] M. B. Plenio and S. F. Huelga. Entangled light from white noise. *Phys. Rev. Lett.*, 88:197901, Apr 2002.
- [Pia15] M. Piani. Channel steering. *J. Opt. Soc. Am. B*, 32(4):A1–A7, Apr 2015.

- [PKM14] T. Pramanik, M. Kaplan, and A. S. Majumdar. Fine-grained einstein-podolsky-rosen-steering inequalities. *Phys. Rev. A*, 90:050305(R), Nov 2014.
- [PM13] T. Pramanik and A.S. Majumdar. Improving the fidelity of teleportation through noisy channels using weak measurement. *Phys. Lett. A*, 377(44):3209–3215, 2013.
- [PM20] B. Paul and K. Mukherjee. Shareability of quantum steering and its relation with entanglement. *Phys. Rev. A*, 102:052209, Nov 2020.
- [Pop94] S. Popescu. Bell’s inequalities versus teleportation: What is nonlocality? *Phys. Rev. Lett.*, 72:797, Feb 1994.
- [PR94] S. Popescu and D. Rohrlich. Quantum nonlocality as an axiom. *Found. Phys*, 24:379–385, Mar 1994.
- [PS07] A.K. Pati and P.K. Sahu. Sum uncertainty relation in quantum theory. *Phys. Lett. A*, 367(3):177–181, 2007.
- [Pus13] M. F. Pusey. Negativity and steering: A stronger peres conjecture. *Phys. Rev. A*, 88:032313, Sep 2013.
- [PW15] M. Piani and J. Watrous. Necessary and sufficient quantum information characterization of einstein-podolsky-rosen steering. *Phys. Rev. Lett.*, 114:060404, Feb 2015.
- [PWK04] N. A. Peters, T.-C. Wei, and P. G. Kwiat. Mixed-state sensitivity of several quantum-information benchmarks. *Phys. Rev. A*, 70:052309, Nov 2004.
- [PZF<sup>+</sup>03] X. Peng, X. Zhu, X. Fang, M. Feng, M. Liu, and K. Gao. Experimental implementation of remote state preparation by nuclear magnetic resonance. *Phys. Lett. A*, 306(5):271, 2003.
- [QLSN07] H. T. Quan, Y.-x. Liu, C. P. Sun, and F. Nori. Quantum thermodynamic cycles and quantum heat engines. *Phys. Rev. E*, 76:031105, Sep 2007.
- [Qua09] H. T. Quan. Quantum thermodynamic cycles and quantum heat engines. ii. *Phys. Rev. E*, 79:041129, Apr 2009.
- [QVC<sup>+</sup>15] M. T. Quintino, T. Vértesi, D. Cavalcanti, R. Augusiak, M. Demianowicz, A. Acín, and N. Brunner. Inequivalence of entanglement, steering, and bell nonlocality for general measurements. *Phys. Rev. A*, 92:032107, Sep 2015.

- [QZL<sup>+</sup>16] Q. Quan, H. Zhu, S.-Y. Liu, S.-M. Fei, H. Fan, and W.-L. Yang. Steering bell-diagonal states. *Sci. Rep.*, 6:22025, Feb 2016.
- [RBM<sup>+</sup>21] S. Roy, A. Bera, S. Mal, A. Sen(De), and U. Sen. Recycling the resource: Sequential usage of shared state in quantum teleportation with weak measurements. *Phys. Lett. A*, 392:127143, 2021.
- [RBV<sup>+</sup>07] W. Rosenfeld, S. Berner, J. Volz, M. Weber, and H. Weinfurter. Remote preparation of an atomic quantum memory. *Phys. Rev. Lett.*, 98:050504, Feb 2007.
- [Rei89] M. D. Reid. Demonstration of the einstein-podolsky-rosen paradox using nondegenerate parametric amplification. *Phys. Rev. A*, 40:913–923, Jul 1989.
- [Rob29] H. P. Robertson. The uncertainty principle. *Phys. Rev.*, 34:163–164, Jul 1929.
- [RPWL17] S. Rana, P. Parashar, A. Winter, and M. Lewenstein. Logarithmic coherence: Operational interpretation of  $\ell_1$ -norm coherence. *Phys. Rev. A*, 96:052336, Nov 2017.
- [RWasidZB13] M. Rådmark, M. Wieśniak, M. Żukowski, and M. Bourennane. Experimental multilocation remote state preparation. *Phys. Rev. A*, 88:032304, Sep 2013.
- [SAP17] A. Streltsov, G. Adesso, and M. B. Plenio. Colloquium: Quantum coherence as a resource. *Rev. Mod. Phys.*, 89:041003, Oct 2017.
- [SB13] G. Strübi and C. Bruder. Measuring ultrasmall time delays of light by joint weak measurements. *Phys. Rev. Lett.*, 110:083605, Feb 2013.
- [SBW<sup>+</sup>13] J. Schneeloch, C. J. Broadbent, S. P. Walborn, E. G. Cavalcanti, and J. C. Howell. Einstein-podolsky-rosen steering inequalities from entropic uncertainty relations. *Phys. Rev. A*, 87:062103, Jun 2013.
- [Sch35] E. Schrödinger. Die gegenwärtige situation in der quantenmechanik. *Naturwissenschaften*, 23:807–812, Nov 1935.
- [Sch36] E. Schrödinger. Probability relations between separated systems. *Math. Proc. Cambridge Philos. Soc.*, 32(3):446, 1936.
- [SCP<sup>+</sup>17] M. Schiavon, L. Calderaro, M. Pittaluga, G. Vallone, and P. Villoresi. Three-observer bell inequality violation on a two-qubit entangled state. *Quantum Science and Technology*, 2(1):015010, 2017.

- [SDMM18] S. Sasmal, D. Das, S. Mal, and A. S. Majumdar. Steering a single system sequentially by multiple observers. *Phys. Rev. A*, 98:012305, Jul 2018.
- [SGGP15] R. Silva, N. Gisin, Y. Guryanova, and S. Popescu. Multiple observers can share the nonlocality of half of an entangled pair by using optimal weak measurements. *Phys. Rev. Lett.*, 114:250401, Jun 2015.
- [Sha48a] C. E. Shannon. A mathematical theory of communication. *The Bell System Tech. Jour.*, 27(3):379–423, 1948.
- [Sha48b] C. E. Shannon. A mathematical theory of communication. *The Bell System Technical Journal*, 27(4):623–656, 1948.
- [SHDH<sup>+</sup>19] A. Shenoy H., S. Designolle, F. Hirsch, R. Silva, N. Gisin, and N. Brunner. Unbounded sequence of observers exhibiting einstein-podolsky-rosen steering. *Phys. Rev. A*, 99:022317, Feb 2019.
- [Sho97] P. W. Shor. Polynomial-time algorithms for prime factorization and discrete logarithms on a quantum computer. *SIAM J.Sci.Statist.Comput.*, 26(5):1484–1509, 1997.
- [SJWP10] D. J. Saunders, S. J. Jones, H. M. Wiseman, and G. J. Pryde. Experimental epr-steering using bell-local states. *Nat. Phys.*, 6:845–849, Nov 2010.
- [SKB12] A. Streltsov, H. Kampermann, and D. Bruß. Quantum cost for sending entanglement. *Phys. Rev. Lett.*, 108:250501, Jun 2012.
- [SMC<sup>+</sup>04] D. R. Solli, C. F. McCormick, R. Y. Chiao, S. Popescu, and J. M. Hickmann. Fast light, slow light, and phase singularities: A connection to generalized weak values. *Phys. Rev. Lett.*, 92:043601, Jan 2004.
- [SMSS21] C. Srivastava, S. Mal, A. Sen(De), and U. Sen. Sequential measurement-device-independent entanglement detection by multiple observers. *Phys. Rev. A*, 103:032408, Mar 2021.
- [SNC14] P. Skrzypczyk, M. Navascués, and D. Cavalcanti. Quantifying einstein-podolsky-rosen steering. *Phys. Rev. Lett.*, 112:180404, May 2014.
- [SP13] C. Shukla and A. Pathak. Hierarchical quantum communication. *Phys. Lett. A*, 377(19):1337–1344, 2013.
- [SPHM18] S. Sasmal, T. Pramanik, D. Home, and A. S. Majumdar. A tighter steering criterion using the robertson–schrodinger uncertainty relation. *Phys. Lett. A*, 382(1):27–32, 2018.

- [SPS22] C. Srivastava, M. Pandit, and U. Sen. Entanglement witnessing by arbitrarily many independent observers recycling a local quantum shared state. *Phys. Rev. A*, 105:062413, Jun 2022.
- [SSdRG11] N. Sangouard, C. Simon, H. de Riedmatten, and N. Gisin. Quantum repeaters based on atomic ensembles and linear optics. *Rev. Mod. Phys.*, 83:33–80, Mar 2011.
- [STP17] C. Shukla, K. Thapliyal, and A. Pathak. Hierarchical joint remote state preparation in noisy environment. *Quant. Info. Proc.*, 16:205, Jul 2017.
- [Str15] A. Streltsov. Quantum correlations beyond entanglement. *Springer Briefs in Physics*, 2015.
- [SW97] B. Schumacher and M. D. Westmoreland. Sending classical information via noisy quantum channels. *Phys. Rev. A*, 56:131–138, Jul 1997.
- [SW06] B. Schumacher and M. D. Westmoreland. Quantum mutual information and the one-time pad. *Phys. Rev. A*, 74:042305, Oct 2006.
- [SYX<sup>+</sup>18] K. Sun, X.-J. Ye, Y. Xiao, X.-Y. Xu, Y.-C. Wu, J.-S. Xu, J.-L. Chen, C.-F. Li, and G.-C. Guo. Demonstration of einstein–podolsky–rosen steering with enhanced subchannel discrimination. *npj Quantum Information*, 4:12, Feb 2018.
- [SZ13] A. Streltsov and W. H. Zurek. Quantum discord cannot be shared. *Phys. Rev. Lett.*, 111:040401, Jul 2013.
- [TDL01] B. M. Terhal, D. P. DiVincenzo, and D. W. Leung. Hiding bits in bell states. *Phys. Rev. Lett.*, 86:5807–5810, Jun 2001.
- [TR11] M. Tomamichel and R. Renner. Uncertainty relation for smooth entropies. *Phys. Rev. Lett.*, 106:110506, Mar 2011.
- [UCNG20] R. Uola, A. C. S. Costa, H. C. Nguyen, and O. Gühne. Quantum steering. *Rev. Mod. Phys.*, 92:015001, Mar 2020.
- [VB96] L. Vandenberghe and S. Boyd. Semidefinite programming. *SIAM Review*, 38(1):49–95, 1996.
- [VDD01] F. Verstraete, J. Dehaene, and B. DeMoor. Local filtering operations on two qubits. *Phys. Rev. A*, 64:010101, Jun 2001.
- [Ved02] V. Vedral. The role of relative entropy in quantum information theory. *Rev. Mod. Phys.*, 74:197–234, Mar 2002.

- [VPRK97] V. Vedral, M. B. Plenio, M. A. Rippin, and P. L. Knight. Quantifying entanglement. *Phys. Rev. Lett.*, 78:2275–2279, Mar 1997.
- [VT99] G. Vidal and R. Tarrach. Robustness of entanglement. *Phys. Rev. A*, 59:141–155, Jan 1999.
- [Wat11] J. Watrous. *Theory of Quantum Information Lecture notes*. 2011.
- [Wer89] R. F. Werner. Quantum states with einstein-podolsky-rosen correlations admitting a hidden-variable model. *Phys. Rev. A*, 40:4277–4281, Oct 1989.
- [Wis02] H. M. Wiseman. Weak values, quantum trajectories, and the cavity-qed experiment on wave-particle correlation. *Phys. Rev. A*, 65:032111, Feb 2002.
- [WJD07] H. M. Wiseman, S. J. Jones, and A. C. Doherty. Steering, entanglement, nonlocality, and the einstein-podolsky-rosen paradox. *Phys. Rev. Lett.*, 98:140402, Apr 2007.
- [WKR<sup>+</sup>21a] K-D. Wu, T. V. Kondra, S. Rana, C. M. Scandolo, G-Y. Xiang, C-F. Li, G-C. Guo, and A. Streltsov. Operational resource theory of imaginarity. *Phys. Rev. Lett.*, 126:090401, Mar 2021.
- [WKR<sup>+</sup>21b] K-D. Wu, T. V. Kondra, S. Rana, C. M. Scandolo, G-Y. Xiang, C-F. Li, G-C. Guo, and A. Streltsov. Resource theory of imaginarity: Quantification and state conversion. *Phys. Rev. A*, 103:032401, Mar 2021.
- [WLCL10] W. Wu, W-T. Liu, P-X. Chen, and C-Z. Li. Deterministic remote preparation of pure and mixed polarization states. *Phys. Rev. A*, 81:042301, Apr 2010.
- [WLZZ09] Z.-Y. Wang, Y.-M. Liu, X.-Q. Zuo, and Z.-J. Zhang. Controlled remote state preparation. *Communications in Theoretical Physics*, 52(2):235–240, aug 2009.
- [Woo98] W. K. Wootters. Entanglement of formation of an arbitrary state of two qubits. *Phys. Rev. Lett.*, 80:2245–2248, Mar 1998.
- [WSG<sup>+</sup>11] S. P. Walborn, A. Salles, R. M. Gomes, F. Toscano, and P. H. Souto Ribeiro. Revealing hidden einstein-podolsky-rosen nonlocality. *Phys. Rev. Lett.*, 106:130402, Mar 2011.
- [WYG21] M-Y. Wang, F. Yan, and T. Gao. Remote preparation for single-photon state in two degrees of freedom with hyper-entangled states. *Front. Phys.*, 16:41501, Mar 2021.

[WZ82] W. K. Wootters and W. H. Zurek. A single quantum cannot be cloned. *Nature*, 299:802–803, Aug 1982.

[XLYG05] G-Y. Xiang, J. Li, B. Yu, and G-C. Guo. Remote preparation of mixed states via noisy entanglement. *Phys. Rev. A*, 72:012315, Jul 2005.

[YL17] R-Y. Yang and J-M. Liu. Enhancing the fidelity of remote state preparation by partial measurements. *Quant. Info. Proc.*, 16:1, 2017.

[ZF21] T. Zhang and S.-M. Fei. Sharing quantum nonlocality and genuine nonlocality with independent observables. *Phys. Rev. A*, 103:032216, Mar 2021.

[Zur03] W. H. Zurek. Decoherence, einselection, and the quantum origins of the classical. *Rev. Mod. Phys.*, 75:715–775, May 2003.